

Solid-State NMR Investigations of the ATP Binding Cassette Multidrug Transporter LmrA

Dissertation zur Erlangung des Doktorgrades
der Naturwissenschaften

vorgelegt dem Fachbereich Biochemie, Chemie, Pharmazie
Institut für Biophysikalische Chemie
Johann Wolfgang Goethe Universität Frankfurt am Main
Zentrum für Biomolekulare Magnetische Resonanz

von

Alena Sjarheyeva

aus Minsk

Frankfurt am Main 2006

vom Fachbereich: Biochemie, Chemie, Pharmazie.....

Johann Wolfgang Goethe – Universität als Dissertation angenommen

Dekan: Prof. Dr. Schwalbe

Gutachter:

Datum der Disputation

Fachbereich 14
der Johann Wolfgang Goethe- Universität

Der Bewerber.....

hat heute das Promotionsverfahren im Fach.....

mit der Gesamtnote.....

abgeschlossen.

Die einzelnen Prüfungsleistungen wurden wie folgt bewertet:

Dissertation:.....

Disputation:.....

Das Recht zur Führung des Dokortitels wird nicht durch diese Bescheinigung, sondern erst durch die Aushändigung der Urkunde erworben.

Frankfurt am Main, den

(Siegel)

Der Dekan
(Unterschrift)

(Siegel der Universität)

Der Fachbereich 14

der Johann Wolfgang Goethe-Universität

verleiht

Alena Sjarheyeva

aus Minsk

den Grad eines Doktors der Naturwissenschaften

nachdem sie in ordnungsgemäßem Promotionsverfahren

durch die Arbeit

Solid-state NMR investigations of the ATP binding cassette multidrug transporter LmrA

und eine öffentliche Disputation ihre wissenschaftliche Befähigung erwiesen hat. Die

Promotionsleistung wurde mit

(Gesamtnote) beurteilt.

Frankfurt am Main, den

Der Dekan

(Unterschrift)

Summary

The development of resistance to multiple drugs is a major problem in treatment of number of infectious diseases and cancer. The phenomenon of multidrug resistance (MDR) is based on the synergetic interplay of a number of mechanisms such as target inactivation, target alteration, prevention of drug influx as well as active extrusion of drugs from the cell. The latter is mediated by over-expression of multidrug efflux pumps. The first discovered and the best characterized until now the human MDR transporter is P-glycoprotein. It is a member of the ATP binding cassette (ABC) superfamily and acts as an active transporter for a variety of anticancer agents using the energy released by ATP hydrolysis. The closest structure and functional homologue of P-glycoprotein found in bacteria is LmrA from *Lactococcus lactis*.

The major goals of this work are to establish the selective isotope labelling of LmrA in *Lactococcus lactis*, to optimize LmrA sample preparation for solid-state NMR, and finally to perform first solid-state NMR investigations on LmrA shedding light on its catalytic cycle and substrate binding. For a long time the solid-state NMR applications to biological science has been limited to investigation of small molecules mostly. Recently, the solid-state NMR methods have shown potential for structural- and non-perturbing, site directed functional studies of large membrane proteins as well as ligands bound to them. However, to our knowledge neither selective isotope amino acid labelling of any ABC transporter, nor NMR investigations on full-length ABC transporter have been reported to date. Solid-state NMR experiments on a membrane protein require reconstitution of purified proteins into a membrane environment at a high density and either isotopic enrichment of the protein or bound drugs or inhibitors. Therefore, the large quantities of LmrA reconstituted at a high density in lipid membranes, sufficient for advanced NMR studies have been produced and its functional state in reconstituted form has been assessed. In the next step, a procedure for cost effective selective amino acids isotope labelling of LmrA in *Lactococcus lactis* has been established.

Using this protocol deuterium alanine labelled LmrA reconstituted into *E. coli* liposomes has been prepared. Deuterium NMR has been used extensively to assess the proteins dynamics in past.

However, it has never been applied to ABC transporter. Here, we report ^2H NMR on selective alanine isotope labelled LmrA which has been used to shed light on the dynamics changes in the protein occurred under AMP-PNP, non-hydrolysable ATP analogue, binding and in ATP/ADP-Vanadate trapped state. It has been found that the major conformation changes affecting the protein motional characteristics occur in the ATP binding domains but not in the transmembrane domains.

Additionally, the binding of several substrates to LmrA has been studied by fluorescence spectroscopy as well as by ^{19}F and ^{31}P solid-state NMR. The binding constants for several LmrA substrates have been obtained by fitting the concentration dependant tryptophan intrinsic fluorescence quenching curves. Based on the fluorescence studies and solid-state NMR data, the conformation changes in LmrA under substrate binding have been discussed.

In addition, the preferable location of nine LmrA and P-glycoprotein substrates within the model membrane has been studied via ^1H -MAS-NOESY-NMR. The results have been interpreted with respect to LmrA and P-glycoprotein binding site accessibility from the membrane interface region.

Zusammenfassung

Die Entstehung von Resistenzen gegenüber mehreren Wirkstoffen ist ein großes Problem bei der Behandlung einiger ansteckender Krankheiten und Krebs.

Multiwirkstoff Resistenzen (MDR) basieren auf einem synergetischen Zusammenspiel mehrerer Mechanismen wie der Inaktivierung oder Veränderung des Angriffziels, Verhinderung des Stoffeinstroms ebenso wie der aktive Transport von Wirkstoffen aus der Zelle heraus.

Der letztere wird durch die Überexpression von Multidrug Effluxpumpe vermittelt. Der erst entdeckte und am besten charakterisierte ist der menschliche MDR Transporter P-Glycoprotein.

Er gehört zur Superfamilie der ATP Bindekassetten (ABC) und wirkt als aktiver Transporter für mehrere Anti-Krebs Stoffe. Die Energie wird durch ATP Hydrolyse gewonnen. Die ähnlichste Struktur und funktionelles Homolog von P-Glykoprotein, das in Bakterien gefunden wurde, ist LmrA von *Lactococcus lactis*.

Das Hauptziel dieser Arbeit ist es, LmrA in *Lactococcus lactis* aminosäureselektiv mit Isotopen zu markieren, die Probenpräparation für Festkörper NMR zu optimieren und letztendlich erste Festkörper NMR Untersuchungen an LmrA durchzuführen, um den katalytischen Zyklus und die Substrat-Bindung aufzuklären.

Seit längerer Zeit waren die Anwendungen der Festkörper NMR im Bereich der Biologie meist auf die Untersuchung kleiner Moleküle beschränkt. Kürzlich haben die Methoden der Festkörper NMR Potential für strukturelle und nicht-störende ortsspezifische funktionale Studien großer Membranproteine sowie ihrer Liganden gezeigt. Es gibt bis jetzt jedoch nach unserem Wissen weder aminosäureselektive Isotopen-Markierung von ABC Transportern, noch NMR Untersuchungen an einem gesamten ABC Transporter. Festkörper NMR Experimente an einem Membranprotein erfordern die Rekonstitution mit einer hohen Konzentration und entweder Anreicherung von Isotopen des Proteins oder gebundener Wirkstoffe oder Inhibitoren. Deshalb wurden große Mengen von LmrA mit einer hohen Konzentration in Lipidmembranen für Festkörper-NMR rekonstituiert. Im nächsten Schritt wurde ein Verfahren für effiziente selektive Markierung von Aminosäuren von LmrA in

Lactococcus lactis etabliert.

Unter Verwendung dieses Protokolles wurde LmrA, das mit deuteriertem Alanin markiert war und in *E. coli* Liposomen rekonstituiert war, hergestellt.

Deuterium NMR wurde in der Vergangenheit umfangreich genutzt um die Dynamik der Proteine zu untersuchen. Sie wurde jedoch niemals auf ABC Transporter angewendet. Hier werden ^2H NMR experimente an Alanin-Isotopen markiertem LmrA vorgestellt, um die Veränderungen der Dynamik in dem Protein bei Bindung von AMP-PNP, einem nicht hydrolysierbares ATP Analogon, und in einem im ATP/ ADP-Vandat eingefangenen Zustand zu zeigen. Es stellte sich heraus, dass die wichtigsten Konformationsänderungen, die die Bewegung des Proteins beeinflussen, in der ATP-Binde-Domäne auftreten, nicht aber in den Transmembran-Domänen.

Zusätzlich wurde die Bindung mehrerer Substrate an LmrA mit Fluoreszenz Spektroskopie untersucht als auch mit ^{19}F und ^{31}P Festkörper NMR. Die Bindungs-Konstanten für mehrere LmrA Substrate wurden mittels Tryptophan Fluoreszenz-Quenching erhalten. Bezogen auf die Fluoreszenz-Untersuchungen und Festkörper NMR Daten wurden die Konformations-Änderungen von LmrA bei der Substrat Bindung diskutiert.

Zusätzlich wurde die bevorzugte Lokalisierung von neun Substraten von LmrA und P-Glykoprotein innerhalb der Modell-Membran durch ^1H -MAS-NOESY-NMR untersucht. Die Ergebnisse wurden in Bezug auf die Zugänglichkeit der Bindungs-Stelle in LmrA und P-Glykoprotein von der Membranzwischenschicht interpretiert.

Acknowledgements

I would like to express my extreme gratitude to Professor Clemens Glaubitz who gave me the opportunity, resources and support to complete the work for this thesis. He was always happy to answer my questions, helped me a lot with NMR measurements, and was extremely patient to me, not a small feat! His enthusiasm in the laboratory was infectious, equally, in a time when things went well and not quite well.

I would like to thank Dr. James Mason for helping me with many biochemical and NMR aspects. He devoted some considerable time especially in the beginning of my PhD to channel my energy in the right direction.

Dr. Jakob Lopez and Dr. Mark Lorch were always ready for discussions of any kind and helped me solving many problems; therefore I am very grateful to them.

I am indebted to Ingrid Weber and Simona Kobylka for their highly efficient administrative power. They both are always helpful, reliable, and accessible.

I am thankful to the other members of the Glaubitz group past and present: Nicole Pflieger, Christoph Kaiser, Ines Lehner, Thilo Ziehm, Daniel Basting, Ute Hellmich, Sarika Shastri for all their advice, help and company they gave me over these years.

Outside of the Glaubitz group I would like to thank Prof. van Veen from the University of Cambridge in UK for providing LmrA expression stain, Dr W. Haase from MPI Frankfurt for performing electron microscopy on reconstituted samples, and members of my thesis committee, Prof. W. Kühlbrandt, Prof. V. Dötsch, and Prof. B. Ludwig, for devoting considerable time to take part in my thesis committee meetings, for their questions and valuable advice along the whole PhD time.

I am thankful to International Research school MPI of Biophysics in general, and Dr. J. Vonck and Prof. W. Kühlbrandt in particular, for permanent support and their extremely welcoming attitude.

I am also grateful to my friends in MPI of Biophysics and University of Frankfurt. Special thought goes to Roman Gorbunov, Elena Olkhova, Elena Herzog.

I would especially like to thank my parents for their encouragement and help. I would not be completing a PhD without them.

Abbreviations

MDR - multidrug resistance

IC – inhibitor concentration

pmf - proton motive force

ABC family - ATP-binding cassette family

RND family - resistance/nodulation/cell division family

MATE family - multidrug and toxic compound family

SMR family - small multidrug transporter family

IM - inner membrane

OM - outer membrane

PGP – P-glycoprotein

ATP - adenosine 5'-triphosphate

TMDs – transmembrane domains

NBDs - nucleotide binding domains

ICDs - intracytoplasmic domains

TAP - transporter associated with antigen processing

LPS – lipopolysaccharide

EPR – electron paramagnetic resonance

CFTR - cystic fibrosis conductance regulator

MIANS - 2-(4'-maleimidylanilino)naphthalene-6-sulfonic acid

BCECF-AM - 2', 7'-bis-(2-carboxyethyl)-5-(and-6)-carboxyfluorescein

FRET - fluorescence resonance energy transfer

ATR-FTIR - Attenuated Total Reflection Fourier Transform Infrared spectroscopy

TMA-DPH - 1-[4-(trimethylamino)phenyl]-6-phenylhexa-1,3,5-triene

SSNMR - solid-state NMR

RF - radiofrequency

PAF - the principal axis frame

MAS - magic-angle spinning

CSA - chemical shift anisotropy

CP - cross polarization

CW - continuous irradiation

TPPM - two pulse phase modulation

FSLG - frequency-switched Lee-Goldburg

DRT - dipolar recoupling techniques

DRAMA - dipolar recovery at the magic angle

RFDR - radiofrequency driven recoupling

NICE - nisin controlled expression system

egg PC – egg phosphatidylcholine

brain PS – brain phosphatidylserine

egg PE – egg phosphatidylethanolamine

DDM - dodecyl maltoside

OG - octylglycoside

ISOVs – inside out vesicles

PM - purple membrane

TPP⁺ - tetraphenylphosphonium

TMR - tetramethylrosamine

CDF - chemically defined media

OD – optical density

CMC – critical micelle concentration

DMPC - 1,2-dimyristoyl-sn-glycero-3-phosphocholine

DMPG – 1,2-dimyristoyl-sn-glycero-3-phosphoglycerol

NOESY MAS NMR – magic angle spinning nuclear Overhauser enhancement spectroscopy

List of Figures

- Figure 1.1** Drug resistance mechanisms of various origins.
- Figure 1.2** Representative members of five characterized families of MDR transporters.
- Figure 1.3** Structures of MsbA and BtuCD transporters.
- Figure 1.4** NBDs association models.
- Figure 1.5** Contrasting transport models for ABC transporters.
- Figure 1.6** 3D atomic model of LmrA.
- Figure 1.7** Comparison of the amino acid sequence of LmrA from *L. lactis*, MsbA from *E. coli*, the N-, and C-terminal halves of human P-glycoprotein.
- Figure 1.8** Topology model for LmrA.
- Figure 1.9** Chemical shift tensor.
- Figure 1.10** Effect of chemical shift anisotropy.
- Figure 1.11** The magnetic moment of nuclear spin generates a magnetic field.
- Figure 1.12** The effect of heteronuclear dipolar coupling on NMR spectrum.
- Figure 1.13** The first-order quadrupolar powder lineshape for spin-1.
- Figure 1.14** MAS experiment.
- Figure 1.15** Cross polarization for heteronuclear spin pairs.
- Figure 1.16** Pulse sequence for cross polarization experiment.
- Figure 1.17** High-power decoupling pulse sequence.
- Figure 1.18** TPPM decoupling pulse.
- Figure 1.19** Pulse sequences for WAHUHA decoupling sequence and the Lee-Goldburg sequence.
- Figure 1.20** Pulse sequence for the DRAMA homonuclear dipolar recoupling sequence.
- Figure 1.21** REDOR experiment sequence.
- Figure 2.1** *L. lactis* grows in the chemically defined media without certain amino acids.
- Figure 2.2** *L. lactis* grows in the chemically defined media without certain amino acids.

- Figure 2.3** *L. lactis* growth in the rich medium and in the chemically defined medium.
- Figure 2.4** Hoechst-33342 transport in the membrane vesicles.
- Figure 2.5** ^{13}C CPMAS spectra of ^{13}C glycine labeled LmrA ISOV.
- Figure 2.6** ^{13}C CPMAS spectra of ^{13}C tyrosine labeled LmrA ISOV.
- Figure 2.7** *L. lactis* growth in the chemically defined medium.
- Figure 2.8** SDS-PAGE analysis as an evidence of LmrA overexpression.
- Figure 2.9** ^{13}C CPMAS spectra of ^{13}C tyrosine labeled LmrA ISOVs prepared from *L. lactis* cells strains NZ9000 and 8048 transferred from the M17 media into the defined medium.
- Figure 2.10** Hoechst-33342 transport assay results obtained for the membrane ISOVs performed for *L. lactis* cells transferred from the M17 media into the defined medium.
- Figure 2.11** ^{13}C CPMAS spectra of ^{13}C tyrosine LmrA ISOVs prepared from *L. lactis* cell grown on the chemically defined medium containing full and half amount of ^{13}C tyrosine.
- Figure 2.12** ^{13}C CPMAS spectra of ^{13}C labelled phenylalanine LmrA ISOV.
- Figure 3.1** The standard reconstitution strategy: preparation of liposomes, step-by-step detergent addition, protein addition and detergent removal.
- Figure 3.2** Gel filtration analysis of purified LmrA.
- Figure 3.3** SDS-PAGE analysis of purified LmrA.
- Figure 3.4** ^{13}C CPMAS spectra and SDS-PAGE analysis of *E. coli* liposomes vesicles reconstituted LmrA by detergent solubilization method.
- Figure 3.5** The freeze fracture electron micrographs and the sucrose gradient of LmrA reconstituted into *E. coli* liposomes using detergent liposome solubilization method.
- Figure 3.6** The freeze-fracture micrographs and SDS-PAGE analysis of *E. coli* liposomes reconstituted LmrA by liposomes destabilization method.
- Figure 3.7** ^{13}C CPMAS spectra and the sucrose gradient of *E. coli* lipids vesicles reconstituted LmrA by detergent destabilization method.
- Figure 3.8** The freeze-fracture micrographs and sucrose gradient of *E. coli* reconstituted LmrA by liposomes destabilization method under detergent exchange conditions.
- Figure 3.9** The colorimetric ATPase assay performed on ISOVs containing overexpressed LmrA

and on liposomes reconstituted protein.

- Figure 3.10** Hoechst-33342 transport assay results obtained for proteoliposomes reconstituted LmrA.
- Figure 3.11** ^{13}C CPMAS spectra of ^{13}C tyrosine labelled LmrA reconstituted in lipid vesicles.
- Figure 3.12** ^{15}N CPMAS spectra of ^{15}N tyrosine labelled LmrA reconstituted in lipid vesicles.
- Figure 3.13** The freeze-fracture micrographs of PC/PG/cardiolipin, and PE/PG lipids mixture reconstituted LmrA by liposomes destabilization method.
- Figure 4.1** SDS acrylamide gel of full-length LmrA, NBDs left in supernatant after isolating the membrane-embedded LmrA domain with proteinase K, LmrA without cytoplasmic domain, and LmrA-MD.
- Figure 4.2** ^2H NMR spectra of ^2H alanine selective labelled LmrA reconstituted *E. coli* liposomes in a resting state and trapped with AMP-PNP.
- Figure 4.3** Experimental and simulated spectra of ^2H alanine selective labelled LmrA reconstituted *E. coli* liposomes in a resting state.
- Figure 4.4** ^2H spectra of ^2H alanine selective labelled membranous LmrA domain obtained with proteinase K cleavage procedure and of LmrA-MD.
- Figure 4.5** ^2H MAS spectra of *E. coli* liposomes reconstituted LmrA in a resting state, and with AMP-PNP bound recorded at 235K, 260K, and 280K.
- Figure 4.6** The ^{31}P spectra of *E. coli* liposomes reconstituted LmrA in a resting state, with AMP-PNP bound, LmrA-MD, LmrA, without NBDs, LmrA trapped with ATP/ADP vanadate, and of free liposomes.
- Figure 4.7** ^2H NMR spectra of ^2H alanine selective labelled LmrA reconstituted *E. coli* liposomes in a resting state in a state trapped with ATP/ADP-Vanadate.
- Figure 4.8** The comparison of the spin-relaxation rates for LmrA TMDs and loops and NBDs in a protein resting state and ATP/ADP-Vanadate bound state.
- Figure 4.9** Proposed LmrA conformation changes affecting the protein dynamics under ATP binding and hydrolysis.
- Figure 5.1** The chemical structures of vinblastine, TPP^+ , and norfloxacin.

- Figure 5.2** The chemical structure of leupeptin.
- Figure 5.3** Fluorescence emission spectra for LmrA reconstituted into *E. coli* liposomes.
- Figure 5.4** Binding of norfloxacin and vinblastine to LmrA reconstituted into *E. coli* liposomes.
- Figure 5.5** ^{19}F MAS NMR spectrum of reconstituted LmrA with added norfloxacin.
- Figure 5.6** Binding of TPP^+ to LmrA reconstituted *E. coli* liposomes as assessed by tryptophan intrinsic fluorescence quenching.
- Figure 5.7** ^{31}P MAS spectrum of proteoliposomes reconstituted with LmrA without TPP^+ and with TPP^+ .
- Figure 5.8** ^{31}P MAS spectra of liposomes reconstituted LmrA with added TPP^+ recorded using direct polarization and cross polarization.
- Figure 5.9** Real-time fluorescence measurement of Hoechst-33342 transport blockage by leupeptin.
- Figure 5.10** The colorimetric ATPase assay presents linear fit of non simulated and leupeptin stimulated ATPase LmrA activity.
- Figure 5.11** Location of tryptophan residues in LmrA sequence.
- Figure 6.1** Energy levels for a pair of spin-1/2 nuclei I and S, showing the six possible relaxation pathways.
- Figure 6.2** NOESY pulse sequence.
- Figure 6.3** Chemical structures of nine PGP substrates.
- Figure 6.4** 400 MHz ^1H MAS NMR spectra of DMPC/ D_2O dispersions containing nine different substrates.
- Figure 6.5** The comparison of cross relaxation rate of nocardipine obtained using one mixing time approach and spin-pair interaction approach.
- Figure 6.6** ^1H MAS NOESY contour plot of a DMPC/cholesterol mixture and the cross peak volumes as a function of mixing time of 40 % cholesterol in DMPC.
- Figure 6.7** Two-dimensional ^1H MAS NMR NOESY spectra of quinidine and penicillin G DMPC dispersions in D_2O .

- Figure 6.8** Following the single mixing time analysis, normalized DMPC–substrate cross peak volumes are plotted in the order of increasing distance from the hydrophobic core of the membrane.
- Figure 6.9** Using the single mixing time analysis, normalized DMPC/DMPG–substrate cross peak volumes are plotted in the order of increasing distance from the hydrophobic core of the membrane
- Figure 6.10** Comparison of chemical shifts and location profiles of doxorubicin and chloramphenicol buffered at pH 7.4 and pH 8.5 and in pure deuterated water.
- Figure 6.11** Drugs are proposed to enter the protein from the membrane interface region.
- Appendix 1** ^{19}F CPMAS of purple membrane M163C mutant labeled with 3-bromo-1, 1, 1-trifluoro-aceton (BTA), and of control lipid vesicles resuspended in BTA and spinned down for NMR measurement.
- Figure 1**
- Appendix 2** The ^{31}P static spectra of PC/PG liposomes: free, reconstituted leupeptin, and
- Figure 2** reconstituted LmrA.

Contents

Summary	5
Zusammenfassung	7
Acknowledgements	9
Abbreviations	10
List of Figures	12
1. Introduction	21
1.1 Multidrug resistance transporters	21
1.1.1. MDR phenomenon	21
1.1.2. Families of MDR transporters	23
1.1.3. MDR transporters of the ABC family	25
1.1.4. Structure investigations on ABC transporters	26
1.1.5. Conformational changes during substrate binding and transport	30
1.2. LmrA – a bacterial ABC MDR transporter as a model of P-glycoprotein	34
1.3. Solid-State NMR	41
1.3.1. Chemical shift	42
1.3.2. Dipolar coupling	44
1.3.3. Quadrupolar coupling	46
1.4. Spectral resolution in solid-state NMR	48
1.4.1. Magic-angle spinning	48
1.4.2. Cross polarization	49
1.4.3. Decoupling techniques	52
1.4.4. Recoupling techniques	55
1.5. Solid-state NMR in application to membrane transporters	58

Aims of the thesis	59
2. Development of defined media for isotope labelling of LmrA from <i>Lactococcus lactis</i>	61
2.1. Introduction	61
2.2. Materials and methods	64
2.2.1. Optimization of defined media composition	64
2.2.2. Metabolic labelling of LmrA ISOVs with ¹³ C labeled amino acids	67
2.2.3. Attempts to enhance protein yield and labelling efficiency	68
2.3. Results	69
2.3.1. Optimization of defined media composition	69
2.3.2. Metabolic labelling of LmrA ISOVs with ¹³ C labeled amino acids	72
2.3.3. Attempts to enhance protein yield and labelling efficiency	73
2.4. Discussion	78
2.4.1. Optimization of defined media composition	78
2.4.2. Metabolic labelling of LmrA ISOVs with ¹³ C labeled amino acids	81
2.4.3. Attempts to enhance protein yield and labelling efficiency	81
Conclusion	83
3. Purification and reconstitution of LmrA in various lipids for solid-state NMR	85
3.1. Introduction	85
3.2. Materials and methods	89
3.2.1. Solubilization and purification of LmrA	89
3.2.2. Reconstitution of LmrA	90
3.3. Results	92
3.3.1. Solubilization and purification of LmrA	92
3.3.2. Reconstitution of LmrA	93

3.4.	Discussion	102
3.4.1.	Solubilization and purification of LmrA	102
3.4.2.	Reconstitution of LmrA	103
	Conclusion	106
4.	LmrA dynamics as studied by deuterium NMR line shape analysis and relaxation measurements	109
4.1.	Introduction	109
4.2.	Materials and methods	111
4.3.	Results	115
4.4.	Discussion	123
	Conclusion	131
5.	Ligand binding to LmrA as observed by fluorescence and solid-state NMR spectroscopy	133
5.1.	Introduction	133
5.2.	Materials and methods	138
5.2.1.	LmrA tryptophan intrinsic fluorescence quenching with various substrates	138
5.2.2	¹⁹ F and ³¹ P SSNMR SSNMR measurements of substrates bound to LmrA	139
5.2.3	Modulation of Hoechst-33343 LmrA transport and ATPase LmrA activity by leupeptin	140
5.3.	Results	140
5.3.1.	LmrA tryptophan intrinsic fluorescence quenching with norfloxacin and vinblastine	140
5.3.2	¹⁹ F SSNMR on norfloxacin bound to LmrA	142
5.3.3	LmrA tryptophan fluorescence quenching with TPP ⁺	143
5.3.4	³¹ P SSNMR on TPP ⁺ bound to LmrA	144
5.3.5	Modulation of Hoechst-33343 LmrA transport and ATPase LmrA activity by leupeptin	147

5.4.	Discussion	149
5.4.1.	LmrA tryptophan intrinsic fluorescence quenching with norfloxacin and vinblastine	149
5.4.2	¹⁹ F SSNMR on norfloxacin bound to LmrA	152
5.4.3	LmrA tryptophan fluorescence quenching with TPP ⁺	152
5.4.4	³¹ P SSNMR on TPP ⁺ bound to LmrA	153
5.4.5	Modulation of Hoechst 33343-LmrA transport and ATPase LmrA activity by leupeptin	154
	Conclusion	155
6.	The localization of multidrug transporters substrates within the model membrane by ¹H MAS NMR	159
6.1.	Introduction	159
6.2.	Materials and methods	163
6.3.	Results	165
6.4.	Discussion	173
	Conclusion	178
	Outlook	179
	Appendix 1	180
	Appendix 2	183
	Literature	186
	Zusammenfassung	214
	Lebenslauf	221
	Publications	222
	List of conference contributions and talks	223

1. Introduction

1.1. Multidrug resistance transporters

1.1.1. MDR phenomenon

Multidrug resistance (MDR) is typically defined as the ability of a living cell to show resistance to a wide variety of structurally and functionally unrelated compounds. In mammals, tumours, which are initially sensitive to cytotoxic agents, often develop resistance to a broad spectrum of structurally unrelated drugs. The widespread occurrence of MDR in tumour cells represents a major impediment to successful cancer chemotherapy. MDR has evolved as a protective mechanism whereby bacterial or tumor cells survive initial treatment and develop resistance against several structurally unrelated classes of compounds.

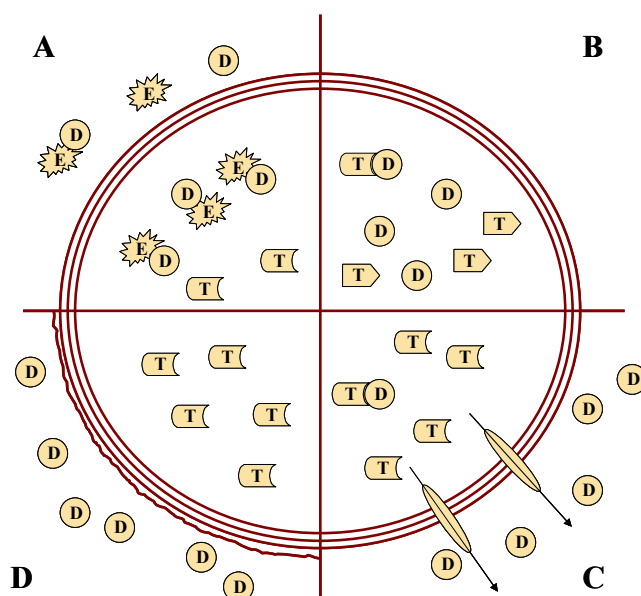


Figure 1.1: Drug resistance mechanisms of various origins: A) enzymatic (E) degradation or modification of drug (D); B) alteration of the drug target (T); C) active extrusion of drugs by transport proteins; D) prevention of drug entry.

The primary mechanisms that give rise to MDR include: (1) modification of drugs, and hence their inactivation, by enzymes of the target cell; (2) alteration of the cellular target through mutation or

post-translation modification; (3) in bacteria, increased cell wall and outer membrane impermeability to drugs, which can be further amplified by the loss of one or more porins, and (4) active efflux transporters (Brennan, 2001) (Figure 1.1).

Analysis of available genome sequences of various bacteria revealed that known and putative drug efflux transporters constitute between 6 % to 20 % of all transporters (Paulsen et al., 1998). In the genome of *E. coli* and *Saccharomyces cerevisiae* about 15-20 % of the genome may code for this type of proteins (Van Bambeke *et al.*, 2003). A growing number of studies demonstrate that resistance to almost any antibiotic could be achieved through the activity of multidrug efflux pumps (Kumar and Schweizer, 2005; Paulsen, 2003; Blackmore *et al.*, 2001). However, the connection between drug efflux and clinical examples of MDR is still not clear. Generally speaking, wild type expression of MDR pumps provides moderate increase in IC₅₀ (the concentration of an inhibitor that is required for 50% inhibition of an enzyme in vivo), which puts a question mark on their clinical relevance (Lynch and Martinez, 2002; Mazzariol et al., 2000). However, the concomitant expression of several efflux pumps has been shown to lead to apparently 'high level' resistance phenotypes (Van Bambeke *et al.*, 2003). There can be multiple reasons why these 'high level' resistance phenotypes appear. The first reason is the exposure of the targets to insufficient drug concentrations. The second reason is the ability of antibiotics to serve as inducers and regulators of some efflux pumps gene transcription or mRNA translation (treatment with rifampicin induces both cytochrome P450 and MDR expression in human whilst erythromycin, tetracycline and aminoglycosides lead to MexXY expression in *P. aeruginosa* (Li et al., 2000; Masuda et al., 2000; Roberts, 1996; Hebert et al., 1992)). The third reason for concomitant MDR pumps overexpression is dissemination. In several classes, the genetic elements encoding MDR pumps and their regulators are located on plasmids (such as Tet transporters in Gram-positive bacteria), or on conjugative or transformable transposons located either on plasmids (Tet transporters also, in Gram-negative bacteria), or on the chromosome (mef genes in *Streptococcus pneumoniae*) (Del Grosso et al., 2002).

So far, MDR transporters are found in almost every cell from bacteria to human. MDR has been reported in gram-negative bacteria including *E. coli*, *S. typhimurium* and *Klebsiella pneumoniae*, in gram-positive bacteria such as *Listeria monocytogenes*, *Staphylococcus aureus*, *Streptococcus*

pneumonia (van Veen *et al.*, 1998a). Besides bacteria, parasitic protozoa are also responsible for some of the most devastating and prevalent diseases of humans and domestic animals, such as malaria (*Plasmodium* spp.), mucocutaneous and visceral leishmaniasis (*Leishmania* spp.), African sleeping sickness (*Trypanosoma brucei gambiense*, *Trypanosoma brucei rhodensiense*), South-American Chagas' disease (*Trypanosome cruzi*), amoebic dysentery (*Entamoeba* spp.), and toxoplasmosis (*Toxoplasma* spp.) (van Veen *et al.*, 1998).

1.1.2. Families of MDR transporters

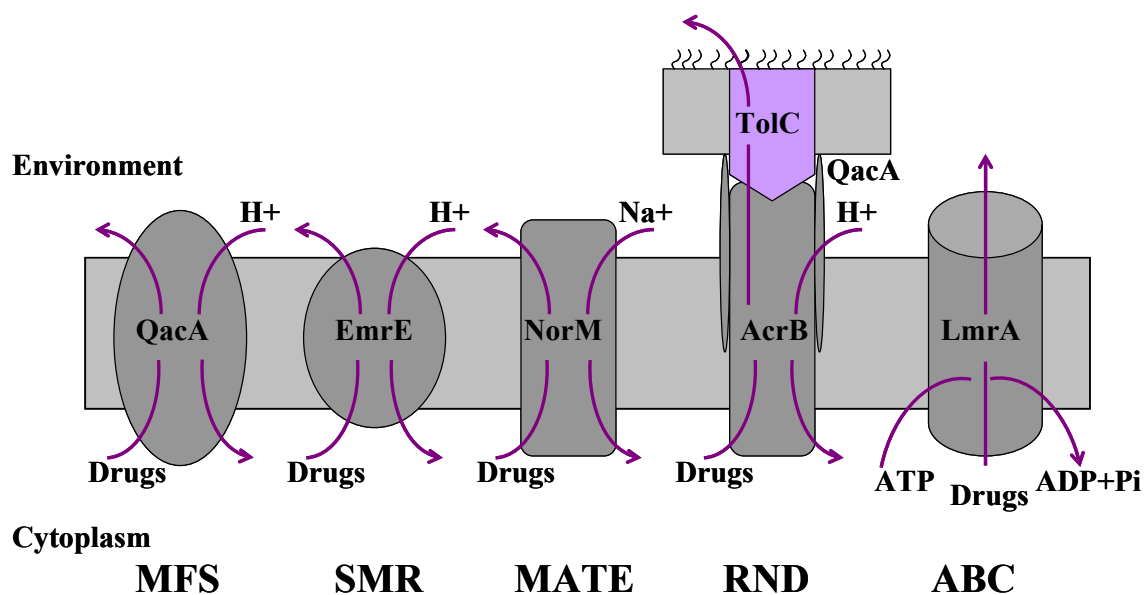


Figure 1.2: Representative members of the five characterized families of MDR transporters: the ATP-binding cassette superfamily (ABC), the resistance/nodulation/cell division family (RND), the multidrug and toxic compound family (MATE), the small multidrug transporter family (SMR), and the major facilitator superfamily (MFS).

The families of MDR transporter include some members of the ATP binding cassette (ABC) transporters family which couple the hydrolysis of ATP to drug efflux, and five families of proteins, which use the proton motive force (pmf) to expel drugs primarily through drug:proton antiport. The latter include the major facilitator superfamily (MFS), resistance/modulation/division (RND), drug/metabolite transporters (DMT) and multi antimicrobial extrusion (MATE) proteins (Brennan, 2001) (Figure 1.2, Table 1.1). A newly discovered superfamily, the multidrug endosomal transporters (MET), which is limited to the endosomal, late Golgi and lysosomal membranes has also been

described (Kumar and Schweizer, 2005).

Multidrug efflux systems for gram-positive, gram-negative bacteria and eukaryotes are quite different. In gram-negative bacteria each efflux pump consists of three components: the inner membrane (IM) transporter, the outer membrane (OM) channel and the periplasmic accessory lipoprotein (Zgurskaya and Nikaido, 2000). In this arrangement, efflux complexes transverse both, the inner and the outer membranes and thus facilitate direct passage of the substrate from the cytoplasm or the cytoplasmic membrane into the external medium. Direct efflux of drugs into the medium is advantageous for gram-negative bacteria because, in order to come in again, the expelled drug molecules must cross the physical barrier that is the OM. The synergetic function of transporters and membrane barrier explains hypersusceptibility of gram-negative bacteria to various drugs. MDR pumps from gram-negative bacteria belong to several families of transporters (Nikaido, 2001).

Family	Selected representatives	Organism	References
MFS	Bmr LmrP MdfA QuacA	<i>Bacillus subtilis</i> <i>Lactococcus lactis</i> <i>Escherichia coli</i> <i>Staphylococcus aureus</i>	(Neyfakh, 2002) (Bolhuis <i>et al.</i> , 1996c) (Edgar and Bibi, 1999) (Mitchell <i>et al.</i> , 1999)
SMR	EmrE QacE YkkC, YkkD	<i>Escherichia coli</i> Gram-negative bacteria <i>Bacillus subtilis</i>	(Rotem and Schuldiner, 2004) (Paulsen, 2003) (Jack <i>et al.</i> , 2000)
RND	AcrB MexB YhiV	<i>Escherichia coli</i> <i>Pseudomonas aeruginosa</i> <i>Escherichia coli</i>	(Murakami <i>et al.</i> , 2002) (Poole <i>et al.</i> , 1993) (Ma <i>et al.</i> , 1995)
MATE	NorM YdhE	<i>Vibrio parahaemolyticus</i> <i>Escherichia coli</i>	(Brown <i>et al.</i> , 1999) (Brown <i>et al.</i> , 1999)
ABC	LmrA PGP	<i>Lactococcus lactis</i> <i>Humans</i>	(van Veen <i>et al.</i> , 1996) (Higgins, 1992)

Table 1.1: Multidrug transporter families.

However, most of the efflux transporters that mediate resistance to relevant antibiotics belong to the resistance/nodulation/cell division family (RND). The best studied drug transporter complexes from gram-negative bacteria are AcrA-AcrB-TolC of *E. coli* and MexB-OprM of *P. aeruginosa* (Zgurskaya and Nikaido, 2000). They pump mostly lipophilic and amphiphilic compounds, including antibiotics, heavy metals, dyes, detergents, and solvents (Nikaido, 1996).

Gram-positive bacteria lack the outer membrane and therefore rely mostly on expression of MDR pumps in order to protect themselves against multiple drugs. Gram-positive bacteria MDR pumps belong to at least three unrelated families: MFS, SMR, and ABC. According to substrate-specificity they can be subdivided into macrolide-specific (MefE, MefA), tetracycline-specific (TetK, TetL, and TetZ), and polyspecific (LmrA, LmrP) (Markham and Neyfakh, 2001).

At present all known MDR transporters in eukaryotes belong to ABC family. The first described and the best characterized MDR ABC transporter in humans is P-glycoprotein (PGP). It provides resistance to a broad spectrum of compounds including anticancer chemotherapeutic agents (Ambudkar *et al.*, 1999).

1.1.3. MDR transporters of the ABC family

ABC transporters have four core domains. Two transmembrane domains (TMDs) each consist of multiple membrane spanning α -helices, which together form the pathway for substrates, crosses the lipid bilayer. Two nucleotide binding domains (NBDs) contain the ATP binding sites and couple conformational changes induced by ATP binding, ATP hydrolysis and ADP release to the transport process (Higgins, 1986a).

The ABC transporters family is large and diverse. What ties the family together is a number of highly conserved ABC cassette motifs, many of which are directly involved in the binding and hydrolysis of ATP (Geourjon *et al.*, 2001). These conserved motifs are P-loop or Walker-A motif (GXXGXGKST, X denotes any amino acid), the Walker-B motif (hhhhD, h any hydrophobic amino acid), a glutamate residue in the Q-loop, and a histidine residue in the switch region. In addition, ABC cassettes invariably possess a D-loop with a short polypeptide stretch (...LSGG...), which is specific for all ABC cassettes. It is often referred as the 'ABC signature sequence'. In general, NBD can be divided

into domain 1 (the catalytic domain, containing the Walker A and B motifs) and domain 2 (the so called signaling domain, containing the signature motif) (Figure 1.4).

One of the best characterized MDR ABC transporter is undoubtedly P-glycoprotein and it is considered as a framework for the whole ABC MDR family. Therefore, the whole upcoming discussion will be held in relation to PGP.

1.1.4. Structure investigations on ABC transporters

Structure investigations of full length ABC transporters

Membrane proteins are notoriously recalcitrant to purification and crystallization. Despite this, considerable progress has been achieved in structural analyses of ABC transporters. The past five years have seen several structures of the ABC transporter MsbA (Reyes and Chang, 2005; Chang, 2003a; Chang and Roth, 2001) and the structure of BtuCD transporter of *E. coli* (Figure 1.3). Additionally, the low resolution structures of PGP up to 8 Å, TAP at 35 Å, 22 Å MRP1, 20 Å CFTR, and YvcC at 25 Å are available (Rosenberg et al., 2005; Rosenberg et al., 2004; Chami et al., 2002; Lee et al., 2002; Rosenberg et al., 2001a; Rosenberg et al., 2001b; Rosenberg et al., 1997).

The low (25 Å, single particle analysis) and medium (8-10 Å, electron microscopy) resolution structures showed that PGP has a shape of a cylinder, 10 nm in diameter and about 8 nm high. About half of the molecule resides in the membrane. The α -helices span the membrane a total of 12 times and organized in two TMDs. In the nucleotide bound state five of the α -helices from each TMD are related by a pseudo-two-fold symmetry, whilst the sixth breaks the symmetry (Rosenberg et al., 2005). TMDs form an aqueous chamber in the membrane, open at the cytoplasmic leaflet. Gaps between two TMDs appear to form side-entrance into the chamber from the lipid phase, which may permit access of substrate to the chamber. Hydrophilic intracytoplasmic domains (ICDs) of the TMDs were observed at a resolution of 8 Å, which interact directly with NBDs. At the resolutions available for PGP not much can be concluded about NBDs arrangement. However, both structures of the

MJ0796 and the BtuCD NBDs can be modeled into PGP 3D structure obtained from 2D crystals (Rosenberg et al., 2005).

The first MsbA (from *E. coli*) structure was solved in the absence of substrate and nucleotide. It shows a chamber in the membrane formed by two MsbA monomers (Figure 1.3 A). The α -helices of this chamber are arranged in the way so that chamber is open ($\sim 25\text{\AA}$) to the cytoplasmic side of the membrane. NBDs are placed relatively far from each other. TMDs are connected to NBDs by extensive helical intracellular regions (ICDs). In general, it is difficult to make any conclusions about NBDs organization, because the N-terminal region (residues 341-418) is not visible. So, the exact role and position of NBDs are obscure (Chang and Roth, 2001).

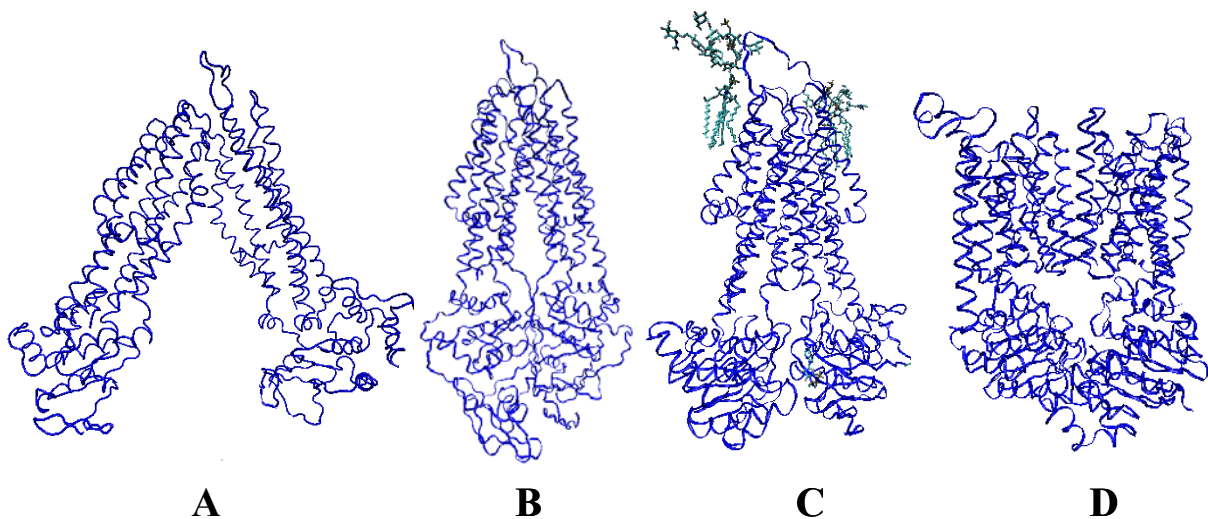


Figure 1.3: Structures of MsbA and BtuCD. Views of MsbA in the open (A) and closed (B) conformation, and LPS and ATP bound (C), and of BtuCD (D). The picture is made in VMD (Humphrey, W., Dalke, A. and Schulten, K., "VMD - Visual Molecular Dynamics", J. Molec. Graphics, 1996, vol. 14, pp. 33-38).

The MsbA from *Vibrio cholera* was crystallized in the closed apo conformation (Figure 1.3 B). In this structure both the TMDs and NBDs are closely packed, a large internal chamber accessible from cytoplasm is formed between the interacting TMDs (Chang, 2003a).

The crystal structure of MsbA of *S. typhimurium* was solved in complex with Mg·ADP·Vanadate and LPS (Figure 1.3 C). This structure when compared to closed MsbA structure exhibits a large rigid-body rotation and translation that result in a $\sim 15\text{\AA}$ opening toward the periplasmic ends and a $\sim 15\text{\AA}$ closing of the NBD-associated ICD helices, which allow a chamber accessibility from the periplasm

but not from cytoplasm (Chang, 2003a). Additionally, in this latest MsbA structure, the bound LPS is seen on the outer membrane leaflet side. Interestingly, several conserved residues between MsbA and PGP map to the binding interface of the LPS, which suggests that this region could be a general binding site for other amphipathic compounds (Chang, 2003a). One more remarkable feature of this MsbA crystal structure is the NBDs architecture. It is better resolved in contrast to both early solved MsbA structures and its organization reminiscent of the dimer sandwich structures of the ABC transporter BtuCD and MJ0796 (Chang, 2003a).

The three structures suggest significant helices tilting movement of the TMDs during the substrate transport, allowing accessibility to an internal chamber from the periplasm but not from the cytoplasm. This ‘tilting’ may impose a large amount of physical stress on both leaflets of the membrane and even require lipid reorganization to counterbalance the different space requirements of MsbA during the catalytic cycle (Schmitt, 2002). Interestingly, this arrangement of MsbA α -helices is consistent with site-directed spin labelling electron paramagnetic studies (EPR) (Dong et al., 2005; Buchaklian et al., 2004) on MsbA and inconsistent with PGP structures at low and medium resolution as well as with in vivo cross-linking data for the TMDs of PGP (Loo *et al.*, 2003). These differences can reflect different conformation stages, different transport cycles (MsbA is a lipid flippase), or be an artifact of crystallization. Moreover, it has been proposed that the dimer interface has been wrongly observed and by the counter-clockwise rotation of both MsbA monomers the *spiral* MsbA has been obtained. This *spiral* MsbA dimer exhibits an interface between the two NBDs identical to that observed in BtuCD, the DNA repair protein Rad50, the homodimeric NBD of ABC transporter MJ0796. Additionally, the packing of TM helices and distances between the membrane spanning helices like in *spiral* MsbA similar to arrangement in PGP (Shilling et al., 2003).

The *E. coli* BtuCD structure is different from all other available MsbA structures (Figure 1.3 D). All 20 (not 12 like in MsbA, and PGP) BtuCD α -helices form the translocation pathway through the membrane that is closed to the cytoplasm by a gate region. The TMD helices tight packing reminiscent the one shown by multiple cross-linking studies on PGP (Loo and Clarke, 2005). Consequently, the NBDs of BtuCD are not separated; they are in contact with each other. In contrast to MsbA and PGP, no ICD was identified in BtuCD and the NBDs are in direct contact with the

TMDs via a cytoplasmic loop, which located between TM helices 6 and 7. The overall fold of ABC domain in BtuCD resembles that of HisP, MalK, TAP1, MJ1267, MJ0796, and the DNA repair enzyme Rad50 (Locher et al., 2002). The core consists of a six-stranded β -sheet that is surrounded by nine α -helices, and a peripheral, three-stranded β -sheet. Each BtuCD ABC domain contains the nucleotide bound at the dimer interface between ABC signature motif of one subunit and the P-loop of the other. At present, the BtuCD structure is considered as a framework for ABC family, whereas MsbA ‘open’ conformation structure is under debates. However, one should keep in mind that MsbA has the highest end-to-end sequence similarity with PGP and LmrA, whereas BtuCD has sequence similarity with these two MDR ABC transporters only in the NBDs.

Structure investigations of the isolated nucleotide binding domains

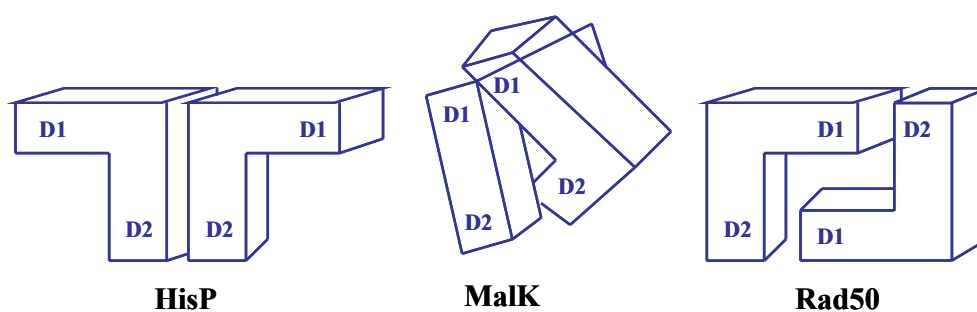


Figure 1.4: NBDs association models. D1 and D2 are two domains of each ATP binding cassette.

The first high resolution structure of an ABC domain – HisP, the NBD of histidine permease – was reported in 1998 (Hung et al., 1998). It shows a dimeric organization of HisP with a ‘back-to-back’ orientation. The dimer interface was formed by the outer β strand of domain 2 (D2), the ATP-binding sites are exposed, and the signature motifs were far away to interact with the bound nucleotide. The X-ray structure of Rad50, a DNA repair enzyme, shows different dimeric organization. The nucleotide-binding site in Rad50 is located in the dimeric interface and formed by the Walker A motif in monomer 1 and the C-loop of monomer 2, which resulted in a ‘head-to-tail’ orientation (Hopfner et al., 2000). One more dimer orientation has been shown for the ABC domain of MalK from *Thermococcus litoralis* (Diederichs et al., 2000). Here, the interface adopted a ‘head-to-head’ orientation, with the largest amount of buried surface area (Figure 1.4).

The following years brought a few more X-ray structures of other ABC domains (Karcher et al., 2005; Lewis et al., 2004; Schmitt et al., 2003; Gaudet and Wiley, 2001; Karpowich et al., 2001; Yuan et al., 2001). So, in the crystal structure of a putative ABC domain MJ1267 of *M. janaschii* and RLI ABC ATPase RNase-L inhibitor of *P. furiosus*, the NBDs adopted a dimer interface that is identical to the one in Rad50 (Karcher et al., 2005; Smith et al., 2002). This NBDs organization is supported by biochemical data obtained for MalK (Fetsch and Davidson, 2002). Thus, it seems to be established that each monomer of ABC domain participate in ATP binding and sensing, thereby forming a dimer interface with a head-to-tail orientation (Schmitt and Tampe, 2002).

A large body of biochemical studies, and computer simulations clearly demonstrated that ATP binding initiates NBDs dimerization (Zaitseva et al., 2005; Oloo and Tieleman, 2004). Interestingly, recent studies on MalK have shown that ATP promotes dimerization, whereas ADP does not (Lu et al., 2005). The dimerization process seems to have two components. First, ATP binding to Walker A/B and Q loop motifs reorients the domain 1 and 2. Second, recognition of the ATP γ -phosphates by the signature motifs from the opposing NBD induces a clamp-like motion in the NBD to form a tight NBD-ATP-NBD sandwich (Karcher et al., 2005). However, whilst deriving the general model for NBDs dimerization, care should be taken, because ATPases from different families might have different dimerization mechanisms.

At which stage of ABC domain catalytic cycle, nucleotide or nucleotides are hydrolyzed, is currently a matter of debate. Two models have been proposed. In the progressive clamp model, both nucleotides in the dimer are hydrolyzed, and the NBDs dissociate before reloading the ATP. In the alternative catalytic site model, hydrolysis occurs in the first catalytic site, followed by opening of this domain while the second catalytic site remains closed. After reloading of ATP in the first site, this site is closed, and hydrolysis takes place in the second catalytic site (for review see (van der Does and Tampe, 2004)).

1.1.5. Conformational changes during substrate binding and transport

Mechanism of ABC transporters is a puzzle despite a number of exhaustive studies performed by biochemists and structural biologists. Due to similarities in NBDs of different transporters, it is

generally accepted that all ABC cassettes bind and hydrolyze ATP in a similar fashion and therefore use a common mechanism to power the translocation of substrate through the membrane. Our understanding of mechanisms of ABC transporters function originates from the low resolution structures of PGP obtained at several conformation stages supported by a number of biochemical assays. Analysis of the two-dimensional crystals by cryo-electron microscopy revealed that major conformation changes within TMDs occur upon ATP binding, which significantly reduces the affinity for drug binding and opens a central pore along its length. These conformation changes can, potentially, facilitate movement of hydrophobic compounds from the lipid bilayer to the aqueous pore of the transporter (Rosenberg et al., 2003; Rosenberg et al., 2001b). Recently, the opening of ion channel in the TMDs was directly linked to NBDs dimerization using single-channel recording electrophysiological method on intact cystic fibrosis conductance regulator (CFTR) from the ABC family (Vergani et al., 2005).

Biochemically, the putative conformation changes of PGP have been studied extensively via cysteine-scanning approach combined with oxidative cross-linking by Loo and Clarke. They have determined that the major conformation changes take place in TM 6, 11, 12 (Loo *et al.*, 2003). Intrinsic fluorescence and MANS quenching approaches have been used as an indication of conformation changes for PGP (Sharom et al., 2001) and LmrA (Vigano *et al.*, 2002).

On the bases of the limited structural information and the extensive available biochemical data two models of the ABC transporters mechanism were generated (Figure 1.5). The two-cylinder model and ATP switch model (Higgins and Linton, 2004; van Veen *et al.*, 2000a). In the two-cylinder model proposed for LmrA, there is no transfer of substrate from one site to another; rather, substrate is translocated while bound to a single site whose affinity and orientation changes as a result of ATP hydrolysis. For PGP it has been proposed that drug initially binds to one side near cytoplasmic surface and transferred to a second (release) site when affinity of the first site is reduced as a result of ATP hydrolysis (Ramachandra et al., 1998; Dey et al., 1997). In any case, the power stroke for substrate translocation is provided by ATP hydrolysis. In contrast, the ATP switch model suggests the transport is initiated by substrate binding by facilitating ATP-dependant closed dimer formation. In the next step substrate release occurs followed by ATP hydrolysis aiming to restore transporter resting

Key questions:

Although the large body of data on structural and functional aspects of ABC MDR transporters in general and on PGP in particular are accumulated, there are still many questions remain unclear. Among those questions are 1) what is a nature of substrate and ATP binding, 2) how many ATP molecules are hydrolyzed per transport of one substrate molecule, 3) how the conformation changes are transferred from NBDs to TMDs and the other way round, 4) what is a sequence in a transport cycle, and 5) how the transport cycle is regulated. In addition, crystal structures of ABC MDR transporter in open and closed states, as well with bound substrate are awaited to be determined.

Mammalian proteins are hard to work on and it is often difficult to produce sufficient amount of material not only for crystallization trials but even for biochemical investigation. Therefore, a convenient model system to perform structural and functional investigation is a bacterial ABC MDR transporter like LmrA.

1.2. LmrA—a bacterial ABC MDR transporter as a model of P-glycoprotein

At present, several different MDR-like transport systems in *L. lactis* strain MG1363 are known. These MDR transport systems vary in substrate specificity (anionic versus cationic substrates), and in their mode of energy coupling to drug transport (pmf – versus ATP-dependant). The secondary MDR transporter of *L. lactis* strain MG1363 is LmrP from MFS family. The ABC family in *L. lactis* strain MG1363 is represented by LmrA, the first identified bacterial MDR ABC transporter, and very recently described LmrCD (Lubelski *et al.*, 2006; Lubelski *et al.*, 2004; van Veen *et al.*, 1996). LmrCD is a first known ABC MDR transporter with a heterodimeric composition. Interestingly, in LmrCD not only TMDs but also NBDs are structurally and functionally distinct (Lubelski *et al.*, 2006). A homologue of LmrA was found in a bacteriocin LsbA and LsbB producing strain of *L. lactis* (Mazurkiewicz *et al.*, 2005). Evidence exists that *L. lactis* strain MG1363 also possesses anion transporter and anion-conjugate transporter (Mazurkiewicz *et al.*, 2005; Yokota *et al.*, 2000).

LmrA, a 590-amino acids MDR transporter, belongs to the ABC family. LmrA confers resistance to several natural and synthetic chemotherapeutic drugs (Table 1.2). LmrA shares significant sequence similarity with the human MDR protein PGP (34 % identity and an additional 16 % similarity (van Veen *et al.*, 1996)) and the lipid flippase MsbA from *E. coli* (28 % overall sequence identity (Chang and Roth, 2001)) (Figure 1.7). PGP and LmrA substrate specificity overlap remarkably. Moreover, LmrA, when expressed into insect and human lung fibroblast cells, is able to functionally complement PGP. LmrA is not only properly targeted to the plasma membrane but also confers multiple resistances in the human cells (van Veen *et al.*, 1998b).

The homodimeric organization of LmrA transporter has been shown by the experiments on dominant-negative mutants mixed with wild-type protein (van Veen *et al.*, 2000a). Each monomer in LmrA consists on six membrane spanning regions (putative α -helices) in the amino-terminal hydrophobic domain, followed by large hydrophilic domain containing ATP-binding site (van Veen *et al.*, 1996) (Figure 1.6 - 1.8). The α -helical organization of TMDs has been determined by cystein scanning mutagenesis and Attenuated Total Reflection Fourier Transform Infrared spectroscopy (ATR-FTIR) studies (Poelarends and Konings, 2002; Grimard *et al.*, 2001). Additionally, $^1\text{H}/^2\text{H}$ exchange ATR-

FTIR experiments revealed fast exchange implying that the transmembrane helical segments of LmrA are more flexible and accessible than any segments described before in the literature. This points out to large translation and rotation movements of the certain segments of transmembrane helices (Grimard *et al.*, 2001). Electron microscopy analysis of purified and reconstituted LmrA revealed small, uniform particles with a diameter of 8.5 nm by 5 nm, similar to that previously observed for PGP (Poolman, unpublished results).

Class	Antibiotic	Increased resistance (fold)
Aminoglycosides	Gentamicin	2
	Kanamycin	3
β -Lactams	Ampicillin	2
	Ceftazidime	3
	Meropenem	1
	Penicillin	4
Glycopeptides	Vancomycin	1
Lincosamides	Clindamycin	14
Macrolides	Azithromycin	33
	Clarithromycin	23
	Dirithromycin	264
	Erythromycin	53
	Roxithromycin	35
	Spiramycin	35
Quinolones	Ciprofloxacin	2
	Ofloxacin	4
Streptogramins	Dalfopristin	163
	Quinupristin	31
	RP59500	55
Tetracyclines	Chlortetracycline	28
	Demeclocycline	12
	Minocycline	138
	Oxytetracycline	8
	Tetracycline	14
Others	Chloramphenicol	11
	Trimethoprim	1

Table 1.2: Effect of LmrA expression on the resistance to antibiotics of *E. coli* CS1562, which is hypersensitive to drugs due to a deficiency of the TolC porin. Data obtained from (Putman *et al.*, 2000).

On the basis of available crystal structures of *V. cholera* MsbA and monomeric TAP1, Ecker and co-workers have built a homology model of LmrA. In this model, the TMDs are predicted to form a helical bundle, which lines a central aqueous pore open to the extracellular space. The central pore is lined by TM helices 1, 3, 5, and 6 of each monomer. TM helices 2 and 4 are shielded from the aqueous environment by other helices (Ecker *et al.*, 2004; Pleban *et al.*, 2004) (Figure 1.6).

Using several analogues of the fluorescent membrane probe diphenyl-hexatrien (DPH), it has been shown that LmrA preferably transports cationic derivatives of DPH, whereas neutral and anionic DPH derivatives are not transported (Bolhuis *et al.*, 1996a). This rule, however, is not strict to neutral substrates. LmrA as well as PGP can recognize a neutral acetoxymethyl ester derivative of 2', 7'-bis-(2-carboxyethyl)-5-(and-6)-caboxyfluorescein (BCECF-AM) (Bolhuis *et al.*, 1996a; Homolya *et al.*, 1993). Based on the kinetics of the extrusion of 1-[4-(trimethylamino)phenyl]-6-phenylhexa-1,3,5-triene (TMA-DPH) by LmrA, it has been concluded that drugs enter the protein from the inner membrane leaflet and are transported to the exterior (Bolhuis *et al.*, 1996a).

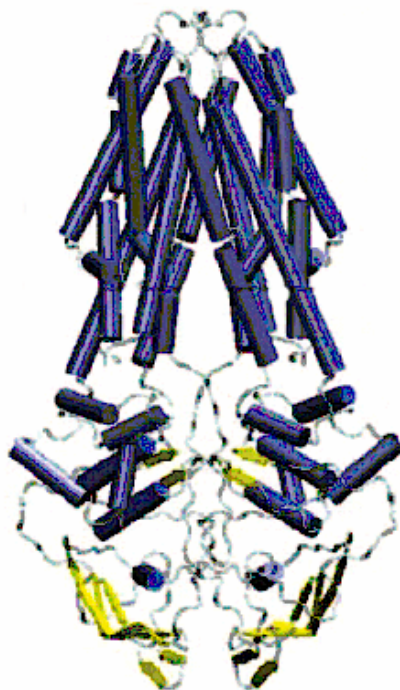


Figure 1.6: 3D atomic model of LmrA generated by the software package Insight II, using *V. cholera* MsbA (Ecker *et al.*, 2004).

human PGP. The last residue in each row is numbered. The roman numbers refer to the predicted transmembrane α -helices of PGP. The ABC signature sequence and Walker A and B motifs are indicated. Different types of residues are highlighted with different colors, subsequently, acidic with blue, basic with magenta, hydroxyl, amine, basic-Q with green, small, hydrophobic with red, and others with grey. In alignment the following symbols denote the degree of conservation observed in each column: * - residues are identical in all sequences; - conserved substitutions have been observed, according to the colors above, . – semi-conserved substitutions are observed. Alignment is done with ClustalW (WWW Service at the European Bioinformatics Institute <http://www.ebi.ac.uk/clustalw>).

Two binding sites, with a low and high affinity, allosterically coupled, have been demonstrated for LmrA (van Veen *et al.*, 2000a). Only low-affinity, outside-facing binding site is accessible in the vanadate-trapped state (van Veen *et al.*, 2000a). On the basis of a detailed analysis of the LmrA drug binding sites, vinblastine equilibrium binding determinations, and photoaffinity labelling studies, an alternating two-site mechanism for drug transport was suggested. Accordingly to this model protein oscillates between two configurations, high-affinity, inside-facing, and low-affinity, outside facing (van Veen *et al.*, 2000a).

To generate a three-dimensional model of the substrate binding sites, LmrA in three different states (resting, with AMP-PNP, and ATP/ADP-Vanadate bound) were labeled with propafenone-type photoaffinity ligands, proteolytically degraded and analyzed using matrix-assisted laser desorption ionization/time of flight mass spectrometry. Data revealed that propafenones bind to LmrA in certain regions within TM helices 3, 5, and 6 for all three protein states, meaning that these helices 3, 5, and 6 are directly involved in drug binding and are accessible to the central cavity (Ecker *et al.*, 2004).

To obtain structural information of LmrA solute translocation pathway, a cysteine scanning mutagenesis approach has been applied. Cysteine mutations were introduced in each hydrophilic loop, and in TMD 6. In the next step their accessibilities were probed with fluorescein maleimide. The periodicity of cysteine accessibility showed that helix 6 has one face exposed to an aqueous cavity along its full length. Interestingly, cysteines in all loops external and internal were accessible to fluorescein maleimide. Taken all together it was concluded that under non-energized conditions the LmrA transporter forms an aqueous chamber within the membrane, which is open to the intracellular milieu (Poelarends and Konings, 2002).

Recently it has been reported that LmrA can operate not only in unidirectional fashion, like it is

accepted to be the case for ABC transporter family members, but can mediate reverse transport (uptake) of ethidium with an apparent K_t of 2.0 μM in presence of an inwardly directed drug concentration. In analogy to ‘traditional’ drug efflux, ethidium uptake can be competitively inhibited by the LmrA substrate vinblastine, and reduced under E314A and E512Q substitutions (Figure 1.8).

Moreover, under ATP-depleted conditions LmrA has been shown to play a direct role in the ATP synthesis reaction (Balakrishnan *et al.*, 2004). In the latter work, the same authors have further investigated the role of a conserved glutamate residue 314. It has been found that the transmembrane pH gradient has a dramatic influence on drug transport of E314D LmrA mutant. So, the active ethidium efflux by the E314D mutant of LmrA is hampered at pH 7.0 and can be almost rescued at pH 8 (Shilling *et al.*, 2005).

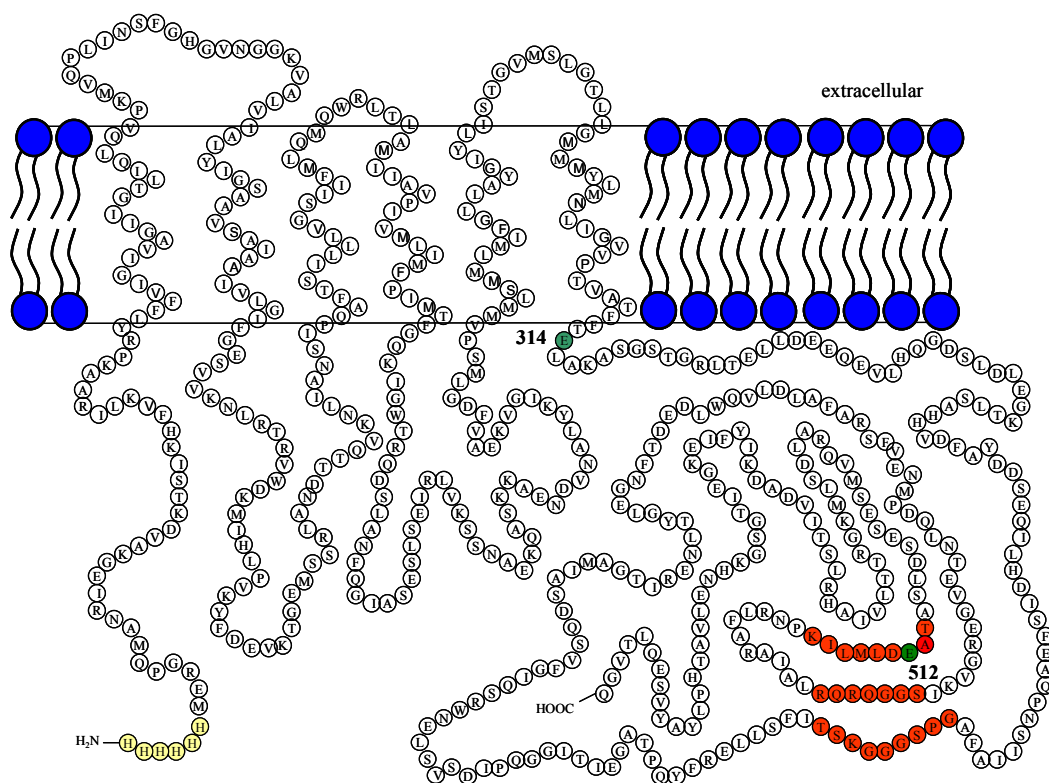


Figure 1.8: Topology model for LmrA (monomer). Conserved residues mentioned in the text are highlighted with green, His-tag with yellow, Walker A, B, and C-loop with red. Picture is adapted from U. Hellmich.

Additionally, it has been shown that LmrA-MD (LmrA mutant lacking NBDs) is able to mediate the uptake of ethidium in cells in co-transport with protons in a reaction driven by the $\Delta\Psi$ (interior

negative) and the transmembrane chemical proton gradient (ΔpH , interior alkaline) (Venter *et al.*, 2003). It has been suggested that glutamate 314 for LmrA plays a role similar to carboxylates in proton translocation by proton-motive force-dependent transporters and primary pumps (Shilling *et al.*, 2005; Abramson *et al.*, 2003; Yerushalmi and Schuldiner, 2000). So, its protonation and deprotonation somehow facilitates conformation changes enabling substrate transport (Shilling *et al.*, 2005). Moreover, it has been shown that LmrA mediated Hoechst-33342 transport is sensitive to uncouplers that collapse the proton gradient, and to *N,N'*-dicyclohexylcarbodiimide, an inhibitor of the F_0F_1 -ATPase (van Berg van Saparoea *et al.*, 2005).

In support to function similarities of LmrA to secondary transporters, a significant sequence similarity has been observed between LmrA and MexB, a secondary transporter from RND family. The shared sequence corresponds to a harpin region of two membrane-spanning helices and the connecting loop between these helices (Venter *et al.*, 2005).

In addition to drugs, LmrA reconstituted into *L. lactis* lipids can transport specific lipids, namely fluorescent phosphatidylethanolamine, but not of fluorescent phosphatidylcholine (Margolles *et al.*, 1999). Recently, it has been shown that LmrA displays an ATP-dependent $^{109}\text{Cd}^{2+}$ uptake stimulated by glutathione (Achard-Joris *et al.*, 2005).

Interestingly, the ABC transporter LmrA shares overlapping substrate specificity not only with PGP but with pmf-driven transporter of *L. lactis* LmrP (van Veen *et al.*, 2000b). The expression of LmrA and LmrP is thought to be up-regulated, because the energy-dependant drug extrusion can be facilitated by growing bacteria in the presence of increasing concentrations of toxic compounds (Mazurkiewicz *et al.*, 2005; Bolhuis *et al.*, 1994). Although, the physiological role of LmrA and LmrP is not known, they are vital for *L. lactis*: all attempts to delete both *lmrA* and *lmrP* transporters genes were unsuccessful. Moreover, the deletion of one of the MDR transporters led to increased expression of the other (Bolhuis *et al.*, 1994).

1.3. Solid-State NMR

The nuclear magnetic resonance history started in December 1945 when Torrey and Pound detected weak radiofrequency signals generated by the nuclei of atoms in ordinary matter, namely paraffin. Almost in the same time Bloch and Packard independently observed radio signals from the atomic nuclei in water. These experiments gave life to nuclear magnetic resonance (NMR) (Levitt, 2001).

These paragraphs briefly introduce the physical basis of the NMR phenomenon, emphasize difficulties faced by solid-state NMR and shortly explain the most common solid-state NMR (SSNMR) techniques.

Nuclei, when placed in a strong external static and uniform magnetic field, \mathbf{B}_0 , start to precess around \mathbf{B}_0 with Larmor frequency ω_0 , which is related to \mathbf{B}_0 by the following equation (Levitt, 2001):

$$[1] \quad \omega_0 = -\gamma \mathbf{B}_0,$$

where γ is the gyromagnetic ratio and is nucleus dependent, \mathbf{B}_0 is the applied magnetic field.

In the absence of a magnetic field, spins have different orientations with the same energy. Therefore net magnetization can not be detected. To create a net magnetization a strong magnetic field has to be applied. In this case the quantization axis for nuclei coincides with the applied field direction. However, magnetic fields created by nuclei wished to be observed is negligibly small compared with the static \mathbf{B}_0 field applied to create net magnetization. For this reason, another magnetic field is applied in direction perpendicular to \mathbf{B}_0 called radiofrequency pulse (RF). This RF pulse rotates net magnetization in the plane perpendicular to \mathbf{B}_0 , where it can be detected. Apart from the external applied magnetic fields described above, there are more sources of magnetic fields, which are internal to the sample. The most important of those are chemical shift anisotropy, dipole coupling and quadrupole coupling. To describe the motions and interactions of all the nuclei and all the electrons the Schrödinger equation [2] is used. The Hamiltonian operator in the Schrödinger equation involves all the interactions between these particles (Levitt, 2001).

$$[2] \quad d/dt | \Psi_{\text{full}}(t) \rangle = -i \hat{\mathbf{H}}_{\text{full}} | \Psi_{\text{full}}(t) \rangle,$$

where $\hat{\mathbf{H}}_{\text{full}}$ is the Hamiltonian of the system, $| \Psi_{\text{full}}(t) \rangle$ is a wave function containing information

about the positions, velocities, and spin states of all the electrons and nuclei.

Equation 2 is complete, but only partly relates to our experiment. Considering only those interactions which are important for NMR, namely nuclear spin state, the spin Hamiltonian can be presented as follows (Levitt, 2001):

$$[3] \quad d/dt | \Psi_{\text{spin}}(t) \rangle = -i \hat{\mathbf{H}}_{\text{spin}} | \Psi_{\text{spin}}(t) \rangle.$$

The nuclear spin Hamiltonian involves external ($\hat{\mathbf{H}}_{\text{ext}}(t)$), internal electric and magnetic interactions ($\hat{\mathbf{H}}_{\text{int}}(t)$). The external part of the spin Hamiltonian is (Levitt, 2001):

$$[4] \quad \hat{\mathbf{H}}_{\text{ext}}(t) = \hat{\mathbf{H}}_{\text{static}} + \hat{\mathbf{H}}_{\text{RF}}(t),$$

where $\hat{\mathbf{H}}_{\text{static}}$ is the interaction of each spin with the longitudinal static field \mathbf{B}_0 , and $\hat{\mathbf{H}}_{\text{RF}}$ is the interaction of each spin with the transverse radiofrequency field \mathbf{B}_{RF} . The internal spin Hamiltonian in diamagnetic substances contains following contributions: chemical shift terms, $\hat{\mathbf{H}}_{\text{CS}}(t)$, quadrupolar coupling, $\hat{\mathbf{H}}_{\text{Q}}(t)$, direct dipole-dipole, $\hat{\mathbf{H}}_{\text{DC}}(t)$, coupling, j-coupling, spin-rotation interactions (Levitt, 2001):

$$[5] \quad \hat{\mathbf{H}}_{\text{int}}(t) = \hat{\mathbf{H}}_{\text{CS}}(t) + \hat{\mathbf{H}}_{\text{DC}}(t) + \hat{\mathbf{H}}_{\text{Q}}(t).$$

1.3.1. Chemical shift

Each nucleus within the molecule is surrounded by electrons, which induce an additional magnetic field. This additional magnetic field contributes to the total field and therefore changes the nuclei resonance frequency. This frequency shift is called the chemical shift. The shielding interactions have two main components: diamagnetic (opposite to the applied field) and paramagnetic (supports the applied field). The chemical shift shielding Hamiltonian operator acting on a spin I has the following form (Duer, 2002):

$$[6] \quad \hat{\mathbf{H}}_{\text{CS}} = -\gamma \hbar \hat{\mathbf{I}} \cdot \boldsymbol{\sigma} \cdot \mathbf{B}_0,$$

where $\hat{\mathbf{I}}$ is a nuclei I spin operator, $\boldsymbol{\sigma}$ is a second-rank tensor, called the chemical shift tensor, and \mathbf{B}_0 is the applied magnetic field generating the electron current and as a result the shielding magnetic field. A second rank tensor $\boldsymbol{\sigma}$ is used to describe the shielding properties associated with a nucleus due to the electron distribution around it, because the size of the electron current around the field, and hence the size of the shielding depend on the orientation of the molecule within the applied field \mathbf{B}_0 .

The NMR spectrum is affected only by the symmetric part of the shielding tensor, and the coordinate system can be chosen in a way that the shielding tensor becomes diagonal. This axis frame is called the principal axis frame (PAF), or x^{PAF} , y^{PAF} , z^{PAF} (Figure 1.9). The numbers along the resulting diagonal of σ^{PAF} are the principal values, which can be expressed as the isotopic value σ_{ISO} , the anisotropy Δ_{CS} , and the asymmetry value η_{CS} (Duer, 2002):

$$\begin{aligned}
 [7] \quad \sigma_{\text{ISO}} &= 1/3 (\sigma^{\text{PAF}}_{\text{XX}} + \sigma^{\text{PAF}}_{\text{YY}} + \sigma^{\text{PAF}}_{\text{ZZ}}) \\
 \Delta_{\text{CS}} &= \sigma^{\text{PAF}}_{\text{ZZ}} - \sigma_{\text{ISO}} \\
 \eta_{\text{CS}} &= (\sigma^{\text{PAF}}_{\text{XX}} - \sigma^{\text{PAF}}_{\text{YY}}) / \Delta_{\text{CS}}.
 \end{aligned}$$

The frequency of the observed NMR signal is composed of the nucleus Larmor frequency, and a chemical shift contribution. Because of a shielding tensor axial symmetry, $\sigma^{\text{PAF}}_{\text{XX}} = \sigma^{\text{PAF}}_{\text{YY}}$ and $\eta_{\text{CS}} = 0$ through the polar angles (θ and φ) (Figure 1.9.) the equation for the spectral frequency simplifies to (Duer, 2002):

$$[8] \quad \omega_{\text{CS}}(\theta) = -\omega_0 \sigma^{\text{PAF}}_{\text{ZZ}} \frac{1}{2} (3\cos^2\theta - 1).$$

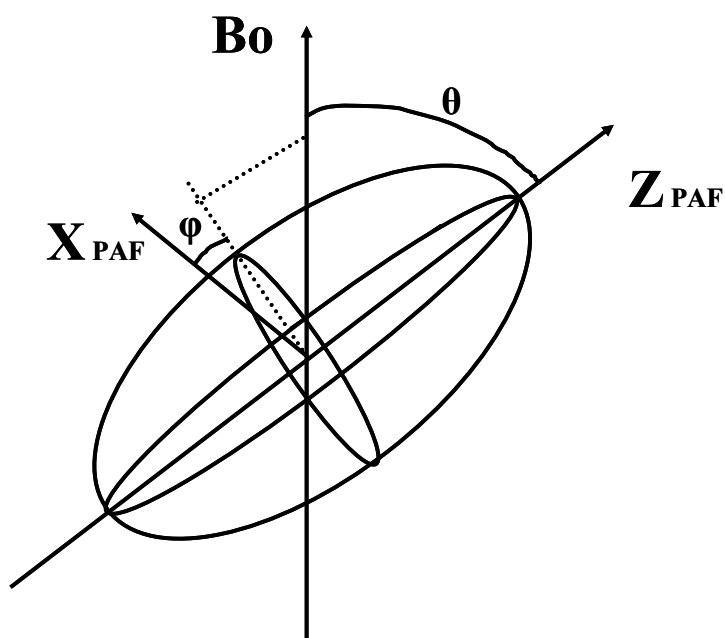


Figure 1.9: Chemical shift tensor. The polar angles, θ and φ , defining the orientation of B_0 field in the principal axis frame (PAF) are defined.

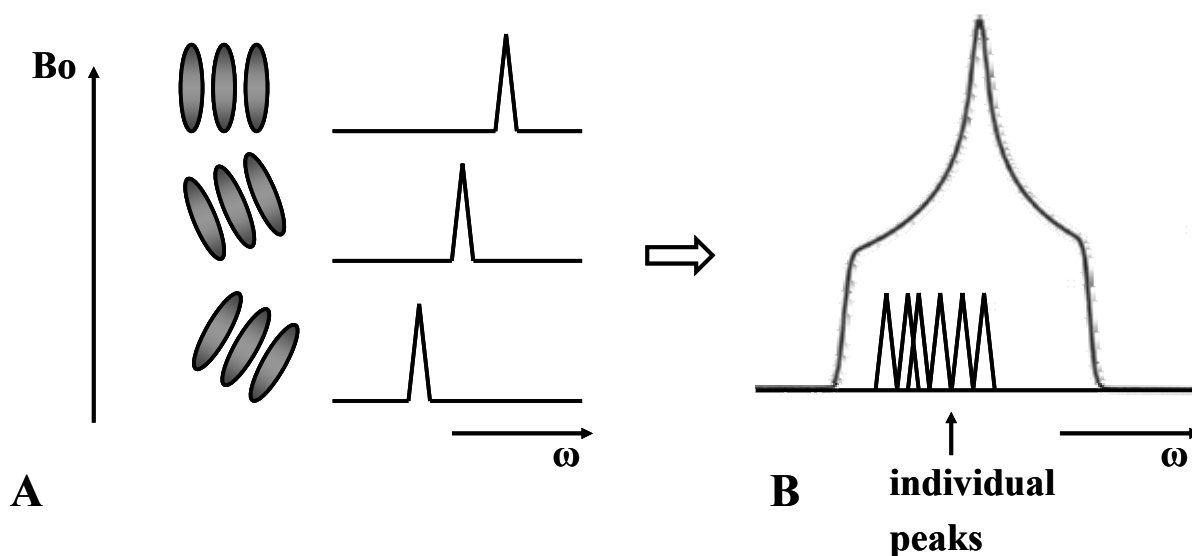


Figure 1.10: Effect of chemical shift anisotropy. (A) In a crystal, the chemical shift anisotropy depends on the solid with respect to the magnetic field. (B) Presence of different molecular orientations gives rise to a powder pattern.

Equation 8 has a direct implication. In a powder sample all orientations are present, meaning all values of the angle θ are possible. Therefore, each different molecular orientation implies a different orientation of the principal axis frame with respect to the applied field B_0 , and so has a different chemical shift associated with it. As a result the spectrum takes the form of a powder pattern with lines from the different molecular orientations covering a range of frequencies (Figure 1.10 B). So, the powder pattern has a so called centre of ‘mass’ or ‘mean value’, the isotropic frequency ω_{iso} .

1.3.2. Dipolar coupling

Each nuclear spin possesses a magnetic moment; therefore spins can interact through space (Figure 1.11). This interaction is called dipole-dipole coupling. The dipolar coupling may have intramolecular and intermolecular origin and be homonuclear (when the spins I_j and I_k are the same species) and heteronuclear (when spins I_j and I_k are different).

The direct dipole-dipole interaction between spins I_j and I_k can be presented by the spin Hamiltonian which in angular frequency units can be expressed in $\text{Rad}^{s^{-1}}$ (Duer, 2002):

$$[9] \quad \hat{\mathbf{H}}_{dd} = -(\mu_0/4\pi) \gamma_j \gamma_k \hbar ((\mathbf{I}_j \cdot \mathbf{I}_k / r^3) - 3((\mathbf{I}_j \cdot \mathbf{r})(\mathbf{I}_k \cdot \mathbf{r}) / r^5)),$$

where \mathbf{r} is the vector between point magnetic dipoles, r is the distance separating two magnetic dipoles spins I_j and I_k , \mathbf{I}_j and \mathbf{I}_k spin operators of nuclei I_j and I_k , μ_0 is the magnetic permeability of free space, and γ_j and γ_k are the gyromagnetic ratios for nuclei j and k .

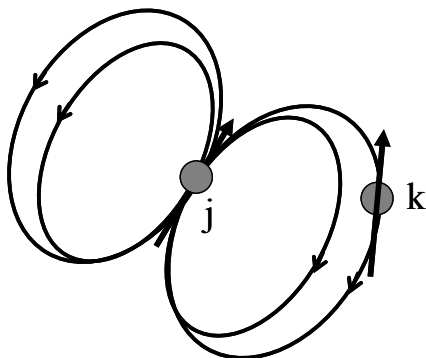


Figure 1.11: The magnetic moment of nuclear spin generates a magnetic field. Magnetic fields originating from different nuclei interact through space like bar magnets. This interaction is called dipole-dipole coupling.

For the homonuclear dipolar coupling case, using the rotating frame formalism the Hamiltonian can be presented as follows (Duer, 2002):

$$[10] \quad \hat{\mathbf{H}}_{dd} = -d(3\cos^2\theta - 1) [\hat{\mathbf{I}}_{jz} \hat{\mathbf{I}}_{kz} - \frac{1}{2}(\hat{\mathbf{I}}_{jx} \hat{\mathbf{I}}_{kx} + \hat{\mathbf{I}}_{jy} \hat{\mathbf{I}}_{ky})],$$

Term A and B

where d is the dipolar coupling constant given as (Duer, 2002):

$$[11] \quad d = \hbar(\mu_0/4\pi) (1/r^3) \gamma_j \gamma_k.$$

The terms A and B in equation 10 cause a large range of transition frequencies (Duer, 2002). It results in very broad lines in NMR spectrum in case of homonuclear dipolar coupling.

In the case of heteronuclear coupling between spins I_j and I_k the term B in equation 10 is absent, because it is associated with the transverse component of the local field due to spin I_k and it is important only if this component precesses at or near the resonance frequency of the other spin I_j . Therefore the effect of heteronuclear coupling on NMR spectrum is simpler and the general form of the lineshapes in found to be that shown in Figure 1.12.

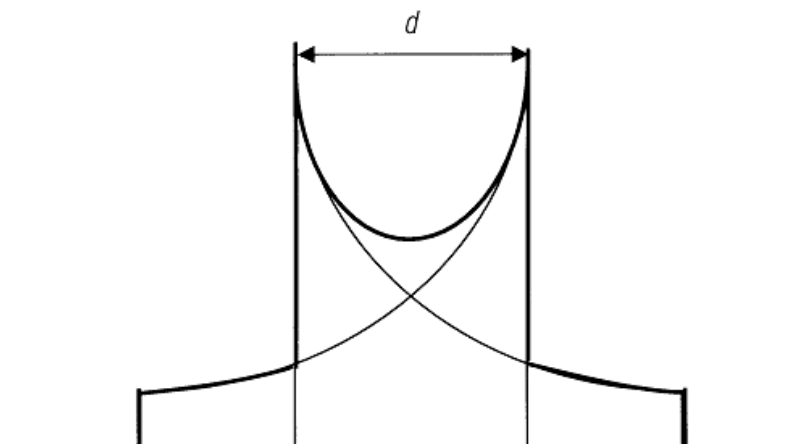


Figure 1.12: Heteronuclear dipolar coupling results in the powder lineshape (pake pattern) of a NMR spectrum. The splitting of the 'horn' is equal to the dipolar coupling constant (d , eq. 11).

1.3.3. Quadrupolar coupling

About 74 % of NMR active nuclei have a spin greater than $\frac{1}{2}$. In addition to a magnetic dipole moment, they possess an electric quadrupolar moment. Therefore, these nuclei interact not only with the applied magnetic field and all local magnetic fields, but also with any electric field gradient present. This interaction additionally affects the nuclear spin levels. The strength of the quadrupolar interaction depends on the orientation of a molecule with respect to the applied magnetic field \mathbf{B}_0 , even though this is not a magnetic interaction. The form of the quadrupolar Hamiltonian describing the interaction between a nuclear quadrupole moment of a nucleus with a spin I and an electric field gradient in tensorial form is (Duer, 2002):

$$[12] \quad \hat{\mathbf{H}}_Q = (eQ/6I(2I - 1)) \mathbf{I} \cdot \mathbf{eq} \cdot \mathbf{I}$$

where \mathbf{eq} is a tensor describing the electric field gradient, and eQ is the electric quadrupolar moment, constant for a given nuclei and does not change with the chemical environment of the nuclei for instance (e is a proton charge).

Figure 1.13 shows the first-order quadrupolar powder lineshape for a spin-1 nucleus at a site of axial symmetry. The term m is the z component of spin in the initial spin level of a transition, so can take values $m = +1$ to $m = 0$ and $m = 0$ to $m = -1$, which gives rise to mirror image powder pattern

lineshapes. The sum of these two powder patterns produces a 'pake pattern' like spectrum. The splitting of the 'pake pattern' is equal to three quarter of the quadrupolar coupling constant (Duer, 2002):

$$[13] \quad \chi = e^2qQ/h.$$

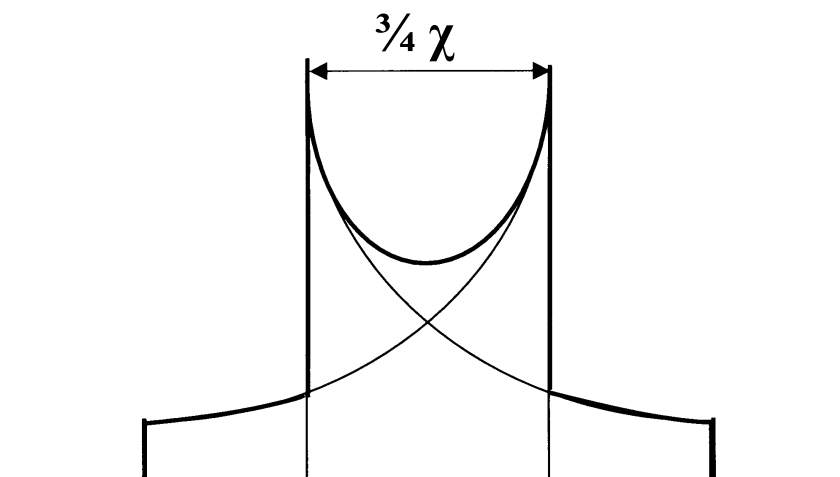


Figure 1.13: The first-order quadrupolar powder lineshape for spin-1 at a site of axial symmetry. The splitting of the 'horn' in the pattern is equal to $\frac{3}{4} \chi$, where χ is the quadrupolar coupling constant. The horns are created by crystallites in which the principal axis z of the quadrupolar coupling tensor is perpendicular to the applied field B_0 .

It is worth mentioning that the quadrupolar interaction for the majority of the quadrupolar nuclei is in the order of MHz and modern NMR spectrometers produce RF pulses in a range of 100 kHz, therefore in these cases the quadrupole coupling dominates through the whole experiment. However, fortunately, it is not the case for the most often used in SSNMR quadrupolar nuclei, deuterium. For ^2H the quadrupolar coupling constant is about 160-190 kHz, which simplifies experiments.

1. 4. Spectral resolution in solid-state NMR

Experimental techniques strongly differ between solution and solid state NMR. In solid-state NMR the information may be extracted from the anisotropic interactions which are averaged in solution state NMR. However, exactly these interactions may cause line broadening and need to be removed and selectively introduced to obtain structural information (Duer, 2002).

1.4.1. Magic-angle spinning

Line broadening in SSNMR is caused mainly by chemical shift anisotropy and dipolar coupling. The symmetric chemical shift anisotropy (CSA) can be removed when the vector connecting two nuclei forms an angle 54.74° with respect to \mathbf{B}_0 . This could be accomplished by using a single crystal in which the CSA ellipsoid is oriented at an angle 54.74° with respect to \mathbf{B}_0 . However, it is hard to perform, because single crystals are hard to obtain. In reality, we often deal with the samples lacking a unique CSA axis orientation. In such cases rapid spinning of a polycrystalline sample at the angle 54.74° makes average CSA look like ellipsoid whose axis is aligned with the spinning axis. It happens because the angle θ (Figure 1.14) varies with time as the molecules rotate with the sample.

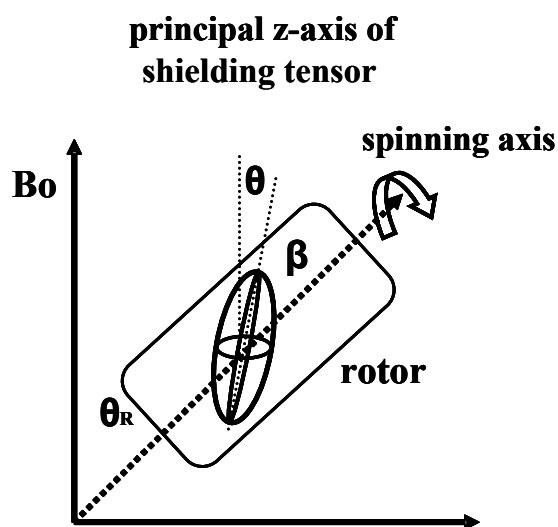


Figure 1.14: The MAS experiment. The value for angle θ_R is at the magic angle with respect to the applied magnetic field and it is under control during the experiment. The chemical shift tensor is represented by an ellipsoid. The angle θ is the angle between \mathbf{B}_0 and the principal z-axis of the shielding tensor, β is the angle between the z-axis of the shielding tensor principal axis frame and the spinning axis.

The average orientation dependence of the nuclear spin is (Duer, 2002):

$$[14] \quad \langle 3\cos^2\theta - 1 \rangle = 1/2(3\cos^2\theta_R - 1) (3\cos^2\beta - 1).$$

The angle β is fixed for each nuclei and the angle θ can have all possible values in a powder sample. The angle θ_R is set to 54.74° ($(3\cos^2\theta_R - 1) = 0$). Therefore, the molecular orientation dependence of the nuclear spin interactions ($3\cos^2\theta - 1$) is removed if the spinning speed is fast enough to average θ compared with the anisotropy of the interaction (Duer, 2002). This technique is known as magic-angle spinning (MAS). If the spinning frequency is not high enough to average the anisotropic interactions, the spectrum consists of a line of isotropic chemical shift and a pattern of sidebands that are spaced by the rotation frequency. The intensity distribution of the sidebands still contain the information about the chemical shift anisotropy and consequently about the molecular geometry in the sample.

1.4.2. Cross polarization

	^1H	^2H	^{13}C	^{15}N	^{19}F	^{31}P
Nuclear Spin, I	1/2	1	1/2	1/2	1/2	1/2
Nuclear magnetic Moment, μ	2.793	0.857	0.702	-0.283	2.689	1.131
Gyromagnetic ratio, γ (rad T $^{-1}$ s $^{-1}$)	$26.75 \cdot 10^7$	$4.11 \cdot 10^7$	$6.73 \cdot 10^7$	$-2.71 \cdot 10^7$	$25.16 \cdot 10^7$	$10.83 \cdot 10^7$
Quadrupole moment		$2.73 \cdot 10^{-31}$				
Relative sensitivity	1.00	$9.65 \cdot 10^{-3}$	$1.59 \cdot 10^{-2}$	$1.04 \cdot 10^{-3}$	0.83	$6.63 \cdot 10^{-2}$
Natural abundance	99.985	0.015	1.10	0.37	100	100

Table 1.3: Comparison of gyromagnetic ratios, natural abundance, and relative sensitivity of the most used nuclei in solid-state NMR (adapted from Mason J. A. PhD thesis 2001).

Apart from the problem associated with anisotropic broadening and short transverse relaxation times characteristic for solid-state NMR, there is one more factor. SSMAS spectra are characterized by poor signal to noise ratio. The reasons for that are multiple. Signal-to-noise ratio roughly scales with the inverse of the linewidths, as the integral intensity of the whole line is constant. The linewidths in SSNMR are typically 10-100 times broader compared to solution-state NMR (Opella, 1982). Another

reason is given by the type of nuclei which are used in SSNMR. The most popular nucleus for solution state NMR, ^1H often can not be used in SSNMR because of its high abundance and significant homonuclear dipole-dipole coupling. Nuclei like ^{13}C , ^{15}N and ^{31}P are characterized by lower anisotropy but have a smaller gyromagnetic ratio and are less sensitive for NMR (Table 1.3).

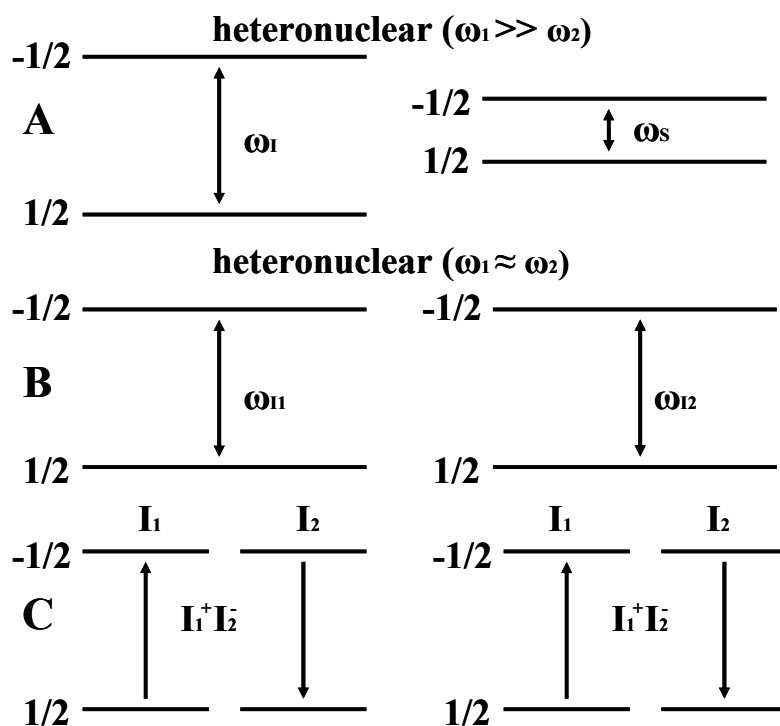


Figure 1.15: Cross polarization for heteronuclear spin pairs. A) at different transition frequencies of two spins ω_1 and ω_2 , no energy-conserving transitions occur; B) when $\omega_1 = \omega_2$, C) the spins can exchange magnetization through an energy-conserving ‘flip-flop’ interaction (Laws *et al.*, 2002).

The situation is further complicated by the fact that longitudinal relaxation times are longer in solid state than in solution. A smaller number of scans can be accumulated in a given time. Overall, it is clear that without techniques allowing us to enhance the signal, the experiments on such a nucleus like ^{13}C are close to impossible.

To enhance the signals from rare nuclei such as ^{13}C and ^{15}N , many SSNMR experiments are today routinely performed involving the transfer of polarization from abundant nuclei (usually ^1H) by using a technique called cross polarization (CP). The process of CP occurs through the tendency of the

magnetization to flow from highly polarized nuclei to nuclei with lower polarizations when the two are brought into contact. For homonuclear spins, the magnetization can be exchanged through mutual energy conserving spin flips. For heteronuclear pairs such as ^1H and ^{13}C , these spins flips are not energy conserving at high magnetic fields (Figure 1.15). Therefore, the exchange of magnetization is driven externally by the application of RF fields.

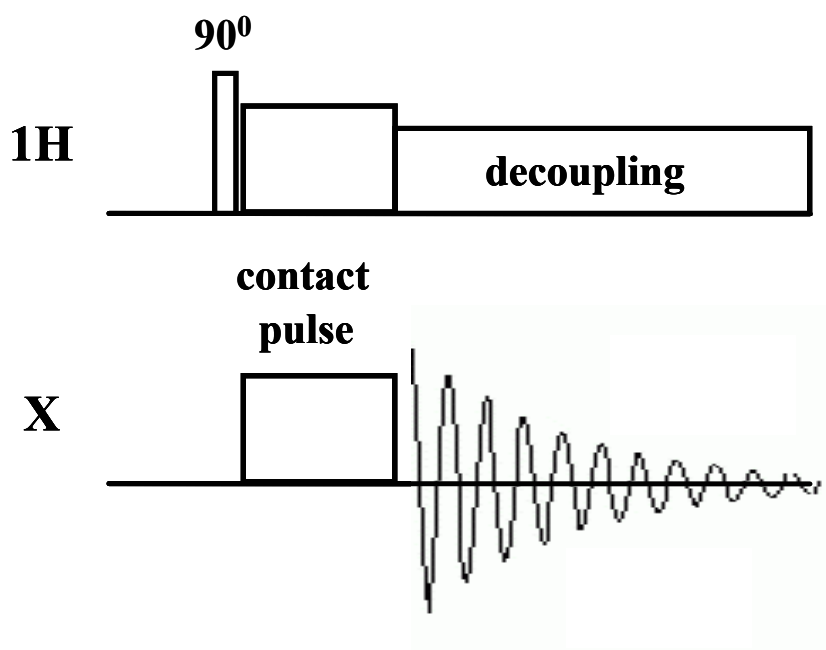


Figure 1.16: Pulse sequence for cross polarization experiment (Hediger *et al.*, 1994; Metz *et al.*, 1994; Peersen *et al.*, 1993; Stejskal *et al.*, 1977).

Among the techniques for establishing a dipolar contact between two different spin systems, a particularly effective approach is that of Hartmann and Hahn. This approach involves the simultaneous application of two continuous RF fields, one at the resonance frequency of one spin and one at the resonance frequency of the other spin in a way that the Hartmann-Hahn condition is satisfied (Laws *et al.*, 2002):

$$[14] \quad \gamma_{\text{C}}B_1^{\text{C}} = \gamma_{\text{H}}B_2^{\text{H}}$$

then the magnetization can be exchanged between two nuclei in energy conserving way by spin flip-flop. The carbon signal enhancement is proportional to $\gamma_{\text{C}}/\gamma_{\text{H}} \approx 1/4$, which is comparable with the NOE enhancement in solution state NMR. Moreover, as the polarization required for the experiment comes from protons and its longitudinal relaxation time is much faster that of any other nucleus, the

experiment can be repeated more frequently. The cross polarization experiment in solid-state NMR is often combined with the MAS and proton decoupling during detection. The standard CP pulse sequence is shown in Figure 1.16.

1.4.3. Decoupling techniques

In solution, dipole-dipole couplings are averaged to their isotropic value by molecular tumbling. This is not the case in solids; here the spectra` quality is strongly influenced by homo- and heteronuclear dipolar coupling between the nuclei. As discussed previously, the dipolar coupling depends directly on the magnitude of the distance between the two spins. Therefore, it not only causes linebroadening but can also provide a means to obtain internuclear distances and as a result leads to determination of the molecule geometry and conformation. There are many pulse sequences designed to remove and to selectively reintroduce dipolar coupling.

Heteronuclear decoupling

In most cases, proton coupling is needed to be removed. The simplest technique to remove heteronuclear proton dipolar coupling is through continuous high-power decoupling (Figure 1.17).

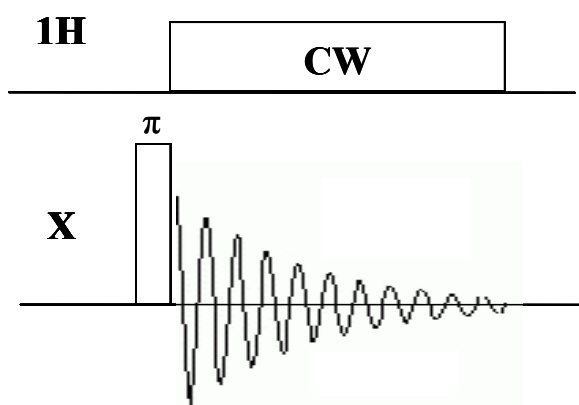


Figure 1.17: High-power decoupling removes the effect of the effect ^1H dipolar coupling on the NMR spectrum of X nucleus.

The method includes applying continuous irradiation (CW) of very high power (100-1000 Watts) at the frequency of the proton resonance. The effect of the close-to-resonance RF irradiation is that

proton spins undergo repeated transitions at a rate determined by the amplitude of the RF irradiation and ^1H Larmor frequency. Therefore, the time dependent z-component of the ^1H spin in the dipolar coupled spin pair, which is affecting the X spin spectrum, approaches zero.

More sophisticated methods to achieve heteronuclear decoupling are via applying TPPM (Takegoshi et al., 2001; Bennet et al., 1995), SPINAL (Fung et al., 2000), SPARC (Yu and Fung, 1998), FMPM (Gan and Ernst, 1997), and C12 (Eden and Levitt, 1999) pulse sequences. They all have similar efficiency, so our detailed consideration will be limited to TPPM decoupling pulse sequence.

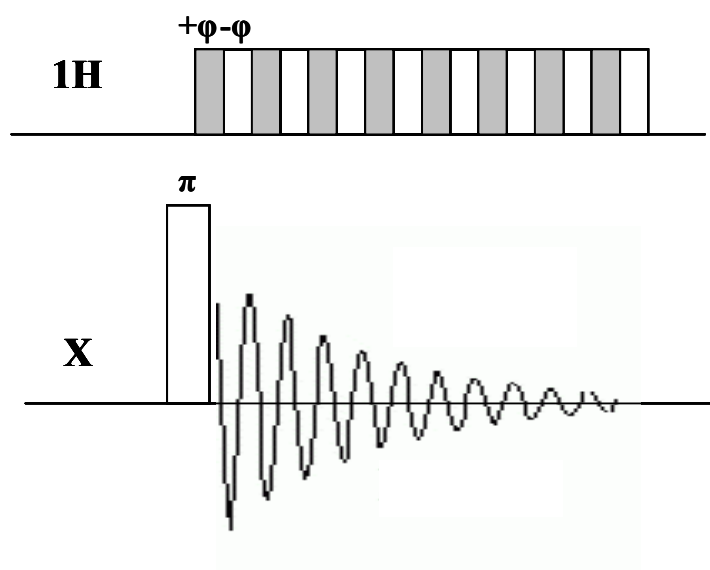


Figure 1.18: TPPM decoupling pulse sequence of alternating phase $\phi_p + \Delta\phi_p$, each of flip angle θ_p .

The two pulse phase modulation (TPPM) pulse sequence consists of continuous irradiation with two pulses of flip angle θ_p and phases which differ by $\Delta\phi_p$ (Figure 1.18). The used RF power is usually about 100-150 kHz. The optimal values of θ_p and $\Delta\phi_p$ are determined for each particular case experimentally, θ_p is often close to 180° and $\Delta\phi_p$ is in a range of $10 - 70^\circ$.

Homonuclear decoupling

In the simplest case, the effect of homonuclear dipolar coupling may be removed by magic-angle spinning. If MAS is not sufficient to remove homonuclear decoupling, special pulse sequences are designed to deal with it. One of the first implemented were WAHUHA (Haeberlen and Waugh, 1968) and MREV-8 (Rhim et al., 1973) (Figure 1.19). Although the WAHUHA sequence is not used any more, it still serves as a good illustrative example of how such techniques works (Laws et al., 2002).

Here, the pulses are placed in a cycle through the period of induction decay in such a way that there is one detection point per cycle until the magnetization decay completely. In comparison to TPPM, WAHUHA does not average the geometrical part of $\hat{H}_{dd}^{\text{homo}}$ but deals with the spin factor $\hat{H}_{dd}^{\text{homo}}$.

While implementing WAHUHA pulse sequences together with MAS, it is necessary to synchronize the pulse sequence and free induction decay collection. Synchronization is not needed if the decoupling pulse sequence is used in the t_1 dimension of a 2D pulse sequence.

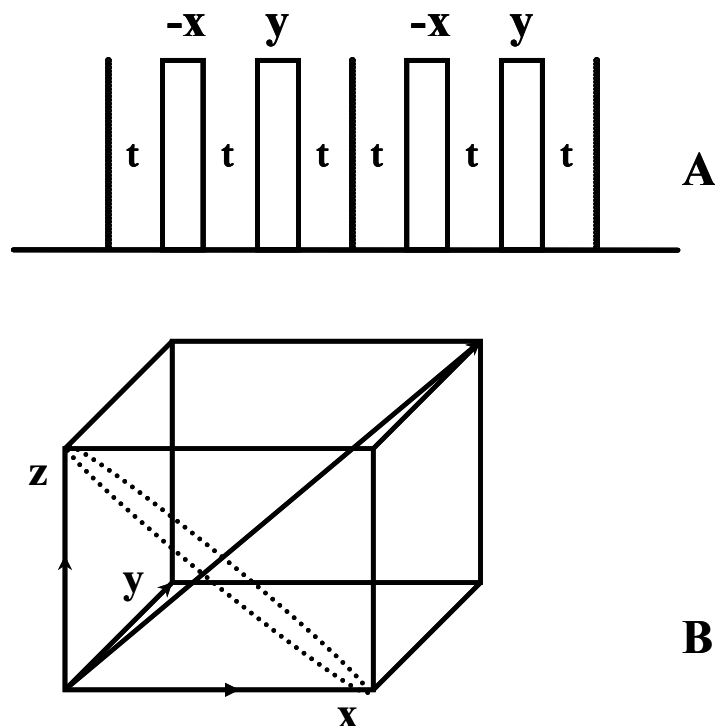


Figure 1.19: A) pulse sequence for one cycle of the four-pulse WAHUHA decoupling sequence. B) The Lee-Goldburg sequence is the continuous analogue, in which spins undergo rotation about an axis inclined at the magic angle in spin space.

One more homonuclear decoupling sequence worth mentioning is frequency-switched Lee-Goldburg (FSLG) (Bielecki et al., 1990; Bielecki et al., 1989) (Figure 1.19). In FSLG the pulses of 360° are applied continuously when decoupling is needed. The pulses are off resonance by amount of $\Delta\omega$ in a way that the effective field experienced by nuclei in the rotating frame is oriented at the magic angle with respect to \mathbf{B}_0 . As a result the spin magnetization precesses completely by one turn around the effective field and the average homonuclear dipolar coupling is zero.

1.4.4. Recoupling techniques

The above sections of this Chapter address the questions how to remove undesirable effects of chemical shift anisotropy and dipolar coupling, and how to approach the resolution of SSNMR spectra close to the resolution of solution state NMR spectra. However, in doing so, we lose all the information about the environment of the nuclei contained in CSA and dipolar coupling. To reintroduce the dipolar coupling and CSA for selected periods of experiments the certain pulse sequences are designed. Using these techniques the distances can be measured and the correlations based on proximity can be established.

Homonuclear dipolar recoupling

One of the first dipolar homonuclear recoupling techniques (DRT) is DRAMA (dipolar recovery at the magic angle) (Tycko and Dabbagh, 1990). During this sequence, two $\pi/2$ pulses per rotation period toggle the reference frame interrupting the averaging producing by MAS. DRAMA recouples not only dipolar coupling but the CSA as well. Therefore, additional π pulses are included usually in the experiment to refocus the CSA (Figure 1.20).

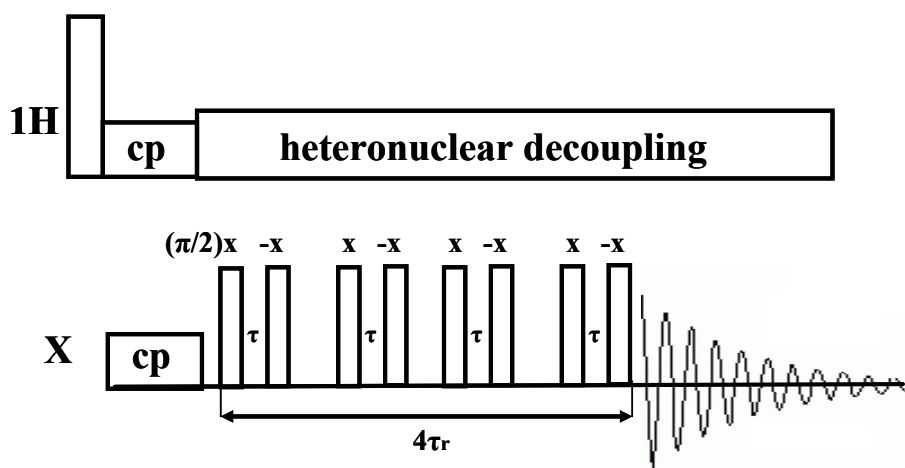


Figure 1.20: Pulse sequence for one cycle of the DRAMA homonuclear dipolar recoupling sequence consisting of $\pi/2$ pulses only. τ_r is a rotor period (Laws et al., 2002).

The alternative approach to observe homonuclear dipolar coupling is to use the rotational resonance phenomenon. If the sample spinning speed is equal to or n times chemical shift difference between the

two spins of interest, the term B in equation 10 is reintroduced (Duer, 2002). The rotational resonance condition is achieved only between two spins, whose the dipolar coupling is measured (Raleigh et al., 1988). In addition to DRAMA and rational resonance, a plethora of homonuclear recoupling sequences have been developed. In practice the most and commonly used DTR seem to be is RFDR (radiofrequency driven recoupling) and C7 (Brinkman et al., 2000; Carravetta et al., 2000).

Heteronuclear dipolar recoupling

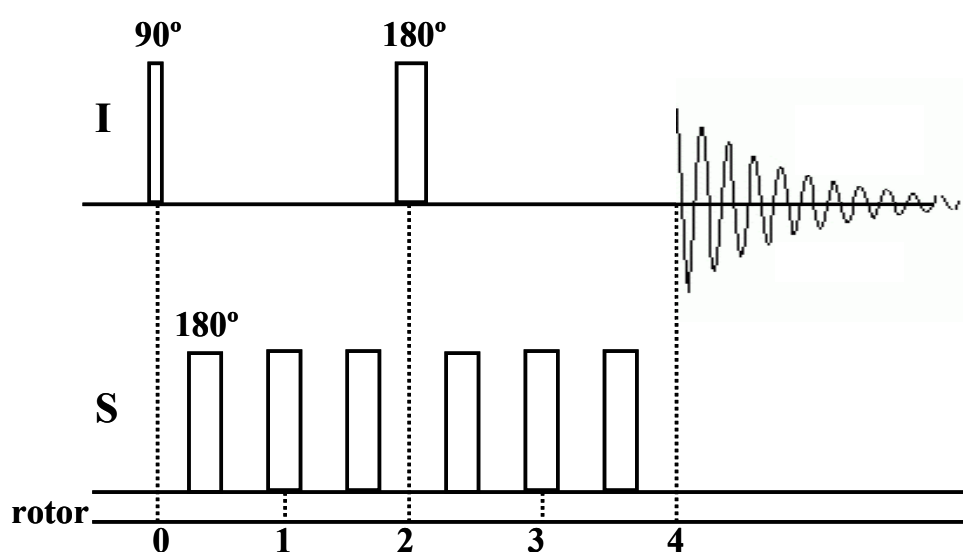


Figure 1.21: REDOR experiment sequence.

A number of experiments have been designed to measure the heteronuclear dipolar coupling, based on the same principle and similar to the well known rotation-echo double resonance experiment (REDOR) (Figure 1.21) (Gullion and Schaefer, 1989). The general idea of this experiment is that magnetization of spin I, which is created by a simple 90° pulse, is left to refocus under the influence of S spin. The refocusing of dipolar coupling is prevented by a series of rotor-synchronized 180° pulses applied to spin S. To obtain the value of dipolar coupling between spin I and S, the extent of I dephasing is monitored as a function of the number of rotor periods for which the dephasing is allowed.

As the strength of the heteronuclear dipolar coupling approaches $\sim 25\text{Hz}$, it becomes very difficult to

determine distances by using REDOR. This corresponds to a $^{15}\text{N} - ^{13}\text{C}$ distance of $\sim 5 \text{ \AA}$ and $^{13}\text{C} - ^{31}\text{P}$ distance of $\sim 7.5 \text{ \AA}$. These distances exceed those typically studied by solution-state NMR and they can provide useful constraints in structural studies of solids. This approach is, unfortunately, not suitable for large dipolar couplings, because in this case the magnetization is completely dephased in one or two rotor periods. Under these circumstances, there are not enough data points to perform a careful analysis (Laws et al., 2002).

1.5. Solid-state NMR in application to membrane transporters

As stated previously, high-resolution structures of membrane transporters as well as of high molecular weight complexes are rare. Membrane transporters are difficult to crystallize; membrane proteins are surrounded by lipids and may aggregate when removed from their normal environment. The same characteristics also hinder solution spectroscopy which is also not suitable for very large complexes due to the lack of fast isotropic tumbling needed for good spectral resolution.

Solid-state NMR is not limited by these problems and, in principal, can be readily applied to almost of those systems. The molecular weight limit that can be studied by solid state NMR is almost unreachable and the field has seen a number of publications on high molecular weight proteins (Basting and Lehner, 2006; Luca *et al.*, 2005; Creemers *et al.*, 2004; Williamson *et al.*, 2001; Glaubitz *et al.*, 2000; Spooner *et al.*, 1998; Watts *et al.*, 1998; Opella, 1982).

For the first time SSNMR has been applied to transporters by Watts and co-workers who have detected the substrate glucose bound to GalP transporter (Spooner *et al.*, 1994). First SSNMR investigations on GalP transporter were followed by studying *E. coli* FucP (Spooner *et al.*, 1998) GusB, NupC transporters (Patching *et al.*, 2004b; Patching *et al.*, 2004a), and EmrE MDR pump (Glaubitz *et al.*, 2000), as well as *Streptococcus thermophilus* LacS transporter (Spooner *et al.*, 1999). These and some other studies aiming to obtain structural information on substrate binding are listed in introduction to Chapter 5.

Interestingly, in all cases the studies have been limited to drug-protein interaction with labeled substrate and in no cases isotope labeled proteins were used.

Aims of the thesis

ABC transporters compose a family of membrane proteins that is associated with many genetic disorders as well as with the resistance to antibiotics and cancer chemotherapy. The latter is mediated by over expression of multidrug efflux pumps. The first discovered and the best characterized until now the human MDR transporter ABC transporter is P-glycoprotein. The closest structure and functional homologue of P-glycoprotein found in bacteria is LmrA from *Lactococcus lactis*.

ABC transporters are extremely difficult for structural analysis and whilst a number of advances have been made, progress in this field remains relatively slow. Solid-state NMR is a powerful technique for obtaining structural constraints and in the past years SSNMR has showed its potency for getting those constraints for membranes, relatively small proteins and peptides. As SSNMR can deal with membrane embedded and/or membrane associated proteins and peptides, it has a potential to produce high-resolution information for such proteins like membrane transporters.

This thesis aims to approach ABC MDR transporters for characterization at atomic level with SSNMR. In doing so, several goals have to be achieved.

1. It will be demonstrated how large quantities of functionally active and selectively isotope labeled LmrA reconstituted at a high density in lipid membranes, sufficient for advanced NMR studies can be produced.
2. Using selectively CD₃ alanine labeled LmrA reconstituted into *E. coli* liposomes, it will be investigated if LmrA undergoes conformational changes affecting the dynamics protein properties upon AMP-PNP binding and in ATP/ADP-Vanadate trapped state.
3. Using isotope non-labelled protein reconstituted into proteoliposomes, the ligand binding will be explored via intrinsic tryptophan fluorescence quenching approach and solid-state NMR spectroscopy.
4. The membrane preferential location of nine LmrA and P-glycoprotein substrates will be investigated via ¹H-NOESY NMR spectroscopy and the results will be correlated with existing ABC MDR transporters binding sites models.

2. Development of defined media for isotope labelling of LmrA from *Lactococcus lactis*

Abstract

The aim of this chapter is to present a cost efficient procedure for biosynthetic selective amino acids labelling of the ABC MDR transporter LmrA expressed in *L. lactis* for SSNMR. A variety of techniques have been established for biosynthetic uniformly and selective amino acid labelling of proteins expressed in *E. coli*. However, to our knowledge isotope labelling has never been shown for proteins expressed in *L. lactis*.

The results of this Chapter have been partially published: Mason A.J., Siarheyeva A., Haase W., Lorch M., van Veen H., Glaubitz C., Amino acid type selective isotope labelling of the multidrug ABC transporter LmrA for solid-state NMR studies, FEBS Letters 568 (1-3): 117-121 June 18 2004.

2.1. Introduction

Unlike in solution-state NMR, the proton resonance alone is not sufficient for resonance assignment of large biomolecules in solid-state NMR, because even sophisticated resolution enhancement techniques such as combined rotation and multiple pulse sequences are not able to reduce the linewidths to achieve the resolution needed. Therefore, problems associated with direct ^1H observation in solid-state NMR has made isotope labelling an absolute requirement. Commonly stable isotopes such as ^{13}C , ^{15}N , ^{19}F and ^2H are enriched. In particular low- γ nuclei, like ^{13}C or ^{15}N are commonly used, primarily because they have relatively large chemical shift ranges and small dipolar couplings. The combined labelling approach opens a door to the development of higher dimensional experiments and allows larger proteins to be studied (Straus, 2004; Lian and Middleton, 2001b). The labels can be introduced into the protein and peptide structure by chemical modifications or biosynthetically. Solid-phase synthesis is widely used to directly synthesize polypeptides with length that are between 2 to 40 residues long. The chemical modification strategy includes such methods as

methylation of the lysine side groups, covalent modification of cysteine sulfhydryl groups or ^{15}N tyrosine nitration (Lian and Middleton, 2001a; Goto and Kay, 2000; Danielson and Falke, 1996b). The biosynthetic approach includes usage of ^{15}N and ^{13}C labeled precursors as the sole nitrogen or carbon sources, or selectively labeled amino acids as a source of nutrients during protein expression. As an example, extensive ^{13}C labelling in *E. coli* can be achieved by substitution of glucose or acetate in a growth medium by their fully labeled analogues or by adding fully labeled glycerol as the only carbon source (Lian and Middleton, 2001a; Goto and Kay, 2000; Hong and Jakes, 1999; Stryer, 1988). To achieve full ^{15}N labelling, ^{15}N -labelled ammonia can be used as the sole nitrogen source (Castellani et al., 2002). An alternative approach is to apply selective extensive labelling. Selective labelling can be achieved using partly labeled glucose or glycerol (Lian and Middleton, 2001b; LeMaster, 1994). In a similar manner, sample deuteration can be obtained, when the deuteration is needed to simplify NMR spectra aiming to improve relaxation properties of the remaining protons. This is used mainly in solution state NMR to increase the protein molecular mass limit (Goto and Kay, 2000; Morgan *et al.*, 2000). Amino acid type selective isotope labelling can be used to observe selected amino acids (Goto and Kay, 2000). For this purpose the amino acids of interest are replaced by their isotope labeled analogues in the growth media. This biosynthetic approach can be complicated however by cross-labelling and isotopic dilution. The problems can be solved by using the appropriate auxotrophic strains. For the case of *E. coli* a complete library of auxotrophic strains exists in the genetic Stock Centre at Yale University (Lian and Middleton, 2001b). For protein production in quantities suitable for NMR experiments the strain auxotrophy must be further combined with over expression of the desired protein. Examples of multi-domain membrane proteins that can be heterologously expressed at levels suitable for structural studies are rare and examples where such proteins have been labeled for NMR purposes are even rarer (Creemers et al., 1999; Eilers et al., 1999).

Whilst the bacterium *E. coli* is one of the most popular systems in which to overexpress membrane proteins (Drew *et al.*, 2003; Lian and Middleton, 2001b), recently protocols have been developed to express membrane proteins in alternative protein expression systems including *Pichia pastoris*, Chinese hamster ovary cell, SF9 cells, and Semliki forest virus cells (Chen *et al.*, 2006; de Lamotte *et*

al., 2001; Goto and Kay, 2000; Morgan *et al.*, 2000). Cell free synthesis has been successfully applied to membrane proteins (Klammt *et al.*, 2004) but may not be capable of producing such large proteins as ABC transporters in a correctly folded and functional state.

For this reason, we have sought to take advantage of the ability to produce large amounts of functional LmrA in *L. lactis* to prepare samples for NMR experiments. The *L. lactis* expression system has many advantages, (1) the organism is easy and inexpensive to culture; (2) the expressed membrane proteins are normally targeted to the cytoplasmic membrane, (3) it has a single membrane and (4) relatively mild proteolytic activity (to date only two proteinases are known) and (5) methods for genetic manipulations as well as a nisin induction system are established and available (Mierau and Kleerebezem, 2005). To create the nisin-controlled expression system (NICE), the auto-induction properties of nisin were used. So, the signal transduction system *nisK* and *nisP* were isolated from the nisin gene cluster and inserted into the chromosome of *L. lactis* strain MG1363 (nisin-negative), creating the strain NZ9000. When the gene of interest is subsequently placed behind the inducible promoter P_{nisA} on a plasmid (pNZ8048), expression of that gene can be induced by addition of sub-inhibitory amounts of nisin (0.1 – 5 ng/ml) to the culture medium (Mierau and Kleerebezem, 2005).

Lactococci lack various biosynthetic pathways when compared with *E. coli* for example, so that they require certain nutrients, especially amino acids and vitamins (Konings *et al.*, 2000). The strain used here, pNH LmrA NZ9000 is Glu (or Gln), Leu, Ile, Val, His and Met auxotrophic (Kunji *et al.*, 2003). This multiple auxotrophy, allows efficient isotopic labeled amino acid incorporation, but eliminates the possibility of uniformly labelling using minimal medium. The use of the *L. lactis* expression system for NMR studies on selectively and uniformly labeled membrane proteins is complicated by the fact that to date, knowledge about both carbon and nitrogen metabolism of *L. lactis* bacterium for growth in chemically defined media is limited.

Earlier attempts to define the composition of chemically defined medium for *Lactococcus* or *Lactobacillus* strains allowed the basic components and the composition of this medium for *L. lactis* strain 2118 to be highlighted (Novak *et al.*, 1997; Coccagn-Bousquet *et al.*, 1995a; Poolman and Konings, 1988; Otto *et al.*, 1983). The general outcome of many studies made on *Lactococcal* species is that with respect to specific requirements for nutrient this group is heterogeneous (Mierau *et al.*,

2005; van Niel and Hahn-Hagerdal, 1999) and for each strain the nutrients requirements must be considered separately. For *L. lactis* strain pNZ9000 used for LmrA over expression neither the components nor the concentration of the various components of defined medium has been previously optimized.

In this chapter the development of the chemically defined medium for *L. lactis* strain pNZ9000 has been demonstrated. Using *L. lactis* expression system large quantities of selectively ¹³C-glycine labeled LmrA (ca. 1mg LmrA/liter culture), sufficient for solid-state NMR experiments are produced. First solid-state NMR spectra are presented showing the suitability of this system for further studies of LmrA structure and function. In so doing, a large (64 kDa) ABC transporter becomes accessible, for the first time, to NMR techniques previously restricted to much smaller proteins. In addition, attempts to enhance the labelling efficiency and protein yield are described.

2. 2. Materials and methods

2.2.1. Optimization of defined media composition

Materials

L. lactis strains pNH LmrA NZ9000 and NZ9700 was a gift from H.W. van Veen (University of Cambridge). Difco Laboratories' M17 medium was obtained from BD, Sparks, MD; n-dodecyl-β-D-maltoside (DDM) from Glycon Biochemicals GmbH, Luckenwalde, Germany; Ni²⁺ nitriloacetic acid (Ni-NTA) resin from Qiagen Inc. All other materials were reagents of analytical grade.

Microorganism and media

L. lactis strain NZ9000 was used as a host for expression vector pNH LmrA, strain 8048 non over expressing LmrA was used as a control whilst NZ9700 was used as a nisin producing strain (Margolles *et al.*, 1999) Cells were cultured overnight at 30°C in M17 medium or defined medium, both supplemented with 0.5 % (w/v) glucose and 5 µg/mL chloramphenicol, and used to start large scale cultures grown at 30° without shaking.

Nisin production

L. lactis NZ9700 was grown in M17 medium until $OD_{660} \sim 0.9$ and then the cells were harvested. The nisin contained in the supernatant was stored in 1 ml aliquots at -20°C . To induce LmrA expression it was diluted 1000 fold in the growth medium.

Preparation of a defined medium

Amino acids, g/L		Salts, g/L	
Alanine	0,3	NH ₄ CL	3,75
Arginine	0,36	KH ₂ PO ₄	2,5
Asparagine	0,48	K ₂ HPO ₄	3,25
Aspartic acid	0,04	MgSO ₄	0,87
Cysteine	0,12	NaCL	0,525
Glutamic acid	0,48		
Glutamine	0,48		
Glycine	0,12		
Histidine	0,12		
Isoleucine	0,36	Vitamins, g/L	
Leucine	0,84	Thiamine	0,0001
Lysine	0,72	Riboflavine	0,001
Methionine	0,20	Niacine	0,001
Phenylalanine	0,36	Pyridoxal HCL	0,0023
Proline	0,6	Aminobenzoic acid	0,0001
Serine	0,12	Folic acid	0,001
Threonine	0,36	Biotin	0,0001
Tryptophan	0,09		
Tyrosin	0,24		
Valine	0,6		
Adenine	trace		
Guanine	trace		
Uracil	trace		

Table 2.1: Chemically defined medium.

The medium (Table 2.1) was prepared as follows. Phosphates, magnesium, ammonium salts and all amino acids were dissolved and autoclaved separately. Glucose was prepared as a 20 % stock solution, chloramphenicol as a 30 mg/ml stock solution in ethanol, vitamins as a 100-fold stock solution, stored at 4°C (Phan-Thanh and Gormon, 1997). The pH of the medium was 6 – 6.5 and was maintained without further adjustments. The bacterial growth was followed by measuring the culture optical density at wavelength 660 nm every 40 minutes on a UV-550 Jasco spectrophotometer. Over expression of LmrA was achieved by induction with 1 % nisin at OD₆₆₀ 0.7.

Optimization of a chemically defined medium was done by comparing *L. lactis* growth with different concentrations of amino acids. The concentration of amino acids was increased in 20 % steps starting with 80 % of the original recipe (Table 2.1). To examine the auxotrophy for selected amino acids, *L. lactis* strain NZ9000 over expressing LmrA was grown on the chemically defined media (CDF) lacking glycine, tryptophan, serine, or both serine and glycine.

Preparation of inside out vesicles

Preparation of inside-out vesicles was done as described previously (van Veen *et al.*, 2000a). *L. lactis* cells were harvested by centrifugation, washed with 100 mM Tris, 50 mM KCl buffer, pH 7 and resuspended in approximately 20 mL of the same buffer. 1 mL of lysozyme stock solution (200 mg/mL) was then added to digest the cell walls. The dissolved pellets were incubated for 30 minutes at 30°C and the cells were lysed by passage through a cell disrupter (1.5 kPa). 20 µl (100 µg/mL) DNase I and 200 µL of 1 M MgSO₄ were added to the cell suspension, which was further incubated for 15 min at 30°C. Unbroken cells and cell debris were removed by centrifugation 10000 rpm for 20 minutes at 4°C. The vesicles were harvested by ultracentrifugation for 30 minutes at 50000 rpm. The protein concentrations in the vesicles were measured using the Bio-Rad DC protein assay kit as adapted from Lowry (Lowry *et al.*, 1951).

Purification of LmrA

Purification of histigine-tagged LmrA ISOVs were solubilised on ice with the solubilization buffer (100 mM Tris, 50 mM NaCl, 10 % (v/v) glycerol, 3 % (w/v) DDM, pH 8.0) for an hour. The

unsolubilised fraction was removed by ultracentrifugation (55000 rpm, 40 minutes). The supernatant was incubated with Ni-NTA agarose for one hour on ice. Ni-NTA agarose was preliminarily preequilibrated with buffer A (100 mM Tris, 50 mM NaCl, 10 % (v/v) glycerol, 0.05 % (w/v) DDM and 10 mM Imidazole, pH 8.0). After the incubation, the resin was loaded on a column (Pharmacia) attached to an ÄKTA prime HPLC. Non-histidine tagged proteins were washed from the column with buffer A and B (100 mM Tris, 50 mM NaCl, 10 % (v/v) glycerol, 0.05 % (w/v) DDM and 10 mM Imidazole, pH 8.0 and 7.0) respectively. When no further protein was detected in the flow (OD monitored at 280 nm), LmrA was eluted with buffer B supplemented with 250 mM Imidazole. All handlings were carried out at 4°C.

Hoechst-33342 transport in membrane vesicles

20 µL inside-out membrane vesicles (about 6 mg/mL) were diluted to 2 mL volume with 100 mM Tris, 50 mM KCl buffer, pH 7, containing 2 mM MgSO₄. After 1 minute incubation at 30°C 10 µL 1 mM Hoechst-33342 was added. 20 µL 100 mM ATP was added when the intensity of the fluorescence reached a plateau. The experiment was repeated with ADP in place of ATP. All measurements were carried out with excitation and emission wavelengths of 355 and 457 nm respectively and a slit width of 3 nm on the Jasco FP-6300 spectrophotometer (Kamihira et al., 2005; Shapiro and Ling, 1995).

2.2.2. Metabolic labelling of LmrA ISOVs with ¹³C labeled amino acids

The amino acid selective labelling has been probed using ¹³C labeled glycine and tyrosine. Glycine was chosen to be the amino acid of interest because there are 49 glycines in LmrA sequence and it is one of the cheapest amino acids making it a good candidate to perform first NMR experiments aiming to reveal the amenability of LmrA to isotopic labelling. As a next candidate for selective amino acid labelling, tyrosine was chosen. There 14 tyrosines in LmrA sequence and several of them can be involved in substrate binding.

2.2.3 Attempts to enhance protein yield and labelling efficiency

Attempts to enhance protein yield

1. *L. lactis* NZ9000 were grown to OD₆₆₀ 1.44, harvested, washed with 100 mM Tris, 50 mM KCl, pH 7 buffer. In three series of experiments equal amounts of cells (from 1 liter of M17 media) were transferred into different volumes of defined media. The defined media volumes were equal, half, and one fourth of the initial rich medium volumes. In the fresh defined media the cells were left to adapt for 20 minutes and finally induced with nisin. The *L. lactis* cells growths were followed by measuring the OD₆₆₀. After 2.5 hours the cells were harvested. LmrA expression was monitored with SDS-PAGE.

2. The cells were initially grown on the chemically defined media containing 50 % of the initial concentration of non labeled amino acid (tyrosine). The ¹³C isotope labeled tyrosine (50 % of the optimum concentration) was added at the induction stage.

Attempts to inhibit aromatic amino acids synthesis

L. lactis strain pNZ9000 over expressing LmrA was grown on the chemically defined medium containing ¹³CO phenylalanine in place of unlabeled phenylalanine and in the presence of glyphosate (1 g/L) (Kim et al., 1990). Prior to addition, glyphosate has been dissolved in 1 M NaOH.

Solid-state NMR measurements

All experiments were performed on a Bruker Avance 600 spectrometer equipped with a 4 mm MAS DVT probe. The measurements were performed at 150.9 MHz for ¹³C, 70.9 MHz for ¹⁵N using a CPMAS pulse program employing a 80-100% ramped Hartmann-Hahn condition, two pulse phase modulated (TPPM15) heteronuclear ¹H decoupling at a field of 62.5 kHz and a 49 ms acquisition time. CP contact times and recycle delay times were respectively 1.5 ms and 2 s. Spectra were zero filled to 16K points and 100 Hz exponential line broadening was applied during processing. Spectra were referenced externally to the carbonyl resonance of glycine at 176.03 ppm (¹³C), (¹⁵NH₄)₂ SO₄ 27 ppm. For each ¹³C spectrum between 20k to 30k scans were accumulated.

2. 3. Results

2.3.1. Optimization of defined media composition

Figure 2.1A shows that the *L. lactis* growth curve was not significantly affected by varying the amino acids concentrations. Therefore, increasing the amino acid concentration would more likely lead in future to a waste of expensive isotopic labeled amino acids. The usage of the defined medium, composed of variety amino acids, implies that an excess of amino acids facilitates amino acids incorporation, preventing their biosynthetic degradation. For this reason, lowering the amino acid concentration in the chemically defined medium should be done with caution. The optimal concentrations of amino acids are listed in the Table 2.1.

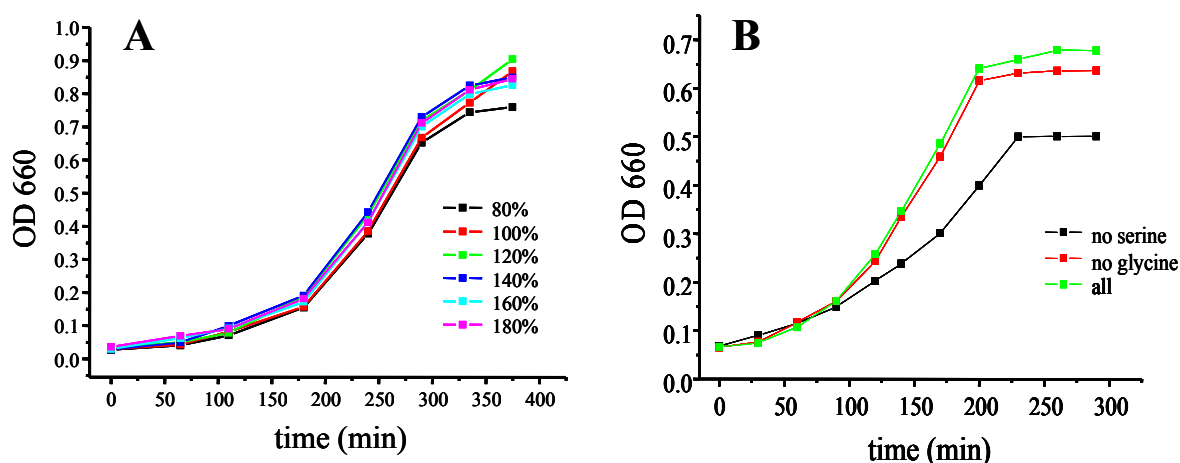


Figure 2.1: (A) Growth of *L. lactis* with different amino acid concentrations, accordingly, 80, 100, 120, 140, 160, 180 % amino acids when comparing with the amounts listed in the Table 2.1. Total protein concentrations in all cases were ca. 3 mg/L. (B) *L. lactis* growths in the chemically defined media with either serine (black line) or glycine (red line) missing; CDF media with complete amount of amino acids (green line) (Table 2.1).

L. lactis growth was not essentially altered when glycine and tryptophan were missing in the defined media, moderate inhibition of *L. lactis* growth was noticed in case of serine (Figure 2.1B, 2.2) as well as when both glycine and serine together were removed from the defined media (Figure 2.2).

Figure 2.3A compares typical *L. lactis* growth curves for the optimized defined medium versus M17 medium. *L. lactis* grow in the chemically defined medium approximately with the same rate as in the M17 medium until OD₆₆₀ reaches 0.8 where the bacteria enter stationary phase in defined media but continued their growth in the rich media. LmrA yield in the defined medium was ca. 1 mg/L which is

three times less when compared with the M17 medium (ca. 3 mg/L). The protein over production and its reproducibility in the chemically defined medium and the M17 is conformed by SDS-PAGE (Figure 2.3B).

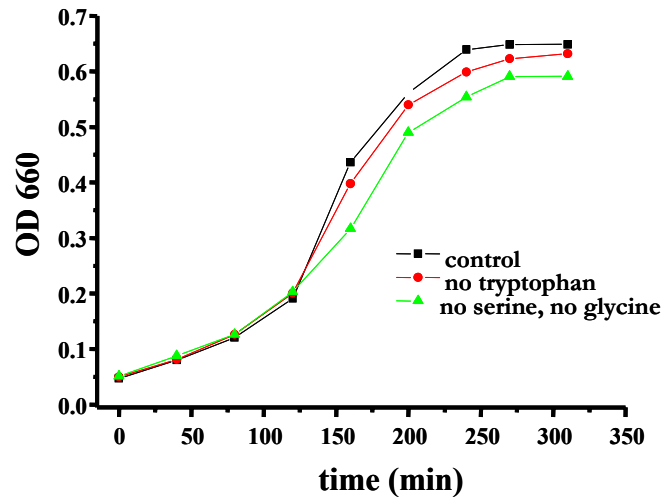


Figure 2.2: *L. lactis* growths in the chemically defined media with either no tryptophan (red line), or no serine and glycine, (green line) defined media with complete amount of amino acids (black line) (Table 2.1).

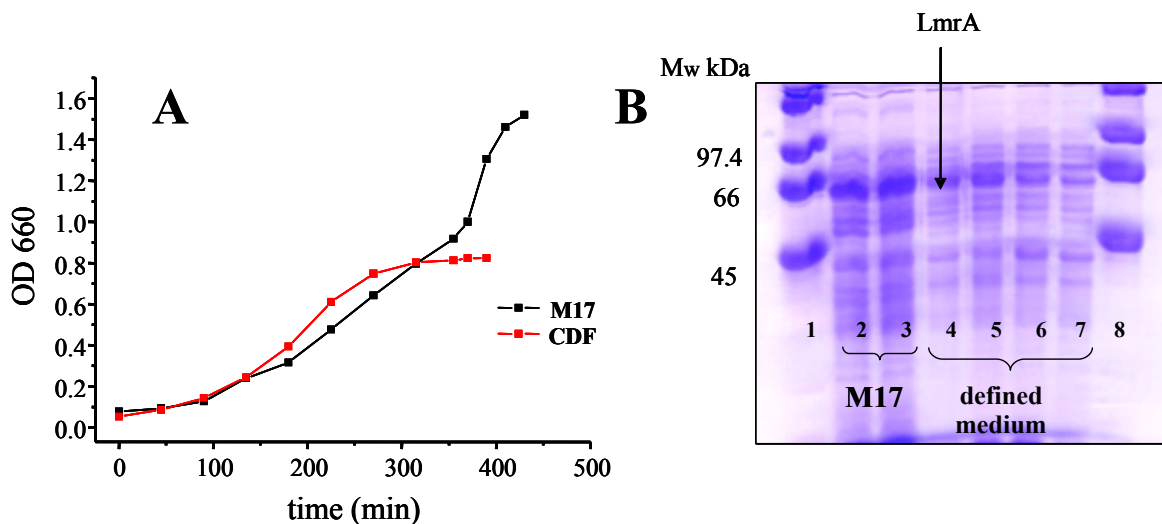


Figure 2.3: (A) *L. lactis* growth in the M17 (ca. 10 mg/L total protein) and in the chemically defined medium (CDF) (ca. 3 mg/L total protein). *L. lactis* grew in CDF approximately to half of the cell density when comparing with the M17 medium and this difference in cell densities is reflected in total protein concentration. (B) SDS - PAGE analysis with 40 % acrylamide gel shows LmrA overexpression in *L. lactis*: 1, 8 -- standards; 2, 3 – *L. lactis* ISOV, M17 media; 4 - 7 – ISOV, the defined medium.

Hoechst transport assay in ISOVs

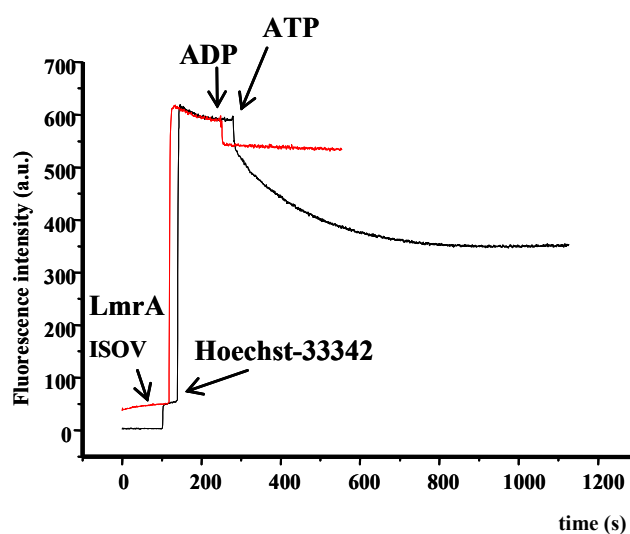


Figure 2.4: Hoechst-33342 transport in the membrane vesicles. LmrA – mediated transport was measured by fluorescence Hoechst-33342 assay. Dye was added after 1 minute of incubation at a room temperature. When intensity of fluorescence reached plateau ATP or ADP was added.

To examine the functional state of LmrA overexpressed in the chemically defined medium a Hoechst transport assay was performed. Hoechst-33342 has been shown to be a substrate for LmrA and P-glycoprotein (Shapiro and Ling, 1995). The Hoechst transport assay is based on the well known fact that Hoechst-33342 dye is fluorescent in lipid environment and non-fluorescent in aqueous environment. Addition of Hoechst-33342 to ISOVs results in a steep increase in fluorescence intensity due to the rapid partitioning of dye into the vesicles (Figure 2.4). Hoechst-33342 binding to the liposomes was essentially complete within 30 seconds, as judged by the fluorescence increase. It has been shown earlier that about 90 % of the Hoechst-33342 added became bound to the lipids (Shapiro and Ling, 1995). At the point when Hoechst-33342 fluorescence reaches equilibrium distribution between the vesicles and buffer environment ATP is added. A 5-10 % fluorescence drop immediately after ATP addition is caused by dilution. Slow fluorescence intensity decrease follows ATP addition because of Hoechst-33342 pumping out of the lipid layer. An ATP regeneration system consisting of creatinine kinase and creatinine phosphatase maintains constant ATP concentration which allows observing pumping on a time scale of up to 1000 seconds. Control experiments are made with ADP place ATP. No changes in Hoechst-33342 fluorescence intensity are observed after addition of ADP.

2.3.2. Metabolic labelling of LmrA ISOVs with ^{13}C labeled amino acids

CPMAS spectra of ^{13}C LmrA ISOVs natural abundance and ^{13}C glycine labeled LmrA ISOVs were recorded at temperature as low as 253K (Figure 2.5). Together with the signal from lipids, the spectra showed increased intensity in the amino acid carbonyl resonance region. Subtraction of CPMAS spectra of ^{13}C LmrA ISOVs natural abundance from ^{13}C glycine labeled LmrA ISOVs (Figure 2.5) revealed the presence of the labeled LmrA in the sample manifested as a peak at 172.4 ppm.

The large number of glycine residues and low chemical shift separation precludes the extraction of information from the spectra in Figure 2.5. Less abundant amino acid is tyrosine, there are 14 tyrosine residues in LmrA sequence compared with 49 glycines and several tyrosines are located in the transmembrane helices 5 and 6 which are proposed to be involved in the drug binding and transport (Ecker *et al.*, 2004). It is widely thought that aromatic amino acids like tyrosine might form the binding sites for drugs (Dougherty, 1996). Hence, labeled tyrosines might provide a valuable reporter on LmrA function.

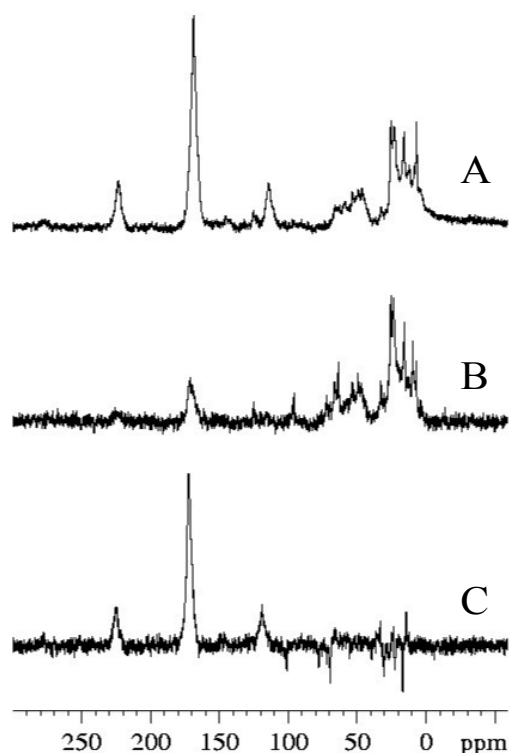


Figure 2.5: ^{13}C CPMAS spectra of LmrA ISOVs A) ^{13}C labeled glycine LmrA ISOV, B) ^{13}C natural abundance LmrA ISOVs, C) spectral subtraction (A from B) revealing contribution from protein. Spectra recorded at 8 kHz MAS spinning frequency and at temperature of 253K.

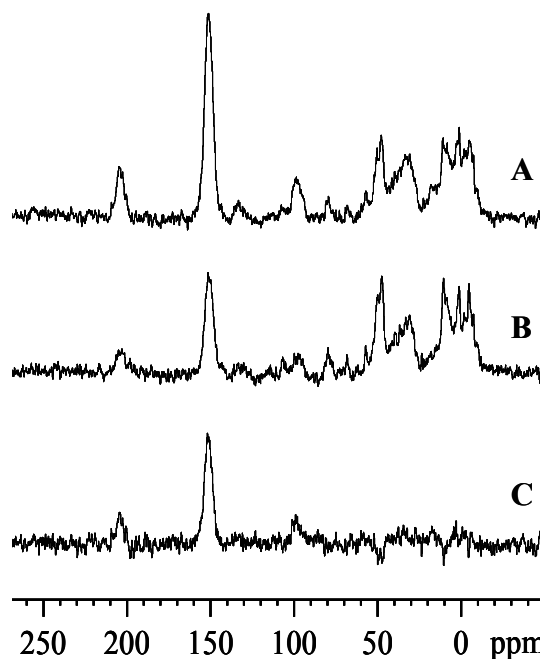


Figure 2.6: ^{13}C CPMAS spectra of LmrA ISOVs A) ^{13}C labeled tyrosine LmrA ISOVs, B) ^{13}C labeled ISOVs prepared from *L. lactis* strain 8048, C) spectral subtraction (A from B) revealing contribution from LmrA. Spectra recorded at 8 kHz MAS spinning frequency and at temperature of 243K.

The CPMAS spectrum of ^{13}C tyrosine labeled LmrA ISOVs was compared with the CPMAS spectrum of ^{13}C tyrosine labeled ISOVs produced by *L. lactis* strain 8048 which does not over express LmrA. Both spectra were recorded at 243K. The subtraction of the first spectrum from the second (Figure 2.6) confirmed the presence of ^{13}C tyrosine labeled LmrA. However the chemical shift resolution of spectrum for fourteen ^{13}C tyrosines is not any better when compared to ^{13}C forty nine glycines. The reasons for this may include high background signal from other labeled proteins in ISOVs and from ^{13}C natural abundance.

2.3.3. Attempts to enhance protein yield and labelling efficiency

Attempts to enhance protein yield

A simple procedure to increase the yield of isotopically labeled proteins presented by Marley (Marly *et al.*, 2001) was applied. The idea is to grow the cells predominantly on unlabelled rich medium

allowing rapid growth to high cell densities and then at induction point to transfer the cells into isotopically labeled defined medium. This method aims for more efficient and targeted incorporation of often expensive isotope labeled amino acids into the protein of interest.

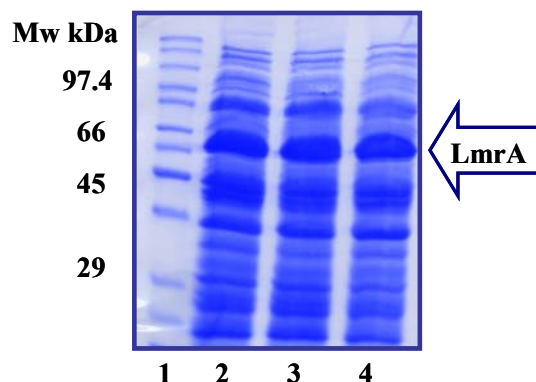


Figure 2.7: SDS-PAGE analysis with 40 % acrylamide gel as the evidence of LmrA over expression in *L. lactis* grown in 1 liter (2), half liter (3), and one fourth liter (4) of the defined media, transferred from 1 liter of M17 media, standards (1).

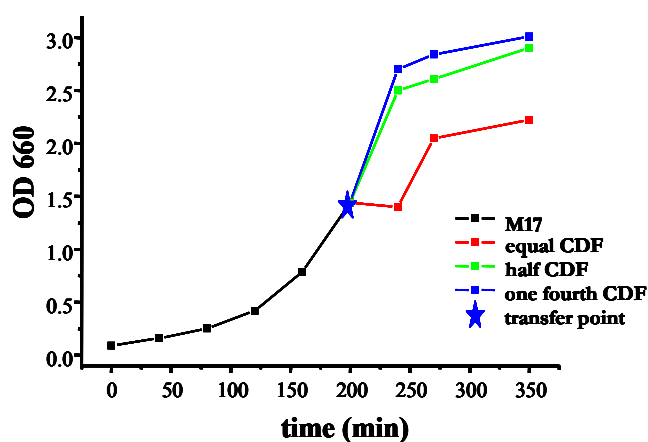


Figure 2.8: *L. lactis* growth in the chemically defined medium. The *L. lactis* cells were grown in the M17 media (black line) and further transferred in equal (red line), half (green line), and one fourth (blue line) volume of the defined media comparing to initial M17 media volume. The growths were followed by measuring OD₆₆₀.

The bacterial growths were followed before and after transferring from the M17 into equal, half and one fourth volume of the chemically defined media compared with the initial volume of rich media, as described in the methods (Figure 2.8). The total protein yields determined for all three cases were accordingly 28, 44 and 144 mg per liter of the defined media. The increased cell densities and total protein concentrations reflect mainly different cells densities at the initial point of cell growth in the

defined media; the real increase in protein expression level is not that high. The LmrA over expression is shown on SDS-PAGE (Figure 2.7). In the next step the ^{13}C tyrosine incorporation with the method described above was compared for the strain 8048 (not over expressing LmrA) and pNH LmrA. The CPMAS spectra for both cases were recorded at 243K (Figure 2.9). The spectrum shows the signal in the protein carbonyl region confirming efficient ^{13}C tyrosine incorporation. Subtraction of the spectra allows an estimate that LmrA comprises approximately 20 % of the total protein. The ^{13}C tyrosine resonances overlap on the spectra (Figure 2.9) and the resonances from different residues can not be resolved.

LmrA his-tagged purification was performed as described in the methods. Unfortunately, it was not possible to purify LmrA although LmrA over expression in ISOVs was clearly shown by SDS PAGE electrophoresis (Figure 2.7). Prolonged protein solubilization time (up to 3 hours) led to the same results.

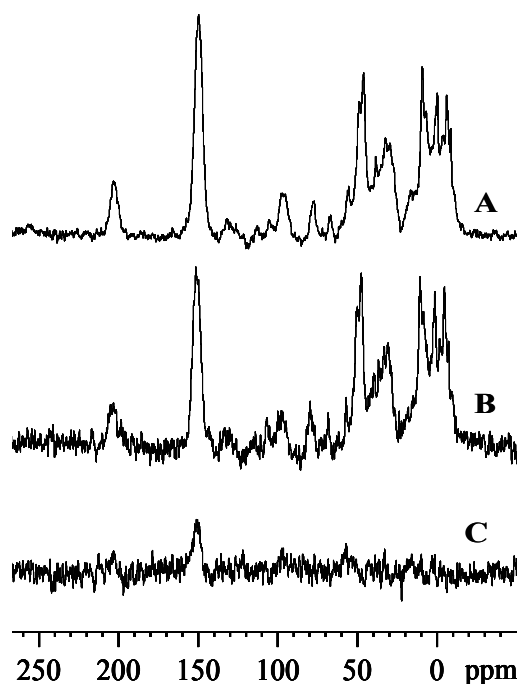


Figure 2.9: ^{13}C CPMAS spectra of LmrA ISOVs A) ^{13}C labeled tyrosine LmrA ISOVs, B) ^{13}C labeled tyrosine 8048 ISOVs. In both cases cells are grown on the M17 medium until OD_{660} 0.9 and transferred into the isotope enriched medium. To prepare LmrA enriched ISOVs, cells were induced after transferring. C) spectral subtraction (A from B) revealing increased signal from ^{13}C tyrosine labeled LmrA. Spectra recorded at 8 kHz MAS spinning frequency and 243K.

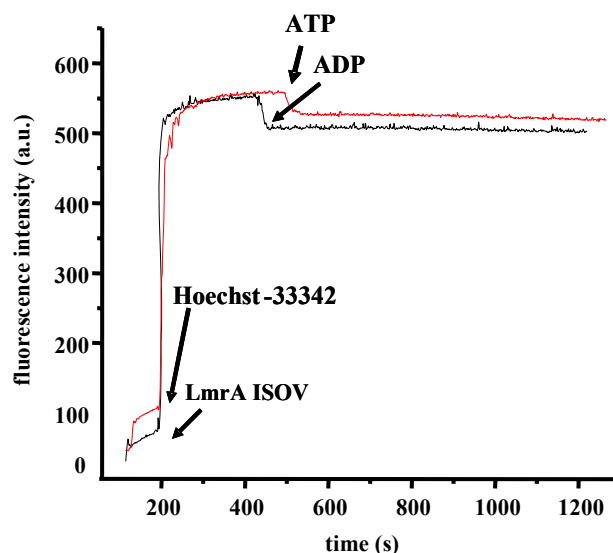


Figure 2.10: Hoechst-33342 transport assay result obtained for the membrane ISOVs performed for *L. lactis* cells transferred from M17 media into equal, half and one fourth volumes of defined media versus initial M17 media volume. Dye was added after 1 minute of incubation at room temperature. When intensity of fluorescence reached plateau ATP or ADP was added.

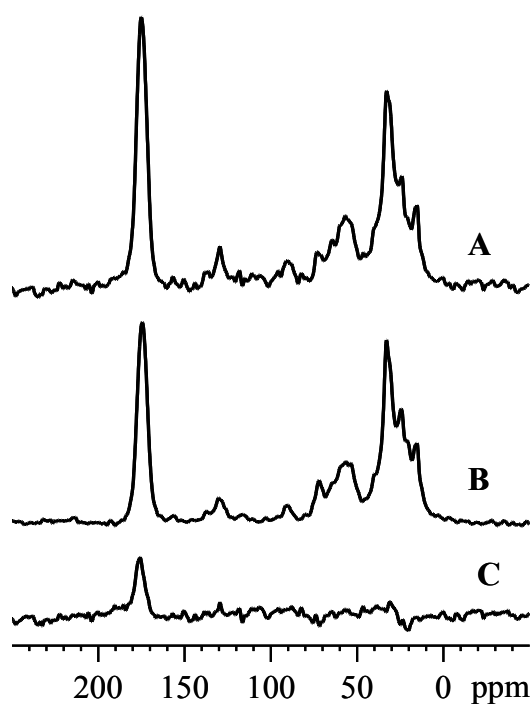


Figure 2.11: ^{13}C CPMAS spectra of LmrA ISOVs A) ^{13}C labeled tyrosine LmrA ISOVs prepared from *L. lactis* cell grown on the chemically defined medium containing full amount of ^{13}C tyrosine from the beginning B) ^{13}C labeled tyrosine ISOVs prepared from the cells grown on the chemically defined medium enriched with half amount of labeled tyrosine at the induction point. C) spectral subtraction (A from B) revealing reduced ^{13}C tyrosine incorporation Spectra recorded at 8.5 kHz MAS spinning frequency and at 260K.

In addition, Hoechst transport assays on ISOVs performed from *L. lactis* cells transferred from M17 media into equal, half and one fourth volumes of defined media versus initial M17 media volume were unable to detect the active protein. Figure 2.10 shows typical Hoechst-33342 transport assay results.

The trial to reduce cost of labels was done using the protocol developed by Cai (Cai et al., 1998) for protein expressed in *E. coli*. For this purpose *L. lactis* cells were grown on the defined media in which half the required amount of the isotope labeled amino acid was added after induction. The ^{13}C spectrum of ISOVs prepared from the cells grown in this way is compared with the spectrum of ISOVs prepared from bacteria cells cultured on defined medium containing the whole amount of isotope labeled tyrosine from the beginning (Figure 2.11). The spectral subtraction reveals that ^{13}CO tyrosine incorporation is slightly reduced when only half amount of labeled amino acid is added after induction point; however the signal in carbonyl region from ^{13}CO tyrosine remains strong.

Attempts to inhibit aromatic amino acids synthesis

A method to achieve more efficient incorporation of labeled aromatic amino acids has been previously introduced for *E. coli* (Kim et al., 1990). The idea of this approach is that the glyphosate inhibits 5-enolpyruvylshikimic acid-3-phosphatesynthase reaction needed for aromatic amino acids biosynthesis. In this way aromatic amino acid synthesis is hampered and bacteria are obliged to incorporate endogenous amino acids. In principle, by applying this method, any aromatic amino acids might be incorporated with similar efficiency to auxotrophic strains (Kim et al., 1990).

Figure 2.12 shows the comparison of ^{13}C spectra of *L. lactis* ISOVs containing ^{13}C labeled phenylalanine. The cells were grown on the chemically defined media with and without glyphosate inhibitor; however the spectra did not show the expected increase label incorporation when inhibitor is used.

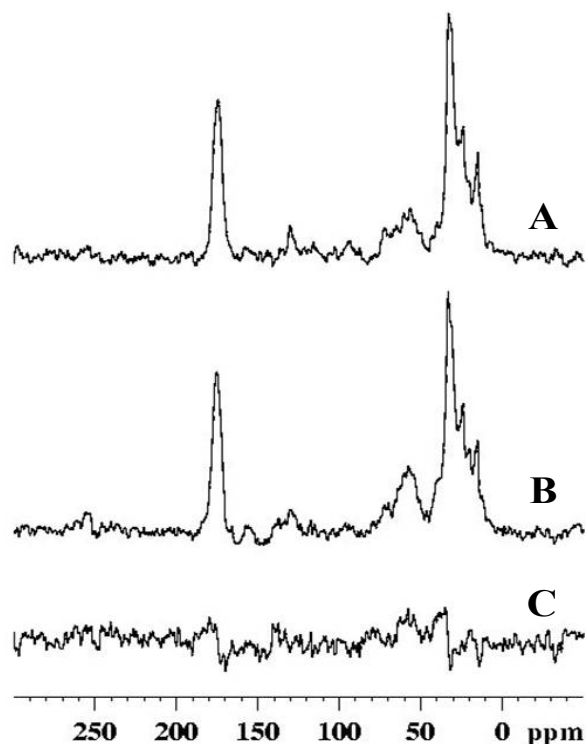


Figure 2.12: ^{13}C CPMAS spectra of ^{13}C labeled phenylalanine LmrA ISOVs, the bacteria were grown in the presence of glyphosate A) and in the absence of inhibitor B), spectral subtraction C) (A from B) revealing no difference in ^{13}C phenylalanine incorporation. Spectra recorded at 8 kHz MAS spinning frequency and 255K.

2. 4. Discussion

2.4.1. Optimization of defined media composition

A rational medium for *S. cremoris* and *S. lactis* growth was first reported nearly 20 years ago (Poolman and Konings, 1988). Based on this work the nutritional requirements for *L. lactis* strain 2118 have been assessed (Cocaign-Bousquet *et al.*, 1995a). However, it is known that each *L. lactis* strain differs in its nutritional requirements, meaning the results obtained for strain 2118 cannot be simply accepted for strain pNZ9000. The optimal conditions must be reconsidered to achieve maximal labelling efficiency along with minimal label scrambling and label cost. Special care was taken checking the amino acid requirement. For biosynthetic labelling, selected amino acids are replaced with their expensive isotope labeled analogues. Therefore, for cost efficient labelling we needed to find optimal concentrations of amino acids allowing sufficient cell growth. In Figure 2.1 the

growth of *L. lactis* with different amino acids concentrations is shown. The optimal amino acids concentrations were obtained (Table 2.1).

To characterize individual amino acids requirements, the LmrA over expressing strain pNZ9000 was grown on the defined medium from which either tryptophan, or serine, or glycine, or both serine and glycine were removed. Glycine and serine was chosen because for strain 2118 their absence in defined media led to important decrease in the growth rate (60 %) and because cheap ^{13}C labeled glycine was planned to be used as a first labelling reporter (Cocaign-Bousquet *et al.*, 1995a). In our case only a moderate decrease in the growth rate was observed when either serine, or glycine, or both serine and glycine were removed. This growth rate decrease was attributed to serine, because its addition to growth medium restored almost correct growth (Figure 2.1B, 2.2). It has been shown for *L. lactis* strain 2118 that serine is normally consumed at a high level and is used for ammonia metabolism (Novak *et al.*, 1997). It is likely that only a moderate growth inhibition is observed in medium lacking serine because the experimental medium contains NH_4Cl as an additional source of ammonia. Our observations together with existing knowledge lead us to think that uniformly ^{15}N labelling might be possible in a medium containing a ^{15}N labeled nitrogen source and ^{15}N labeled serine (Novak and Loubiere, 2000; Otto *et al.*, 1983). Considering uniform ^{13}C labelling, it is known that a small but significant part of glucose is converted into the cell structural material serving as a carbon source giving the totality of nearly all amino acids (Mahmound *et al.*, 2004; Novak and Loubiere, 2000; Otto *et al.*, 1983). Therefore uniform ^{13}C LmrA labelling might be considered in future as well. For this purpose glucose must be replaced by its ^{13}C analogue in the chemically defined medium.

To probe the effect of the aromatic amino acid, tryptophan, on bacterium growth, LmrA expressing *L. lactis* were grown on media lacking tryptophan (Figure 2.2). The absence of tryptophan in defined medium did not lead to any significant growth rate suppression. Comparing the data obtained for serine, glycine and tryptophan for the strain pNZ9000 with results reported for strain 2118 (Cocaign-Bousquet *et al.*, 1995a), we conclude that both strains behave in similar way in respect to these three amino acids. The only difference is that the dramatic suppression of the bacterium growth rate reported for the strain 2118 in case of serine absence is much more pronounced when compared with

the LmrA over expressing strain. Summing up all the results it can be concluded that apart from amino acid concentration all the other components (vitamins and salt) do not need further considerations and their concentrations can be used as defined for strain 2118. Taking into account the importance of serine for ammonia metabolism, we clearly would not be able to label serine with this biosynthetic approach.

L. lactis growth has been further compared in the optimized defined and complex organic (M17) media. *L. lactis* grew with similar rate in both media; however the bacterium entered the stationary phase earlier when grown on the defined medium (Figure 2.3A). The reasons why the cells growth is limited in the defined medium are obscure. As pH remains fairly constant during cell growth (Otto et al., 1983), it can not effect the growth (Mierau et al., 2005). It has been reported that accumulation of H₂O₂ and lactate by *Lactococci* occurred in synthetically defined media. Both H₂O₂ and lactate are toxic and retards growth above certain concentration. For H₂O₂ it is considered that the primary lack of catalase causes destruction of cell components and several of the potentially glycolytic enzymes (glucokinasa, glyceraldehydes-3 phosphate dehydrogenase and fructose-1, 6-dophoshate) are known to be inhibited by H₂O₂ (van Niel et al., 2002). This would also explain the fact that enhancement of amino acids concentration does not increase protein yield (Figure 2.1A) as it would be expected if the medium was simply exhausted at OD₆₆₀ 0.8. SDS-PAGE analysis with 40 % acrylamide gel shows that over expression of *L. lactis* LmrA protein in the defined and in M17 media are comparable (Figure 2.3A).

Nevertheless sufficient cell densities for *L. lactis* growth on defined media can be obtained. The chemically defined medium was tested by selective labelling of LmrA with ¹³CO tyrosine and glycine (Figure 2.5, 2.6). The efficiency of labelling is difficult to estimate. Estimation of labelling levels often relies on mass spectrometry (Cai et al., 1998). However, despite progress made recently in the mass spectroscopy field, a number of technical issues remain to be addressed. Among them are the relationships between the amount of analyzed sample and obtained signal intensity, which is complex and incompletely understood, and technical difficulties in membrane proteins ionization (Meng et al., 2004; Aebersold and Mann, 2003). As a result, the examples of mass spectroscopy on membrane proteins are rare (Venter et al., 2002).

2.4.2. Metabolic labelling of LmrA ISOV with ^{13}C labeled amino acids

The spectra presented on Figure 2.5 and 2.6 show the incorporation of labeled amino acids analogues into the protein sequence. ^{13}C tyrosine and glycine resonances from labeled LmrA overlap on MAS NMR spectra due to the relatively high natural abundance of ^{13}C (1 %) and possible labels incorporation into other than LmrA *L. Lactis* proteins. Subtraction of ^{13}C CPMAS spectrum of labeled ISOVs produced from *L. lactis* strain 8048, which does not over express LmrA, from a spectrum of labeled ISOVs containing 30 % of over expressed LmrA could potentially remove the natural abundance background. However the resolution of the difference spectrum is not sufficient to resolve individual residues. The internal MAS rotor volume is not big enough to increase signal to noise ratio simply by taking more material for measurements. One possible solution could be to enhance the protein concentration in the ISOVs and this way to make signal from labeled protein dominant.

To examine the function state of LmrA overexpressed in the chemically defined medium the Hoechst transport assay was performed (Figure 2.4). Hoechst-33342 is shown to be substrate for LmrA and P-glycoprotein (Shapiro and Ling, 1995). The slow rate of Hoechst-33342 pumping represents the difference between the rate of substrate transport out of the membrane and the rate of rebinding of transported Hoechst-33342 to the membrane.

2.4.3. Attempts to enhance protein yield and labelling efficiency

Attempts to enhance protein yield

An approach to enhance the production of isotope labeled protein was applied accordingly to (Marly *et al.*, 2001). The idea of this method is to generate cell mass using unlabeled rich media followed by exchange into a smaller volume of labeled media. Thus, the consumption of costly isotope labels is reduced, by-products inhibiting cell growth are removed and, finally, a high yield of isotope labeled protein can be achieved. It was shown that a higher level of protein production (Figure 2.7) and labelling (Figure 2.9) can be achieved. Unfortunately, it was not possible to purify protein from the

cells and the over expressed protein in ISOVs was found to be inactive (Figure 2.10).

Apart from the possibility that the protein over expressed under such media exchange condition is not fully matured at the stage of biosynthesis, it is possible that the protein is stably folded, but it adopted a fold which is not the native conformation of the protein. Such misfolding can occur at some point during the protein solubilization or even purification leading to hampered accessibility of the His-tag. The presence of this problem is difficult to detect and solve. There are methods known to correct membrane protein misfolding during solubilization and purification. The usage of protein denaturants (urea, for example) in the presence of detergent can potentially unfold misfolded protein bound to an affinity column, the further removal of denaturant on the column is suggested to lead to protein refolding in to a native-like conformation (Rogl *et al.*, 1998). A second method, known as 'reconstitutive refolding' includes protein purification into dodecylphosphocholine (DPC) micelles followed by mixing with POPC lipids and dialytic removal of DPC (Gorzelle *et al.*, 1999). Unfortunately, both methods could not be applied to LmrA; because the protein is not stable under denaturing conditions and, in our experience, aggregates quickly while dialyzing.

Degradation of membrane proteins can be also an important factor which abolishes the protein production. The mechanism of membrane protein degradation is not well studied, but a couple of examples, such as SecY translocase component, are known. SecY needs to be over expressed together with SecE component, otherwise it is prone to degradation (Kihara *et al.*, 1995). Moreover, protein over production can trigger stress responses and thus degradation of the target protein in the cell (Mierau *et al.*, 2005)

One further way to reduce labelling cost is to add the expensive labeled amino acids after induction and in smaller amounts. The idea is that after induction the cells are mainly involved in expression of the target protein and therefore expensive isotope labels amino acids will be incorporated mostly in the over expressed protein (Lian and Middleton, 2001b). In this way site specific label incorporation can be achieved and theoretically label scrambling might be minimized. In Figure 2.11, reduced but still essential labeled amino acid incorporation is shown, when this method is applied.

Attempts to inhibit aromatic amino acids synthesis

In the next step the trial has been done to improve efficiency of aromatic amino acid incorporation by inhibiting these amino acids synthesis. For this purpose glyphosate, an inhibitor of 5-enolpyruvylshikimic acid-3-phosphate synthase, was added in the defined growth medium. Figure 2.12 shows that the level of ^{13}C phenylalanine incorporation is not altered when glyphosate is added. It is known that *L. lactis* biosynthetic pathways are simpler in comparison with *E. coli*. The result of this simplicity is that the bacterium prefers to consume amino acids rather than to synthesize them (Konings et al., 2000). This way the amino acid incorporation is very efficient and addition of any amino acid synthesis inhibitors has no influence. An alternative explanation could be that glyphosate inhibition is not valid for *L. lactis*. *L. lactis* biosynthetic pathways are less well understood than those of *E. coli* and the effect of different enzyme inhibitors is difficult to predict.

Conclusion

The chemically defined medium needed to perform biosynthetic selective amino acid labelling of ABC transporter LmrA in *L. lactis* for NMR purposes is developed. The first spectra of inside-out vesicles containing 30 % of over expressed and ^{13}CO glycine/tyrosine labeled LmrA conform successful labelling. The method to half reduce isotope labeled amino acid quantities in comparison with amounts listed in Table 2.1 is successfully applied to *L. lactis* system. The functional state of LmrA over expressed in the chemically defined medium was demonstrated with fluorescence Hoechst-33342 assay.

3. Purification and reconstitution of LmrA in various lipids for solid-state NMR

Abstract

SSNMR imposes strict constraints on a sample preparation with respect to protein purity, reconstitution at high protein lipid ratio, and sample homogeneity. As soon as large quantities of selectively isotope labeled LmrA can be produced in *L. lactis*, the next large problem to overcome prior SSNMR experiments is the concentration of liposomes reconstituted with the protein in a NMR rotor. To achieve a decent signal-to-noise ratio while doing SSNMR measurements, the protein incorporation into liposomes has to be of a ratio of about 1:100 mol/mol (protein/lipid). This protein lipid ratio exceeds the ratios used typically for functional assays in approximately 3-5 times. Therefore, the procedure for reconstitution of LmrA into *E. coli* and synthetic lipids at a high protein lipid ratio (1:300 mol/mol) has been established. The homogeneity of reconstitution and protein function state in reconstituted form has been probed subsequently with freeze-fracture microscopy, sucrose gradient, and functional assay.

The results of this Chapter have been partially published: Mason A.J., Siarheyeva A., Haase W., Lorch M., van Veen H., Glaubitz C., Amino acid type selective isotope labelling of the multidrug ABC transporter LmrA for solid-state NMR studies, FEBS Letters 568 (1-3): 117-121 June 18 2004.

3.1. Introduction

As it has been observed, some model membrane system better mimic the structural, dynamic and morphological properties of native bilayers than others. In general, the resemblance to native membrane decreases in the order: vesicles > bicelles > mixed micelles > micelles > amphipoles (Sanders and Oxenoid, 2000). The membrane proteins are extremely difficult to study, therefore every advantage should be taken in preparation of the model system. For a number of membrane proteins satisfactory resolution can be obtained in detergent, however the liposomes surely provide better

interactions that integral proteins require (Krueger-Koplin et al., 2004). The fact that most membrane proteins are fully active only when they are correctly inserted in a lipid bilayer is well known and accepted. Accordingly, in many instances the ability to investigate membrane proteins is limited by the necessity to functionally reconstitute these proteins into liposomes.

Despite the fact that many proteins have been functionally reconstituted into artificial lipid membrane, the molecular mechanisms of membrane reconstitution with integral membrane proteins are still poorly understood and the methods often lack reproducibility. The situation with ABC transporters is even more complicated. In recent years, the purification and reconstitution of only a few members of the ABC transporter family in a functionally active form has been achieved (Hagmann *et al.*, 2002; Mao *et al.*, 2000; Callaghan *et al.*, 1997a; Shapiro and Ling, 1995). For biochemical investigation the proteins are usually reconstituted at high lipid protein ratio to ensure the protein' function state. So, typical protein lipid ratio in proteoliposomes in this case is usually kept in the order of 1:1000 mol/mol. Current solid-state NMR techniques are insufficiently sensitive to this amount of labeled protein and good quality spectra are difficult to obtain. Usually, the amount of nuclear spins in the sample has to be in the order of μM for decent signal-to-noise ratio to obtain. With the rotor active volume of 20-90 μL , the protein concentration must be in the order of 3-20 mM. For ABC transporter with a molecular mass of 64 kDa, this means that at least 10-15 mg of protein need to be inserted into a small MAS rotor container. In the units of protein to lipid ratio, it means approximately 1:100 mol/mol. In this case, anyway, four-fifths of the sample volume in the rotor is still taken by lipids. Further increase of protein to lipid ratio is dangerous, because it can be associated with protein aggregation or lead to 2D crystals formation. In general, 2D crystals are suitable for SSNMR investigations but unfortunately it is not possible to monitor proteins activity in 2D crystal form.

Four basic strategies of membrane protein insertion into liposomes can be outlined: mechanical means, freeze-thawing, organic solvents and detergents (Rigaud and Levy, 2003). The first three methods find very rare applicability because they cause membrane protein degradation. The amphiphilic nature of most membrane proteins requires detergents, not only in the initial step of their solubilization, but also as a mean of keeping the protein in a non-denaturing environment during further purification and even storage. The standard detergent-mediated method of protein

reconstitution contains the following steps: preforming of liposomes, incubation of detergent solubilised protein with liposomes and finally, removing of detergents (Figure 3.1).

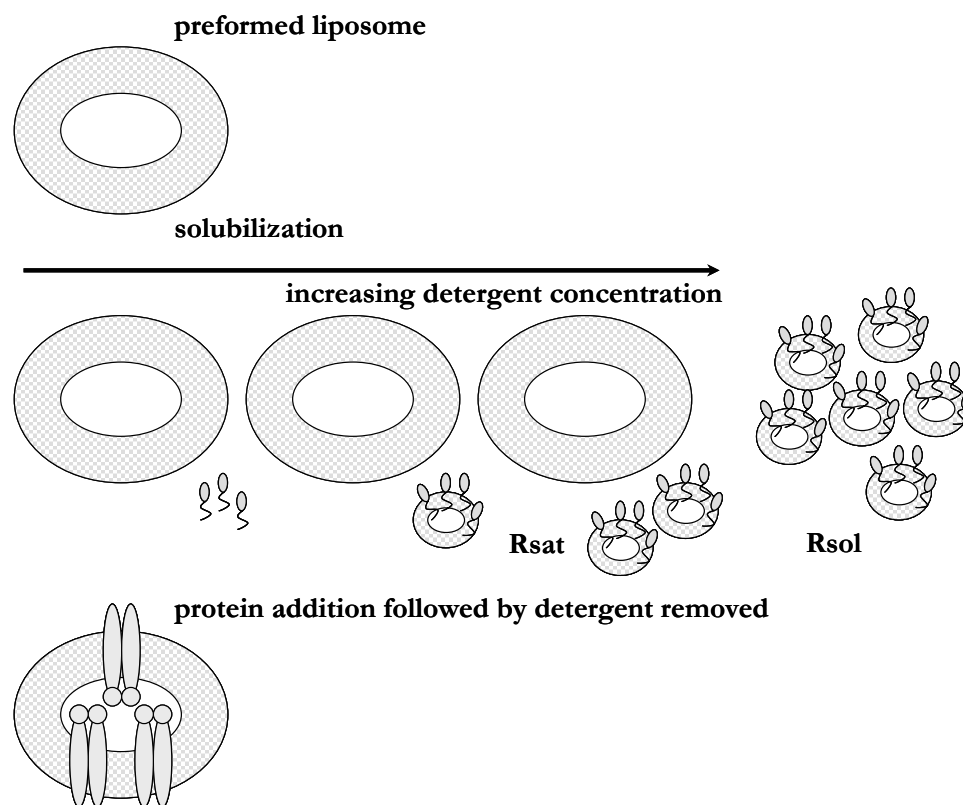


Figure 3.1: The standard reconstitution strategy: preparation of liposomes, step-by-step detergent addition, protein addition and detergent removal.

The liposomes can be preformed in a number of ways, the details can be found elsewhere (Knol et al., 1998). Here lipids are extruded through polycarbonate filters of 100, 200 and 400 nm. The specific internal volumes of liposomes after extrusion through 400 nm filters are $0.90 \pm 0.05 \mu\text{L}/\text{mg}$ of lipids. Subsequent extrusion through 200 nm filters yields a specific volume of $0.73 \mu\text{L}/\text{mg}$ of lipids. The diameter and morphology of liposomes depend on the filters as well. Extrusion through 400 nm filters yields liposomes with average diameter of ~ 350 nm, with only a relatively small fraction being multi-lamellar. Extrusion of these liposomes through 200 nm filters yields lower amounts of multi-lamellar liposomes, whereas the size is reduced to ~ 150 nm. Subsequent extrusion through 100 nm filters reduces the size even further to ~ 100 nm. The latter preparations exhibit irregular shapes and a large

fraction appeared as collapsed structures. In our studies we prepared liposomes exclusively by extrusion through 400 nm filters, as these preparations yield highest level of protein uptake (Knol et al., 1998; Paternostre et al., 1988). This might be especially important in reconstituting such a large protein as LmrA.

The next step in any detergent-mediated reconstitution is solubilization of preformed liposomes. The processes of membrane solubilization can be subdivided into three stages. First, the detergent incorporates into the lipid bilayer (stage 1), which results in a peak of the turbidity at the onset of solubilization R_{sat} (R_{sat} is a maximal detergent concentration at which preformed liposomes are not disturbed by detergent addition). Subsequently the liposomes disintegrate (Stage 2) and a transition takes place from bilayer structures to mixed micelles. Finally, at R_{sol} (R_{sol} is a minimal detergent concentration at which preformed liposomes are solubilised) the liposomes are completely solubilised (Stage 3) and further increase in detergent concentration only affects the ratio of detergents to lipids in micelles. The membrane reconstitution of an integral membrane protein can often be optimized by following the insertion of the protein into preformed liposomes, destabilized by detergents in the range R_{sat} to R_{sol} (Figure 3.1).

The turbidity measurements systematically performed as a function of detergent concentration is a simple and effective technique to qualitatively evaluate the lamellar to micellar transitions and the amounts of detergent bound either to the bilayer or to the micelles (Paternostre et al., 1988). This makes the whole procedure well controlled and highly reproducible.

The association of a protein with lipid detergent mixtures has been shown to be a time dependant process, which depends on the nature and the concentration of detergents used for reconstitution. Depending of the nature of the detergent, proteins can either be incorporated directly into detergent-saturated liposomes at the onset of solubilization (mechanism 1), transferred from mixed micelles to detergent-saturated liposomes (mechanism 2), or participate in proteoliposomes by micellar coalescence (mechanism 3). The final protein orientation depends on the mechanism of association. Dodecylmaltoside (DDM)-mediated reconstitution performed here leads usually (Rigaud and Levy, 2003) to direct protein incorporation into detergent-saturated liposomes (Putman *et al.*, 1999). Theoretically DDM could mediate reconstitution in both directions however, the hydrophilic ATP

domain, which is comparable in size with transmembrane part, may prevent a random insertion of the protein into the membrane and lead to a symmetric distribution of orientations (Knol et al., 1997; Paternostre et al., 1988).

The last step of reconstitution is the removal of detergent from the equilibrated lipid-detergent mixtures. Although there are various methods (dialysis, gel filtration and dilution) in use, absorption of detergent molecules on Bio-beads SM-2 has been demonstrated to be the most efficient.

To date, the existing protocol allows LmrA reconstitution with a large excess of lipids. This protocols allows only very limited amount of LmrA, less than 0.1 mg of LmrA, to be placed into a NMR rotor. In an effort to overcome this limitation, the reconstitution LmrA into *E. coli* liposomes has been optimized for a protein lipid ratio of 1:300 mol/mol. The function state of LmrA reconstituted at such a high protein to lipid ratio was confirmed by ATPase assay. In addition to *E. coli* liposomes, LmrA has been reconstituted into several synthetic lipids systems at high lipid protein ratio.

3.2. Materials and methods

Materials

Bio-beads, SM-2 from Bio-Rad Laboratories Inc; *E. coli*, 1-Palmitoyl-2-Oleoyl-*sn*-Glycero-3-Phosphoethanolamine (PE), 1-Palmitoyl-2-Oleoyl-*sn*-Glycero-3-Phosphocholine (PC), 1-Palmitoyl-2-Oleoyl-*sn*-Glycero-3-Phospho-*rac*-(1-glycerol) (PG) lipids from Avanti Polar lipids, Alabaster.

3.2.1. Solubilization and purification of LmrA

LmrA purification was performed as described under Materials and Methods in Chapter 2. Directly from the column the purified LmrA was passed through the analytical gel filtration column. Gel filtration analysis was performed using ÄKTA HPLC system (Amersham Pharmacia) at a flow rate of 0.08 mL/min. 50 μ L of the purified LmrA (approximately 1 mg/mL) directly from the Ni²⁺-NTA column was loaded into a Superose 6 3.2/30 column (Amersham Pharmacia) previously equilibrated with 50 mM Tris, 150 mM NaCl, 0.02 % (w/v) DDM pH 8 buffer.

3.2.2. Reconstitution of LmrA

Bio-beads preparation

Bio-beads preliminarily were washed 3 times with methanol, 5 times with 100 mM Tris 50 mM KCl buffer (pH 7), incubated with *E. coli* lipids suspension (30 µg lipids per 20 mL 100 mM Tris 50 mM KCl pH 7 buffer) for at least 40 minutes and finally washed 3 times with the same buffer. This procedure aims to reduce loss of lipids during the reconstitution procedure.

Detergent solubilization method

E. coli total lipid extract was resuspended in 100 mM Tris 50 mM KCl buffer (pH 7) to a final concentration 4 mg/mL and the suspension were clarified by drop-wise addition of 10 % (w/w) DDM solution. Purified LmrA protein in solution taken directly from the column was added to solubilised *E. coli* lipids. The solution was incubated for 40 minutes and finally 1.5 g bio beads were added per 100 mg DDM in solution. The mixture was placed on a rocking table and became cloudy within 2 hours. The molar ratio of protein to lipids was about 1 to 100.

Liposome destabilization method

Lipids at a starting molar ratio of 200 lipids per protein were suspended in 100 mM Tris, 50 mM KCl buffer at pH 7 to a concentration of 4 mg/mL. The lipid suspension was vortexed briefly and then extruded (Northern Lipid Extruder) 11 times through a 400 nm filter. The liposome suspension was then titrated with a 0.02 M DDM solution as described (Fang *et al.*, 1999; Cocaign-Bousquet *et al.*, 1995b) and mixed with detergent solubilised LmrA. The destabilized liposomes and protein were incubated for 30 minutes on a rocking table at room temperature before bio beads (80 mg/mL) were added. The mixture was incubated for a further 30 minutes on a rocking table at room temperature and then overnight at 4°C. After incubation, the increased turbidity of the solution indicated vesicle formation. After removal of bio beads, the protein-lipid vesicles were pelleted by centrifugation (55000 rpm for 40 min) and layered over a discontinuous sucrose gradient (10-20-30 %). Bands were

collected from the sucrose gradient and washed with 100 mM Tris, 50 mM KCl, 10 mM EDTA buffer at pH 7 before being pelleted and loaded into 4 mm MAS rotor (Bruker GmbH, Karlsruhe, Germany). Protein concentrations were measured using the Bio-Rad DC protein assay kit (Lowry *et al.*, 1951).

Reconstitution into PE/PG and PC/PG/cardioliipin mixtures

For both reconstitutions the lipids were dissolved in methanol chlorophorm mixture 1:1 (v/v). Organic solvents were removed under rotor evaporation. Remaining organic solvents were removed under vacuum for at least 4 hours. Dry lipid film was then resuspended in reconstitution buffer (100 mM Tris, 50 mM KCl, pH 7). The following reconstitution was applied as described for detergent liposome destabilization method above. The molar lipid ratio in PC/PG/cardioliipin mixture was approximately 5:3:2. The molar ratio in PE/PG mixture was 7 to 3.

Electron microscopy

For freeze-fracturing, reconstituted membrane vesicles in suspension were placed between two small copper blades and frozen by plunging into ethane cooled to -180°C by liquid nitrogen. Samples were fractured in a freeze-fracture (400T from Balzers, Lichtenstein) and shadowed with platinum/carbon at an angle of 45 degrees. Replicas reinforced by pure carbon shadowing at an angle of 90 degrees were cleaned from organic material in chromo-sulfuric acid and later analyzed by electron microscopy (EM208S, Philips, Eindhoven, The Netherlands).

Solid-state NMR

All experiments were performed on a Bruker Avance 600 equipped with a 4 mm MAS DVT probe. Experiments were performed at 150.9 MHz and 60.8 MHz for ^{13}C and ^{15}N using a CPMAS pulse program employing an 80-100% ramped Hartmann-Hahn condition, two pulse phase modulated (TPPM15) heteronuclear ^1H decoupling at a field of 62.5 kHz and a 49 ms acquisition time. CP contact times and recycle delay times were respectively 1.5 ms and 2 s for ^{13}C experiments. Spectra were zero filled to 16K points and 100 Hz exponential line broadening was applied during processing. Spectra were referenced externally as described in Chapter 2. Number of scans accumulated for each

measurement varied and indicated in subsequent figure legend.

Enzyme assay

The ATPase assay of reconstituted LmrA was based on a colorimetric ascorbic acid/ammonium molybdate assay to measure the liberation of Pi from ATP. 50 mM ATP and 10 mM vanadate stock solutions were freshly prepared. Reconstituted LmrA was washed twice with 20 mM K-HEPES (pH 7), 5 mM MgSO₄ buffer and resuspended at a final concentration of 2.5 mg/mL. ATPase assays were performed at 30°C in a reaction volume of 20 mL. Following incubation of reconstituted LmrA and ATP (final concentration 5 mM) for 10 minutes, the ATPase reactions were terminated by addition of 40 mL of a freshly prepared acidic solution consisting of 0.48 % (w/w) ammonium heptamolybdate tetrahydrate, 6.6 % (v/v) concentrated sulfuric acid, 0.01 % (w/w) potassium antimonyl tartrate and 0.42 % (w/w) ascorbic acid. Following the addition of 140 mL H₂O and 30 min of incubation at 30°C in the dark, the absorbance was measured at 690 nm. ATPase activity measurements in the presence of 1 mM orthovanadate were obtained in parallel and subtracted from the reading.

Hoechst 33342 assay

Hoechst-33342 assay on LmrA reconstituted liposomes was performed as described under section Materials and Methods in Chapter 2.

3. 3. Results

3.3.1. Solubilization and purification of LmrA

Solubilization of LmrA was performed essentially as described in (Margolles *et al.*, 1999). It has been shown that 1 % (w/v) DDM solubilises 91 % of LmrA, whereas other detergents showed clearly worse results (Margolles *et al.*, 1999). In agreement with Margolles and co-workers, SDS-PAGE analysis revealed that almost all protein is solubilised from ISOVs (Figure 3.3).

The purification was carried out in a single affinity chromatography step as described in (Margolles *et*

al., 1999). The eluted fraction containing his-tagged LmrA was typically at a concentration of 1 mg/mL, and the procedure yielded about 1 mg of LmrA from 15 mg of total membrane protein. Fractions collected at different steps of the purification procedure, and purified protein was analyzed by SDS-PAGE. Analysis of SDS-PAGE gels showed that LmrA is isolated at high purity (Figure 3.3). In addition, van Veen and co-workers have analyzed SDS-PAGE gels and immunoblots with the purified protein using densitometry. It was shown that LmrA can be isolated at levels of approximately 97 % of purity (Margolles *et al.*, 1999).

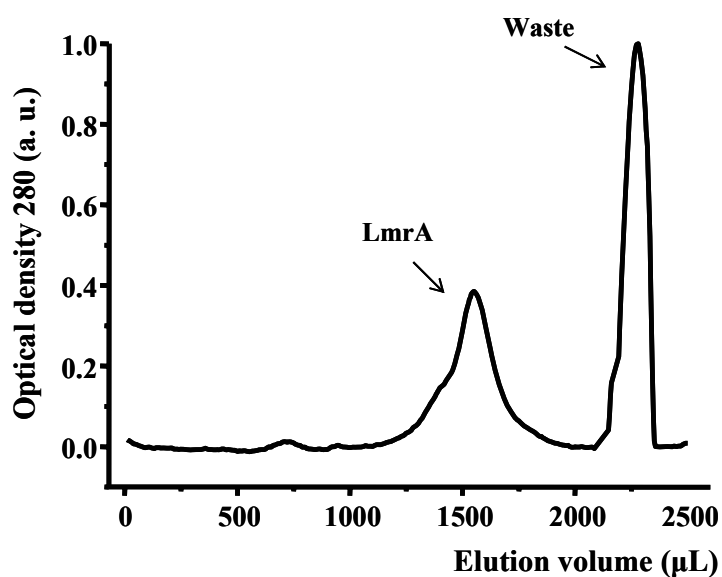


Figure 3.2: Analysis of the purified LmrA (approximately 1 mg/mL) performed by gel filtration on Superose 6 (3.2/30). The 64 kDa LmrA was eluted as a single peak.

In addition, to probe the protein purity, LmrA was loaded into a gel filtration column. The gel filtration showed that purified LmrA in DDM detergent micelles elutes as a single peak, no evidences of aggregated proteins as well as of contaminations from other proteins were visible on gel filtration chromatogram (Figure 3.2).

3.3.2. Reconstitution of LmrA

In both the detergent lipids solubilised and detergent liposome destabilized methods of protein reconstitution, detergent DDM and *E. coli* lipids extracts were used. Polar lipid extracts from *E. coli*

are commonly used in membrane protein reconstitution (White et al., 2000), and they are good model biological membrane. DDM was chosen for liposomes solubilization and destabilization because this detergent is used for protein purification and possible detergent exchange could extend the reconstitution procedure.

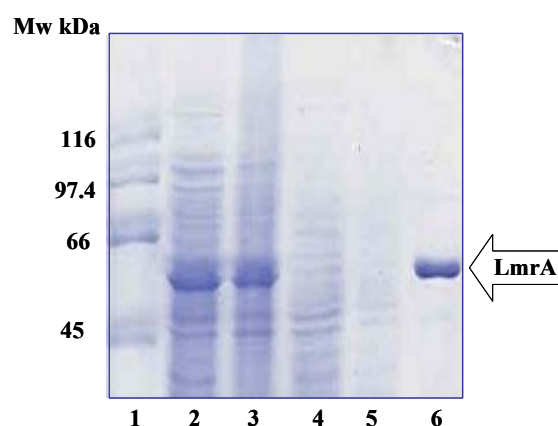


Figure 3.3: Analysis of the purified LmrA (approximately 1 mg/mL) performed by SDS-PAGE analysis with 40 % acrylamide (1) standards, (2) ISOVs containing over expressed LmrA, (3) 3 % DDM solubilised LmrA, (4) Unsolubilised material, (5) wash from the purification column, (6) LmrA purified.

Detergent solubilization method

Detergent solubilised LmrA, eluted from the Ni-NTA column was used immediately for reconstitution at high protein to lipid ratios. Lipids (4 mg/mL) were dissolved completely in the presence of DDM, and mixed with purified LmrA (1 mg/mL). In the next step, detergent was removed rapidly over the course of a few hours with polystyrene beads. The resulting protein-lipid vesicles were collected by centrifugation and the presence of LmrA in the vesicles was confirmed by SDS-PAGE gel analysis (Figure 3.4). In addition, the presence of the labeled LmrA in the sample was confirmed by comparing the spectrum for the reconstituted sample with that of *E. coli* lipids (Figure 3.4). However, electron microscopy revealed that reconstitution is not efficient. The freeze-fracture microscopy showed the liposomes contain no or rare protein incorporations. A substantial amount of protein is simply aggregated (Figure 3.5). Moreover, the sucrose gradient confirmed that the reconstitution is not homogenous. For visual inspection it is clear that LmrA in all three bands is mostly in aggregated form (Figure 3.5).

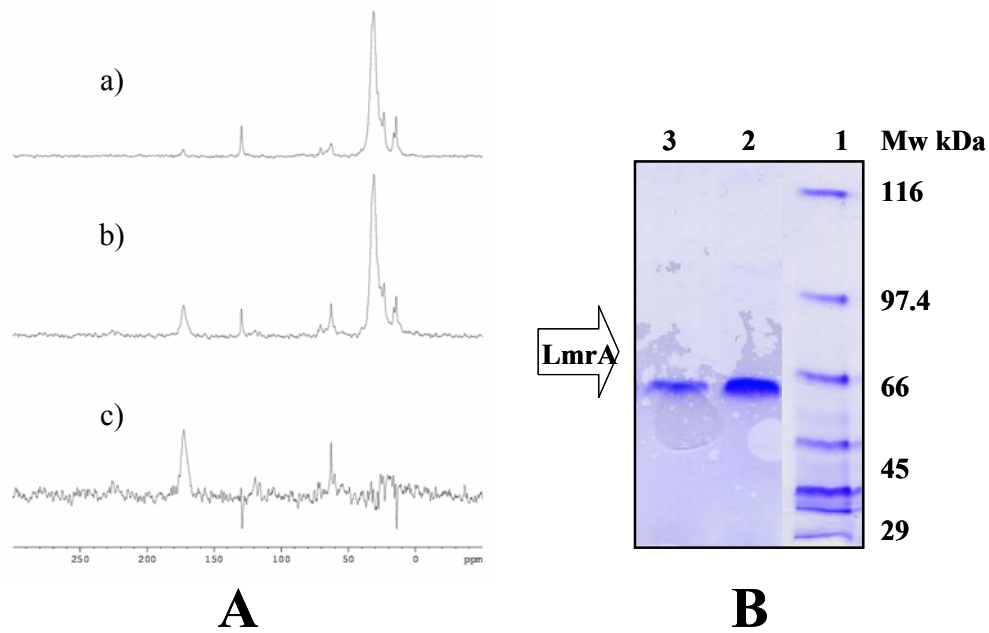


Figure 3.4: A) ^{13}C CPMAS spectra of *E. coli* liposomes reconstituted LmrA by detergent solubilization method; a) protein free lipid vesicles, b) ^{13}CO glycine labeled LmrA reconstituted in lipid vesicles, c) spectral subtraction (a from b) revealing contribution from protein. Spectra recorded at 8 kHz MAS spinning frequency and 253K. B) SDS-PAGE analysis with 40 % acrylamide 1) standards, 2) LmrA purified, 3) LmrA reconstituted into *E. coli* liposomes using detergent liposome solubilization method. Approximately 30k scans were accumulated per each spectrum.

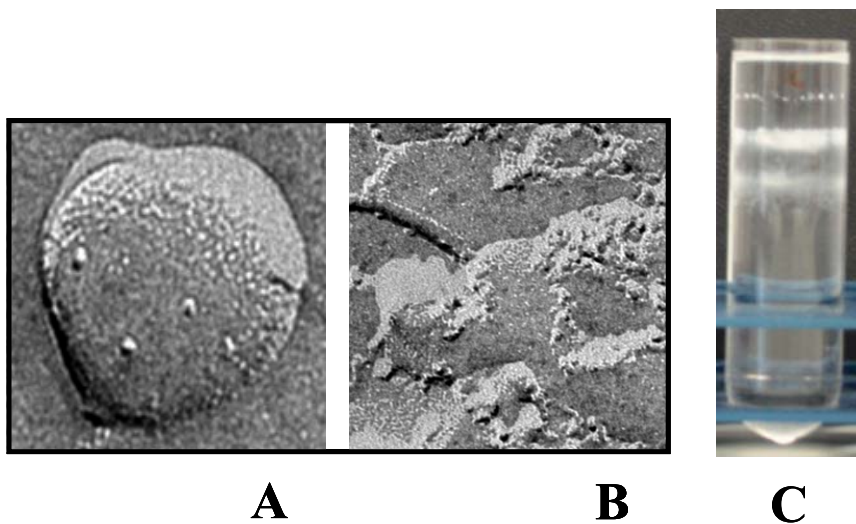


Figure 3.5: The freeze fracture electron micrographs of *E. coli* lipid reconstituted LmrA by detergent lipids solubilization method. A) Free lipid vesicles with limited protein incorporation, B) protein aggregates. The freeze-fracture microscopy was performed by Dr. W. Haase for MPI of Biophysics, Frankfurt. The freeze-fracture micrographs are shown in 16K magnification. C) The 10-20-30 % sucrose gradient of LmrA reconstituted into *E. coli* liposomes using detergent liposome solubilization method. LmrA aggregates are clearly visible in all three bands.

Liposome destabilization method

LmrA was reconstituted by mixing the purified protein with preformed DDM destabilized liposomes, followed by the slow detergent removal. The onset of solubilization (liposomes saturated with detergent) was reached at a concentration of 1 μ mole of DDM /mg of lipid. SDS gel showed (Figure 3.6D) that protein efficiently reconstituted into liposomes and its presence can not be detected in supernatant left after reconstitution. Analysis of proteoliposomes reconstituted LmrA using detergent liposome destabilization method by freeze fracture microscopy showed the presence of protein free liposomes, LmrA aggregates as well as liposomes containing reconstituted LmrA (Figure 3.7A, B, C). The aggregated protein can potentially hamper NMR lineshapes. To clarify how much of protein is actually aggregated the 10-20-30% sucrose gradient was performed. The protein free liposomes were clearly separated from LmrA reconstituted liposomes but not the aggregated protein. The aggregates are kept on the liposomes surface by some kind of interactions, possibly electrostatic. To disturb the electrostatic interactions, the reconstitution buffer was supplemented with 10 mM EDTA. This way the aggregated protein was separated from free and LmrA reconstituted liposomes as it can be seen on a sucrose gradient (Figure 3.7).

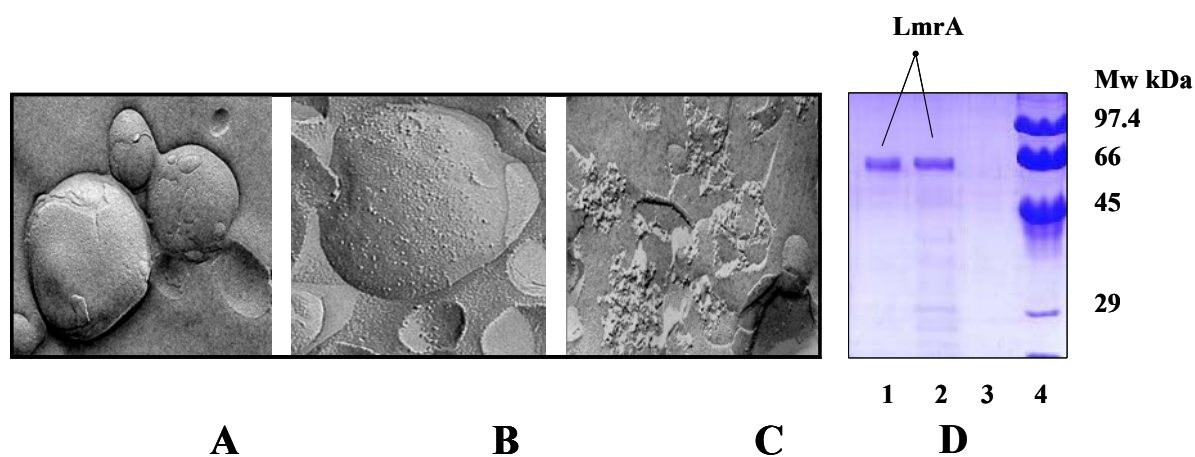


Figure 3.6: The freeze-fracture micrographs of *E. coli* reconstituted LmrA by liposomes destabilization method after 10-20-30% sucrose gradient. A) empty liposomes, B) the liposomes with sufficient LmrA incorporation, and C) aggregates separated from the liposomes. The freeze-fracture microscopy was performed by Dr. W. Haase for MPI of Biophysics, Frankfurt. The corresponding freeze-fracture micrographs are shown at 10K, 16K, and 20K magnification respectively. (D) SDS - PAGE analysis with 40 % acrylamide (1) LmrA purified, (2) LmrA *E. coli* liposomes reconstituted, (3) supernatant from reconstitution, and (4) standards.

To further analyze the quality of reconstitution, LmrA was labeled with ^{13}C glycine how it is

described in Chapter 2, purified and reconstituted into *E. coli* liposomes by detergent destabilization approach in presence of 10 mM EDTA, and loaded on the 10-20-30% sucrose gradient.

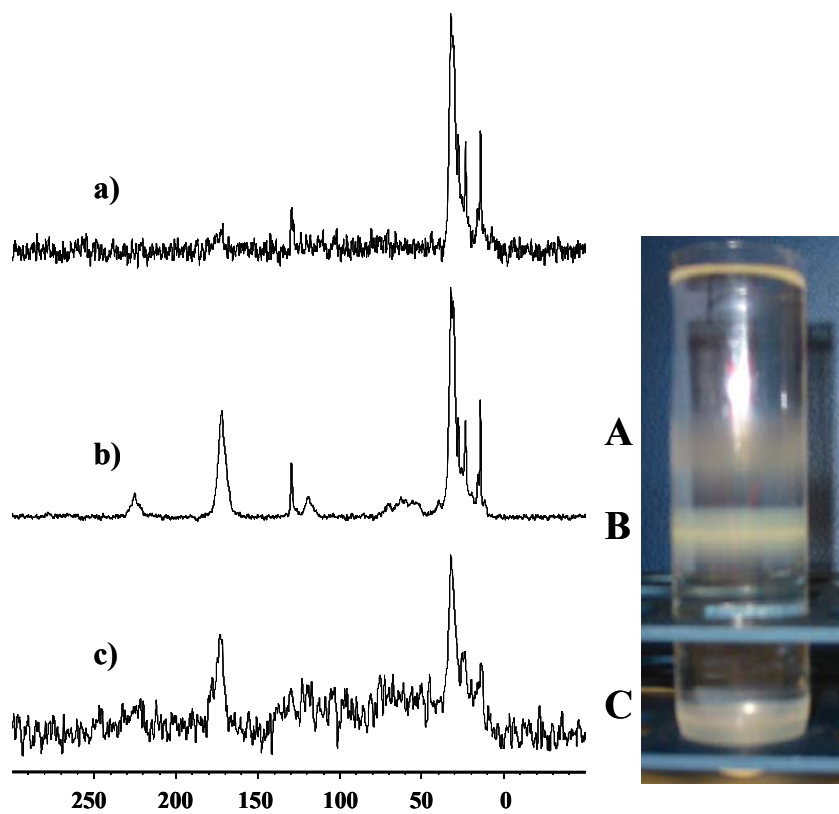


Figure 3.7: ^{13}C CPMAS spectra of *E. coli* lipids vesicles reconstituted LmrA by detergent destabilization method; a) protein free lipid vesicles, b) ^{13}CO glycine labeled LmrA reconstituted in lipid vesicles, c) aggregated protein. Spectra recorded at 8 kHz MAS spinning frequency and 253K. 62K (b) and 56K (a, c) transients were acquired for each spectrum. The 10-20-30 % sucrose gradient of LmrA *E. coli* liposomes reconstituted in buffer supplemented with 10 mM EDTA. A) Free liposomes (9 % sucrose); B) liposomes reconstituted LmrA (17 % sucrose); C) aggregated protein (28 % sucrose). Approximately 30 K scans were accumulates per each spectrum.

Three bands were collected and analyzed by ^{13}C CPMAS NMR. The lowest density band (9 % sucrose) contained only protein free liposomes. The spectrum of this band was characterized by natural abundance signals from lipids and a lack of any intense signal in the carbonyl region from ^{13}CO glycine labeled LmrA. The second band (17 % sucrose), an increased intensity at 172.4 ppm indicated the presence of ^{13}CO glycine labeled LmrA. Comparison of resonance intensity of the carbonyl resonance (172.4 ppm), from 49 labeled glycine resonances, with that of the lipid CH_2 natural abundance resonance (30.8 ppm) yields an approximate protein lipid ratio of 1/6 (w/w). The

aggregated protein was found to accumulate in the third band (28 % sucrose). The ^{13}C CPMAS spectrum of this sample was characterized by low intensity and was composed largely of signal from aggregated protein (175.8 ppm) with some associated lipids (Figure 3.7). All presented spectra were recorded with similar numbers of scans allowing us to estimate contribution from aggregated protein and free liposomes. The contribution from the aggregated protein is not high.

Unfortunately, using ATPase assay, it was found out that *E. coli* liposomes reconstituted LmrA after sucrose gradient is not active. So, taking into account that contribution from aggregated protein is not dramatic and free liposomes resonances do not affect with protein resonances it was decided to use reconstituted LmrA without sucrose gradient step.

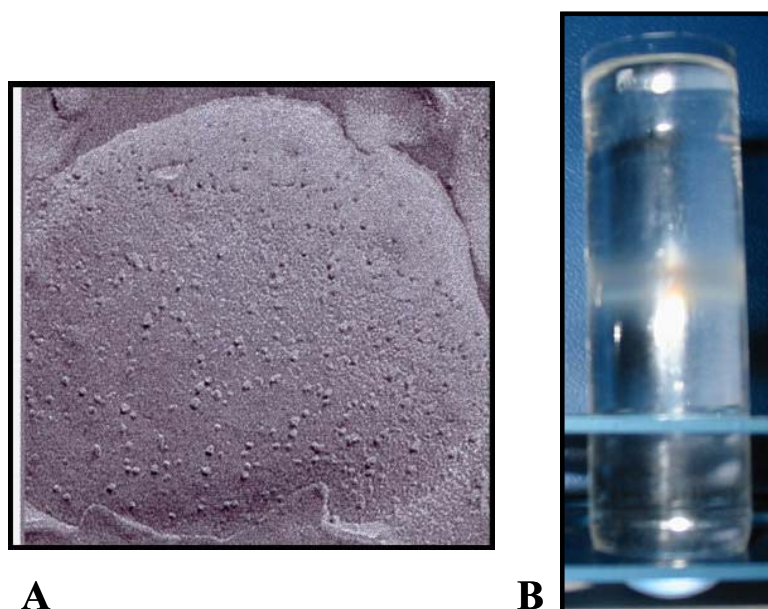


Figure 3.8: A) The freeze-fracture micrographs. The freeze-fracture microscopy was performed by Dr. W. Haase for MPI of Biophysics, Frankfurt. The freeze-fracture micrographs are shown in 16K magnification. B) 0-10-20-30 % sucrose gradient of *E. coli* reconstituted LmrA by liposomes destabilization method under detergent exchange condition. Both bands (18 % and 21 % sucrose) visible on sucrose gradient contain LmrA.

In the next step, detergent destabilized reconstitution of LmrA in *E. coli* liposomes was probed under detergent exchange conditions. Meaning the protein was purified as always in DDM micelles, but the liposomes were destabilized by step-by-step addition of oyl glycoside place DDM. In Figure 3.8 the freeze-fracture of LmrA reconstituted into *E. coli* liposomes shows that under detergent exchange conditions the protein incorporation is even higher. So, this way the quality of reconstitution is further improved. Moreover, the sucrose gradient shows that the reconstitution is more homogenous, there is

no protein aggregations on the bottom of the tube and two bands (18 % and 21 % sucrose), both from liposomes reconstituted LmrA are close (Figure 3.8B).

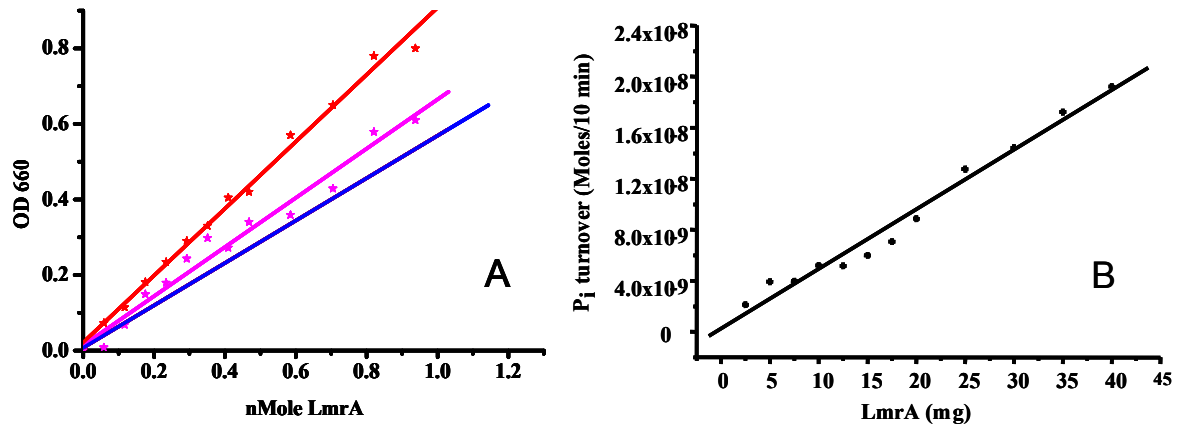


Figure 3.9: The colorimetric ATPase assay performed on A) ISOV containing overexpressed LmrA (red and purple lines show ATP hydrolysis accordingly without and with vanadate, blue line is the difference between red and purple line, corresponding to LmrA vanadate sensitive activity, B) functionally reconstituted LmrA (in proteoliposomes) compares inorganic phosphate turnover with increasing amounts of LmrA over 10 minutes.

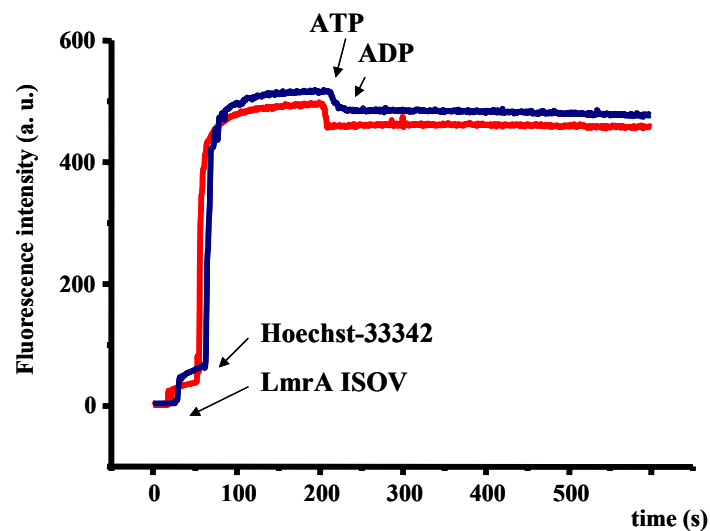


Figure 3.10: Hoechst-33342 transport assay result obtained for proteoliposomes reconstituted LmrA. Dye was added after 1 minute of incubation at room temperature. When intensity of fluorescence reached plateau ATP or ADP was added.

Compared with previously published results (Vigano *et al.*, 2002) the enzyme function assay detecting ATP turnover showed much reduced activity when protein was reconstituted by detergent liposome

solubilization method and slightly reduced activity of NBDs for LmrA reconstituted by detergent destabilization method. The vanadate sensitive ATP activity for detergent liposome destabilization method was determined to be 47 nmole/min/mg of protein (Figure 3.9B). Interestingly, the vanadate sensitive ATP activity in ISOV was determined to be in the same ranges as reconstituted system – 40 nmole/min/mg of protein (Figure 3.9A). Lower activity in ISOVs can be contributed to variation in LmrA over expression level.

Hoechst-33342 transport by proteoliposomes reconstituted LmrA was measured as described in Chapter 2. No Hoechst-33342 transport was detected (Figure 3.10).

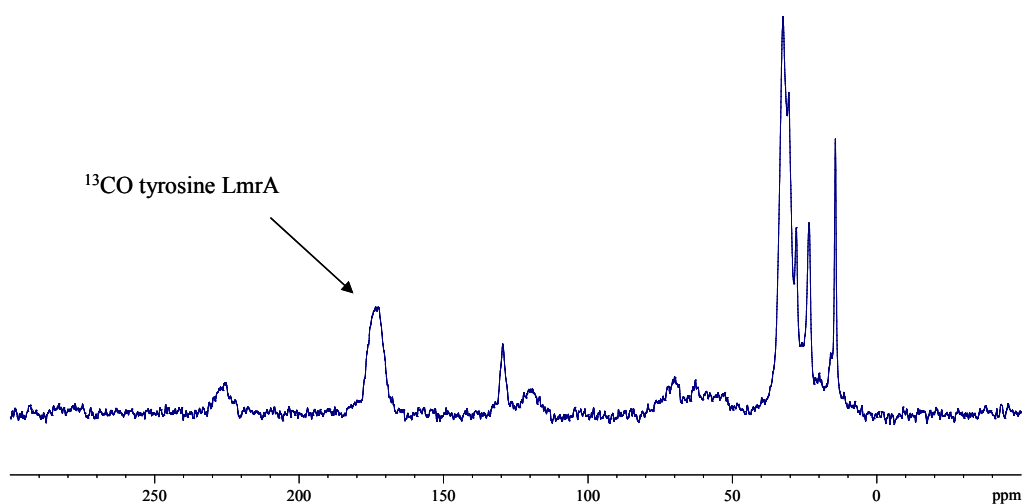


Figure 3.11: ^{13}C CPMAS spectra of ^{13}CO tyrosine labeled LmrA reconstituted in lipid vesicles. Spectra recorded at 8 kHz MAS spinning frequency and 253K. Approximately 40 K scans were accumulated per spectrum.

To probe the selective amino acid labelling approach and reconstitution using liposome destabilization method, ^{13}C tyrosines were incorporated into LmrA. Figure 3.11 shows that 14 LmrA tyrosine signals can not be resolved on a MAS carbon spectrum. ^{13}C carbon has better sensitivity than ^{15}N , however ^{15}N has advantage of very low natural abundance (0.36 %) in contrast to ^{13}C (1.11 %). Therefore, in the next step ^{15}N labeled tyrosines were incorporated into LmrA (Figure 3.12). However, due to low ^{15}N sensitivity, no statements can be made about resolution of individual LmrA sites (Figure 3.12).



Figure 3.12: ^{15}N CPMAS NMR spectra of ^{15}N tyrosine labeled LmrA reconstituted in lipid vesicles. Spectra recorded at 8 kHz MAS spinning frequency and 253K. Approximately 250 K scans were accumulated per spectrum.

LmrA reconstitution in synthetic lipid mixtures



Figure 3.13: The freeze-fracture micrographs of A) PC/PG/cardiolipin, B) PE/PG lipids mixture reconstituted LmrA by liposomes destabilization method. The molar lipid ratio in PC/PG/cardiolipin mixture was approximately 5:3:2. The molar ratio in PE/PG mixture was 7 to 3. The freeze-fracture microscopy was performed by Dr. W. Haase for MPI of Biophysics, Frankfurt. The freeze-fracture micrographs are shown in 16K magnification.

LmrA reconstitution was probed for lipids mixtures PE/PG and PC/PG/cardiolipin. These lipids mixtures were chosen for reconstitution because PE/PG mimics *E. coli* membrane and

PC/PG/cardiophilin mixture resembles eukaryotic membrane. The freeze-fracture micrographs for both lipid mixtures are presented in Figure 3.13. For PE/PG lipids mixture freeze-fracture micrographs shows well formed liposomes and sufficient reconstitution. For PC/PG/cardiophilin the liposomes are replaced by long lipids sheets containing sufficient protein incorporation.

3.4. Discussion

3.4.1. Solubilization and purification of LmrA

The solubilization of membrane proteins requires that the proteins are taken from their natural environment and that lipid bilayer is replaced by the detergent micelle. The choice of the detergent used for protein solubilization is crucial and to a large extent determines the quality of purification.

LmrA solubilization and purification was performed essentially as described in (Margolles *et al.*, 1999). van Veen and co-workers have examined several detergents on their ability to solubilised LmrA. The best results were obtained for DDM and Triton-100, they solubilised respectively 91 % and 87 % of LmrA from ISOVs. However, due to often inhibition of the transport activity of membrane transporters by Triton-100, DDM was selected for the purification of LmrA (Margolles *et al.*, 1999; Putman *et al.*, 1999; Callaghan *et al.*, 1997b). The solubilization of LmrA was probed by SDS-PAGE analysis. The results revealed that almost all protein is solubilised from ISOVs (Figure 3.3).

The purification of LmrA was achieved by applying a single nickel-chelate affinity chromatography step. The eluted fraction containing his-tagged LmrA (1 mg/mL) was loaded on a gel filtration column and on SDS gel. Gel filtration and SDS-PAGE analysis showed that LmrA is isolated at high purity (Figure 3.2 and Figure 3.3). Slight broadening of a peak from the purified LmrA on the gel filtration chromatogram can be associated with non homogeneous size distribution of DDM detergent micelles (Figure 3.2).

3.4.2. Reconstitution of LmrA

The method of LmrA reconstitution into preformed liposomes by detergent liposome destabilization method was found to yield a lot higher protein incorporation in comparison with liposome solubilization method (Figure 3.3-3.7). The final protein lipids ratio was estimated to be 1 to 6 (w/w). This ratio is sufficient to provide high enough protein concentration in NMR rotor needed for NMR measurements. The further increase in protein lipid ratio we considered dangerous because aberrant oligomerization could take place.

As it was shown by electron microscopy the fraction of liposomes after reconstitution is not homogenous. Together with LmrA reconstituted liposomes, there are some free liposomes and aggregated protein. Presence of free liposomes is harmful for NMR measurements in case when ^{13}C experiments are performed (high natural ^{13}C abundance 1 %) and when critical amount of free liposomes competes with proteoliposomes for the place in small MAS NMR rotor. More problems come from aggregated protein, because the contribution from aggregated protein broadens resonances. To estimate contribution from free liposomes and aggregated protein, ^{13}CO glycine isotope labeled LmrA reconstituted into *E. coli* lipid liposomes were separated on a sucrose gradient. ^{13}C MAS NMR spectra of all the three bands (Figure 3.7), corresponding to empty liposomes, proteoliposomes and aggregated protein, were compared (Figure 3.7). From the spectra comparison it was concluded that the contribution from free liposomes and aggregated protein is not dramatic. So, keeping in mind ABC transporters instability, the gradient step was excluded in further experiments.

From detergents used for membrane protein solubilization and purification, the most popular candidate is DDM. It is relatively mild detergent and is usually well tolerated by membrane proteins. It has been previously reported that its long alkyl chain protect the hydrophobic portion of integral membrane proteins better than shorter detergents like octylglyside (Callaghan *et al.*, 1997a). DDM was applied for solubilization and reconstitution of number of membrane proteins including LmrA and LmrP from *L. lactis* (van Veen *et al.*, 2000a; Putman *et al.*, 1999). However, considering liposome formation DDM is clearly not the best choice. It has been shown that it is difficult to remove DDM from liposomes because of its low CMC. Presence of detergent in liposomes add unnecessary lipid dynamics, initiates proteoliposomes leakage and as a result complicates activity assays,

determines swelling of liposomes and formation of multilamellar vesicles (Otten et al., 2000). In particular cases, the presence of detergent molecules leads to liposomal disintegration, followed by formation of small micelles, which can not maintain protein incorporation. In addition, prolonged contact with detergent facilitates slow protein degradation. Therefore, we considered the possibility to exchange detergent during the reconstitution procedure. For reasons mentioned before, DDM can not be excluded from LmrA purification procedure but its usage can be avoided in case of liposome destabilization.

In contrast to DDM, the complete detergent removal from the proteoliposomes, as well as smoother liposome morphology distribution has been shown in case of octylglycoside (OG) usage (Fang et al., 1999; Knol et al., 1997). Functional octylglycoside mediated reconstitution as well as lower OG detergent induced protein ATPase activity and drug binding inhibition in comparison to DDM have been shown for P-glycoprotein (Callaghan *et al.*, 1997a). The liposomes were destabilized by OG. The efficiency of LmrA reconstitution was assessed by migration profiles of liposomes and protein through sucrose gradients and by freeze-fracture microscopy (Figure 3.8). The sucrose gradient revealed two major bands: at 21 % and 18 % (w/v) sucrose (Figure 3.8B). Surprisingly, both bands contained protein. Existence of two bands corresponding to proteoliposomes can be addressed to two main peaks in liposomes size distribution profile. In comparison to DDM mediated reconstitution, no band corresponding to aggregated protein was found. Taken together, octylglycoside mediated LmrA reconstitution allows an optimized reconstitution procedure. The freeze-fracture microscopy revealed sufficient protein incorporation into liposomes (Figure 3.8A). This novel detergent liposomes destabilization approach can be advantages if the protein dynamics is studied.

As soon as successful reconstitution is confirmed by electron microscopy, the functional state of the protein must be assessed. Available methods to check the protein function state depends on both the protein and on the model membrane system used. For example, the enzymatic activity can typically be measured regardless of the model system (Vinogradova et al., 1998). For some classes of proteins in some media, functional assays are not possible. For example, the channel activity can not be assessed in micelles (Sanders and Oxenoid, 2000). In this case evidence for native protein structure must be obtained by indirect methods such as measurements of ligand binding capacity, and protein

thermodynamic stability (Sanders and Oxenoid, 2000; Lau and Bowie, 1997), additional information can be acquired using so called ‘finger-print’ methods like near- and far-UV circular dichroism, amide H-D exchange measurements, and fluorescence. Once this data are obtained the comparison between the structural data obtained under conditions known to provide correctly folded protein and the data received for tested conditions can be done.

The ATPase turnover was estimated using a colorimetric assay, the reported activity (47 nmole/min/mg) is lower than earlier reported activity for LmrA in ISOVs (150 nmol/min/mg) (Vigano *et al.*, 2002) (Figure 3.9). It is interesting to note, that for P-glycoprotein the reported activity varies from 6 to 900 nmol/min/mg (Ambudkar *et al.*, 2003; Ambudkar *et al.*, 1999; Callaghan *et al.*, 1997a). The activity in reconstituted system may be underestimated, since many ATP binding sites can be buried in the vesicles lumen and are not accessible to ATP. Moreover, low ATPase activities are typically observed before for proteins reconstituted at a high protein lipids ratio (Poolman, personal communications).

Hoechst-33342 was used to assess the functional state in studies of several reconstituted membrane proteins, including MDR transporters LmrP, P-glycoprotein and LmrA (van Veen *et al.*, 2001; Putman *et al.*, 1999; Shapiro and Ling, 1995). Our study unfortunately showed no ATP mediated Hoechst-33342 transport in LmrA reconstituted proteoliposomes (Figure 3.10). The Hoechst-33342 transport assay requires well formed and sealed liposomes. In the case of reconstitution of LmrA into *E. coli* lipids (Figure 3.6) we observed a broad distribution of vesicles size, including some fused liposomes, and high protein density in majority of the vesicles. It is known that such a high density of protein in membrane changes the membrane bilayer properties a lot. As a result, the vesicles are not stable and leaky. The additional liposome fusion and aggregation can be caused by Hoechst-33342 itself (Shapiro and Ling, 1995). Overall, these facts suggest that the proteoliposomes can be significantly leaking. To detect Hoechst-33342 transport the rate of transport must be much higher than the rate of rebinding of Hoechst-33342 to the membrane. In addition, significant detergent retention during the reconstitution procedure (approximately 1 mol of DDM per 15-20 mol of phospholipids) can affect transport. The detergent can potentially affect the passive drug flip-flop from one membrane leaflet to the other and thereby interfere with net drug transport indirectly.

Taking all together it is not surprising that we were not able to detect Hoechst-33342 transport even when the protein is active as the ATPase assay presented here shows.

As soon as functional reconstitution is confirmed, the selective ^{13}C glycine and tyrosine labelling of LmrA were performed as described in Chapter 2. The quality of spectra of ^{13}C as well as ^{15}N tyrosine and glycine labeled LmrA reconstituted into *E. coli* liposomes do not allow us to resolve individual components (Figure 3.11, 3.12). Such spectra quality deterioration can be due to many reasons. Firstly, we certainly meet frequent problem of the frozen membrane samples: conformational micro heterogeneity of the protein of interest where each component yields its own distinct spectrum, and the spectra of many individual conformers overlap. The possible solution could be preparation of microcrystals or protein with careful precipitation with agents as ammonium sulphate or polyethylene glycole (Sanders and Oxenoid, 2000). However, crystallization of MDR ABC transporters is difficult if not impossible and in both cases (crystallization and precipitation) we would deal with not functional protein.

Reconstitution of LmrA in synthetic lipid mixture

A number of NMR measurements were planned in our laboratory in future to assess the protein lipid interactions. For this purpose, the reconstitution trials were extended to include not only *E. coli* lipids but also mixture of synthetic lipids. In Figure 3.13 the freeze-fracture micrographs of PE/PG and PC/PG/cardioliipin reconstituted LmrA are shown. PE/PG reconstitution case resembles *E. coli* lipid reconstitution; well formed liposomes with essential incorporation are shown. PC/PG/cardioliipin reconstitution is appeared to be different, with the protein incorporation occurring not in liposomes but in lipid sheets.

Conclusion

LmrA has been successfully reconstituted into natural *E. coli* lipids and mixture of synthetic lipids (PE/PG, and PC/PG/cardioliipin) using detergent liposome destabilization approach at high protein lipid ratio (1:6 w/w). For comparison, the previously established protocol allowed to reconstitute LmrA into lipids at 1:100 w/w ratio (Margolles *et al.*, 1999). The quality of reconstitution and the

protein function state in reconstituted form have been assessed subsequently by freeze-fracture microscopy, sucrose gradient, SDS-PAGE, ATPase assay, and Hoechst 33342 transport assay. The first spectra of ^{13}C and ^{15}N tyrosine labeled LmrA reconstituted into *E. coli* liposomes revealed good signal to noise ratio and confirm that the amount of selectively isotope labeled LmrA sufficient for SSNMR experiments are produced. This makes for the first time the 64 kDa membrane protein LmrA, and therefore the ABC transporter superfamily accessible to NMR analysis.

4. LmrA dynamics as studied by deuterium NMR line shape analysis and relaxation measurements

Abstract

As it is well accepted that the conformation changes in ABC MDR transporters leading to substrate transport are driven by ATP binding and hydrolysis, it is a question of great importance to investigate ATP binding to MDR pumps. In this chapter dynamics changes in ABC MDR transporter LmrA under ATP and ATP/ADP-Vanadate binding have been followed by deuterium solid-state NMR.

4.1. Introduction

The existence of a structural cooperation between membrane and cytosolic domains propose significant conformation rearrangements within these domains. These rearrangements might be associated with altering of the proteins NBDs and TMDs dynamics behaviour. Therefore, the dynamics information is an important complement to static structural data and studying of the protein internal dynamics is of fundamental interest. The dynamic information for large membrane proteins like ABC transporter is difficult to extract. Recently, long-time dynamics of BtuCD ABC-transporter and AcrB MDR transporter were approached using B-factor analysis. However, only qualitative dynamics description was obtained in both cases (Lu *et al.*, 2006; Tanizaki and Feig, 2006). Concerning MDR ABC transporters, to our knowledge, there were no reports on any studies concerning their dynamics.

There are several methods to investigate the proteins internal dynamics (Stopar *et al.*, 2005). One of the most powerful approach is solid-state ^2H NMR (Tiburru *et al.*, 2004; Sparrman and Westlund, 2003; Millet *et al.*, 2002; Palmer, 1997; Bienvenue *et al.*, 1982). It allows studying molecular dynamics of membrane embedded proteins spanning a wide range of time scales extending over many orders of magnitude (Tiburru *et al.*, 2004; Rozovsky and McDermott, 2001; Keniry *et al.*, 1984b; Davis, 1983; Batchelder *et al.*, 1982; Bienvenue *et al.*, 1982). Indeed, several pulse sequences for measuring of fast and intermediate rate processes, as well as two-dimensional chemical exchange

experiments for measuring slow rate processes allow following molecular dynamics in motional frequencies from 10 to 10^{10} Hz (Palmer, 2004; Siminovitch, 1998). In doing so, the correlation time of $5 \cdot 10^5$ Hz and a three-jump rotation at 10^8 Hz were estimated subsequently for (ϵ - $^2\text{H}_2$) tyrosine ring and (β - $^2\text{H}_3$) alanine in selectively labelled photosynthetic bound protein (Kikuchi *et al.*, 2000).

Deuterium is a convenient probe of macromolecular dynamics. The relaxation of this nucleus is completely dominated by the quadrupolar interaction. This is characterized by the quadrupole coupling constant χ and the asymmetry parameter η_Q . For deuterons the quadrupolar coupling constant is known to be relatively small ($\chi \sim 160 - 190$ kHz) and because the quadrupolar interaction is dominated by intramolecular contributions from the axially symmetric deuterons bond the asymmetry parameter is close to zero (Beshah *et al.*, 1987). These features result in relatively simple spectra and lineshapes that are sensitive to both molecular structure and motions (Hologne and Hirschinger, 2004; Kristensen *et al.*, 1999). Therefore, the interpretation of the ^2H relaxation data is straight forward in contrast to the case for relaxation data from other nuclei, for example with spin $\frac{1}{2}$. For spin half nuclei the relaxation rates contain the contributions from interactions like dipolar coupling, and chemical shift anisotropy (Muhandiram *et al.*, 1995; Torchia, 1984). These interactions are negligible in ^2H spectra. Moreover, the angular dependence of the NMR frequency is the same for the chemical shift and quadrupole interactions, therefore molecular motions affects chemical shift and ^2H powder patterns in essentially the same way (Torchia, 1984).

Additionally, concerning proteins internal dynamics studies, solid-state NMR has an advantage over solution state NMR. In solids, in contrast to liquids the orientation-dependent NMR parameters of protein motion are not covered by the rapid overall motion of the protein (Torchia, 1984).

For our study we have selected CD_3 alanine groups as a probe of internal protein dynamics for variety of reasons. These reasons are 1) alanine high frequency occurrence in proteins coupled with their distribution at various positions; 2) methyl groups in alanine are directly attached to the α -carbon allowing to look at the backbone dynamics; 3) methyl groups reorientation is sensitive to local environment and information on the actual rate of motion as well as on type of motion can be deduced directly from the line shape analysis and relaxation measurements (Leo *et al.*, 1987; Smith and Oldfield, 1984).

In the past, several proteins and peptides have been extensively studied on a subject of their macromolecular dynamics using ^2H solid-state NMR. Among those are gramicidin, collagen, the coat protein of bacteriophage fd, bacteriorhodopsin in the purple membrane of *Halobacterium halobium*, egg white lysozyme, pancreatic A_2 phospholipase, triosephosphate isomerase, and photosynthetic membrane-bound protein (Rozovsky and McDermott, 2001; Kikuchi *et al.*, 2000; Mack *et al.*, 2000; Prosser and Davis, 1994b; Allerrini *et al.*, 1985; Torchia, 1984; Jelinski *et al.*, 1980a).

The main goal of this study is to shed light on dynamic properties of membrane and cytoplasmic LmrA domains and to investigate how the ATP binding and hydrolysis affect these protein characteristics. Because of relatively high basal ATP hydrolysis rate, 47 nmole/min per mg of protein, ATP is not a good candidate for ^2H SSNMR measurements which can last up to several days. Therefore, to investigate dynamic properties of LmrA under ATP binding, non-hydrolysible ATP analogue AMP-PNP was used place ATP. This analogue has been used extensively to trap several ABC transporters including PGP and LmrA in pre-hydrolysis state (Ecker *et al.*, 2004; Rosenberg *et al.*, 2003). To trap the protein in post-hydrolysis state in addition to ATP vanadate was added to the reconstituted LmrA. It is well know that vanadate traps ADP at one of the two nucleotide-binding sites by mimicking the transition state of the γ -phosphate of ATP during ATP hydrolysis. In addition, vanadate trapping at one site inhibits ATP hydrolysis at the second site (Fetsch and Davidson, 2002; Loo and Clarke, 2002; van Veen *et al.*, 2000a).

In our study we used deuterium solid-state NMR approach. Severe line distortions of the static spectra of selectively alanine CD_3 labeled LmrA with AMP-PNP and ATP/ADP-Vanadate bound when compared to LmrA resting state spectra were interpreted as an evidence of restricted motions of the cytosolic and membrane spanning protein domains.

4.2. Materials and methods

Materials

L-(3, 3, 3- d_3) alanine (98 % atom ^2H) was obtained from Sigma Aldrich. Deuterium-depleted water

was purchased from Aldrich Chem. Proteinase K was from Sigma and phenylmethylsulfonyl fluoride (PMFS) from Serva. All the other reagents were of analytic grade.

Labelling

LmrA and LmrA-MD were labeled with L-(3, 3, 3-*d*3) alanine biosynthetically following the protocol adapted from Cai (Cai *et al.*, 1998) (Chapter 2). For this purpose *L. lactis* cells were grown on the defined media in which half the required amount of the isotope labeled amino acid was added after induction point. After induction the bacteria were left to overexpress LmrA or LmrA-MD and incorporate L-(3, 3, 3-*d*3) alanine for 2.5 hours.

Expression, purification and reconstitution

Full-length LmrA

Purification and reconstitution of full length LmrA have been done how it was described in Chapter 2 and 3.

The LmrA reconstituted proteoliposomes were washed with a total of 10 mL of 100 mM Tris 50 mM KCl pH 7 buffer made on deuterium depleted water by suspension and centrifugation. Samples of LmrA were trapped respectively with ATP non-hydrolysable analogue AMP-PNP, and ATP/ADP - Vanadate. For this purpose AMP-PNP or ATP 20 mM, and MgSO₄ 5 mM were solubilised in 100 mM Tris 50 mM KCl pH 7 buffer made in deuterium depleted water, added into the LmrA reconstituted vesicles up to total volume of 5 mL, incubated for 20 minutes on a rocking table at a room temperature, and harvested at 55000 rpm for 40 minutes.

LmrA-MD

LmrA-MD (N-terminally His₆-tagged LmrA truncated in the linker region (His 353) that connects the MD to the NBD) expression strain NZ9000 was a gift from H. van Veen, University of Cambridge, UK (Venter *et al.*, 2003). Truncated LmrA (LmrA-MD) was detected as a 36 kDa protein by SDS-polyacrylamide-gel electrophoresis (SDS-PAGE) (Figure 4.1). Purification and reconstitution

of LmrA-MD has been performed as it is described for full-length LmrA (Chapter 2, and 3).

Proteolysis of LmrA

As an alternative to LmrA-MD, NBDs were removed from LmrA full length by proteolysis. To do that and thus to isolate the membrane-embedded domain together with loops connecting transmembrane segments of LmrA, the proteoliposomes (3 mg of LmrA /mL) were incubated with proteinase K (4 mg/mL) at a room temperature on a rocking table for 30 minutes. The proteolytic digestion was stopped by addition of phenylmethylsulfonyl fluoride to a final concentration of 1 mM. The proteoliposomes containing LmrA-MD and LmrA without proteinase K cleaved NBDs were then diluted in 100 mM Tris, 50 mM KCl, pH 7, pelleted by centrifugation for 40 minutes at 50000 rpm, and subsequently washed twice with 100 mM Tris 50 mM KCl buffer made on deuterium depleted water. Sample was analysed by SDS-PAGE (Figure 4.1).

***E. coli* lipid liposomes**

The liposomes for ^{31}P measurements were prepared as described in Chapter 3 for detergent liposomes destabilization method, including extrusion, detergent destabilization, and final detergent removal and harvested by centrifugation for 30 minutes at 50000 rpm.

^2H NMR measurements

All ^2H NMR experiments were performed on a Bruker Avance 600 spectrometer equipped with a 4 mm MAS DVT probe. The measurements were done at 92.123 MHz. For all static measurements a solid echo experiment pulse program was used with the acquisition time of 8.123 ms, the 90° pulse of 4 μs , the recycle delay time was 0.4 s, and the echo delay of 50 μs . The spectral width for ^2H was set to 303030 Hz. Spectra were zero filled to 4892 points and 2500 Hz exponential line broadening was applied during processing. The number of scans collected for each measurement was approximately 400K. Each experiment took ca. 48 hours.

For MAS ^2H NMR measurements a rotor synchronized Hahn echo experiment with the 90° pulse of 4 μs , recycling delay of 1 s, spectral width of 303030 Hz, data size of 8K, and acquisition time of 12.99

ms were used. Hahn echo experiment was used because it solves the problem of a dead time better than starting Fourier transformation at the first rotor echo. The number of scans collected for each measurement was approximately 50K. Each experiment took ca. 6 hours. The linebroadening of 200 Hz was applied during processing.

For the T_1 measurements the inversion-recovery technique has been used. In the inversion recovery pulse sequence, the spin system is first inverted with a 180 degree pulse (of 10 μ s). It is then allowed to evolve during a variable delay (0 - 200 ms) and finally detected the magnetization is detected with a 90 degree observe pulse (of 5 μ s) and acquired with the acquisition time of 8.123 ms. The relaxation delay must be at least $5T_1$. Typically, 15 – 20 points were obtained for each experiment. Experimental data were fitted to the following equation (Claridge, 1999)

$$[4.1] \quad M(t) = (M(0) - M_0) \exp(-t/T_1) + M_0$$

where M_0 is magnetization at thermal equilibrium, $M(t)$ is +z magnetization at a time point t , and T_1 is the longitudinal relaxation. Data conversion, calculations and fitting were done with the help of the open source software packages Tcl/Tk (Welch, B.B., <http://dev.scriptics.com>), SIMPSON ((Bak *et al.*, 2000), <http://nmr.imsb.au.dk/bionmr/software/simpson.php>), and GNUPLOT (version 4.0, Thomas Williams and Colin Kelley, <http://www.gnuplot.info>). Each experiment took ca. 60 hours.

The ^{31}P measurements were performed on a Bruker Avance 400 spectrometer equipped with a 4 mm MAS DVT probe. The measurements were performed at 161.923 MHz. The ^{31}P spectra were acquired using a Hahn echo pulse sequence, with echo delay of 15 μ s and ^{31}P excitation pulse with a length of 3 μ s. The continuous wave homonuclear ^1H decoupling was applied during the acquisition. The line broadening of 250 Hz were applied to all spectra. The number of scans collected for each measurement was approximately 4K. Each experiment took ca. 3 hours.

The temperature was regulated by a Bruker temperature control. All spectra were processed and analysed using routines in TOPSPIN. The low temperature experiments were run first to minimize the sample degradation.

4.3. Results

^2H static spectra of LmrA in a resting state

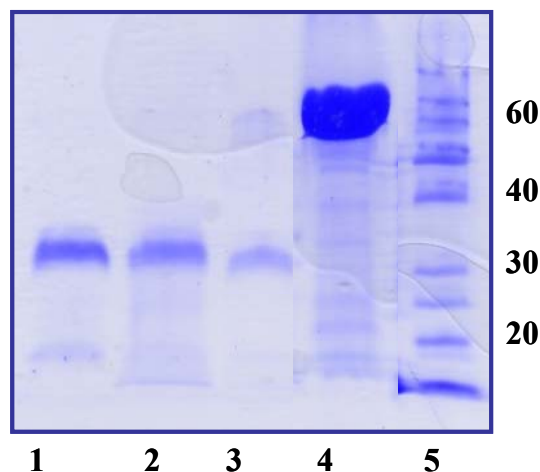


Figure 4.1: SDS acrylamide gel: 1) LmrA-MD (36 kDa), 2) LmrA after proteolysis without cytoplasmic domain (35 kDa), 3) NBD left in supernatant after isolating the membrane-embedded LmrA domain with proteinase K, 4) full-length LmrA (65 kDa), and 5) standards.

Characteristic quadrupolar echo spectra of selectively alanine CD_3 labelled LmrA in a resting state are shown in the Figure 4.2A as a function of temperature. Examination of Figure 4.2A reveals that at low temperature ^2H spectra of LmrA in a resting state have a typical powder pattern lineshape. The ^2H alanine selective labelled LmrA quadrupolar coupling of 49 kHz is close to quadrupolar coupling 56 kHz known for crystalline form of CD_3 alanine, how it was found by SIMPSON simulations (Figure 4.3) (Beshah *et al.*, 1987). Increasing the temperature causes dramatic changes in the LmrA spectra. Namely, at increasing temperatures an isotropic component appears in the spectra. For this isotropic component the quadrupolar coupling constant has collapsed to an apparent value of 159 Hz from 49 kHz, how it was found by SIMPSON simulations (Figure 4.3). Such a dramatic motion narrowing can be associated with correlation times of ca. 10^{-4} s and be originated from deuterons' orientation over a wide angular range in a time several-fold less than the inverse of the frequency of the rigid quadrupolar splitting, that is $\ll 10^{-5}$ s (Leo *et al.*, 1987).

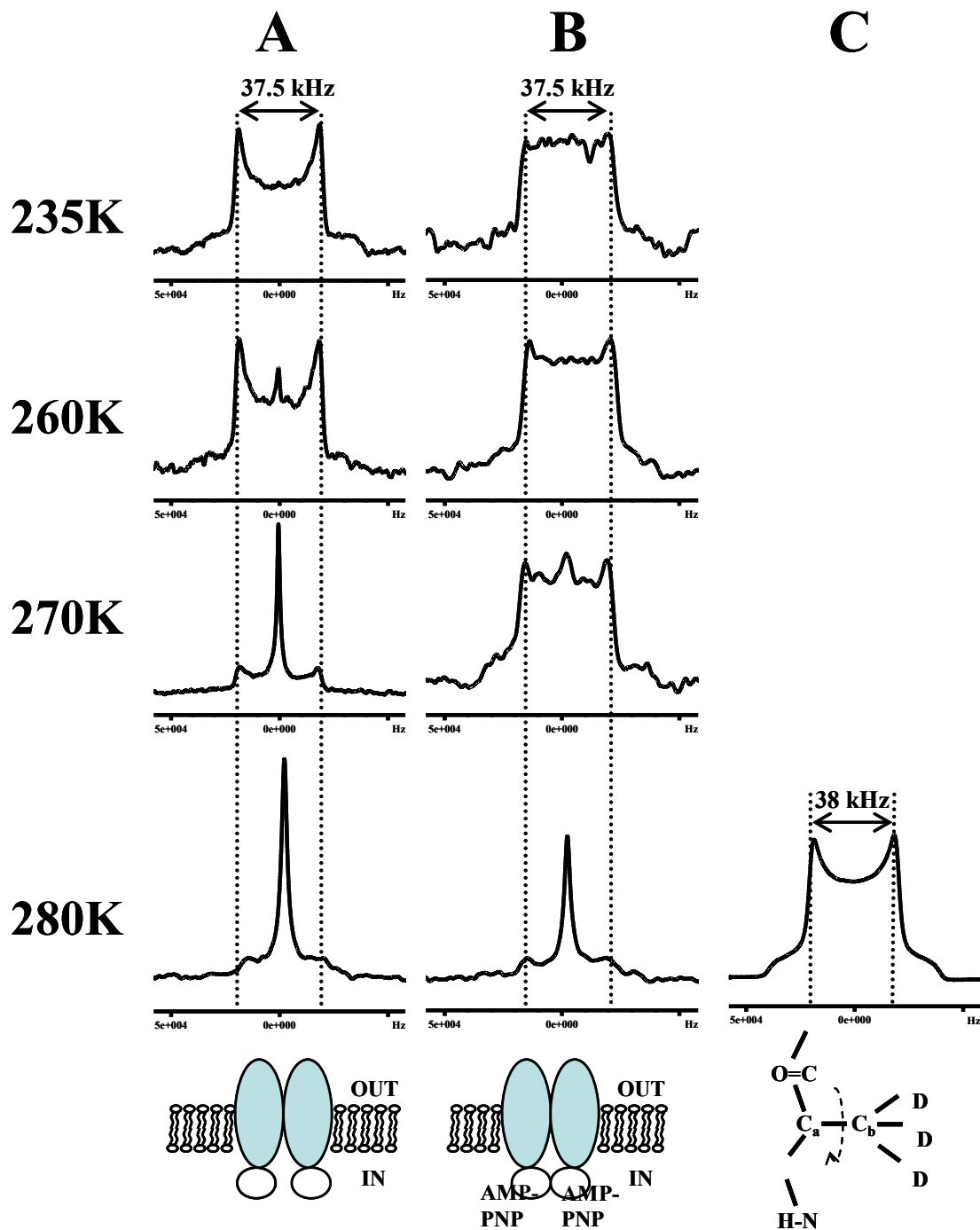


Figure 4.2: ^2H NMR spectra of ^2H alanine selective labelled LmrA reconstituted *E. coli* liposomes in a resting state (A) and trapped with AMP-PNP (B). The spectra recorded at increasing temperatures 235K, 260K, 270K, and 280K and arise from 48 alanines in the LmrA (~ 147 deuterons). The spectrum of powder CD_3 labelled alanine recorded at 280K is shown for comparison (C).

It is known that T_1 is sensitive to motions with broad range of correlation times. Table 4.1 shows the spin-lattice relaxation times of LmrA as a function of temperature. A continuous increase of the

values with increasing temperatures is found. This T_1 behaviour is consistent with the results observed for DPPC with incorporated peptide and without (Prosser *et al.*, 1992) and for hydrochloride form of L-CD₃-alanine (Keniry *et al.*, 1984b). However, no general conclusion can be drawn since the limited measurement time did not allow following the T_1 temperature behaviour any longer and systematically analyse the relaxation data as a set of temperature-dependant parameters.

Temperature	T_1 , ms: TMDs Rigid (R)	T_1 , ms: NBDs Dynamic (D)
235K, LmrA resting state	12.3±1	-
260K, LmrA resting state	14.4±0.7	-
280K, LmrA resting state	20.4±1.5	28.5±2.2
280K, ATP/ADP-Vanadate trapped	17.5±2.0	36.0±2.7

Table 4.1: The spin-lattice relaxation values obtained at different temperatures in two protein states: the resting state and trapped with ATP-ADP-Vanadate.

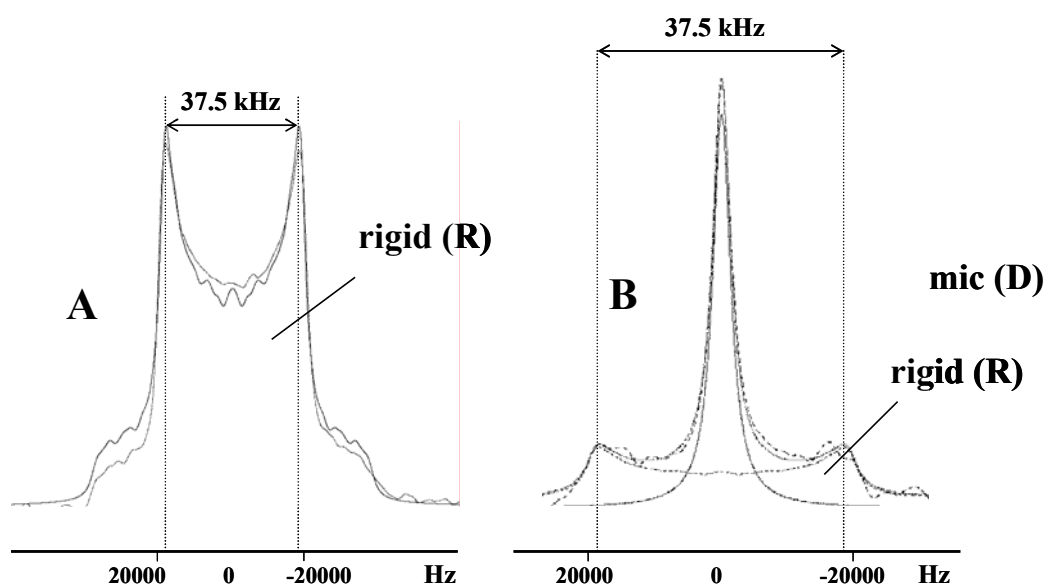


Figure 4.3: Experimental (---) and simulated (—) ²H spectra at (A) 235K and (B) 280K. At 280K the simulated spectrum is a sum of dynamic and rigid components. The dynamic component corresponds mostly to mobile NBDs and rigid mostly to TMDs. The calculated rigid spectrum has the quadrupolar coupling constant of 49 kHz and the dynamic component subsequently 159 Hz. Additionally, the width at the half height of 150 Hz was determined for the dynamic component at linebroadening of 0 Hz. The line broadening of 1500 Hz was

applied during simulation and on compared experimental spectra.

LmrA proteolysed

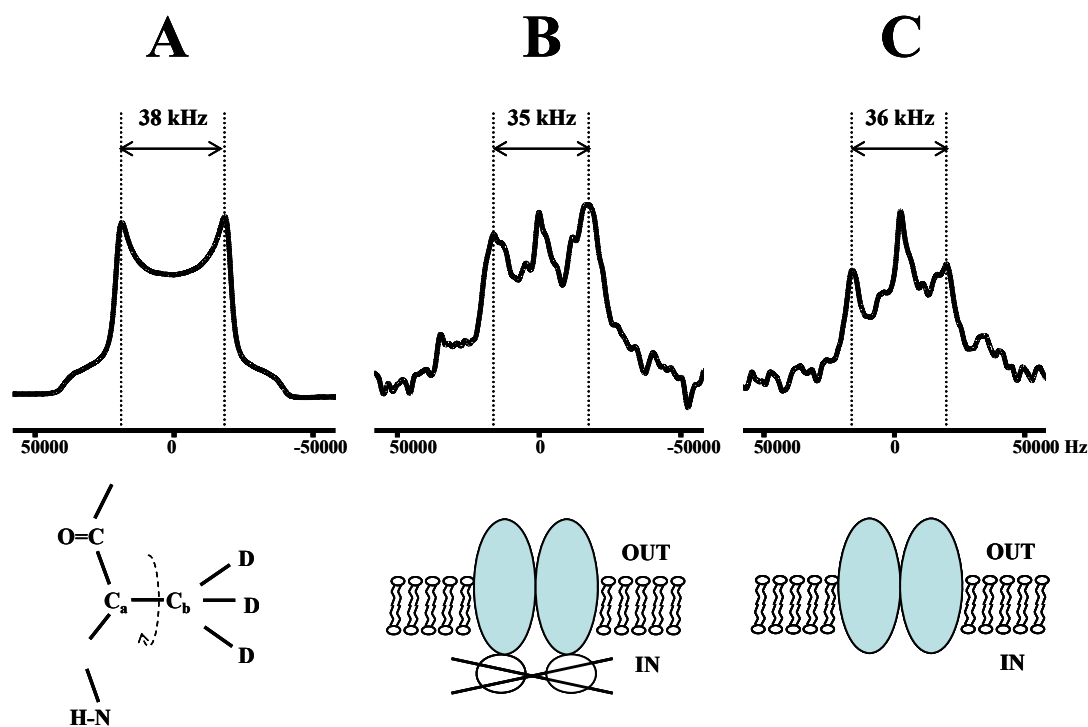


Figure 4.4: ^2H spectra of ^2H alanine selective labelled membranous LmrA domain obtained with proteinase K cleavage procedure (B) and LmrA-MD (C). Both, LmrA proteolysed and truncated, are *E. coli* liposomes reconstituted. The spectrum of powder alanine CD_3 is shown for comparison (A). The spectra were recorded at 280K.

To isolate the membrane-embedded domain of LmrA, proteoliposomes containing reconstituted full-length LmrA was treated with proteinase K. This procedure allows selectively removing of the cytoplasmic domain and leaves intact the membranous domain and vesicles interior parts of the protein. Figure 4.1 shows that no band of the intact protein is observed after the proteolysis as well as of other peptides associated with protein or lipids. Van Veen and co-workers who were the first to apply this procedure to LmrA, have blotted the 35 kDa membranous LmrA domain on a PVDF membrane, sequenced and proved that this peptide is the six transmembrane helices and the loops connecting them according to the protein predicted model (Grimard *et al.*, 2001). ^2H NMR spectrum

of the LmrA was recorded at 280K and compared to powder pattern alanine CD₃ (Figure 4.4). The spectra comparison reveals that quadrupolar splitting of proteolysed LmrA is narrowed from 38 kHz (d3-alanine) to 35 kHz and the isotopic component is dramatically reduced when compared to full length LmrA (Figure 4.2).

LmrA-MD

Truncated LmrA-MD (36 kDa) was detected at SDS-PAGE (Figure 4.1). The spectrum of LmrA-MD was recorded at 280K and compared to powder alanine CD₃ (Figure 4.4). The spectra comparison reveals that that quadrupolar splitting is narrowed from 38 kHz to 36 kHz and the isotopic component is dramatically reduced when compared to full length LmrA (Figure 4.2). However, this reduction is slightly less pronounced, than the one observed for proteolysed LmrA. This slightly smaller reduction of an isotropic component can be associated with the fact that LmrA-MD (36 kDa) has longer, suppositively mobile, intracellular domain connecting the TMDs and NBDs, than proteolysed LmrA (35 kDa). Interestingly, both LmrA-MD and proteolysed LmrA run at SDS-PAGE on approximately the same level (Figure 4.1). It can be explained by 'low' resolution of SDS-PAGE and possible differences in electrophoretic behaviour of both proteins (Venter *et al.*, 2002).

²H-MAS NMR

The contribution from the natural abundance water can be approximated from deuterium MAS NMR experiment which allows clearly resolving the water and the protein components. Figure 4.5 shows the ²H MAS NMR spectra of LmrA in a resting state, and trapped with AMP-PNP. For all cases at 280K the water peak is clearly separated from the protein peak and its contributions is not dominant. Interestingly, for all cases we did not observe expected improvement in spectra intensity when compared to ²H static spectra and in addition observe loss of spectra intensity with increasing temperatures (Figure 4.2 and 4.5). It could mean that the particular LmrA domains are in an intermediate motion regime (μsec), at which that the sidebands broaden significantly and as a result ²H MAS NMR loses its advantage of high resolution and sensitivity.

Another interesting feature of ²H MAS spectra is sidebands pattern in each spectrum at 280K. The

sidebands are significantly reduced in all cases at 280K when compared to the subsequent spectra recorded at 235K and 260K but less for LmrA AMP-PNP trapped state (Figure 4.5). This more pronounced sidebands pattern of LmrA trapped with AMP-PNP deuterium spectra could be correlated with subsequent static deuterium spectra, showing reduced NBDs mobility (Figure 4.2 and 4.5).

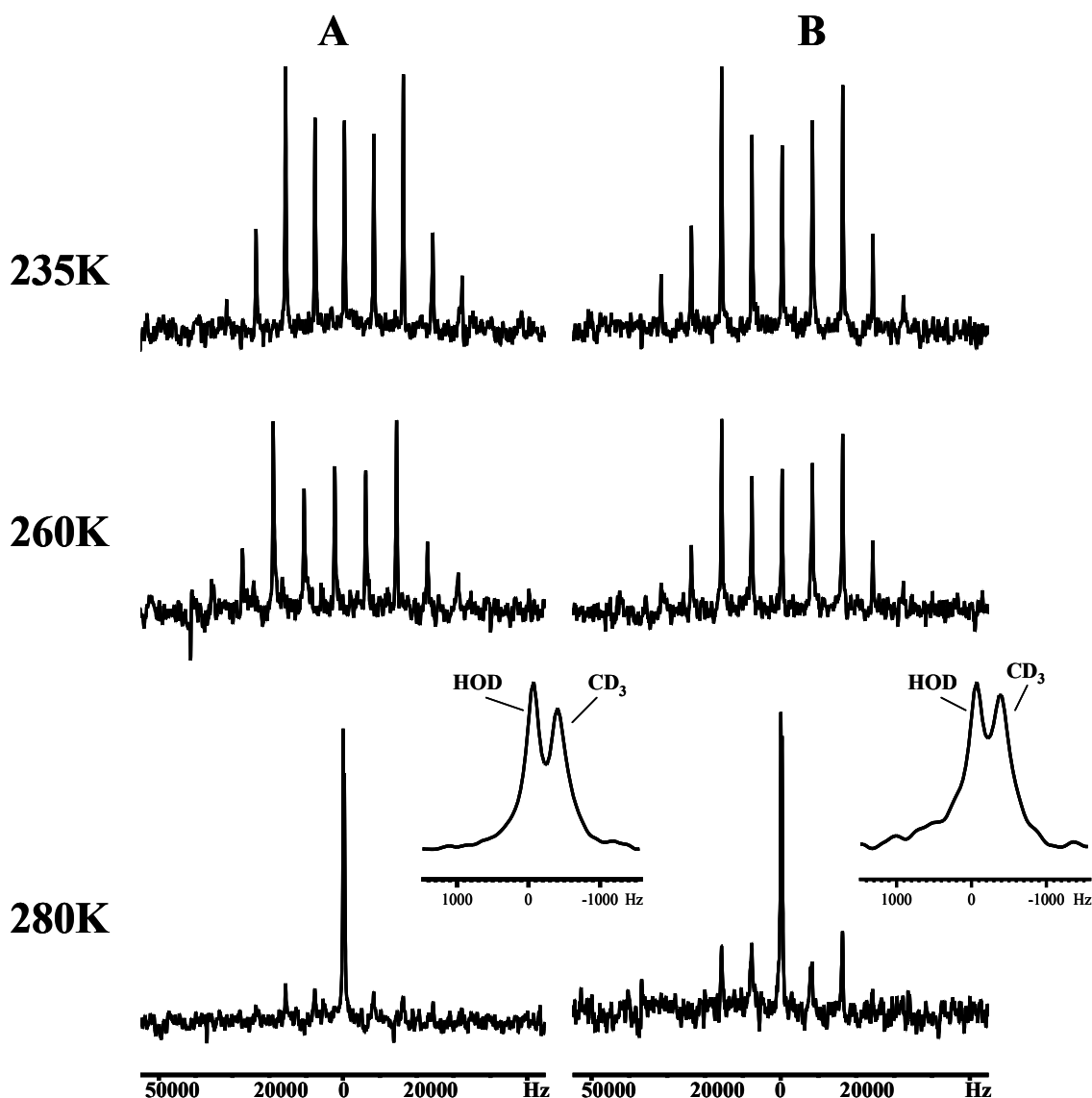


Figure 4.5: ^2H MAS NMR spectra of *E. coli* liposomes reconstituted LmrA in a resting state (A), and with AMP-PNP bound (B). The temperature was set at 235K, 260K and 280K.

^{31}P NMR

One of the possible origins of the central component is fast tumbling protein associated with non-

bilayer lipid complexes or with small unilamellar vesicles (Herzfeld *et al.*, 1987; Jelinski *et al.*, 1980a). To exclude this possibility, the ^{31}P NMR was used to monitor changes in the phase behaviour of the phospholipids bilayer upon interaction with the protein (Ravault *et al.*, 2005). Figure 4.6 shows a comparison of ^{31}P spectra of *E. coli* liposomes reconstituted LmrA and *E. coli* lipid unilamellar liposomes prepared in the same way as for reconstitution, including detergent destabilization and detergent removal with bio-beads. All spectra are clearly dominated by the chemical shift anisotropy of the phosphate groups averaged by fast axial rotation of lipid molecules. This confirms that the lipid systems remain in the liquid crystalline lamellar phase when it contains reconstituted LmrA in full and truncated form. Additionally, the freeze-fracture micrographs presented in Chapter 3 (Figure 3.8) clearly demonstrate that the systems used here were liposomal. Nonliposomal or amorphous structures were not seen.

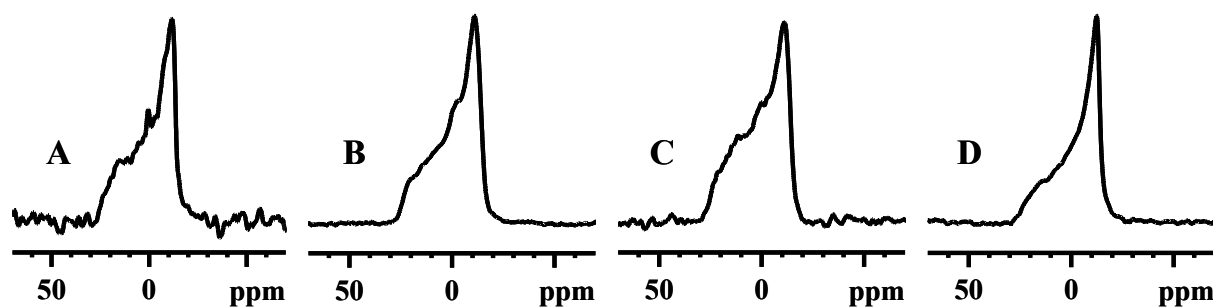


Figure 4.6: The ^{31}P NMR spectra of *E. coli* liposomes reconstituted LmrA in (A) a resting state (B) with AMP-PNP bound, (C) LmrA-MD, (D) free liposomes prepared in a way like for LmrA reconstitution. The temperature was set at 300 K.

Comparison of ^2H NMR spectra of LmrA in a resting state and a state when AMP-PNP bound

In the next step the static spectra of alanine CD_3 labeled LmrA in complex with AMP-PNP at the most representative temperatures, 235K, 260K and 280K, were recorded. Figure 4.2 shows a comparison of ^2H alanine CD_3 spectra in the LmrA resting state and in complex with AMP-PNP. From the visual inspection it is clear that at the temperature as high as 280K the difference between the spectra of both protein states is in the size of a central component. It is considerably reduced when AMP-PNP is bound to LmrA. The quadrupolar splitting of both spectra are equal to the one of the resting state LmrA at every measured temperature. However, the powder pattern of the protein with

AMP-PNP bound exhibit severe spectra distortions at 235K, and 260K, when compared to spectra of LmrA in a resting state.

Comparison of ^2H spectra and T_1 relaxation for LmrA in a resting state, and ATP/ADP-Vanadate trapped state

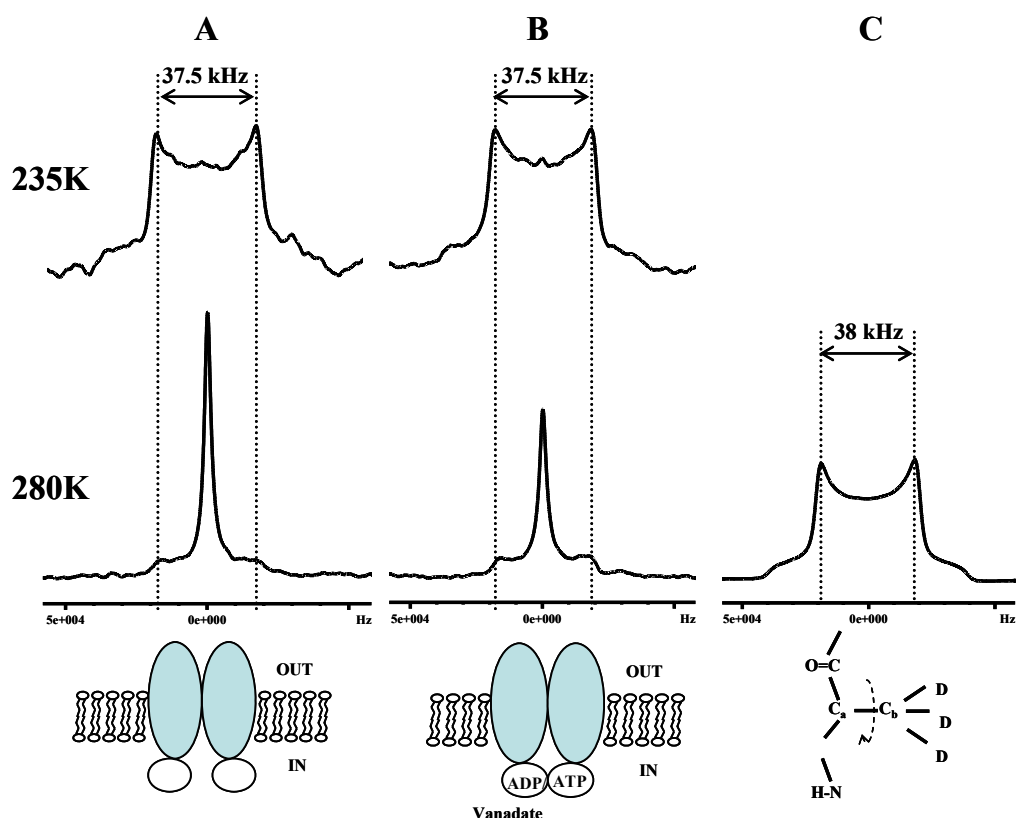


Figure 4.7: ^2H NMR spectra of ^2H alanine selective labelled LmrA reconstituted *E. coli* liposomes in a resting state in a state trapped with ATP/ADP-Vanadate. The spectra recorded at increasing temperatures 235K, and 280K. The spectra arise from the 48 alanines in the LmrA (~ 147 deuterons).

To investigate the dynamics behaviour of LmrA in post-hydrolysis state, LmrA was trapped with ATP/ADP-Vanadate in a state when one ATP molecule is hydrolysed and product ADP still bound to nucleotide binding site and another ATP is waiting to be hydrolysed. The comparison of spectra of full-length LmrA in a resting state and in ATP/ADP-Vanadate trapped state at 280K revealed that the central component is reduced for ATP/ADP-Vanadate trapped state in a way similar to the one observed for LmrA trapped with AMP-PNP. Interestingly, in contrast to AMP-PNP trapped LmrA, no

differences were observed between the spectra of LmrA in a resting state and in ATP/ADP-Vanadate trapped state recorded at 235K. The direct comparison of deuterium NMR spectra of LmrA trapped with AMP-PNP and ATP/ADP-Vanadate could cause error because these two samples belong to different preparation batches and these two different preparation batches might slightly differ in deuterium natural abundance water content, which could be estimated for each case only qualitatively. In addition, the T_1 values have been obtained for both rigid and dynamic part of ATP/ADP-Vanadate trapped LmrA state spectra and compared to values obtained for LmrA resting state (Figure 4.8 and Table 4.1).

It was found that the T_1 values for rigid part of ^2H spectrum are not significantly changed, the difference is in the ratio of experimental mistake. In contrast, the T_1 values for the dynamic component are clearly different for two protein states. Although quantitative analysis of deuterium spin-lattice relaxation is straight forward, it has to be done with care if multiple motions are present. Therefore, even having the whole set of T_1 values, it is not possible to deduce a correlation time of CD_3 group motion in LmrA.

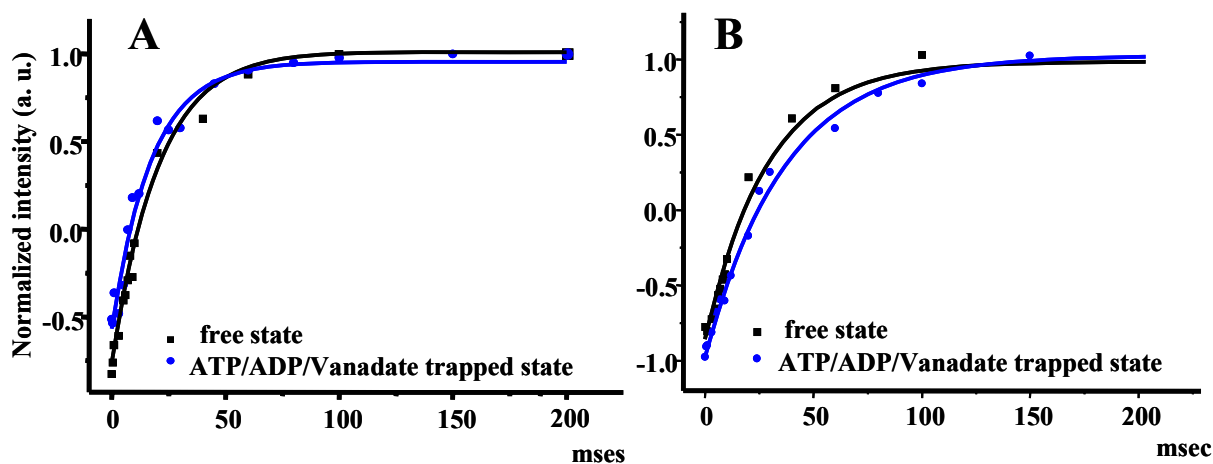


Figure 4.8: The comparison of the spin-relaxation rates for LmrA TMDs and loops (A) and NBDs (B) in the protein resting state (black line) and ATP/ADP-Vanadate trapped state (blue line).

4.4. Discussion

Due to the necessity to study membrane proteins in membrane embedded form, structural and dynamic information is extremely difficult to obtain. Recently, the most precise structures of ABC

family members were obtained for MsbA and BtuCD transporters (Locher *et al.*, 2002; Chang and Roth, 2001). However, it provides no information about the overall macromolecular proteins dynamics as well as about dynamics of these proteins particular domains.

Labelling

Here we exploit the deuterons as a spin-spy probe of molecular dynamics of the ABC transporter LmrA transmembrane and ATP binding domains. For this purpose, deuterium labelled (CD₃ group) alanine was incorporated in the LmrA, using the procedure adopted from Cai (Cai *et al.*, 1998). The alanine methyl groups were chosen because of their direct attachment to the α -carbon what allows to look at the backbone dynamics (Leo *et al.*, 1987). Thus, any motions influencing the line shape, other than threefold methyl reorientation about the C _{α} -C _{β} bond axis, must arise from the protein backbone (Leo *et al.*, 1987). Moreover, non-methyl deuterons suffer from severe difficulties of signal detection (Jones *et al.*, 1997).

Alternative ways to incorporate the deuterium probes into the protein of interest have been used for egg white lysozyme and gramicidin A. All exchangeable groups in hen egg white lysozyme were labeled with deuterium by mild thermal denaturation in ²H₂O. Using this approach via T₁ measurements the correlation times for a fully hydrated crystalline protein was determined. The spin-lattice relaxation measurements at different NMR fields indicated the presence of additional slow motions in the range of 10⁻⁷ – 10⁻⁶ sec (Mack *et al.*, 2000). Another example is the indole ring protons of the gramicidin A tryptophan residues, which were deuterated via exchange in deuterated trifluoroacetic acid. From the experimentally determined quadruple echo decay time, the rotation correlation time was obtained which was consistent with formation of the peptide dimer (Macdonald and Seelig, 1988). Both methods, however, is not suitable for membrane transporters in general, and LmrA in particular, because the conditions for reversible renaturation for these proteins are not known.

Examination of ²H static LmrA in a resting state

At low temperatures the spectra of selectively alanine methyl group deuterated LmrA in a resting state

has the powder pattern typical for crystalline form of CD₃ alanine with asymmetry parameter of $\eta \sim 0$. It has a featureless line shape indicative of slow molecular dynamics with the quadrupolar coupling constant of 49.0 kHz, corresponding to a powder width of 37.5 kHz. At higher temperatures together with the rigid component the second central isotopic component appears in the spectra (Figure 4.2). The quadrupolar splitting of the rigid component at higher temperatures does not differ from the one at low temperatures. This indicates that particular domains in LmrA remain almost immobilized at low as well as at high temperatures whereas other LmrA domains exhibit high level of motion at increasing temperature. It implies that the alanine methyl groups in the LmrA domains corresponded to the rigid component in ²H spectra exhibit no reorientation in addition to 3-fold rotation. Similar no change in quadrupolar splitting of the ²H spectra rigid component recorded between -85 and 75°C has been shown previously for ²H₅ Trp labeled bR (Kinsey *et al.*, 1981). Therefore, it was concluded that bR Trp residues undergo no large amplitude motions on a time scale below $< 10^{-5}$ s below 75°C (Kinsey *et al.*, 1981).

Central component

The central isotopic component similar to the one we observed at increasing temperatures has been reported in the literature before. There can be multiple reasons for this central component to appear. Firstly, it can originate from deuterium natural abundance in water. Although prior to NMR measurements the protein reconstituted into proteoliposomes was extensively washed with buffer prepared on deuterium depleted water, the water containing natural abundance (0.015 %) concentration of deuterium can not be completely washed from the vesicles interior. Therefore, one could expect certain intensity in the isotopic central peak originating from deuterated water in natural abundance. For the unlabelled collagen it has been shown that approximately one-third of the sharp peak in the center of the spectrum is due to deuterium natural abundance in water, whereas two-third of the central component intensity comes from the alanine residues residing in the nonhelical termini of the molecule (Jelinski *et al.*, 1980b). Using ²H MAS NMR we have made a rough estimation of natural deuterium abundance water content in our samples. How it can be seen from Figure 4.5, this contribution is not significant.

Secondly, the central component can originate from partly degraded protein, which lost its connection with the proteoliposomes or from soluble proteins which associated with the membrane and were not removed during the purification procedure. This possibility can be excluded as the SDS-PAGE analysis and gel filtration (Figure 4.1 and Figures 3.2 and 3.3, Chapter 3) reveal that the procedure we use for the samples preparation yields pure protein without contaminations from soluble proteins. Additionally, the ATPase assays performed on those samples as well as substrate induced intrinsic tryptophan fluorescence quenching experiments had concentration-dependent character. This proves the function state of the protein reconstituted *E. coli* liposomes and allows us to exclude the presence of aggregated protein in our samples (Chapter 3, 5).

Thirdly, using ^{31}P NMR we have excluded the possibility that this component comes from fast tumbling protein attached to non-bilayer lipid complexes or small unilamellar vesicles (Figure 4.6).

Alternatively, in some cases, this central isotopic component has been assigned to the amino acids located on the protein surface (Keniry *et al.*, 1984a). Similar reduction of the spectral width (in our case to 150 Hz width at the half height for a resting state LmrA measured at 280K) has been reported for the protein in solution. Here, it has been addressed to free rotation of the molecules about its long axis (Jelinski *et al.*, 1980a). However, in the same study it was proposed that the sharp component may be due to some alanine C_α - C_β bond axes which make the ‘magic angle’ with respect to the helix axis, or corresponds to residues residing in non-helical termini of the molecule (Jelinski *et al.*, 1980a).

In addition, very strong argument comes from the deuterium NMR measurements of LmrA-MD and proteolysed LmrA. So, it has been clearly shown that this central component can be almost removed from the spectrum if the NBDs are cleaved or if LmrA is expressed in truncated version without NBDs (LmrA-MD) (Figure 4.4).

Taking all together, it can be concluded that this central isotopic component originates from the residues located in NBDs. The NBDs are not embedded into lipid matrix, so the overall motion characteristics of NBDs can be quite different from the motion characteristics of the TMDs and even resemble the motion behaviour of the protein in solution. The central isotopic component has a dramatically reduced quadrupolar constant of 159 Hz (from 49.0 kHz of a rigid part). Such a quadrupolar constant reduction can be associated with (1) three-fold methyl hops or rotations, which

are not limited by the membrane in cytoplasmic domain, as well as by (2) additional rotation motions about the protein long molecular axis, (3) rotation about the C_{α} - C_{β} and C_{β} - C_{γ} bond axes, (4) librational motions corresponded to wobbling of methyl groups, and (5) by backbone mobility (Tiburu *et al.*, 2004). Similar two components ^2H spectrum for deuterated fd coat protein was obtained. The rigid spectrum part was assigned to immobile alanine residues whereas dynamic part to alanine residues of experiencing isotropic motions (Leo *et al.*, 1987). At that time the structure of fd coat protein in the lipid bilayer was not available (McDonnell *et al.*, 1993). So it was not possible to complete the picture and associate different alanine amino acids dynamic characteristics with their membrane buried and surface location (Leo *et al.*, 1987).

The relative integrals of rigid and dynamic parts in deuterium static spectra of LmrA in a resting state were calculated to be approximately 1 to 1 (Figure 4.2). This ratio is well matched to the number of residues in TMDs/loops LmrA part and LmrA NBDs, which is subsequently 27 to 21. However, it is known that the intensities in the ^2H quadrupolar echo experiments are not proportional to the number of spins except for the slow and fast limit regimes due to substantial intensity loss of groups undergoing intermediate rate ($\approx 10^5 \text{ s}^{-1}$) (Siminovitch, 1998). Therefore, a relation between the integrated intensities of the two spectra components may not reflect a relation between numbers of amino acids contributing to them, and have to be interpreted with caution.

^2H static spectra of LmrA in a resting state and in a state when LmrA is trapped with AMP-PNP and ATP/ADP-Vanadate

To investigate the effect of AMP-PNP binding on LmrA overall dynamics, deuterium NMR spectra of CD_3 alanine labeled LmrA in complex with ANP-PMP were recorded at 235K, 260K, and 280K. Figure 4.2 shows a comparison of LmrA spectra at 235K, 260K, and 280K for both protein states. Interestingly, the AMP-PNP binding to LmrA leads to the clear changes in the LmrA spectra at all studied temperatures. The difference in the deuterium spectra at 235K and 260K evidences changes in the protein mobility which is difficult to address to particular LmrA domains. In contrast, at 280K, at which the rigid spectra component was assigned to mostly TMDs and dynamic component to NBDs, the only difference is that the spectrum of LmrA in complex with AMP-PNP has considerably

reduced central component. It may indicate the reduced mobility of NBDs.

In the next step the spectrum of ATP/ADP-Vanadate trapped LmrA were compared to a resting state LmrA spectrum (Figure 4.7). Interestingly, at a temperature as high as 235K the spectrum of ATP/ADP-Vanadate trapped LmrA resembles the one of a resting LmrA state, whereas at 280K the one for AMP-PNP trapped LmrA (Figure 4.2 and Figure 4.7). This interesting spectra behaviour points out that motionally ATP/ADP-Vanadate trapped LmrA state is neither equal to LmrA resting state nor to AMP-PNP trapped state.

T₁ measurements

In general T₁ measurement is a useful mean to investigate the protein dynamics (Allerrini *et al.*, 1985; Keniry *et al.*, 1984b; Opella, 1982; Jelinski *et al.*, 1980a). The spin-relaxation measurements are extremely sensitive to internal motions of proteins side chains in the range 10⁻⁷ to 10⁻¹⁰ s. It is possible to determine a unique correlation time from a single set of relaxation spectra and often to discriminate among possible models of motion (Torchia, 1984). In our case the T₁ measurements contain limited information because there too many probes in the protein, 48 deuterated alanines (~147 deuterons). Each of them might be motionally inequivalent and the resulting T₁ values might be an average of many of different values. However, T₁ values comparison for different protein states can certainly add to a qualitative understanding of dynamic process occurring in the protein under AMP-PNP and ATP/ADP-Vanadate binding.

The spin-relaxation was investigated as a function of temperature. For LmrA resting state, it is shown (Table 4.1), that the T₁ values increase with the temperature. Similar increase of T₁ values with a temperature has been observed before for myoglobin (Keniry *et al.*, 1983). It has been suggested that for methyl groups in L-amino acids methyl rotation dominates the relaxation at low temperatures. In contrast, at higher temperatures an additional large-amplitude motions occurs that effect the relaxation and often ²H NMR line shapes. At 280K the T₁ values were obtained separately for two spectra components, the rigid and the dynamic, corresponded respectively to TMDs and loops and to NBDs. The obtained spin-lattice relaxation vales for TMDs and loops was 20.4±1.5 ms and for NBDs was 28.5±2.2 ms. To compare, the motional characteristics of membrane spanning domains and nucleotide

binding domains during the LmrA transport cycle the T_1 values for LmrA in the resting protein state and in the state where LmrA is trapped with ATP/ADP, and vanadate were obtained (Figure 4.8, Table 4.1). The spin-lattice relaxation values indicated that in the ATP/ADP-Vanadate trapped state, the LmrA has motional characteristics clearly different from the resting state. Moreover, it was shown (Figure 4.8, Table 4.1) that the major dynamic changes effecting the dynamics occur not in membrane spanning region, but in nucleotide binding region.

Summarizing to say, at 280K temperatures the deuterium spectra of LmrA in a resting state and trapped with AMP-PNP and ATP/ADP-Vanadate had two components: the rigid with a quadrupolar splitting of powder CD_3 labeled alanine and central isotropic part. Usage LmrA-MD and LmrA proteolysed allowed us to correlate the central component with NBDs and the rigid with TMDs and loops. Examination of deuterium static spectra of LmrA trapped with AMP-PNP and ATP/ADP-Vanadate revealed that NBDs in both protein states have reduced mobility when compared to LmrA resting state. In addition, LmrA trapped with AMP-PNP is more motionally restricted then LmrA trapped with ATP/ADP-Vanadate.

Relation with the ABC transporters transport cycle

Strong evidence exists that ABC transporters NBDs dimerization occurs under ATP binding, and subsequent ATP hydrolysis leads to opening of NBDs dimer (Lu *et al.*, 2005). Such a dramatic structural rearrangement (Figure 4.9) may lead to altering of the overall protein dynamics characteristics what may have direct influence on deuterium spectra lineshapes in a way we detected. Interestingly, we have observed that all the LmrA state: resting, pre-hydrolysis, and post-hydrolysis are not motionally equivalent. In past, conformational non-equivalence between those three protein conformations have been reported for PGP on 2D crystals and by cross-linking studies and on LmrA by mass spectroscopy (Ecker *et al.*, 2004; Rosenberg *et al.*, 2003; Loo and Clarke, 2002).

Concerning the ABC transporters transmembrane domain, it is well established that the transmembrane helices exhibit conformation rearrangements under substrate and/or ATP binding (Vigano *et al.*, 2002; Rosenberg *et al.*, 2001b; van Veen *et al.*, 2000a). However, limited structural

data do not allow to reliably conclude on a nature of these rearrangements. The fact that changes in the dynamics characteristics of LmrA transmembrane helices were not detected on ^2H static spectra recorded at 280K and by T_1 measurements at 280K (Figure 4.2) in the presence of AMP-PNP and ATP/ADP-Vanadate subsequently does not imply that no conformation changes occur in TMDs under ATP and ATP/ADP binding. We can speculate that rotation or translation movements of the α -helices which may be involved in restructuring of the membrane embedded domain do not affect the overall dynamics of TMDs in a way to be detected by low resolution ^2H NMR (Figure 4.9). Biochemical evidences of such transmembrane helices movements have been reported previously for LmrA and PGP (Vigano *et al.*, 2002; Rosenberg *et al.*, 2001b).

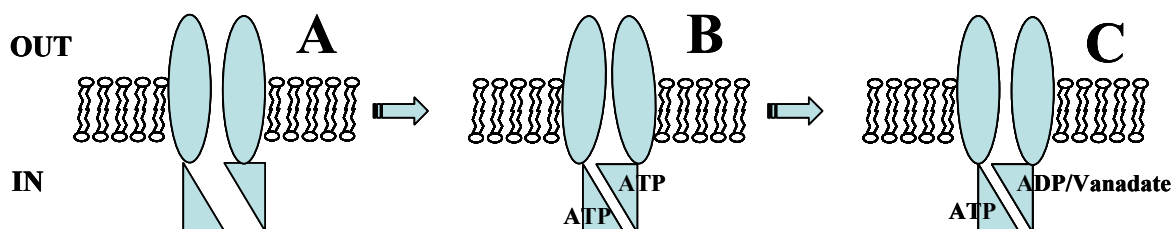


Figure 4.9: Proposed LmrA conformation changes affecting the protein dynamics under ATP binding and hydrolysis.

Approach advantages and limitations

The work presented in this chapter is the first attempt to study the dynamic behaviour of full-length ABC transporter LmrA in three protein states: resting, pre-hydrolysis and post-hydrolysis. This approach has its advantages and limitations.

While it does not allow for studying the internal dynamics of individual sites within the protein, this approach has several advantageous features. It allows associating particular signals with the protein TMDs, loops and NBDs and in parallel following the dynamics changes under ATP binding and hydrolysis separately for the membrane spanning and ATP binding domains. Similar results would be difficult to obtain with the smaller number of probes. In the absence of the high resolution structure and in the presence of limited biochemical data on LmrA, we would not be able to speculate on the dynamic changes in the whole system. However, such a study could potentially make analysis of ^2H

NMR spectra lineshapes more quantitative.

The results reported in this Chapter would be difficult to obtain by means of solution state NMR, because the internal motion of interest would be most likely superimposed by the overall protein tumbling, which is the dominant effect in determining T_1 and other relaxation parameters (Mack *et al.*, 2000). In contrast, in solid-state NMR no significant overall molecular motions occurs on the NMR time scale and relaxation is induced by internal motions alone (Mack *et al.*, 2000).

In addition to high sensitivity towards motional changes in the protein, the approach we used here is free of necessity to perform the signal assigning and the low natural abundance of deuterium (0.015 %) virtually eliminates background signals due to unlabelled material in natural abundance.

Conclusions

^2H static NMR studies thus demonstrated that the dynamic behaviour of LmrA domains is complex. The deuterium LmrA spectra at 280K had two components: the rigid with a quadrupolar splitting of powder CD_3 labeled alanine and central isotropic part. The rigid spectra part was related to TMDs and loops and isotopic to NBDs. The comparison of spectra at several temperatures 235K, 260K, and 280K allows to conclude that the LmrA TMDs are relatively immobile on NMR time scale; in contrast NBDs are quite dynamic. The comparison of deuterium lineshapes of LmrA in a resting state and trapped with AMP-PNP and ATP/ADP-Vanadate revealed that the protein is motionally non-equivalent at each state. Concerning motion of certain LmrA domains, it has been observed that under ATP binding and hydrolysis, TMDs remain relatively immobilized on a time scale of NMR measurement, in the same time, NBDs experience considerably reduced mobility.

5. Ligand binding to LmrA as observed by fluorescence and solid-state NMR spectroscopy

Abstract

Having optimized the protocol for reconstitution of LmrA into *E. coli* liposomes at a high protein lipid ratio, the experiments aiming to shed light on drug protein interaction and conformation changes occurring in the protein under substrate binding can be performed. In the first step the binding of TPP⁺, fluoroquinolone drug, norfloxacin and vinblastine were probed using tryptophan intrinsic fluorescence quenching approach. TPP⁺ and norfloxacin both contain NMR active nuclei, respectively ³¹P and ¹⁹F, in their structure. It is give the possibility to assess these drugs binding to LmrA by SSNMR without expensive isotope labelling. Finally, effect of leupeptin, an effective PGP inhibitor, on Hoechst-33342 transport and ATPase activity of LmrA reconstituted into proteoliposomes was investigated.

5.1. Introduction

As one of the major causes of MDR is the overexpression of MDR transporters, the goal of modern pharmaceutical science is to find effective modulators of MDR transporters for clinical application. Therefore detailed knowledge on drug-protein interaction is needed. Numerous studies have been performed to gain insight into the physicochemical aspects of substrate interaction with different types of MDR transporters (Murakami *et al.*, 2002; Zheleznova *et al.*, 2000; Seelig, 1998). However, the substrate interactions and translocation by the MDR proteins family is not well understood.

To observe the drug binding to LmrA and conformation changes in the protein occurred under substrates binding, the tryptophan intrinsic fluorescence quenching with three drugs, TPP⁺, norfloxacin, and vinblastine were performed (Figure 5.1). Two of them, TPP⁺ and vinblastine, are known LmrA substrates (van Veen *et al.*, 2000a; van Veen *et al.*, 1996). Binding of fluoroquinolone drug, norfloxacin to LmrA, in contrast, has never been shown before. Although rapidly emerging

bacterial resistance to this type of agents including resistance through expression of MDR membrane pumps is shown (Blondeau, 2004b; Poole, 2000).

Fluorescence spectroscopy has been very fruitful over the past years in exploration of membrane transporters structure and function (Eckford and Sharom, 2005; Elbaz *et al.*, 2005; Lugo and Sharom, 2005a; Vigano *et al.*, 2002; Liu *et al.*, 2000; Sharom *et al.*, 1999a; Sharom *et al.*, 1999b). Fluorescence measurements can be performed using fluorescent dyes, MDR substrates, using the extrinsic fluorophore 2-(4-maleimidoanilino)naphthalene-6-sulfonic acid (MIANS) at Cys residues or by taking advantage of intrinsic fluorescence of proteins provided by their aromatic acids, tyrosine, tryptophan and phenylalanine (Sharom *et al.*, 2001; Sharom *et al.*, 1999b). These measurements have provided unique information suggesting that the drugs are extracted from the membrane cytoplasmic leaflet and allowing to monitor changes occurring in the transmembrane and cytosolic regions in the presence of drug (Sharom *et al.*, 2001; Mitchell *et al.*, 1999).

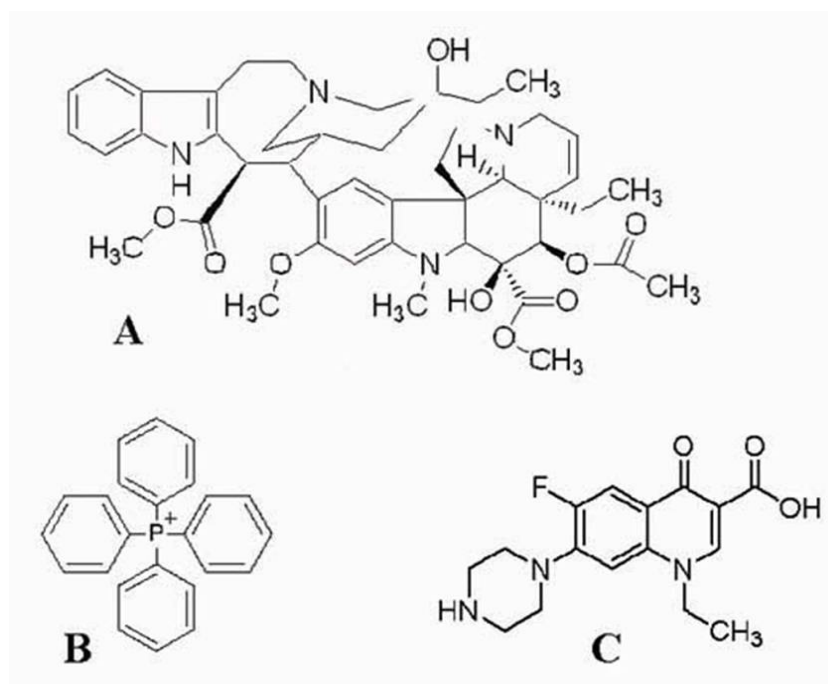


Figure 5.1: The chemical structures of (A) vinblastine, (B) TPP⁺, and (C) norfloxacin.

The intrinsic tryptophan fluorescence of PGP is shown to be highly sensitive to the drugs and

nucleotide binding and can be used to assess the drug affinity of known substrates and screen the drug library to identify new substrates and modulators (Sharom et al., 2001; Liu et al., 2000; Sharom et al., 1999a; Sharom et al., 1999b). Experiments aiming to determine the K_d values for known MDR substrates are extremely important because substrate K_d values are highly correlated with their ability to inhibit. Fluorescence quenching approach application to LmrA has been reported to our knowledge only once (Vigano *et al.*, 2002). In this case, Trp fluorescence quenching by acrylamide has been carried out in the presence and absence of the substrate daunorubicin and ATP. The experiments show that drug binding influences the structure of cytosolic regions of LmrA and a conformational change is transmitted from the TMDs to NBDs (Vigano *et al.*, 2002).

As an alternative technique, NMR has been successfully applied in recent years to identify and characterize a number of compounds in drug discovery process (Wyss et al., 2002; Glaubitz et al., 2000; Spooner et al., 1994). It is a rather useful tool for obtaining site specific information concerning membrane protein drug recognition, binding and transport, because it allows the protein to be studied in the native environment (Boland and Middleton, 2004; Middleton *et al.*, 2004; Patching *et al.*, 2004b; Middleton *et al.*, 2000a; Watts *et al.*, 1998). In addition, NMR is able to determine the structure of bound ligand (Luca et al., 2005).

Solid-state NMR spectroscopy can be applied not only to observe bound ligands, but also to investigate the binding quantitatively by studying CP build-up curves and analyzing binding stoichiometry (Patching *et al.*, 2004a; Xu *et al.*, 2000). The most relevant substrates for this kind of studies are weakly bound substrates. Strongly bound ligands undergo slow dissociation from the membrane receptor and their kinetic is not manifested on NMR time scales. Additionally, resonances of tightly bound ligands experience linebroadening due to chemical shift anisotropy and dipolar interactions. However, strongly bound ligands can be detected by means of CP MAS NMR, because MAS average chemical shift anisotropy and dipolar interactions (Patching et al., 2004b).

Among examples of such investigations are experiments performed on a nucleoside transporter, NucP, and a glucuronide transporter, GusB. For these two transporters not only the binding affinities of ^{13}C -labeled substrates have been determined but, additionally, a novel approach allowing to eliminate signal from non-specific binding by means of a cross-polarization/polarization inversion

recovery NMR has been presented (Patching *et al.*, 2004b). This method might be of interest especially if the chemical shifts of specifically and non-specifically bound ligands overlap or if the signal from non-specifically bound ligand is much stronger than that of specifically bound ligand.

The application of solid-state NMR methods allows structural insight into ligand binding to large membrane proteins to be obtained, which is extremely difficult by other biophysical methods (Zech *et al.*, 2004). An example of such an investigation is a solid-state NMR investigation of glycosides binding to Na⁺/K⁺ ATP-ase. Here, a ¹⁹F/¹³C REDOR NMR strategy was used to determine the structure of an inhibitor in its binding site (Middleton *et al.*, 2000a).

An alternative way to study ligand-protein interactions by SSNMR is through the observation of a labeled protein followed by analysis of chemical shift differences between the drug bound and unbound protein state. This approach is potentially free of difficulties associated with non-specific substrates binding to the membrane in case of membrane reconstituted protein samples, especially in case of weak substrate binding often observed for membrane transporters (Spooner *et al.*, 1998). Using this approach, the ligand binding to the anti-apoptotic protein Bcl-xL has been observed (Zech *et al.*, 2004).

The observation of ligand bound to protein requires isotope labeled ligand or protein. However, examples of isotope labeled drugs are rare and protein labelling is often expensive. Another way to observe bound ligand by NMR spectroscopy is to observe ligands naturally containing NMR active nuclei, such as ³¹P or ¹⁹F (Patching *et al.*, 2004b; Middleton *et al.*, 2000a). ³¹P (100 % abundance) and ¹⁹F (100 % abundance) nuclei are spin half nuclei and are characterized by high sensitivity, which makes them convenient for NMR spectroscopy. In addition, the protein itself does not contain any fluorine or phosphorous nuclei (unless protein is phosphorylated), which makes assignment and removal of background, in case of phosphorous, straight forward (Xu *et al.*, 2000). Two LmrA substrates TPP⁺ and norfloxacin meet these requirements, containing respectively ³¹P and ¹⁹F in their structure.

There are several ways to inhibit the drug transport in MDR proteins. Among them is designing modulators which have affinity for the drug binding site high enough to win the competition for this binding site with other substrates, occupy the binding site, and block the protein function. Another

way to modulate the drug resistance phenomena is to design compounds perturbing interactions between the cytosolic and membrane-embedded domains. Concerning, PGP, up to date numerous compounds have been identified as MDR-reversing agents (Dantzig *et al.*, 2001). There is growing evidence that many hydrophobic peptides are also P-glycoprotein substrates (Lam *et al.*, 2001; Sharom *et al.*, 1998; DiDiodato and Sharom, 1997). Several of them have been seriously investigated with respect to their K_d values, ATPase activity modulation, and ability to block drug transport (Sharom *et al.*, 1998; Sharom *et al.*, 1996). These peptides display a relatively low overall toxicity to intact MDR cells, and inhibit drug transport at concentrations below the toxic range. Therefore, it is suggested that hydrophobic peptides should be given serious consideration for development as clinical chemosensitizing agents (Sharom *et al.*, 1998). Among those peptides are leupeptin, pepstatin A, valinomycin, cyclosporin A. However, despite the growing evidence of hydrophobic peptides ability to modulate MDR, their interaction with LmrA has never been reported. Therefore, we have examined the influence of leupeptin on Hoechst-33342 transport by the multidrug transporter LmrA and on LmrA ATPase activity.

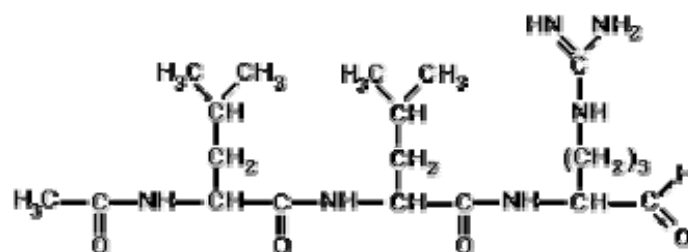


Figure 5.2: The chemical structure of leupeptin (acetyl-Leu-Leu-Arg-al), linear peptide, which was shown to be an effective blocker of colchicine transport for PGP (Sharom *et al.*, 1998).

The present work uses a fluorescence approach to provide insight into the binding of three drugs, norfloxacin, TPP^+ , and vinblastine, to LmrA. So, the binding affinities for three drugs are determined and the nature of their binding to the protein is discussed. The binding of norfloxacin and TPP^+ to LmrA was additionally assessed by solid-state NMR spectroscopy. The real-time fluorescence assay is used to monitor the Hoechst-33342 transport and the transport collapse by LmrA modulator, peptide, leupeptin.

5.2. Materials and Methods

Materials

TPP⁺, leupeptin, norfloxacin, and vinblastine were obtained from Sigma. All other materials were reagents of analytical grade.

LmrA purification and reconstitution into *E. coli* liposomes by detergent liposome destabilization method was done as described under Materials and Methods in Chapter 2 and 3.

5.2.1. LmrA tryptophan intrinsic fluorescence quenching by various substrates

Fluorescence quenching experiments were carried out in suspensions of 1 μ M LmrA reconstituted into *E. coli* liposomes by the detergent destabilized method described above. The necessary proteoliposomes dilutions were performed in 100 mM Tris, 50 mM KCl buffer, pH 7 buffer. Working solutions of drugs were prepared in ethanol (TPP⁺ and norfloxacin) and in DMSO (vinblastine) of highest available purity. The final concentration of solvent in the fluorescence cuvette was always kept to 1 % (v/v). Both solvents alone in such concentration showed negligible effect on intrinsic Trp fluorescence. Quenching experiments were performed by adding 1 μ L aliquots of different drug concentrations to 99 μ L LmrA reconstituted proteoliposomes in 0.5 cm quartz cuvette. After each addition, the sample was excited at 290 nm and the steady-state fluorescence emission was measured at 340 nm. Fluorescence intensities were corrected for ethanol, DMSO, and drugs effect by subtracting the emission spectra of the same drug dilution in appropriate buffer collected in parallel for each sample. Artifacts originating from scattering were corrected by using polarizing filters.

Experimental data showing monophasic quenching behavior were computer-fitted to the following equation (Liu *et al.*, 2000):

$$[5.1] \quad \left(\frac{\Delta F}{F_0} \times 100\right) = \frac{\left(\frac{\Delta F_{\max}}{F_0} \times 100\right) \times [S]}{K_d + [S]}$$

where F_0 is the initial value of fluorescence intensity, ΔF is the value of fluorescence intensity at a given point in the titration, $((\Delta F/F_0) \cdot 100)$ is the percent quenching (percent change in fluorescence relative of the initial value); $[S]$ is the substrate concentration, and K_d is the dissociation constant.

Fitting to a one or two site model was carried out using a nonlinear regression algorithm with Origin 7.0 (Microcal Software Inc., Northampton, MA), the K_d value for monophasic quenching behavior and K_{d1} , K_{d2} for biphasic were extracted.

5.2.2. ^{19}F and ^{31}P SSNMR measurements of substrates bound to LmrA

All experiments were performed on a Bruker Avance 600 spectrometer equipped with a 4 mm MAS DVT probe. The measurements were performed at 242.9 MHz for ^{31}P and 564.5 MHz for ^{19}F . For ^{31}P and ^{19}F observation a CPMAS pulse program employing an 80-100% ramped Hartmann-Hahn condition with two pulse phases modulated (TPPM15) heteronuclear ^1H decoupling was used. For ^{31}P observation the acquisition time was set to 49 ms, CP contact times and recycle delay times were respectively 1.5 ms and 2 s. For ^{19}F observation the acquisition time was set to 20 ms, CP contact times and recycle delay were respectively 1 ms and 4 s. Spectra were zero filled to 16k points and exponential line broadening of 50 kHz and 100 kHz were applied during processing respectively for ^{31}P and ^{19}F . The spinning rate was set to 10 kHz for all ^{19}F experiments and 8 kHz for all ^{31}P measurements. Spectra were referenced externally to phosphoric acid (85 %) at 0 ppm (^{31}P), and to trifluoacetic acid at 0 ppm (^{19}F). The temperature was regulated by a Bruker temperature control. Observations were made in both the L_α (liquid crystalline) and L_β (gel) phase of *E. coli* lipids at 25°C and -20°C respectively. Spectra were analyzed using Topspin (Bruker). Deconvolution of ^{19}F spectra was performed using PeakFit (SeaSolve Software Inc).

For ^{31}P NMR experiments 0.65 μM TPP^+ was added to 5 ml suspension of *E. coli* proteoliposomes reconstituted LmrA (about 0.15 μM of protein) in 100 mM Tris, 50 mM KCl, pH 7 buffer or to 20 mg *E. coli* lipid free liposomes. The mixtures were incubated on a rocking table for 20 minutes and then pelleted for 40 minutes with 50000 rpm.

For ^{19}F NMR experiments the same sample preparation procedure was used, however 10 fold excess of norfloxacin (about 2 μM) was added to the reconstituted protein (approximately 0.2 μM) to ensure efficient protein concentration in the lipid phase.

5.2.3. Modulation of Hoechst-33342 LmrA transport and ATPase activity by leupeptin

Hoechst-33342 transport inhibition

The Hoechst-33342 transport assay was performed essentially in the way described under Materials and Methods in Chapter 2. The only alteration is that Hoechst-33342 pumping under ATP hydrolysis was perturbed by addition of 20 μ L 10 mM leupeptin solution in DMSO. In a control measurement, pure DMSO was added place to leupeptin dissolved in DMSO.

The ATPase activity modulation

The ATPase assay was performed as described under Materials and Methods in Chapter 3. Leupeptin was dissolved in DMSO so that 1 μ L added to reaction mixture provided leupeptin concentrations of 1 mM and 10 mM subsequently for two experiments. For control measurement 1 μ L of pure DMSO was added to reaction mixture.

5.3. Results

5.3.1. Tryptophan intrinsic fluorescence quenching with norfloxacin and vinblastine

LmrA contains 5 tryptophan residues distributed throughout the LmrA polypeptide chain. Accordingly to the proposed topology (van Veen *et al.*, 1996), two of them are located in the NBD and three in loops connecting TM helices (Figure 5.11). Fluorescence quenching studies with the fluoroquinolone norfloxacin, and *Vinca alkaloid* vinblastine were carried out accordingly in 1 μ M LmrA containing proteoliposomes suspension.

The emission spectra of reconstituted LmrA exhibited a maximum at 344 nm, indicating that the tryptophan residues are located in a relatively non-polar environment buried within the protein structure as indicated by their emission spectrum when compared to solubilised Trp, which has an emission maximum at 360 nm (Figure 5.3) (Liu *et al.*, 2000). Two Trp residues are non membrane-embedded and located in nucleotide binding domain. Therefore, they potentially can be accessible to

aqueous surroundings. However, we observe only one emission maximum at 344 nm. This shows that Trp residues in NBD domain are possibly hidden from the aqueous environment and located in the NBD vicinity.

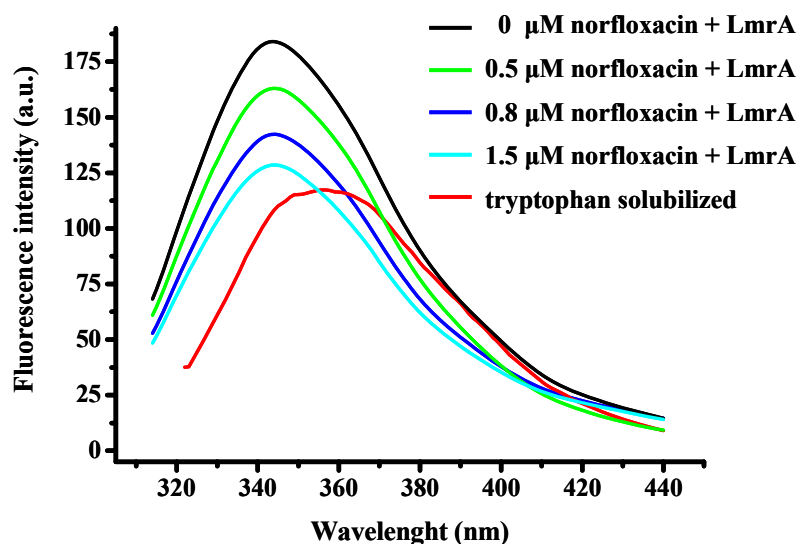


Figure 5.3: Fluorescence emission spectra for LmrA reconstituted into *E. coli* liposomes (1 μM protein) in buffer containing 100 mM Tris, 50 mM KCl, pH 7. The black spectrum is control fluorescence emission spectrum of standard proteoliposomes/buffer mixture containing 1 % (v/v) of pure ethanol. The red spectra show the fluorescence emission for Trp solubilised in 100 mM Tris, 50 mM KCl buffer, pH 7. Fluorescence emission was recorded at 25°C following excitation at 290 nm.

The Trp intrinsic fluorescence quenching for both drugs was measured in the concentration range of 0 – 50 μM . Further titration was limited by low drugs solubility. The usage of ethanol and DMSO in amounts higher than 1 % v/v had to be avoided, as this could potentially lead to the protein degradation. For both drugs, high fluorescence quenching showed the concentration dependent binding of drugs to protein and it was possible to estimate the binding constants for both drugs. In both cases, the data were fitted to a one site binding model. For norfloxacin the binding constant was determined $0.3 \mu\text{M} \pm 0.03 \mu\text{M}$ and for vinblastine $3.79 \pm 0.4 \mu\text{M}$ (Figure 5.4). The control quenching of solubilised Trp analogue N-acetyl-L-tryptophanamide (NATA) by number of substrates including vinblastine has been performed previously and was shown to be fully aqueous (Liu et al., 2000).

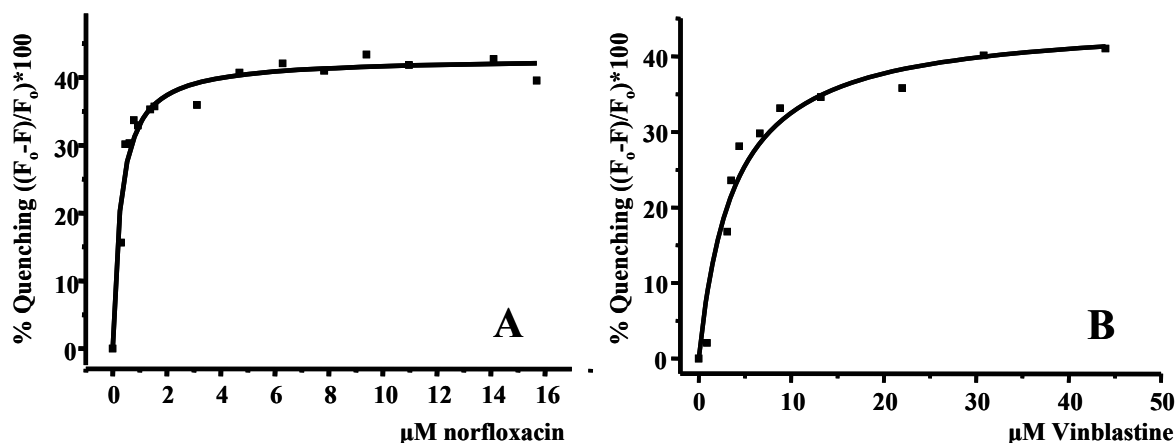


Figure 5.4: Binding of norfloxacin (A) and vinblastine (B) to LmrA reconstituted *E. coli* lipids liposomes as assessed by tryptophan intrinsic fluorescence quenching. The continuous lines represent the best computer-generated fit of the data points (shown by the symbols) to an equation describing interaction of drug with a single type of binding site. The determined affinity constants are $0.3 \pm 0.03 \mu\text{M}$ for norfloxacin and $3.79 \pm 0.4 \mu\text{M}$ for vinblastine.

For both drugs the quenching in percent appears to be relatively mild (less than 50 %). This indicates limited indirect effect of drugs binding on LmrA domains containing Trp residues. Otherwise higher quenching effect would be expected (Sharom et al., 2001). For the residues directly involved into drug binding the typical degree of quenching is much higher, up to 100 % (Sharom et al., 2001). The specificity of the interaction between the drugs and the protein was further confirmed, since neither norfloxacin, nor vinblastine showed any concentration-dependent Trp intrinsic fluorescence quenching when LmrA was thermally denaturated at 100 °C for 20 minutes.

5.3.2. ^{19}F SSNMR on norfloxacin bound to LmrA

As we have clearly demonstrated that fluoroquinolone drug, norfloxacin, binds to LmrA and since little is known concerning its interaction with PGP and LmrA, a solid-state NMR experiment was designed to obtain structural insight in norfloxacin binding to the protein. CPMAS ^{19}F spectrum of norfloxacin bound to LmrA (Figure 5.5B) is compared with control measurement performed on the protein free liposomes incubated with an equal proportion of drug (Figure 5.5A). The significant spectrum overlap hampers the differentiation of drug bound to the protein from the drug residing in the membrane. The observation of bound to protein ligand is further complicated the limited solubility

of norfloxacin. Low norfloxacin solubility leads to the presence of three different peaks from non bound drug molecules associated with presence of different norfloxacin conformers in solution. Nevertheless, by deconvoluting the spectrum containing the signal from substrate bound to protein (Figure 5.5B, box) it was possible to filter out the resonance we are interested in. Figure 5.5B (box) shows deconvoluted ^{19}F spectrum of norfloxacin, where the resonance of ligand bound to the protein is slightly shifted to -42.50 ppm when compared with the signal of unbound ligand at -46.00, -41.20, and -38.46 ppm (norfloxacin conformers).

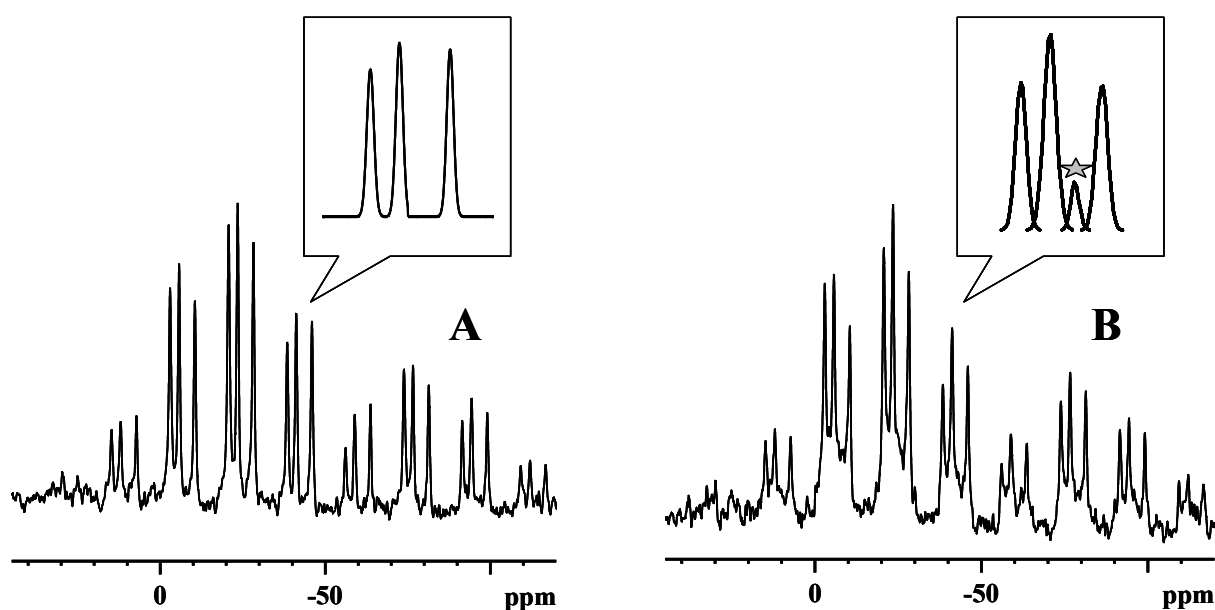


Figure 5.5: ^{19}F MAS spectrum of (A) free liposomes incubated with norfloxacin at a room temperature for 30 minutes, (B) proteoliposomes reconstituted LmrA with added norfloxacin (LmrA : norfloxacin = 1:5 mol/mol). The deconvoluted spectra for both free and protein reconstituted liposomes are shown in the boxes. The resonance signal from ligand non specifically interacting with the membrane is assigned to -46.00, -41.20, and -38.46 ppm, the signal from the substrate bound to LmrA is assigned to -42.50 ppm and marked with a star. The experiment was performed at 245K, at spinning frequency of 10 kHz. Approximately 8 K scans were accumulates per each spectrum.

5.3.3. LmrA tryptophan intrinsic fluorescence quenching with TPP^+

In the next step using tryptophan fluorescence quenching and solid-state NMR approaches TPP^+ binding to LmrA was probed. Figure 5.6 shows that Trp intrinsic fluorescence quenching of LmrA with TPP^+ has the concentration dependent manner. The Trp intrinsic fluorescence quenching curve

was fitted with a two-site binding model. The determined affinity constants are 9.3 ± 3.9 nM for a high affinity binding site and 22.0 ± 3.8 μ M for a low affinity binding site. The massive TPP⁺ binding, manifested in non concentration dependant Trp intrinsic fluorescence quenching, was observed when the titration was prolonged up to concentration of 0.05 M. However, it is obvious that at lower ligand concentrations significant binding to lipids occur as well. This obviously interferes with the results. Therefore, the results must be interpreted with caution.

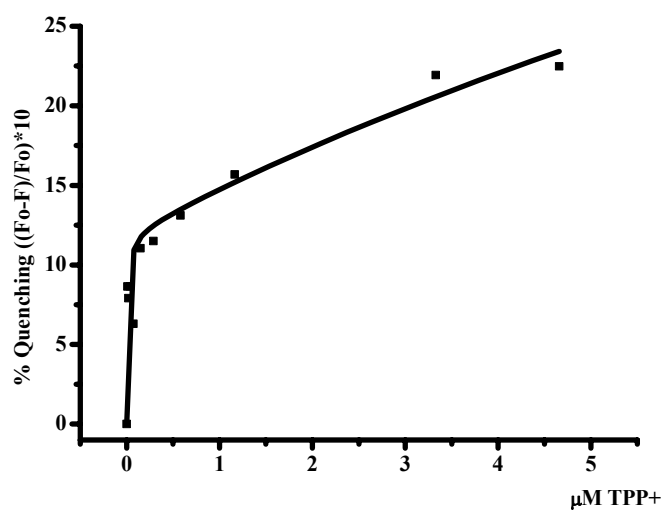


Figure 5.6: Binding of TPP⁺ to LmrA reconstituted *E. coli* lipids liposomes as assessed by tryptophan intrinsic fluorescence quenching. The continuous lines represent the best computer-generated fit of the data points (shown by the symbols) to an equation describing interaction of drug with two-site type of binding model. The determined affinity constants are 9.3 ± 3.9 nM for a high affinity binding site and 22.0 ± 3.8 μ M for a low affinity binding site. The massive TPP⁺ binding was observed when the titration was prolonged, which can interfere with the results. Therefore, the results must be interpreted with caution.

5.3.4. ³¹P SSNMR on TPP⁺ bound to LmrA

In the next the ³¹P CP MAS spectra were recorded on protein free *E. coli* liposomes and proteoliposomes reconstituted LmrA both containing 0.65 μ M TPP⁺, 5 fold excess in relation to total LmrA amount (Figure 5.7). The spinning speed was set to as 8 kHz, but it was not enough to average chemical shift anisotropy, so the spectra contain spinning sidebands together with the isotropic chemical shift. At temperature as high as 253K the TPP⁺ resonance is observed at 23.2 ppm, the chemical shift is consistent with values reported in the literature (Glaubitz et al., 2000). TPP⁺ is a

substrate for LmrA, and expected to bind to the protein under conditions used in the experiment (van Veen *et al.*, 1996). The bound drug molecules might be placed in different environment. In this case, the resonance position from the bound TPP⁺ molecules might be shifted from the non-bound molecules. However, no second peak from TPP⁺, which could correspond to bound drug molecules, was observed.

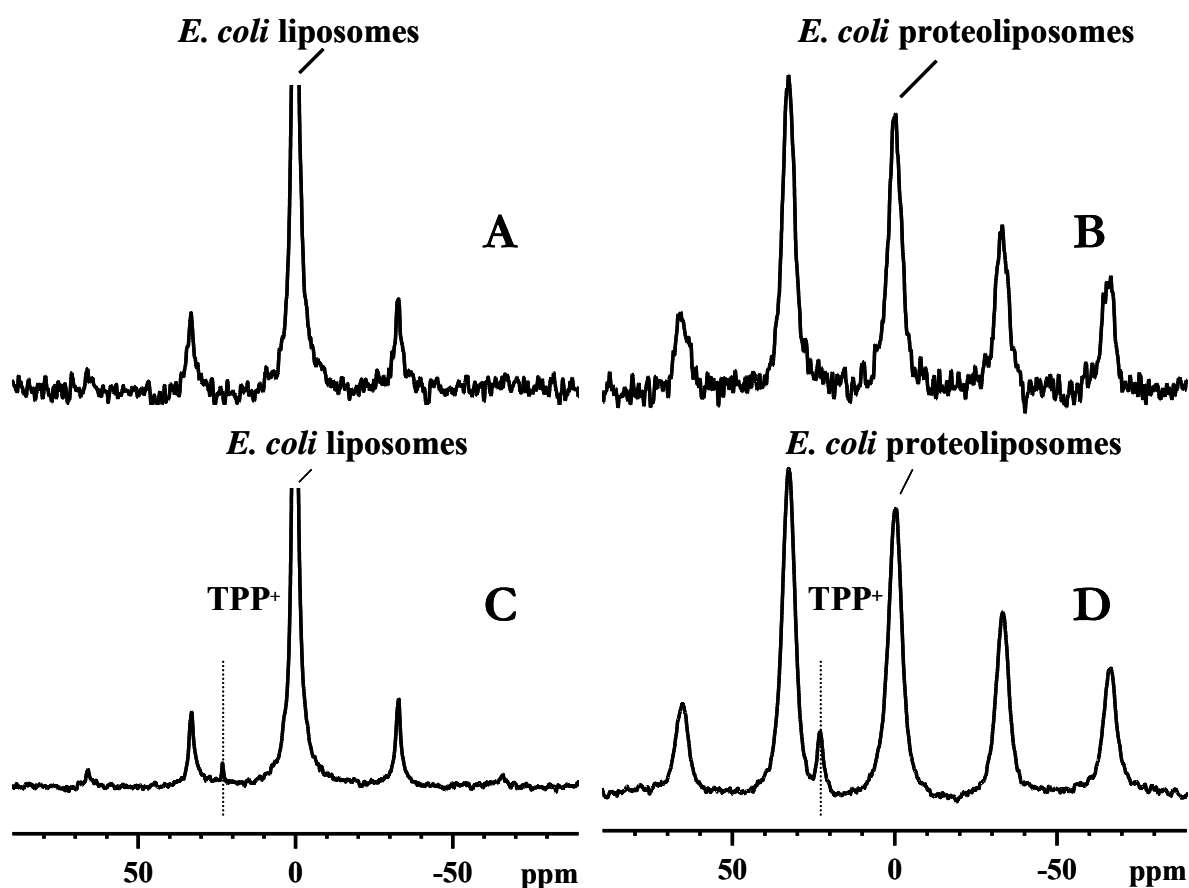


Figure 5.7: ³¹P MAS NMR spectra recorded using cross polarization. Spectra A and C correspond to free liposomes, with (C) and without TPP⁺ (A). Spectra B and D correspond to *E. coli* liposomes reconstituted LmrA, with (B) and without TPP⁺ (D). The isotropic lines are labeled with TPP⁺ (23.2 ppm) and *E. coli* liposomes (0.1 ppm). The experiment was performed at 253K, at spinning frequency of 8 kHz. Approximately 100 k scans were accumulated per each spectrum.

Knowing that under the experimental conditions used here, the substrate binds to LmrA with high affinity, we hypothesized that it was not possible to differentiate between bound and unbound ligands by NMR methods because they have the same chemical shift. However, even if bound and unbound

ligands have the same chemical shift they might have different mobility characteristics. So, limited mobility might be expected for tightly bound ligands. It is possible to selectively detect relatively immobile species by applying cross polarization at increasing experimental temperatures. For effective cross polarization to occur ^{31}P nuclei have to be surrounded by relatively immobile protons as when ligand is tightly bound in the protein binding site. Subsequently, direct polarization allows observing all nuclei independent of their dynamics properties. The increasing experimental temperatures is required because in a frozen state the dynamics difference between more and less mobile molecules might not be manifested. This way, by comparing the spectra recorded under cross polarization and under direct polarization conditions it is potentially possible to differentiate between tightly bound ligands and ligands resided in the membrane or bound non-specifically to the protein.

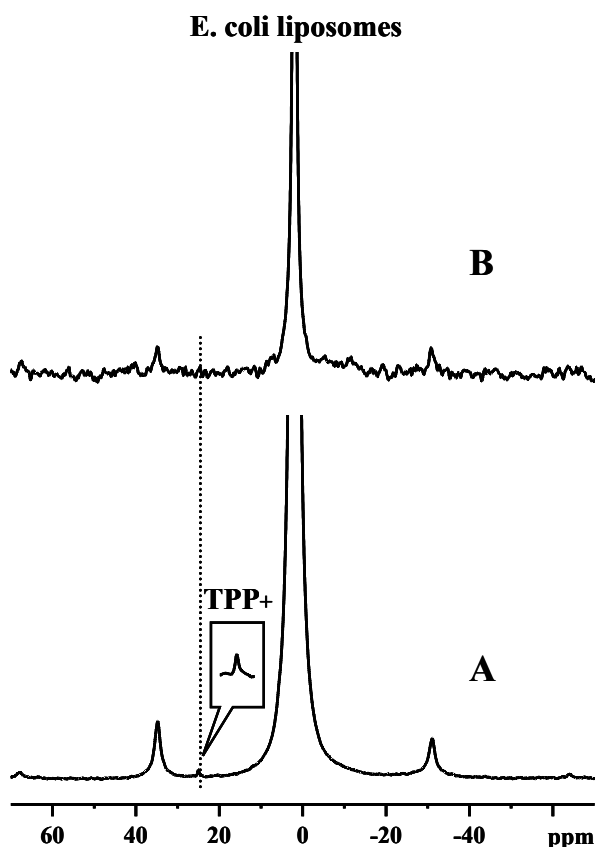


Figure 5.8: ^{31}P MAS spectrum of liposomes reconstituted LmrA with added TPP^+ recorded using direct polarization (A) and cross polarization (B). The isotropic lines are labeled with TPP^+ (25 ppm) and *E. coli* liposomes (1.8 ppm). The experiment was performed at 277K, at a spinning frequency of 8 kHz. Approximately 100 k scans were accumulated per each spectrum.

Figure 5.8 shows the ^{31}P spectra of *E. coli* proteoliposomes with 5 fold mole excess of TPP^+ recorded under direct polarization and cross polarization conditions at temperatures as high as 25°C . The number of scans was doubled in case of cross polarization (Figure 5.8B), however the spectrum intensities obtained using cross polarization are much lower when compared to direct polarization (Figure 5.8A). This is not surprising because at 277K cross polarization is not efficient because there is a lot of mobility taking place in the membrane at temperatures close to physiological.

5.3.5. Modulation of Hoechst-33342 LmrA transport and ATPase LmrA activity by leupeptin

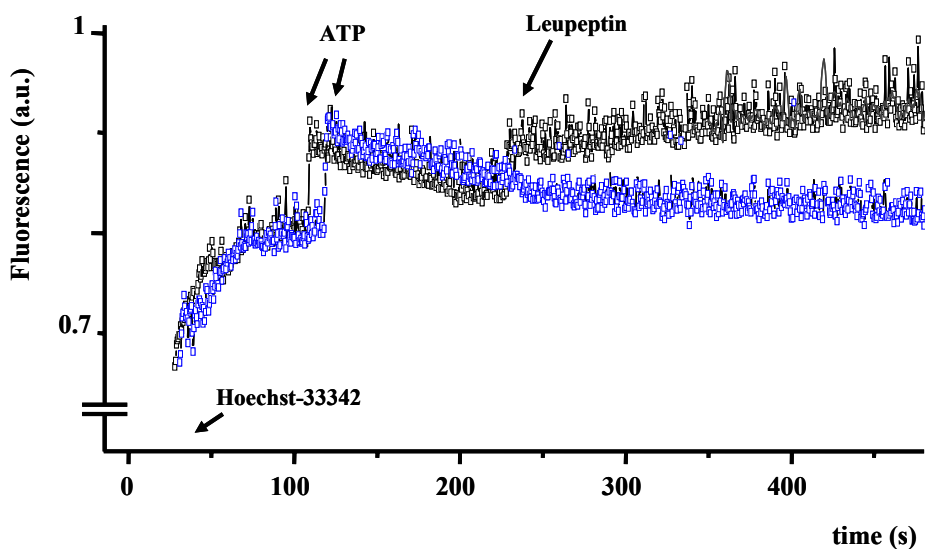


Figure 5.9: Real-time fluorescence measurement of Hoechst-33342 transport blockage by leupeptin. The assay has been performed on the membrane ISOVs prepared for *L. lactis* cells. Fluorescent dye Hoechst-33342 was added after 1 minute of incubation. When the intensity of fluorescence reached plateau, ATP or ADP was added. Leupeptin was added when Hoechst-33342 transport was clearly observed (about 2 minutes after Hoechst-33342 addition). The experiment was performed at a room temperature.

The MDR can be reversed by the action of a group of compounds known as chemosensitizers. This group includes several linear and cyclic peptides. One of them is leupeptin, a small linear peptide. It consists of two leucine and one arginine residues (Figure 5.2). Leupeptin was shown to be an effective PGP modulator with a binding constant of $77.6 \mu\text{M}$. In addition, it was been shown that this peptide is

able to block colchicine transport in PGP (Sharom et al., 1998). As it was not known before if LmrA can bind such peptides, the series of experiments was designed to look if leupeptin can block substrate (Hoechst-33342) transport of LmrA and to find out if leupeptin influence LmrA ATPase activity.

In our experiment Hoechst-33342 fluorescence exhibited enhancement upon interaction with lipid bilayers. Then upon ATP addition a slow decrease in Hoechst-33342 fluorescence is observed. This decrease is an average between active inward pumping of drug by LmrA and outward passive diffusion through the membrane (Lu *et al.*, 2001). The ATP dependant pumping of Hoechst-33342 by LmrA was interrupted by addition of leupeptin. After leupeptin addition, the Hoechst-33342 fluorescence exhibited a slow but stable increase during the measurement period (Figure 5.9). From this experiment it is difficult to conclude whether the Hoechst-33342 transport is completely abolished by leupeptin addition or just inhibited.

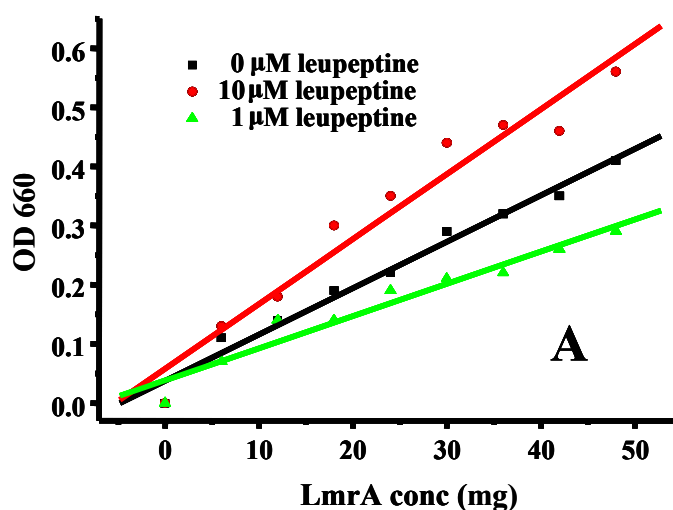


Figure 5.10: The colorimetric ATPase assay performed on the membrane ISOVs prepared for *L. lactis* cells compares inorganic phosphate turnover with increasing amounts of LmrA over 10 minutes. The black line presents linear fit of non simulated ATPase LmrA activity (49 nmole/min per mg of protein), whereas the red and green line show respectively the linear fit of 10 mM (56 nmole/min per mg of protein) and 1 mM (33 nmole/min per mg of protein) leupeptin simulated ATPase LmrA activity.

It was found that PGP substrates and inhibitors can modulate the protein ATPase activity (Sharom et

al., 1999b). The LmrA ATPase activity was examined in basal state (49 nmole/min per mg of protein), and in presence of two different concentrations of leupeptin, 1 mM and 10 mM (Figure 5.10). Interestingly, at lower concentration leupeptin has inhibiting effect on LmrA ATPase activity (33 nmole/min per mg of protein), whereas at higher concentration it has stimulating effect (56 nmole/min per mg of protein).

Experiments similar to real-time fluorescence measurements of Hoechst-33342 transport blockage by leupeptin, has been performed by Sharom and co-workers for PGP reconstituted into proteoliposomes (Lu *et al.*, 2001). In this case the real-time fluorescence measurement of TMR (tetramethylrosamine) transport by P-glycoprotein was inhibited by the MDR modulators cyclosporine A, and verapamil (Lu *et al.*, 2001).

In addition tryptophan intrinsic fluorescence quenching of LmrA (1 μ M) reconstituted in *E. coli* liposomes (1 μ M LmrA) was performed with increasing increasing concentrations of leupeptin (0 to 50 μ M). No concentration dependant tryptophan fluorescence quenching was observed. The possible reason for that is that only low concentrations of leupeptin are accumulated in lipid phase, whereas high concentrations of leupeptin are needed for efficient binding.

5.4. Discussion

5.4.1. Tryptophan intrinsic fluorescence quenching with norfloxacin and vinblastine

The fluoroquinolones present a diverse class of bacterial agents and are effective against gram-positive and gram-negative organisms, including *Streptococcal* and *Staphylococcal* species with multiple applications in variety of infection diseases (Fukuda et al., 2001). Their mechanism of action is to target bacterial DNA synthesis (Walsh, 2003). Recently, rapidly emerging bacterial resistance to this type of agents through expression of MDR membrane pumps, such as MdfA from *E. coli* (Edgar and Bibi, 1999), NorA from *S. aureus*, PmrA from *S. pneumoniae*, Bmr and its regulator BmrR together with Blt from *B. subtilis*, and LfrA from *M. smegmatis* (Poole, 2000) have been observed (Blondeau, 2004a).

The tryptophan fluorescence quenching approach was used to determine whether fluoroquinolones in

general and norfloxacin (Figure 5.3C) in particular can be transported by LmrA and characterize the binding if it takes place. Figure 5.3 and 5.4A shows that LmrA intrinsic tryptophan fluorescence quenching occurs under titration of proteoliposomes reconstituted LmrA mixtures with increasing concentrations of norfloxacin. The experiments on Trp intrinsic fluorescence quenching by vinblastine, a known substrate for PGP and LmrA (Wiese and Pajeva, 2001; van Veen and Konings, 1997), was performed in parallel (Figure 5.3A).

Addition of both drugs resulted in saturable, concentration-dependent quenching of Trp fluorescence (Figure 5.3, 5.4). Tryptophan intrinsic fluorescence quenching with both substrates gave clear monophasic curve, interpreted as evidence of existence of only one binding site, or two with equal affinities, which is unlikely.

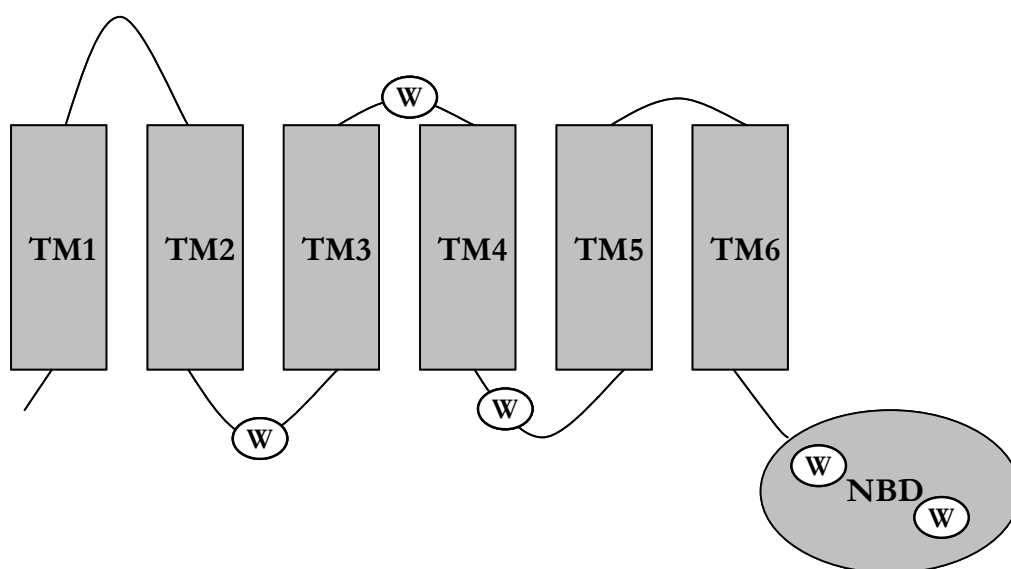


Figure 5.11: Location of tryptophan residues in LmrA.

There are 5 tryptophan residues in the LmrA amino acid sequence. Three of them are located in the predicted loops connecting TM helices 2 and 3, 3 and 4, and 4 and 5, one in extracellular (W172), and two in intracellular (W112 and W201) loops. The other two are found in the predicted NBD (W421 and W457) (Figure 5.11). The indole group of Trp can serve as an intrinsic fluorophore in proteins. Since the emission spectrum is highly sensitive to solvent polarity, it can also reveal information

about its environment, conformation changes in the protein, and/or direct interactions with substrates. The Trp emission spectrum of LmrA reconstituted *E. coli* liposomes has a maximum at 344 nm, much lower than that of the buffer-solubilised Trp, 357 nm, suggesting that all Trp residues are exposed to a relatively hydrophobic environment (Figure 5.3). During the substrate binding the concentration-dependant Trp intrinsic fluorescence is observed but not the shift to the lower wavelength. Moreover, the observed quenching efficiency is less than 50 %. Therefore, it seems more likely that all Trp residues are indirectly involved in the conformation changes within the protein occurred during the binding event. These conformation changes do not include exposing of Trp residues to a polar environment. The results of fluorescence quenching experiments performed by Sharom and co-workers on MANS labeled PGP led to similar conclusion. The MANS labels in their experiments were placed in both NBD (Qu et al., 2003). Quenching of the Trp intrinsic fluorescence by drugs occurs in the absence of ATP, clearly indicating that prior binding of ATP is not necessary for drug interaction with LmrA.

The obtained binding affinity constant for norfloxacin to LmrA was $0.3 \pm 0.03 \mu\text{M}$ and for vinblastine $3.79 \pm 0.4 \mu\text{M}$. The vinblastine binding constant obtained in our measurements was compared to the one known for PGP. It is important to note, that for PGP this binding constant has been obtained using the same approach, Trp intrinsic fluorescence quenching (Liu et al., 2000). So, for PGP the K_d is $0.5 \mu\text{M}$, which is about 10 times higher when compared to the value obtained in our measurement. However, the same author reported the K_d of $1.08 \mu\text{M}$ for PGP with two MANS labels, which is only 3 times different from the value obtained in our measurements and a K_d of $2.32 \mu\text{M}$ which is comparable to our K_d $3.86 \mu\text{M}$ for PGP containing 1 MANS label and vanadate (Qu et al., 2003). To emphasize the difficulties in comparison of K_d obtained using different approaches it is worth mentioning the example of K_d for [^3H] vinblastine obtained by a filtration method by Callaghan and co-workers. Their K_d value was estimated to be 80 nM, which is more than 10-fold higher than the all K_d values obtained by fluorescence quenching approach (Qu et al., 2003; Martin et al., 2001). The main difficulty for measuring drug binding in proteoliposomes is that often the concentration of drug in lipid bilayers is not known.

5.4.2. ^{19}F SSNMR on norfloxacin bound to LmrA

Norfloxacin binding to the LmrA was further assessed by means of solid-state NMR. The ^{19}F CP spectrum of the proteoliposomes reconstituted LmrA incubated with norfloxacin is shown in Figure 5.5. Presence of different norfloxacin conformers as well as high ^{19}F chemical shift anisotropy resulted in severe signals overlap (Figure 5.5). Nevertheless, applying deconvolution method on the spectrum of norfloxacin added to LmrA reconstituted in to *E. coli* liposomes, it was possible to differentiate the signal from unbound and bound to protein substrate (Figure 5.5). The substrate bound to the protein exhibited the shift of -42.5 ppm when compared to unbound -46.00, -41.20, and -38.46 ppm (norfloxacin conformers). Such a shift might be caused by the ring currents of neighboring aromatic residues which are suggested to be involved in the substrate binding (Scrutton and Raine, 1996). The line broadening characteristic for norfloxacin molecules bound to the protein (Figure 5.5B) from one side hamper spectrum analysis, but from the other side it gives information on binding character. Namely, it indicates immobilization of bound ligand. Hence, the observed line broadening can be an indication of the rapid exchange between two ligand states, bound and unbound. However, taking into account that the experiment was performed at temperature as low as 253K, the rapid exchange between bound and unbound ligand states is questionable. In addition, our measurements do not allow us to exclude the possibility that the substrate binding to protein is partly or fully nonspecific. A good way to prove specificity of binding is to titrate proteoliposomes containing reconstituted LmrA and norfloxacin with another known LmrA substrate and follow reduction of signal from bound norfloxacin. However, such fine-tuned experiments are complicated by the fact that signal from unbound norfloxacin is dominant and differentiation of bound norfloxacin from unbound needs spectra deconvolution.

5.4.3. LmrA tryptophan intrinsic fluorescence quenching with TPP^+

In the next step, TPP^+ binding to the LmrA reconstituted proteoliposomes was studied by the tryptophan intrinsic fluorescence quenching (Figure 5.6). The intrinsic tryptophan fluorescence quenching revealed that TPP^+ is bound to LmrA reconstituted under experimental conditions. Two binding site for TPP^+ were found, one TPP^+ molecule is bound to LmrA with high affinity ($9.3 \text{ nM} \pm$

3.8) and one with relatively low affinity ($22 \mu\text{M} \pm 3.8$). Previously, it has been found by two independent measurements that for another MDR transporter from SMR family, EmrE, the binding constants for TPP^+ were 10 nM and 1.9 nM (Elbaz *et al.*, 2005). These values are close to the value obtained for LmrA. The titration of proteoliposomes reconstituted LmrA with higher concentration of TPP^+ showed that massive binding of TPP^+ to membrane lipids. This complicates all experiments and the results must be interpreted with caution.

5.4.4. ^{31}P SSNMR on TPP^+ bound to LmrA

Detection of ligand bound to target by solid-state NMR is based mostly on the observation of the difference in chemical shifts between bound and unbound ligand (Zech *et al.*, 2004). The difference in chemical shifts comes from the fact that bound and unbound ligands are in different chemical environments meaning that bound and unbound ligand nuclei experience different chemical shift shielding. Here, no chemical shift difference was observed between bound and unbound TPP^+ molecules (Figure 5.7). In a similarly designed experiment (Glaubitz *et al.*, 2000), where TPP^+ binding was probed to EmrE, the MDR transporter from the small multidrug resistance family, the peak from bound TPP^+ appeared shifted from the unbound TPP^+ 4.2 ppm to lower frequency. It should be taken into account that for all MDR proteins similar binding mechanism is proposed (Zheleznova *et al.*, 1999). Similar binding mechanism implicates similar influence from the distribution of electrons around the TPP^+ phosphorous atom and as a result similar chemical shifts. There can be multiple reasons why it was not possible to observe a second peak from TPP^+ bound to LmrA. In case of solid-state NMR measurements signal from massively bound to liposomes TPP^+ and intensive resonance peak from lipid phosphorous can hide small resonance peak of TPP^+ bound to LmrA. Moreover, lipids might compete with LmrA in TPP^+ binding, therefore not all TPP^+ binding sites on protein can be occupied, making signal from bound TPP^+ even weaker and more difficult to observe. We have hypothesized that cross polarization performed at 253K might not be suitable for this type of measurements, because at these temperatures with CP all ligand fractions, tightly bound and unbound are observed. To check this possibility, the spectra of proteoliposomes reconstituted LmrA with 5 fold mole excess TPP^+ recorded at 25°C under cross polarization and direct polarization

were compared (Figure 5.8).

Expected significant reduction in intensity was observed under CP condition. The TPP⁺ resonance was visible only under direct irradiation conditions but not under cross polarization conditions. It shows that both TPP⁺ molecule fractions bound to protein and unbound are highly immobile on NMR time scale and can not be cross polarized at this temperature.

So, the observation of ligand bound to the protein is limited. It is possible only if the bound and unbound ligand fractions experience different chemical shift or if their dynamic properties are on time scales accessible for NMR measurements.

Apart from complicated TPP⁺ behavior another interesting feature appears while looking at the CP spectra of free *E. coli* liposomes and liposomes reconstituted LmrA at high mole per mole protein lipid ration (about 300:1) recorded at 253K. This feature is significant increase in chemical anisotropy of lipid resonance of proteoliposomes reconstituted LmrA when compared to free liposomes (Figure 5.7). This difference is almost vanished when the spectra of liposomes reconstituted LmrA obtained under cross polarization and direct observation were recorded at temperature as high as 277K (Figure 5.8). To our opinion high chemical shift anisotropy of lipids resonance in the spectra recorded under CP conditions may correspond to tightly bound to protein lipids. In the same time, lipid signal on the spectrum obtained under direct irradiation originates from all lipids bound and unbound. This way it can be concluded that the lipid moiety in the liposomes reconstituted LmrA has at least two different fractions. One of them might correspond to tightly bound to the protein and therefore relatively immobile lipids and another to bulk free lipids from which membrane is composed. Alternatively, this phosphorous spectra behavior can be related to change in the lipids phase transitions in liposomes containing reconstituted protein when compared with free liposomes. Because the phase transition temperature is a measure of the stability of the packed gel state relative to the fluid state, these changes might indicate that protein incorporation interferes with phospholipids packing.

5.4.5. Modulation of Hoechst-33342 LmrA transport and ATPase LmrA activity by leupeptin

There are two main ways to deal with MDR resistance, to modify the drugs to avoid their interaction with the transporters, and to find relatively non-toxic compounds, which can interfere with the drug

extrusion, somehow blocking the MDR proteins activity. A large number of compounds (chemosensitizers) has been identified for PGP, which are capable of restoring the cytotoxicity of chemotherapeutic drugs. Chemosensitizers appear to compete for substrate binding site in a poorly understood way. Peptides, like leupeptin (Figure 5.2), are of particular interest for pharmaceutical science, because they are relatively non-toxic for cells, and their increased size might enhance their interaction with the transporter, and their synthesis by classical peptide synthetic methods is expected to be relatively low costly (Sharom et al., 1998).

The Hoechst-33342 transport assay has been used before to determine ATP dependent drug pumping in LmrA (van Veen *et al.*, 2000a). We tested the effect of leupeptin, a hydrophobic peptide, the modulator for P-glycoprotein, on Hoechst-33342 transport in inside-out vesicles containing over expressed LmrA. It was shown that leupeptin affected the Hoechst-33342 transport in inside-out vesicles (Figure 5.9). From our experiment it was not possible to conclude whether the Hoechst-33342 transport is blocked or allosterically inhibited by leupeptin addition. The analysis of the kinetic parameters of substrate transport could not be carried on, because the dye concentration in the lipid phase is unknown. In the next step, the ATPase activity of ISOVs vesicles containing overexpressed LmrA was assayed in the presence of different leupeptin concentrations and compared with non-stimulated, basal LmrA ATPase activity (Figure 5.10). It was observed that at 1 mM leupeptin concentration, the peptide inhibit the LmrA ATPase activity, whereas at 10 mM it stimulates the LmrA ATPase activity. The bimodal stimulation profile has been observed before for several PGP chemosensitizers (Sharom et al., 1999b). This bimodal behavior can be caused by interaction of a particular compound with the stimulatory site followed by the interaction with the inhibitory site. This suggestion, however, is speculative because the knowledge of LmrA substrate binding is limited at present.

Conclusions

Tryptophan intrinsic fluorescence quenching experiments were performed on LmrA reconstituted into *E. coli* proteoliposomes. For the first time it was shown that norfloxacin, the antibacterial agent from fluoroquinolones family, is a substrate of LmrA. The binding constants for norfloxacin, vinblastine and TPP^+ have been obtained by fitting the concentration dependant Trp intrinsic fluorescence

quenching (Table 5.1).

By analyzing the LmrA fluorescence emission spectra, a relatively nonpolar localization in the protein interior was concluded for all five tryptophan residues. Moreover, it was shown that under the substrates binding conformation changes are transmitted from transmembrane helices to cytosolic domain. However, these conformation rearrangements do not increase NBDs Trp accessibility towards the solvent. Moreover, we suggest that drug binding initiated Trp intrinsic fluorescence quenching can be used as a binding assay to probe the protein activity.

Binding affinity for interaction of drugs with LmrA reconstituted into proteoliposome of <i>E. coli</i>		
Norfloxacin, K_d (μM)	TPP, K_{d1} and K_{d2} (μM)	Vinblastine, K_d (μM)
0.3 ± 0.03	0.0093 ± 0.0039 22.0 ± 3.8	3.79 ± 0.4

Table 5.1: Binding affinities for interaction of drugs with LmrA reconstituted into proteoliposomes of *E. coli*.

A challenge faced while studying the ligand binding to the proteins reconstituted in the liposomes by SSNMR is to distinguish between specific interaction of ligand with the protein and non-specific interaction of ligand of interest with the surrounding lipids. Taking the advantage of high ^{19}F sensitivity and applying the deconvolution method to the spectrum of norfloxacin titrated into the proteoliposomes containing reconstituted LmrA, it was possible to observe the ligand binding to the protein.

The experiments aiming to observe TPP^+ bound to LmrA have ambiguous results. It allowed better understanding of the limitations in ligand observation by solid-state NMR and showed possible ways to overcome these limitations.

In the present study for the first time it was demonstrated that the real-time Hoechst-33342 transport by LmrA containing inside-out vesicles can be collapsed by addition of leupeptin to the vesicles exterior. Similar experiments can be used to carry out as high-through real-time fluorescence assay aimed to screen the drug library for potential ABC transporters substrates and modulators. In

principal, this real-time approach can be extended to other LmrA fluorescence substrates, like for example, verapamil derivate. The LmrA ATPase was examined at different leupeptin concentrations. Leupeptin gives bimodal ATPase modulation, suggesting existence of LmrA inhibitory and stimulatory sites and leupeptin subsequent interaction with both of them.

6. The localization of multidrug resistance transporters substrates within the model membrane by ^1H MAS NMR

Abstract

Recognition and binding of substrates by LmrA and PGP must be associated with a preferred substrates membrane location, determined by molecular properties and lipid interactions. Therefore, a systematic study on the interaction between seven PGP and LmrA substrates (phenazine, doxorubicin, cephalexin, ampicillin, chloramphenicol, penicillin G, quercetin) and two modulators (quinidine, nicardipine) with 1,2-dimyristoyl-sn-glycero-3-phosphocholine (DMPC) model membranes has been performed. The location profile of these molecules across the membrane has been determined by ^1H -NOESY MAS NMR based on ^1H - ^1H cross peaks between their aromatic finger print region and lipid resonances.

The results of this Chapter are partially published: Siarheyeva A., Lopez J., Glaubitz C.: The localization of P-glycoprotein substrates within model membranes, *Biochemistry*, 2006 in press.

6.1. Introduction

Cells over-expressing PGP and LmrA have been shown to possess an increased resistance to at least eight classes of clinically relevant broad-spectrum antibiotics, including aminoglycosides, lincosamides, macrolides, quinolones, streptogramins, tetracyclines and chloramphenicol, which are neutral or positively charged hydrophobic compounds (Chapter 1, Table 1.2) (Poelarends *et al.*, 2000; Ambudkar *et al.*, 1999). It is difficult to define common specific chemical features for these MDR ABC transporters substrates, but most of them are characterized by a high hydrophobicity, and planar aromatic groups; they frequently contain a basic nitrogen atom especially within non-aromatic rings, and an oxo group bonded to an aliphatic carbon (Ojjima, 2005; Onishi Y., 2003; Seelig, 1998; Klopman *et al.*, 1997; Ueda *et al.*, 1997; Chiba *et al.*, 1996; Scrutton and Raine, 1996).

It has not been quite understood yet how a multidrug efflux pump recognizes and translocates a range of chemically diverse molecules. The translocation of drugs could either be accomplished by a

transporter acting as a ‘classical pump’, as a ‘flippase’ or as a ‘hydrophobic vacuum cleaner’. A flippase mechanism requires the drugs to enter the inner membrane leaflet, where they bind to the protein, which subsequently flips the compounds to the outer leaflet. From there, they could diffuse into the extracellular space as proposed for phosphatidylcholine transport (Higgins and Gottesman, 1992). The ‘vacuum cleaner’ model suggests that drugs diffuse into the lipid phase from where they enter the protein which expels them through a proposed central channel (Poelarends and Konings, 2002; Rosenberg *et al.*, 1997). Both models require a substrate accumulation within the membrane in contrast to the classical pump mechanism. A ‘classical pump’, where the transporter takes up drugs from the aqueous phase and translocates them into extracellular space, seems unlikely, as it has been clearly demonstrated that substrates enter the protein from the membrane as outlined in Chapter 1.

To map the PGP binding sites, multiple amino acids substitutions, cysteine mutagenesis coupled with cross-linking, and photo-affinity labelling have been carried out (Loo and Clarke, 2005; Peer *et al.*, 2005; Pleban *et al.*, 2005b; Loo *et al.*, 2004a; Loo *et al.*, 2004b; Loo and Clarke, 2001; Ueda *et al.*, 1997). These experiments identified residues in trans-membrane helices 4, 5, 6, 8, 9, 10, 11, and 12, as well as in the ATP binding cassette and loops to be important for substrate binding and/or transport. Based on these data, it has been suggested that the PGP drug-binding domain is a large, flexible ‘funnel’ which narrows at the cytoplasmic side. The drug binding according to this ‘pocket’ model occurs through a substrate-induced fit mechanism (Pleban *et al.*, 2005a; Ambudkar *et al.*, 2003; Loo *et al.*, 2003; Loo and Clarke, 2001). From the other side, several experiments using fluorescent PGP substrates (for example, TMA-DPH and Hoechst-33342) map the binding sites locations close to the membrane boundary of the cytoplasmic leaflet (Lugo and Sharom, 2005a; Qu and Sharom, 2002; Shapiro and Ling, 1998; Bolhuis *et al.*, 1996c; Bolhuis *et al.*, 1996b). This controversy drug binding site/sites location makes difficult to hypothesize on the ABC MDR transporters transport cycle. Therefore, knowledge about location of substrate binding sites is required.

The nature of drug binding to some extent could also be influenced by drug-lipid interactions. The membrane-based location of a binding pocket is consistent with the hydrophobicity of many substrates which has been commonly determined from their n-Octanol-water partition coefficient. However, phospholipids bilayers are not homogeneous hydrophobic two dimensional solvents, but

contain partially ordered hydrocarbon chains between highly ordered, charged headgroup regions. It is not known if PGP substrates have a preferable location within lipid bilayers. This knowledge could be essential for the understanding of drug-protein interactions. If structurally diverse molecules show a similar interaction pattern within membrane lipids, a common binding site could be envisaged as all substrates could be located in the same region within the membrane. In contrast, if each substrate behaves differently, a larger, less specific binding pocket within the membrane would be required. The lack of information on substrate-membrane interactions was a motivation to perform a systematic study to determine the location of a set of PGP substrates and modulators within phospholipid bilayers.

MAS-NOESY NMR

Magic angle spinning nuclear Overhauser enhancement spectroscopy (MAS-NOESY) has been shown to be a powerful tool for studying substrate distributions within model lipid bilayers in multilamellar dispersions (Huster et al., 1999).

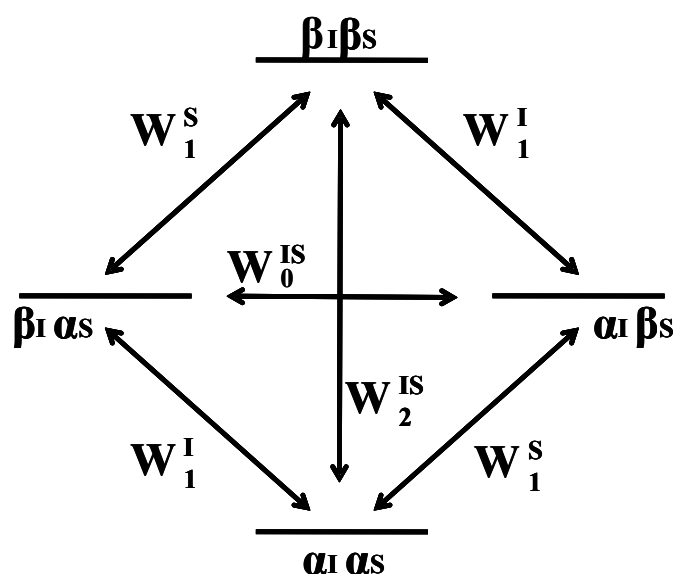


Figure 6.1: Energy levels for a pair of spin -1/2 nuclei I and S, showing the six possible relaxation pathways. W_2^I and W_0^{IS} are cross relaxation pathways, the others are the spin-lattice relaxation processes.

The NOE cause the change in intensity of one resonance (spin I) when the spin transitions of another are perturbed from their equilibrium populations (spin S). This change in intensity of spin I resonance

occurs if spins I and S are dipolar coupled via cross relaxation process. The perturbation occurs by either saturating a resonance that is equalizing the spin population differences across the corresponding transitions or by inverting the population differences across the transitions. On a diagram showing energy levels for a pair of spin $\frac{1}{2}$ nuclei I and S (Figure 6.1) the cross relaxation processes are defined by $\alpha_I\alpha_S \leftrightarrow \beta_I\beta_S$ (both spins flipping in the same direction at rate W_2^{IS}) and by $\alpha_I\beta_S \leftrightarrow \beta_I\alpha_S$ (I and S flipping in opposite directions at rate W_0^{IS}). If both transitions of one nucleus (S) are saturated, spin system may reach equilibrium state by so called ‘cross relaxation’. The saturated spin S transfers magnetization to its dipolar coupled partner I. The change in intensity of the I resonance can be positive (an increase), or negative (a decrease). In an attempt to return to equilibrium, W_2^{IS} and W_0^{IS} relaxation pathways are competing. When the W_2^{IS} pathway dominates, the population difference across the two I transitions increases, causing on enhancement of the I spin resonance intensity; this is then positive NOE. In contrast, when W_0^{IS} dominates, the population difference across the two I transitions decrease; this is then negative NOE. Which relaxation pathway is dominating is determined by molecular motional characteristics of the studied system.

The NOE enhancement is negative for large molecules with an average tumbling rate τc^{-1} much less than ω_0 (Larmor frequency), and positive for small molecules with an average tumbling rate τ_c^{-1} much greater than ω_0 . The magnitude of the NOE between I and S can be quantified by a parameter η , defined in terms of ι the perturbed NMR intensity of spin I, and ι_0 its normal intensity:

$$\eta = (\iota - \iota_0)/\iota_0.$$

The NOE magnitude contains direct information on internuclear separation, so the r^{-6} dependence of the cross relaxation rates in principle gives internuclear distances directly (Claridge, 1999; Hore, 1995). Alternatively, NOEs are often used semiquantitatively to decide whether two nuclei are close to one another or not. Gawrisch and co-workers have shown that NOESY MAS NMR is a powerful tool for studying substrate distribution within model lipid bilayers in multilamellar dispersions. It was found that NOE cross peaks between lipid resonances arise mainly from inter- rather than intramolecular interactions due to the anisotropic nature of molecular motions in membrane bilayers (Huster et al., 1999). Therefore, NOEs between substrate and lipid resonances could serve as a measure for substrate-lipid distances which could be converted into substrate distribution with respect

to the lipids which act as a molecular ruler across the membrane.

The correct interpretation of lipid-lipid NOEs as intermolecular interactions was verified by analyzing the full cross relaxation rate from a series of cross peak built up curves from DPMC/nicardipine MAS-NOESY spectra taken at a range of mixing times (50 to 900 ms), while for substrate-lipid interactions, a simplified single mixing time approximation was used (Huster *et al.*, 1999).

Using this approach, the distribution of ethanol in model lipid membranes (Holte and Gawrisch, 1997), the location of anesthetics and hydrophobic ions in liposomes (Peng *et al.*, 1995; Yokono *et al.*, 1989; Ellena *et al.*, 1987), the preference of flavonoids and tryptophan for the membrane interface (Scheidt *et al.*, 2004; Yau *et al.*, 1998), the interaction of a peptide (Huster *et al.*, 2003b) and, the location and dynamic reorientation of two fluorophores (Huster *et al.*, 2003a) have been investigated. Here, we used the aromatic protons of all nine molecules as molecular reporters to determine the drugs preferable location within the membrane. The substrates were prepared in a complex with DMPC and DMPC/DMPG liposomes. The DMPC lipids was chosen to be a model membrane because in these lipids PGP binds substrates more effectively than in egg PE for example (Romsicki and Sharom, 1999).

6.1. Materials and methods

Materials

The phospholipids 1,2-dimyristoyl-*sn*-glycero-3-phosphocholine (DMPC) and 1,2-dimyristoyl-*sn*-glycero-3-phospho-ras-(1-glycerol) (DMPG) were obtained from Sigma. Penicillin G was obtained from Fluka, BioChemika, ampicillin from Roth. All other reagents were purchased from Sigma.

Sample preparation

Drugs and DMPC (25 mg) were dissolved separately in 2 ml of chloroform and methanol 1:1 and mixed. The drugs/lipids molar ratios were follows: 0.28 phenazine, 0.22 doxorubicin, cephalexin, quinidine, penicillin G, and quercetin, 0.18 ampicillin, 0.26 chloramphenicol, 0.27 nicardipine. The

solvent was removed under stream of nitrogen. The lipid film was re-dissolved in 2 mL cyclohexane, frozen in liquid nitrogen and freeze-dried in a vacuum overnight. Multilamellar vesicles were prepared by hydrating the lipid/drug sample with approximately 20 μL of D_2O . The samples were further homogenized by 5 freeze-thaw cycles. The pellet was transferred to a 4 mm MAS rotor. Before acquiring data, the sample was spun at 8 kHz in the MAS rotor for 15 min to allow for homogeneous sample distribution and equilibration.

NMR measurements

NMR experiments were performed on a Bruker Avance 400 equipped with a 4 mm MAS probe at temperatures 300K and 313K which maintains DMPC lipids in the liquid crystalline phase. All ^1H experiments were carried out at a resonance frequency of 400.131 MHz with spectral width of 8 kHz. Inserts made of Kel-F were used to keep the samples centered within the 4 mm zirconia MAS rotor. Two-dimensional NOESY experiments were acquired in the phase sensitive mode with 90° pulses of 3 μs was used (Figure 6.2). A total of 256 complex data points were collected in the indirect dimensions with 16 transients per increment at a relaxation delay of 4 s between scans. A square sine-bell window function was applied in both dimensions before processing.

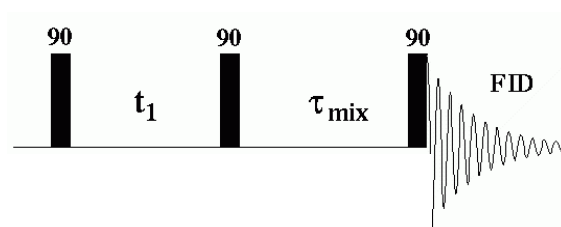


Figure 6.2: NOESY pulse sequence.

All ^1H spectra were referenced with respect to the terminal methyl group of the lipid chains at 0.89 ppm of a DMPC sample in the absence of drug molecules.

Data processing was carried out with XWIN-NMR (Bruker Instruments, Karlsruhe). Assignment and integration of the NOESY crosspeaks were carried out using the software packages Sparky (T. D. Goddard and D. G. Kneller, SPARKY 3, University of California, San Francisco).

In order to assess the cross relaxation rates (σ_{ij}) between the nuclei of the ligand and the lipid matrix, the approximations, which take into account the interactions between just two nuclei whilst ignoring

the effect of other nuclei within dipolar coupling range was used [6.1]. For the diagonal peak volumes:

$$[6.1a] \quad i(t_m) = [A_{ii}(0)/2] [1 + \exp/(-2\sigma_{ij}t_m)] \exp(-t_m T_{ii})$$

and for the cross peak volumes:

$$[6.1b] \quad (t_m) = [A_{jj}(0)/2] [1 - \exp/(-2\sigma_{ij}t_m)] \exp(-t_m T_{ij})$$

where $A_{ii}(t_m)$ and $A_{ij}(t_m)$ are the respective diagonal peak and the crosspeak volumes at mixing time t_m , $A_{ii}(0)$ and $A_{jj}(0)$ are the diagonal peak volumes at a mixing time zero. The values $1/T_{ii}$ and $1/T_{ij}$ define a rate of magnetization leakage toward the lattice. By simplifying the spin pair approach it is possible to calculate the cross relaxation with the use of equation [6.2] (Huster et al., 1999):

$$[6.2] \quad \sigma_{ij} = A_{ij}(t_m)/A_{jj}(t_m)t_m$$

The cross relaxation rate σ_{ij} is estimated by dividing the crosspeak volume A_{ij} by the diagonal peak volume A_{jj} , multiplied by the mixing time t_m of the NOESY spectrum.

In order to ensure the validity of the approximation for our experiments, results using [6.2] were compared with those obtained by using the spin pair interaction model for DMPC-nicardipine H9-proton [6.1]. For these purpose, the NOESY spectra for this ligand, prepared with DMPC liposomes, were obtained at 9 mixing times, ranging between 50 ms and 900 ms.

6.2. Results

The nine substrates used in this study are listed in Table 6.1 and their chemical structures are shown in Figure 6.3. They have been shown to act either as substrates or modulators for PGP and LmrA (Alqwai *et al.*, 2003; Ambudkar *et al.*, 2003; Varma *et al.*, 2003; Poelarends *et al.*, 2000; Ambudkar *et al.*, 1999; van Veen *et al.*, 1998b; VanVeen *et al.*, 1996) and belong to distinct drug classes such as Ca^{2+} channel blockers, antracyclines, cytotoxic agents, antihypertensives or bacteriostatics. Their lipophilicity is estimated in form of the octanol/water partitioning coefficient ($\log P$) as shown in Table 6.1. Its high value indicates that fast drug equilibration within the model membrane can be expected. However, no indication about their detailed location within the lipid bilayer can be derived from the partitioning coefficient.

Drug		Category	log P
A	phenazine	miscellaneous	2.8±0.3
B	doxorubicin	antiracines	2.3±0.7
C	cephalexin	bacteriostatic	0.6±0.3
D	ampicillin	bacteriostatic	1.3±0.3
E	quinidine	Antimalarial	3.4±0.4
F	chloramphenicol	Bacteriostatic	1.0±0.3
G	nicardipine	Calcium channel blockers	5.2±0.6
H	penicillin G	bacteriostatic	1.7±0.2
I	quercetin	bacteriostatic	2.2±1.0

Table 6.1: PGP and LmrA substrates used in this study and their octanol/water partition coefficients (logP) (calculated using Advanced Chemistry Development (ACD/Labs) Software Solaris V4.67 (1994-2005 ACD/Labs)).

Although varying in molecular size and structure, a common feature of all drugs in this study is the occurrence of aromatic moieties in each molecule (Figure 6.3), which seem to be directly involved in protein binding (Varma *et al.*, 2003; Van Bambeke *et al.*, 2000). The NMR signals of the aromatic protons are well resolved and well separated from dominating lipid resonances, as shown in Figure 6.4 for all nine molecules, a fact which makes these groups ideal probes for substrate-lipid interactions. The ¹H chemical shift assignments of substrates and synthetic lipid DMPC have been determined before and are shown in Figure 6.3 and 6.8 (Garipova and Silnikov, 2003; Zolek *et al.*, 2003; Lindholm *et al.*, 2002; Tung *et al.*, 2000; Calzolari *et al.*, 1997; Gaggelli *et al.*, 1992)

The feasibility of one mixing time approach was checked by comparing the results obtained for one mixing time approach and two spin pair approximation. A comparison of the distribution profiles of nicardipine proton 9, 21, 21' within the lipid matrix, calculated with two spin approximation, and single mixing time equation, showed only marginal differences (Figure 6.5).

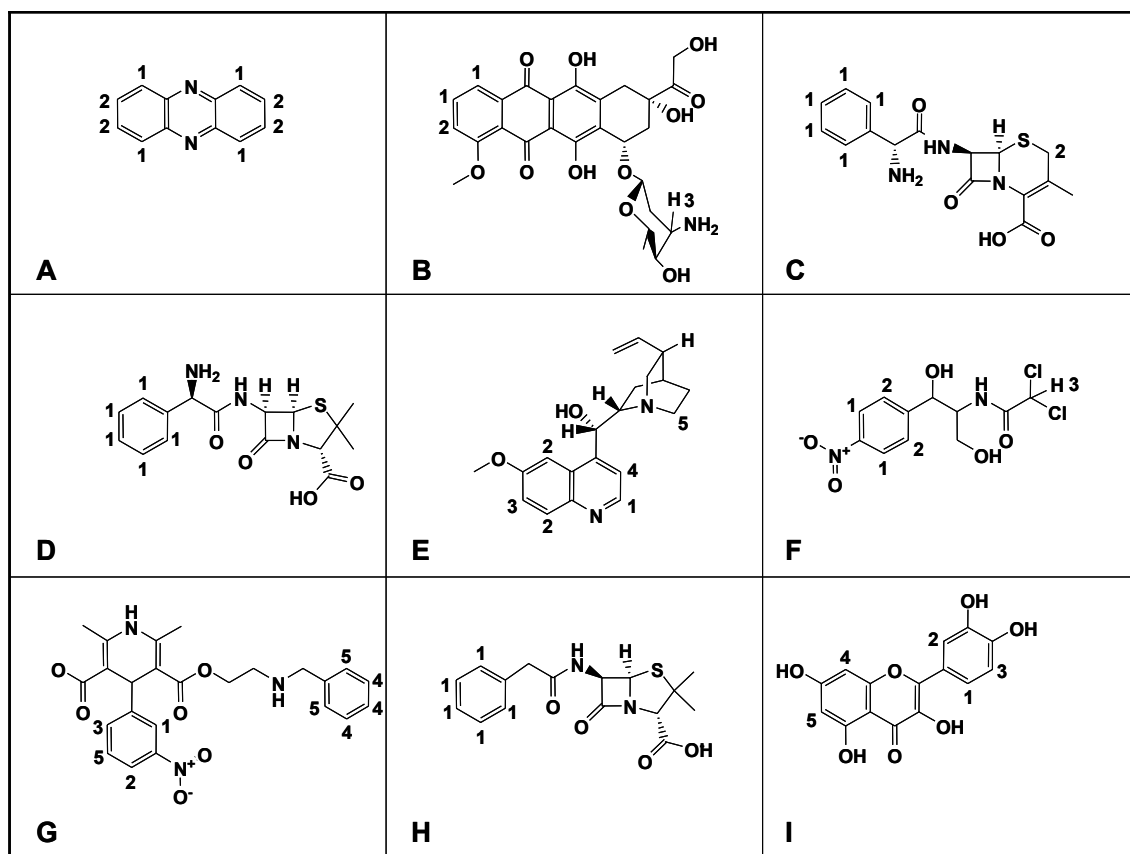


Figure 6.3: Chemical structures of PGP substrates used in this study: (A) phenazine, (B) doxorubicin, (C) cephalixin, (D) ampicillin, (E) quinidine, (F) chloramphenicol, (G) nicardipine, (H) penicillin G, (I) quercetin, and (J) DMPC. The drug categories and partition coefficients are given in Table 6.1.

To ensure the reproducibility of two spin-pair approximation, the 2D MAS NOESY spectra of cholesterol 40 % (w/w) in DMPC were obtained and the cross relaxation rate for 23 proton of cholesterol (Muhl et al., 1996) and the G3 group of DMPC group was fitted by using eq. 6.1b. Figure 6.6 shows the 2D MAS NOESY spectrum of cholesterol 40 % (w/w) in DMPC and the dependence of cross peak volumes for the 23 proton group of cholesterol and the G3 group of DMPC fitted to two spin-pair approximation. The calculated cholesterol cross relaxation rate is 0.00158 ms^{-1} . This number is comparable with the values obtained earlier for the cross relation rates between the saturated *sn*-1 chain methylene groups of PC, PE, and PS and the cholesterol C18 methyl resonance (Huster et al., 1998). Additionally, the comparison of the cross relaxation rates obtained by using the full relaxation matrix method, two spin pair, and one mixing time approximations for quinidine also confirm the

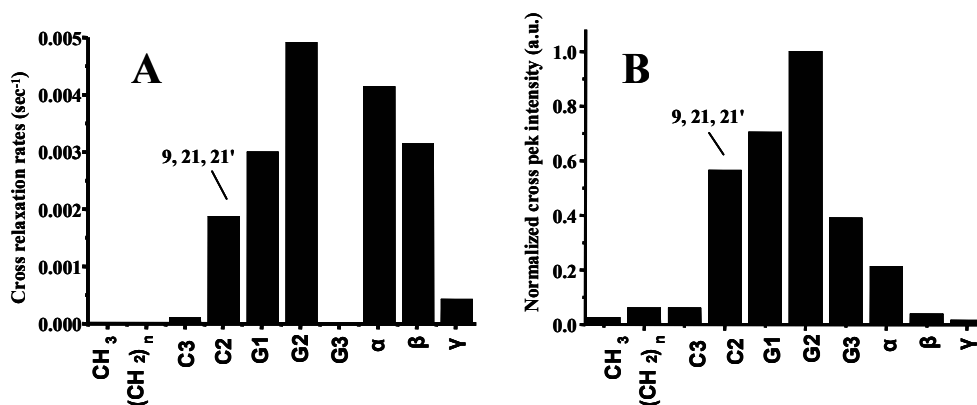


Figure 6.5: The comparison of cross relaxation rate for 9, 21, 21' nicardipine group obtained using spin-pair interaction approach (A) and one mixing time approach (B). Assignment for nicardipine and DMPC is kept as in Figure 6.3 and 6.8.

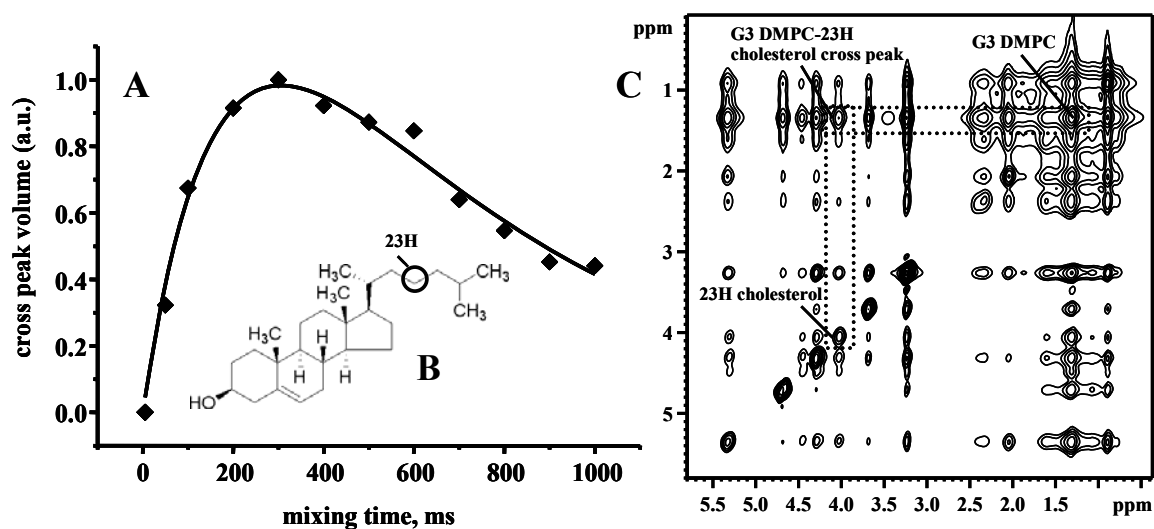


Figure 6.6: (A) The cross peak volumes as a function of mixing time in a 40 % (w/w) cholesterol in DMPC. The solid line represents a fit according to the spin-pair interaction model ($\sigma_{\text{lipid-cho}} = 0.00158 \text{ ms}^{-1}$) as described in the text, (B) cholesterol, (C) ¹H MAS NOESY contour plot of a 14:0 DMPC/cholesterol 40% mixture recorded at a mixing time of 300 ms. The 23 proton of cholesterol and the G3 group of DMPC are highlighted with boxes.

In the single mixing time approximation, cross relaxation rates are proportional to normalized cross peak volumes. By plotting these values for each cross peak between drug and lipid resonance as a function of the corresponding lipid proton location within the membrane, a distribution function of the drug across the membrane is obtained. The results of our measurements are shown in Figure 6.8,

plotted from the hydrophobic core of the membrane to the headgroup region from left to right, respectively. None of the substrates shows a strong correlation with the hydrophobic core region. There is a general pattern of preferred equilibrium location of the aromatic groups of all studied molecules in a layer located below the head group phosphate and above the first segments of the lipid acyl chain.

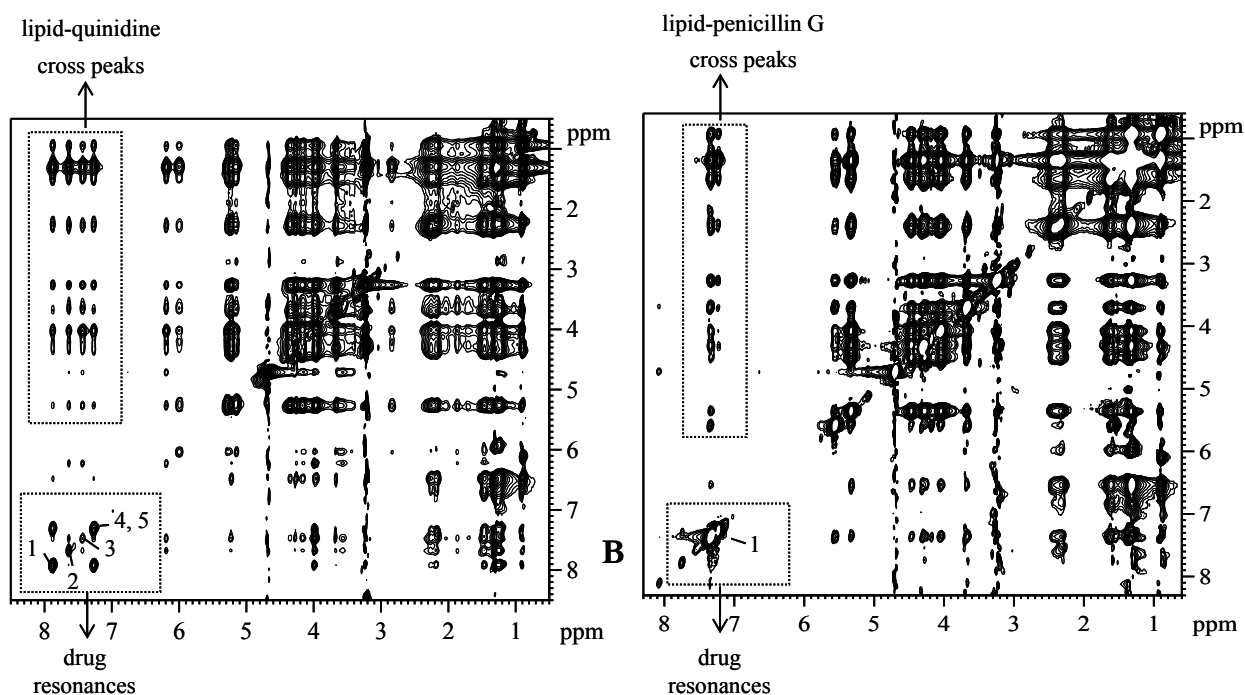


Figure 6.7: Examples for two-dimensional ^1H MAS NMR NOESY spectra of quinidine (A) and penicillin G (B) DMPC dispersions in D_2O recorded with a mixing time of 400 ms and at a temperature of 300 K. Both spectra show intense cross peaks between drugs and DMPC resonances.

Interestingly, in almost all molecules most resolved protons show a similar location profile indicating that they do not take up a preferred orientation within the bilayer

In some cases (Figure 6.8), we observe discontinuities of relative cross peak volumes for contacts around the G1 lipid protons. The α resonance coincides with one of the proton signals of G1 (Figure 6.4) (Holte and Gawrisch, 1997). Therefore, the number of lipid protons by which the volumes of cross peaks have to be corrected do not necessarily reflect the number of lipid protons actually contributing to the lipid-drug interaction.

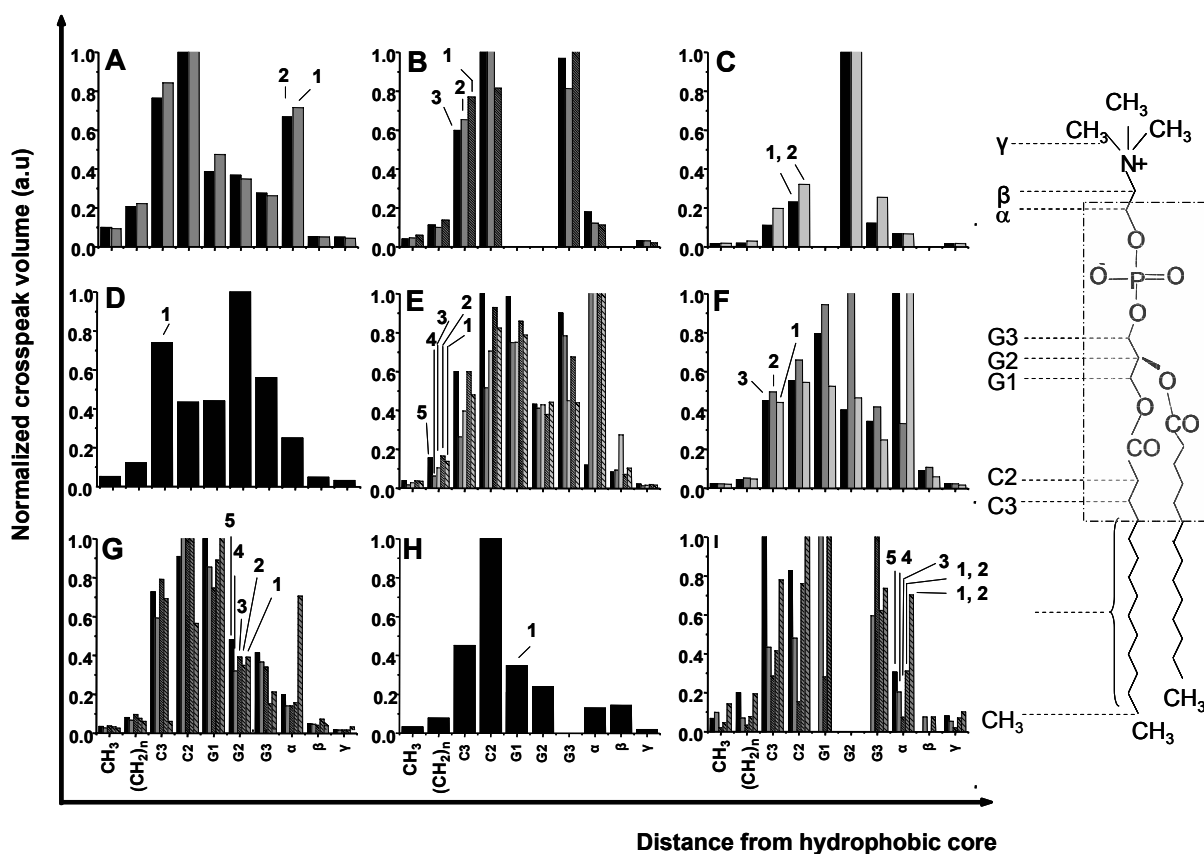


Figure 6.8: Following the single mixing time analysis as discussed in the text, normalized DMPC–substrate cross peak volumes according to the ^1H assignments in Figures 6.3 are plotted in the order of increasing distance from the hydrophobic core of the membrane. All aromatic protons in all nine substrates show a similar interaction profiles indicating a similar location of all aromatic groups within the membrane interface ((A) phenazine, (B) doxorubicin, (C) cephalexin, (D) ampicillin, (E) quinidine, (F) chloramphenicol, (G) nicardipine, (H) penicillin G, (I) quercetin). On the right side, the DMPC proton assignment used for ^1H -NOESY MAS NMR is shown. The labelling corresponds to: $\text{N}(\text{CH}_3)_3$ (α), $\text{N-CH}_2\text{-CH}_2$ (β), $\text{CH}_2\text{-CH}_2\text{-O}$ (γ), $\text{O-CH}_2\text{-CH}$ (G3), $\text{CH}_2\text{-CH-CH}_2$ (G2), $\text{CH-CH}_2\text{-O}$ (G1), $\text{CH}_2\text{-CH}_2\text{-COO}$ (C2), $\text{CH}_2\text{-CH}_2\text{-COO}$ (C3).

The main purpose of this work was to investigate the membrane interaction of the neutral form of all drugs in pure D_2O . Control experiments on doxorubicin which bears a single positive charge in its daunosamine moiety at pH 7.4 and an additional experiment at pH 8.5 did show a very similar location profile as shown in Figure 6.10. We have also altered surface charge and temperature in order to investigate their effect upon membrane distributions of chloramphenicol, nicardipine, penicillin G, and quinidine. Charged model membranes were prepared by mixing anionic DMPG with DMPC

(3:7). At this DMPG/DMPC ratio, the membrane is almost saturated with negative charges (Wiedmer *et al.*, 2001). Our measurements show that the addition of anionic lipids to the model membrane causes no significant change in the overall location probability for all studied (Figure 6.9).

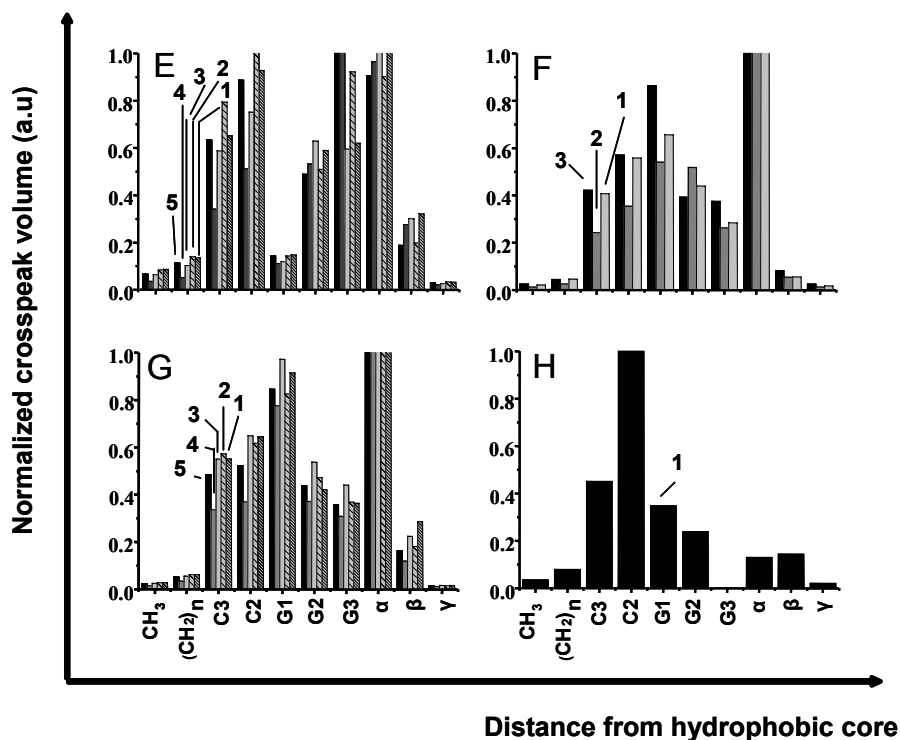


Figure 6.9: Using the single mixing time analysis as discussed in the text, normalized DMPC/DMPG–substrate cross peak volumes are plotted in the order of increasing distance from the hydrophobic core of the membrane. All aromatic protons in all four substrates show similar interaction profiles indicating a similar location of all aromatic groups within the membrane interface ((E) chloramphenicol, (F) nicardipine, (G) penicillin G, and (H) quinidine).

Further experiments at a higher temperature of 313K on chloramphenicol, nicardipine, penicillin G, and quinidine DMPC/DMPG lipid mixtures were carried out. The higher temperature causes shorter lipid and drug correlation times and influences the motional characteristics of lipid-drug interactions. As expected, the relative cross peaks volumes dramatically decreased as correlation times are reduced at higher temperatures (Holte and Gawrisch, 1997). A smoothed drug distribution might be expected as membrane fluidity also rises with temperature, thus facilitating drug diffusion within the lipid matrix. Experiments at 313 K also present a more physiological situation. However, we observed no

change in the resulting drug location probability within the membrane.

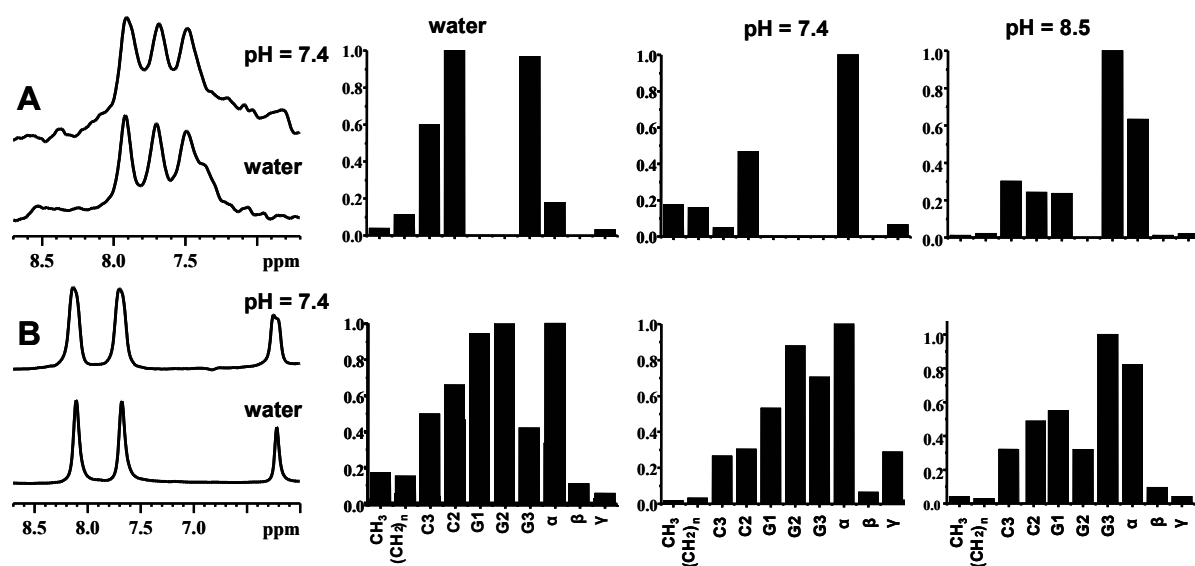


Figure 6.10: Comparison of chemical shifts and location profiles of proton 3 in doxorubicin (A) and proton 2 in chloramphenicol (B) buffered at pH 7.4 and pH 8.5 (10 mM TRIS, 50 mM KCl) and in pure deuterated water.

6.4. Discussion

Our data clearly indicate that all tested drugs accumulate within the membrane, in accord with their high octanol/water partition coefficients (Table 6.1). The relative lipid-drug cross peak volumes shown in Figure 6.8 offer direct evidence for the preferred interfacial location of the aromatic groups of all nine drugs, although their distribution across the hydrophobic core region is less well defined: Protons from each CH_2 chain segment have the same chemical shift but could contribute differently to each cross peak volume due to different contacts to the substrate. A better spatial resolution is offered by other NMR approaches such as ^2H -NMR on selectively chain deuterated lipids or ^{13}C -MAS NMR, as demonstrated for the antidepressants desipramine and imipramine (also PGP substrates). They have been found to show contacts down to the sixth out of fourteen carbons on the lipid acyl chain (Santos *et al.*, 2004; Meadows, 1979). However, there is no doubt that the aromatic groups of all nine tested drugs shown in Figure 6.3 have a preferred equilibrium location within the interface region, i.e. within a narrow layer between upper segments of the lipid acyl chain and below the phosphate of the lipid head group (Figure 6.8).

Drug-membrane interactions

The main reason for this distribution is a balanced interplay between hydrophobic and electrostatic effects. Lipid membranes are characterized by a steep hydrophobicity profile with dielectricity constants ranging from 80 at the aqueous phase to 2 inside the hydrocarbon phase (Subczynski *et al.*, 1994) as well a strong electric dipole potential (Clarke, 2001). The drugs used in his study contain both hydrophilic and hydrophobic groups. They are weak bases or acids which remain mainly uncharged under the conditions used here (Ferte, 2000). Therefore, only their π - π electron systems and to a lesser extent electric dipole- and quadrupole moments would weakly contribute to electrostatic interactions with the dipole of the zwitter-ionic DMPC lipid headgroup (Yau *et al.*, 1998). In addition, the formation of hydrogen bonds between the lipid carbonyls and drug molecules supports a preferred location within the membrane interface (Castaing *et al.*, 2005; Clarke, 2001). Therefore, hydrophobic substances would have a preference for the membrane core region, while electrostatic interactions would cause a preference for the lipid headgroups. These effects could compensate each other in the interface region.

Four of the drugs (doxorubicin, quinidine, penicillin G, ampicillin) used here have already been investigated with respect to their interaction with lipids. Studies on quinidine and its optical isomer quinine have shown that it interacts with both neutral and charged lipids. However, penetration into the bilayer has only been observed in the presence of charged lipids (DMPG) (Porcar *et al.*, 2003). Ampicillin (Casa *et al.*, 1992) and penicillin G (Suwalsky *et al.*, 1996) have been found to interact with model membranes as well, but spatially resolved details could not be obtained.

Anthracyclines, and especially doxorubicin, have been subjected to an especially intense scrutiny by a variety of methods in both neutral and anionic lipids (Parker *et al.*, 2001). Membrane binding involves a complex interplay of both hydrophobic and electrostatic interactions. Using NMR, it was found that it interacts with both surface and buried sites in DMPC/cardiolipin containing bicelles (Parker *et al.*, 2001), while monolayer studies showed no penetration into the hydrophobic region of the membrane. It has been shown that the presence of anionic lipids increases the binding of doxorubicin to the bilayers (Dewolf *et al.*, 1991) but decreases passive transport through the membrane (Speelmans *et al.*, 1994). Interestingly, some fluorescence studies have suggested two binding environments in

PC/cardiolipin bilayers (Karczmar and Tritton, 1979). While our studies have focused on the detailed location of the neutral form of doxorubicin within zwitter-ionic lipids, our data also show a preferred interaction with the interface region. Doxorubicin does not penetrate deeply into the hydrophobic core. Indeed, Figure 5.8 indicates two maxima for the location probability, one more exposed between water and lipid headgroup and a second between lipid headgroup and hydrophobic core region of the lipids.

At physiological pH 7.4, 94% of the doxorubicin molecules bear a positive charge at the daunosamine group (pKa 8.4) leading to strong electrostatic binding to anionic lipids. However, it is the uncharged form of the drug which is transported via passive diffusion across the membranes (Frezard and Garniersuillerot, 1991) and it has also been shown that it is transported better by PGP than charged doxorubicin (Frezard *et al.*, 2001). Our data show a very similar location profile of neutral doxorubicin compared to data acquired at pH 7.4 and pH 8.5 (Figure 6.10). This is consistent with fluorescence studies which did show that drug incorporation in the bilayer does not depend on the presence of a positive charge nor on anionic lipids but on the hydrophobicity of the molecule (Gallois *et al.*, 1996).

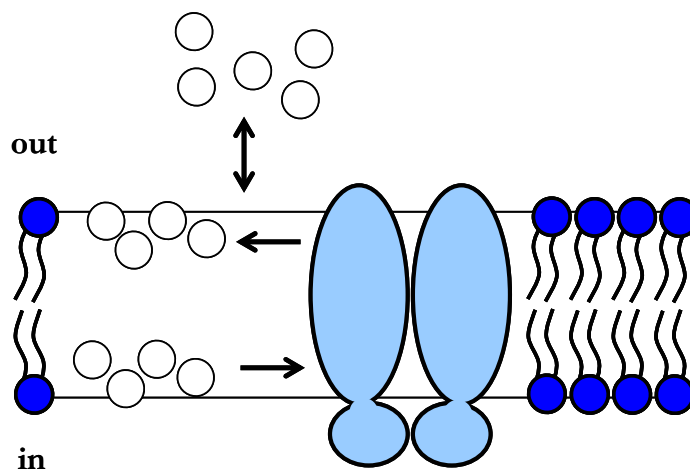


Figure 6.11: Drugs are proposed to enter the protein from the membrane interface region.

Comparison with physiological conditions

Under physiological conditions, the total lipid to drug ratio in cell membranes is significantly lower than the ratios used in our measurements. Our use of higher ratios was a requirement due to the low

signal-to-noise ratio of the observed drug resonances. However, line-width and chemical shifts of lipid resonances did not change significantly compared to drug-free liposomes, indicating an intact bilayer structure. Indeed, we note that previously published studies used comparable drug-lipid ratios (Scheidt *et al.*, 2004; Yau *et al.*, 1998). Although our major goal was a comparative study of the interaction of nine PGP substrates or modulators with neutral/zwitter-ionic lipids, the effect of charged lipids (DMPC/DMPG 7:3) on the drug distribution within the membrane was additionally studied, due to the importance of charged lipids for drug-membrane interactions. The locations of chloramphenicol, nifedipine, penicillin G, and quinidine within the DMPC/DMPG membrane were evaluated. No qualitative change was observed when compared with DMPC membranes. This result, and the fact that substrate-PGP binding affinity has been shown to be higher in DMPC than in PS or PE, indicates that DMPC is a good choice as a model system (Romsicki and Sharom, 1999).

Relevance of our findings for passive uptake models

Due to their mainly lipophilic nature, most drugs “dissolve” and accumulate within the membrane. In contrast to active efflux, drug uptake takes place by passive diffusion across the membrane along the drug concentration gradient. The high substrate concentration in the interface region found here supports the model of a three step process for the drug to cross the membrane: (i) Substrate accumulates in the interface of the outer leaflet, (ii) it flips over to the interface of the inner leaflet and (iii) is found to be in equilibrium with the intracellular space. Therefore, our findings support the previously suggested flip-flop model for passive drug uptake (Eytan, 2005; Eytan *et al.*, 1996).

Relevance of our findings for efflux

Although the binding sites for hydrophobic substrates are assumed to be in the transmembrane region, their exact location is not yet known despite a number of studies using mutagenesis, photo-affinity labelling, and fluorescence spectroscopy (Lugo and Sharom, 2005a; Loo *et al.*, 2004a; Loo *et al.*, 2004b; Loo *et al.*, 2003; Loo and Clarke, 2001; Seelig and Landwojtowicz, 2000; Dougherty, 1996). An important role of aromatic residues for substrate binding has been suggested (Ambudkar *et al.*, 2003; Pawagi *et al.*, 1994), and indeed a common building block of the rather diverse set of substrates

are aromatic ring structures (Seelig and Landwojtowicz, 2000). In this case, drug binding could take place via π - π cation and stacking interactions with aromatic and polar amino acids present in the transmembrane domain of PGP and LmrA (van Veen, 2001; Seelig and Landwojtowicz, 2000; Dougherty, 1996). Aromatic residues in membrane proteins are likely to be exposed to the membrane interface region (von Heijne, 1992), where the substrates studied here have their highest concentrations. Interestingly, the relatively low binding affinity of many PGP substrates (μ M) increases with increasing membrane partition coefficient (Sharom *et al.*, 1999a). This means that increasing substrate concentration in the membrane is needed for efficient binding. Therefore, our data support a model in which drug binding sites are located within or accessible from the membrane interface (Figure 6.11) (Lugo and Sharom, 2005a; Lugo and Sharom, 2005b).

We have included in our study not only PGP substrates (Table 6.1) but also the two modulators nifedipine and quinidine (Ambudkar *et al.*, 2003), which have been found to decrease PGP activity (Wang *et al.*, 2000). Interestingly, we have found no differences in the membrane location for substrates and modulators. This could indicate that substrates and modulators enter the proteins via similar pathways or that substrate and modulator binding sites are both accessible from the membrane interface. The high similarities in structure, partition coefficient and membrane interaction between substrates and modulators may make it very difficult to define molecular properties needed to eventually design a potent inhibitor.

Existing transport models imply that bound substrates are taken up from the inner leaflet, moved across the membrane and released either into the outer leaflet (flippase model) or directly into extra cellular space (hydrophobic vacuum cleaner model). Although substrate-lipid interactions and their well defined membrane location found here can be related to drug uptake and binding, it is difficult to draw any conclusions about their translocation and release. Their preference for the interface region makes a flippase model likely. In this case, the transporter would have to flip drugs at a higher rate than flip-flops observed during passive uptake. In contrast, the existence of an aqueous transmembrane chamber open to extracellular milieu as suggested for PGP or LmrA could also serve to release bound substrates directly (Loo *et al.*, 2003; Poelarends and Konings, 2002; Rosenberg *et al.*, 1997).

Conclusion

The location of seven PGP substrates and two modulators within neutral phospholipid bilayers have been determined by NOESY-MAS-NMR. Although structurally rather diverse, all molecules show a very similar behavior within the membrane and are found predominantly within the membrane interface region, but are less likely to penetrate into the membranes hydrophobic core region. Furthermore, both substrates and modulators show a rather similar membrane location profile. Therefore, substrate and modulator binding sites in PGP are most likely accessible from within the interface region. These findings might also have relevance for the understanding of secondary multidrug efflux pumps due to their partially overlapping substrate specificity and their ability to bind substrates from within the membrane as shown for example for LmrP (Bolhuis *et al.*, 1996a).

Outlook

Nuclear magnetic resonance spectroscopy is unique among the methods available for structure determination (Wüthrich, 2002). In general, although not yet widely used for membrane proteins, solid-state NMR methodology is rapidly developing into a method for protein structure determination.

In this thesis a procedure for preparation of selective amino acids isotope labeled ABC MDR transporter LmrA from *Lactococcus lactis* for solid-state NMR investigations as well as first solid-state NMR experiments on this protein have been demonstrated. This opens a door to apply advanced SSNMR techniques not only to the ABC MDR transporter LmrA but to the whole ABC family.

In future MAS SSNMR experiments can be performed using $^{13}\text{C}/^{15}\text{N}$ uniformly and selectively labeled LmrA reconstituted into *E. coli* liposomes as well as in a variety of synthetic lipids. These experiments can potentially allow detecting conformational changes in LmrA during its catalytic cycle. This can be done via following chemical shift changes in $^{13}\text{C}/^{15}\text{N}$ MAS SSNMR spectra of LmrA in a resting state and in states where LmrA is trapped with either substrates, or ATP and ADP.

In addition, the distance constrains of LmrA ATP-binding domain can be investigated through variety of correlation type 2D $^{13}\text{C}/^{15}\text{N}$ MAS SSNMR experiments taking advantage of LmrA NBDs high mobility by utilizing J-coupling under MAS-NMR conditions. Alternatively distance constrains can be obtained from dipole-dipole interactions between two spins. Example of distance constrains determination is measuring of the internuclear distance in specifically labeled (^{15}N -Leu₃₇, ^{13}C -Leu₃₉) phospholamban peptide (Middleton *et al.*, 2000b).

Experiments could be planned to detect $^2\text{H}/^{13}\text{C}/^{15}\text{N}/^{19}\text{F}$ isotope labeled substrates bound to LmrA via static and MAS SSNMR. Moreover, $^{13}\text{C}/^{15}\text{N}$ 1D and 2D MAS SSNMR experiments can be performed firstly to detect $^{13}\text{C}/^{15}\text{N}$ labeled ATP bound to LmrA and secondly to shed light on the conformation changes occurring in the LmrA NBDs under ATP binding and hydrolysis. Deuterium static SSNMR can be used to add to understanding of the protein-lipids interactions.

Appendix 1

Trifluoroacetyl cysteine labelling of bacteriorhodopsin

Attaching ^{19}F labeled groups to cysteins allows selective labelling of membrane proteins for ^{19}F MAS NMR. The aim is to make use of long range of ^{19}F dipolar coupling and of high ^{19}F sensitivity. Here, ^{19}F labelling of M163C bacteriorhodopsin is demonstrated. Such an approach could be used for LmrA in the future.

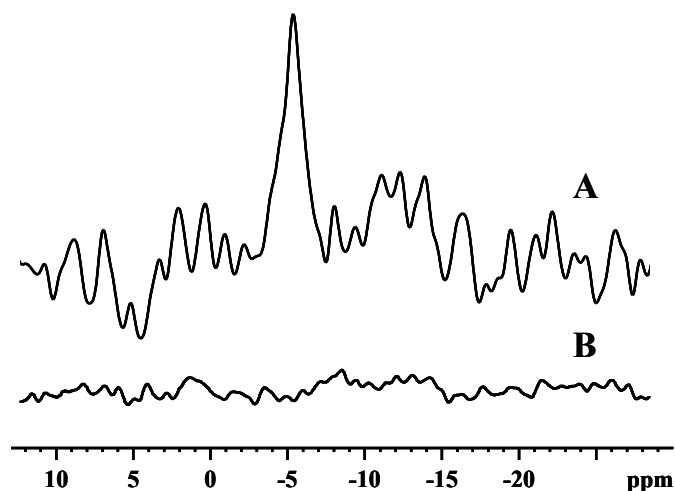
Materials and Methods

Purple membrane (PM) (10.5 mg, 0.4375 μM) was resuspended in 50 mM Tris, 25 mM KCl, pH 7.5 buffer to final concentration 7 mg/mL. Ten fold diluted 97 % 3-bromo-1, 1, 1-trifluoroacetone (BTFA) solution was added to PM suspension to final BTFA concentration of 5 mM. After 30 minutes incubation at room temperature on a rocking table, trifluoroacetyl cysteine labeled bacteriorhodopsin (bR) was pelleted by ultracentrifugation at 50.000 rpm for 40 minutes. To remove excess of labelling reagent, PM pellets was washed twice in low salt buffer (Brauer and Sykes, 1986; Huestis and Raftery, 1978; Milett and Raftery, 1972). ^{19}F CPMAS NMR experiments were performed essentially as described in Chapter 5.

Results

Trifluoroacetyl bR M163C mutant labelling was performed using adapted protocols from (Getmanova et al., 2004; Brauer and Sykes, 1986; Huestis and Raftery, 1978; Milett and Raftery, 1972). Figure 1 shows a comparison of ^{19}F CPMAS NMR spectra of PM M163C mutant labeled with TFA and of control *E. coli* lipids resuspended in BTFA solution and spinned down. PM mutant M163C ^{19}F spectrum has only one resonance at -5.2 ppm corresponding to TFA labeled cysteine. The absence of any other peaks shows that BTFA side reactions with threonine, lysine and histidine have low efficiency and are not significant on NMR scales. Control ^{19}F CPMAS measurements, performed on

BTFA incubated with lipids, revealed no non-specific TFA binding to lipids.



Appendix 1 Figure 1: ^{19}F CPMAS of A) purple membrane M163C mutant labeled with 3-bromo-1, 1, 1-trifluoro-aceton (BTA), B) control lipid vesicles resuspended in BTA and spinned down for NMR measurement. Spectra recorded at 7 kHz MAS spinning frequency and 255K. Spectra were referenced externally to trifluoacetic acid at 0 ppm.

Discussion

^{19}F NMR has been proven to a powerful technique in the study of protein structure and dynamic because ^{19}F nucleus provides a relatively nonperturbing and extremely sensitive probe (the ^{19}F chemical shift range is 100-fold larger than that of ^1H) with no background signals (Danielson and Falke, 1996a). Biosynthetic approach often fails to directly introduce fluorinated amino acids into a protein sequence because they are toxic for majority of bacterial strains (Gerig, 2001; Danielson and Falke, 1996a). We tried to incorporate ^{19}F tryptophan into LmrA by substitution of unlabelled tryptophan with its ^{19}F labeled analogue in CDM. However, the bacterial growth as well as the protein production was dramatically limited. Another way to introduce a fluorine labels into a biological macromolecule is by means of a chemical reaction in which a covalent bond is formed between a functional group of the molecule and some exogenous, fluorine-containing reagent. The most often target for such experiments is the sulfohydryl group of cysteine residues because of the high nucleophilicity of the side chain sulfohydryl group. There are usually relatively few cysteines in

proteins what makes this modification specific. Apart from cysteines, BTFA can react with the amino groups of lysine and of the peptide N-terminus, or the hydroxyl group of a serine or threonine but these reactions have very low yield, so on NMR scale their products are not visible (Gerig, 2001). A number of recent works showed applicability of TFA cysteine labelling approach for studying of such a large macromolecules as mammalian rhodopsin (Getmanova et al., 2004; Loewen et al., 2001; Thomas and Boxer, 2001). Trifluoroacetyl labelling was not tested first on LmrA but on bR because of several reasons. Among them are questionable accessibility of cysteines in LmrA mutants for labelling reagent and dimeric nature of LmrA. These could potentially initiate a wrong interpretation of labelling results if cysteines are not accessible or if each half of LmrA dimer gives separated peaks. For these reasons trifluoroacetyl cysteine labelling was first probed on PM M163C mutant. Figure 1 shows ^{19}F CPMAS spectrum of trifluoroacetyl labeled bR. The peak at -5.2 ppm corresponds to TFA labeled cysteine. The same labelling approach can be used in future for LmrA.

Appendix 2

Alignment of LmrA reconstituted into PC/PG liposomes

Solid-state NMR on aligned membrane proteins is an alternative to solid-state MAS NMR. The main problem however is to prepare well aligned samples of large membrane proteins. Here, first results of alignment tests on LmrA are reported.

Materials and methods

The preparation of the aligned free and leupeptin reconstituted PC/PG liposomes (the molar ration of PC to PG were 3 to 1 for all cases) was accomplished by the procedure outlined by (Hallock *et al.*, 2002). The procedure basically involves co-dissolving lipids, and peptide when necessary, in the chlorophorm-methanol mixture (3:1) to a lipid concentration of 4 mg/ml, depositing the mixture onto glass cover slips, subsequent drying of the cover slips on the air and under vacuum for at last 4 hours, and finally hydrating the samples with H₂O and aligning the lipids or lipid-peptide deposits.

The preparation of aligned LmrA reconstituted PC/PG proteoliposomes were accomplished by two approaches, and simple drying and hydrating on the glass cover slips and by the isopotential centrifugation (Grobner *et al.*, 1997). The first approach included depositing of the suspension of LmrA (4 mg/mL) reconstituted into PC/PG on the glass plates, drying the plates on the air for approximately 20 minutes and hydrating in sealed plates in 93% (93 % KCl) hydration atmosphere for several days. The isopotential centrifugation was performed how it was described in (Grobner *et al.*, 1997).

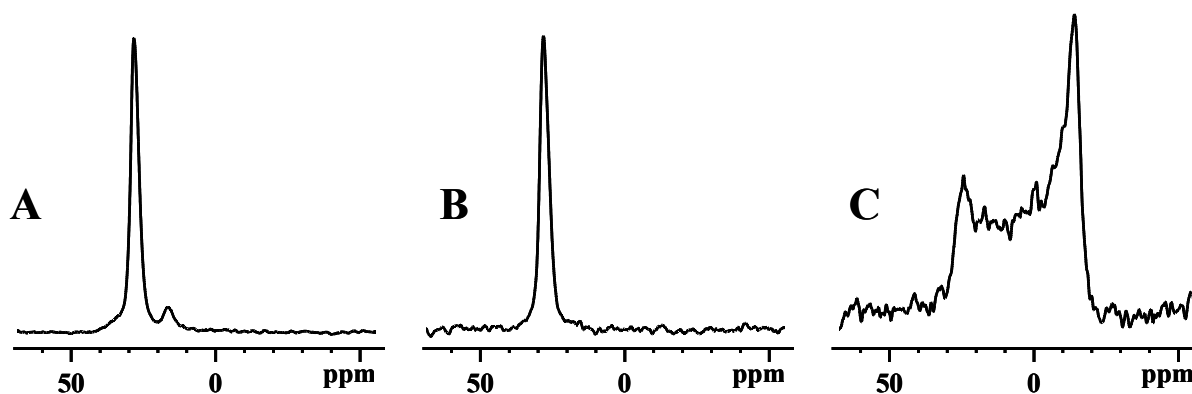
Prior to alignment the cover slips were pre-washed with in methanol and chlorophorm, dried on the open air. The remaining solvent was removed by evaporation under vacuum for at least 3 hours.

For NMR measurements about 15 cover slips were stacked one on top of the other, sealed with paraffin to prevent rehydratation and measured in at 0° with respect to the magnetic field direction at 303K. ³¹P static NMR experiments were performed essentially as described in Chapter 4.

LmrA purification and reconstitution was performed as described in Chapter 2 and 3.

Results

Figure 2 shows proton-decoupled ^{31}P NMR spectra of fully hydrated mechanically aligned PC/PG liposomes: free (Figure 2A), reconstituted with leupeptin (Figure 2B), and non aligned PC/PG proteoliposomes reconstituted with LmrA (Figure 2C) at 25°C. The presence of single intense peak at 29 ppm in Figures 2A and 2B indicates that the PC/PG bilayer normal is aligned parallel to the external magnetic field. In contrast, the presence of a powder pattern indicates that the liposomes reconstituted LmrA are not oriented in magnetic field. The PC/PG lipids' mixture was chosen as preferable lipid matrix for LmrA when compared with total *E. coli* lipids extract, because liposomes made of mixture of *E. coli* lipids in total extract are not well suitable lipids for alignment experiments. Additionally, how it was shown in Chapter 3, LmrA can be reconstituted into several synthetic lipids, including PC/PG lipids mixture.



Appendix 2 Figure 2: The ^{31}P spectra of PC/PG liposomes (A) free, (B) reconstituted leupeptin, 3 amino acid long peptide, and (C) reconstituted LmrA. For all oriented samples, the glass plates are oriented such that the bilayer normal is parallel to magnetic field. The temperature was set at 25°C.

Discussion

Keeping in mind, that the chief advantage of solid-state over solution state NMR is that orientational parameters are analytically related to angles of the reporter group relative to the applied magnetic field, efforts were made to prepare oriented sample. The examples of solid-state NMR studies on

peptides and proteins aligned on the glass plates are rare (Prosser and Davis, 1994a). However, we tried to align LmrA reconstituted into PC/PG liposomes on glass covers. Several alignment methods were probed, namely isopotential centrifugation and sequential proteoliposomes drying on glass plates followed by their slow rehydration. However, it was not possible to align the LmrA reconstituted proteoliposomes on the glass plates. In Figure 1 shows the comparison of aligned PC/PG liposomes free and containing small tripeptide, leupeptin, and non aligned PC/PG proteoliposomes reconstituted LmrA.

Literature

Calculated using Advanced Chemistry Development (ACD/Labs) Software Solaris V4.67 (1994-2005 ACD/Labs).

Abramson, J., Smirnova, I., Kasho, V., Verner, G., Kaback, H.R. and Iwata, S. (2003) Structure and mechanism of the lactose permease of *Escherichia coli*. *Science*. **301**: 610-615.

Achard-Joris, M., van Saparoeva, H.B.V., Driessen, A.J.M. and Bourdineaud, J.P. (2005) Heterologously expressed bacterial and human multidrug resistance proteins confer cadmium resistance to *Escherichia coli*. *Biochemistry*. **44**: 5916-5922.

Aebersold, R. and Mann, M. (2003) Mass spectrometry-based proteomics. *Nature*. **422**: 198-207.

Allerrini, P.R., van Scharrenburg, G.J.M., Sloodboom, A.J., de Haas, G.H. and Seelig, J. (1985) Side-chain dynamics of two aromatic amino acids in pancreatic phospholipase A2 as studied by deuterium nuclear magnetic resonance. *Biochemistry*. **24**: 3268-3273.

Alqwai, O., Poelarends, G., Konings, W.N. and Georges, E. (2003) Photoaffinity labelling under non-energized conditions of a specific drug-binding site of the ABC multidrug transporter LmrA from *Lactococcus lactis*. *Biochem. Biophys. Res. Commun.* **311**: 696-701.

Ambudkar, S.V., Kimchi-Sarfaty, C., Sauna, Z.E. and Gottesman, M.M. (2003) P-glycoprotein: from genomics to mechanism. *Oncogene*. **22**: 7468-7485.

Ambudkar, S.V., Dey, S., Hrycyna, C.A., Ramachandra, M., Pastan, I. and Gottesman, M.M. (1999) Biochemical, cellular, and pharmacological aspects of the multidrug transporter. *Annu. Rev. Pharmacol. Toxicol.* **39**: 361-398.

Bak, M., Rasmussen, J.T. and Nielsen, N.C. (2000) SIMPSON: A General Simulation Program for Solid-State NMR Spectroscopy. *J. Magn. Reson.* **147**: 296-330.

Balakrishnan, L., Venter, H., Shilling, R.A. and van Veen, H.W. (2004) Reversible transport by the ATP-binding cassette multidrug export pump LmrA - ATP synthesis at the expense of downhill ethidium uptake. *J. Biol. Chem.* **279**: 11273-11280.

Bartzatt, R. and Malesa, C. (2003) Synthesis, Structural analysis and antibacterial activity of a butyl ester derivative of ampicillin. *Chemother.* **49**: 213-221.

Basting, D. and Lehner, I. (2006) Investigating transport proteins by solid-state NMR. *Naunyn-*

Schmiedeberg's Arch. Pharmacol. 372 (6): 451-464.

Batchelder, L.S., Sullivan, C.E., Jelinski, L.W. and Torchia, D.A. (1982) Characterization of leucine side-chain reorientation in collagen-fibrils by solid-state ^2H NMR. *Proc. Natl. Acad. Sci. U.S.A.* **79**: 386-389.

Bennet, A.E., Rienstra, C.M., Auger, M., Lakshmi, K.V. and Griffin, R.G. (1995) Heteronuclear Decoupling in Rotating Solids. *J. Chem. Phys. Letters.* **103**: 6951.

Beshah, K., Olejniczak, E.T. and Griffin, R.G. (1987) Deuterium NMR study of methyl group dynamics in L-alanine. *J. Chem. Phys.* **89**: 4730-4736.

Bielecki, A., Kolbert, A.C. and Levitt, M. (1989) Frequency-Switched Pulse Sequences - Homonuclear Decoupling and Dilute Spin NMR in Solids. *Chem. Phys. Letters.* **314**: 443.

Bielecki, A., Kolbert, A.C., de Groot, H.J.M., Griffin, R.G. and Levitt, M. (1990) Frequency-Switched Lee-Goldburg Sequences in Solids. *Adv. Magn. Reson.* **14**: 111.

Bienvenue, A., Bloom, M., Davis, J.H. and Devaux, P.F. (1982) Evidence for protein-associated lipids from deuterium nuclear magnetic resonance studies of rhodopsin-dimyristoylphosphatidylcholine recombinants. *J. Biol. Chem.* **257**: 3032-3038.

Blackmore, C.G., McNaughton, P.A. and van Veen, H.W. (2001) Multidrug transporters in prokaryotic and eukaryotic cells: physiological functions and transport mechanisms. *Mol. Membr. Biol.* **18**: 97-103.

Blondeau, J.M. (2004b) Fluoroquinolones: mechanism of action, classification, and development of resistance. *Surv. Ophthalmol.* **49**: 73-77.

Boland, M.P. and Middleton, D.A. (2004) Insights into the interactions between a drug and a membrane protein target by fluorine cross-polarization magic angle spinning NMR. *Magn. Reson. Chem.* **42**: 204-211.

Bolhuis, H., van Veen, H.W., Molenaar, D., Poolman, B., Driessen, A.J.M. and Konings, W.N. (1996) Multidrug resistance in *Lactococcus lactis*: Evidence for ATP-dependent drug extrusion from the inner leaflet of the cytoplasmic membrane. *EMBO J.* **15**: 4239-4245.

Bolhuis, H., Molenaar, D., Poelarends, G., van Veen H. W., Poolman, B., Driessen, A.J.M. and Konings, W. (1994) Proton motive force-driven and ATP dependant drug extrusion systems in multidrug resistant *Lactococcus lactis*. *J. Bacteriol.* **176**: 6957-6964.

Bolhuis, H., van Veen H. W., Brands, J.R., Putman, M., Poolman, B., Driessen, A.J.M. and Konings, W. (1996b) *J. Biol. Chem.* **271**: 24123-24128.

Borges-Walmsley, M.I., McKeegan, K.S. and Walmsley, A.R. (2003) Structure and function of efflux pumps that confer resistance to drugs. *Biochem. J.* **376**: 313-338.

Brauer, M. and Sykes, B.D. (1986) ¹⁹F nuclear magnetic studies of selectively fluorinated derivatives of G- and F-actin. *Biochemistry.* **25**: 2187-2191.

Brennan, R.G. (2001) Introduction: multidrug resistance. *Semin. Cell Biol.* **12**: 201-204.

Brinkman, A., Eden, M. and Levitt, M. (2000) Synchronous helical pulse sequences in magic-angle spinning nuclear magnetic resonance: Double quantum recoupling of multiple-spin systems. *J. Chem. Phys.* **112**: 8539.

Buchaklian, A.H., Funk, A.L. and Klug, C.S. (2004) Resting state conformation of the MsbA homodimer as studied by site-directed spin labelling. *Biochemistry.* **43**: 8600-8606.

Cai, M., Huang, Y., Sakaguchi, K., Clore, G.M., Gronenborn, A.M. and Craigie, R. (1998) An efficient and cost-effective labelling protocol for proteins expressed in *Escherichia coli*. *J. Biomol. NMR.* **11**: 97-102.

Callaghan, R., Berridge, G., Ferry, D.R. and Higgins, C.F. (1997) The functional purification of P-glycoprotein is dependent on maintenance of a lipid-protein interface. *Biochim. Biophys. Acta.* **1328**: 109-124.

Calzolari, L., Gaggelli, E., Maccotta, A. and Valensin, G. (1997) Nuclear magnetic resonance investigations of calcium-antagonist drugs .4. Conformational and dynamic features of nicardipine {methyl 2- methyl(phenylmethyl)amino ethyl 1,4-dihydro-2,6-dimethyl-4-(3-nitrophenyl)pyridine-3,5-dicarboxylate} in deuterium oxide. *J. Chem. Soc. Perk. T. 2*: 363-367.

Carravetta, M., Eden, M., Zhao, X., Brinkman, A. and Levitt, M. (2000) Symmetry principles for the design of radiofrequency pulse sequences in the nuclear magnetic resonance of rotating solids. *Chem. Phys. Lett.* **321**: 205.

Casa, M., Boissonnade, M.M. and Baszkin, A. (1992) Penetration of chlorcyclizine and ampicillin into mixed phospholipid-oleic acid monolayers. *Colloid Surf.* **68**: 207-214.

Castaing, M., Loiseau, A. and Mulliert, G. (2005) Multidrug resistance modulator interactions with neutral and anionic liposomes: membrane binding affinity and membrane perturbing activity. *J. Pharm. Pharmacol.* **57**: 547-554.

- Castellani, F., Van Rossum, B.J., Diehl, A., Schubert, M., Rehbein, K. and Oschkinat, H. (2002) Structure of a protein determined by solid-state magic-angle NMR spectroscopy. *Nature*. **420**: 98-102.
- Chami, M., Steinfelds, E., Orelle, C., Jault, J.M., Di Pietro, A., Rigaud, J.-L. and Marco, S. (2002) Three-dimensional structure by cryo-electron microscopy of YvcC, a homodimeric ATP-binding cassette transporter from *Bacillus subtilis*. *J. Mol. Biol.* **315**: 1075-1085.
- Chang, G. (2003a) Structure of MsbA from *Vibrio cholera*: A multidrug resistance ABC transporter homolog in a closed conformation. *J. Mol. Biol.* **330**: 419-430.
- Chang, G. (2003b) Multidrug resistance ABC transporters. *FEBS Lett.* **555**: 102-105.
- Chang, G. and Roth, C.B. (2001) Structure of MsbA from *E. coli*: A homolog of the multidrug resistance ATP binding cassette (ABC) transporters. *Science*. **293**: 1793-1800.
- Chen, C.-Y., Cheng, C., Chen, Y.-C., Lee, J.-C., Chou, S.-H. and Chuang, W.-J. (2006) Preparation of amino acid-type isotope labelling of proteins expressed in *Pichia pastoris*. *Proteins-Structure Function and Bioinformatics*. **62**: 279-287.
- Chiba, P., Ecker, G., Schmid, D., Drach, J., Tell, B., Goldenberg, S. and Gekeler, V. (1996) Structural requirements for activity of propafenone-type modulators in P-glycoprotein-mediated multidrug resistance. *Mol. Pharmacol.* **49**: 1122-1130.
- Claridge, T.D.W. (1999) High resolution NMR techniques in organic chemistry. *Pergamon press*.
- Clarke, R.J. (2001) The dipole potential of phospholipid membranes and methods for its detection. *Adv. Colloid Interfac.* **89-90**: 263-281.
- Cocaign-Bousquet, M., Garrigues, C., Novak, L., Lindley, N.D. and Loubiere, P. (1995a) Rational Development of a Simple Synthetic Medium for the Sustained Growth of *Lactococcus Lactis*. *J. Appl. Bacteriol.* **79**: 108-116.
- Creemers, A.F.L., Bovee-Geurts, P.H.M., DeGrip, W.J., Lugtenburg, J. and de Groot, H.J.M. (2004) Solid-state NMR analysis of ligand-receptor interactions reveals an induced misfit in the binding site of isorhodopsin. *Biochemistry*. **43**: 16011-16018.
- Creemers, A.F.L., Klaassen, C.H.W., Bovee-Geurts, P.H.M., Kelle, R., Kragl, U., Raap, J., *et al* (1999) Solid state N-15 NMR evidence for a complex Schiff base counterion in the visual G-protein-coupled receptor rhodopsin. *Biochemistry*. **38**: 7195-7199.
- Danielson, M.A. and Falke, J.J. (1996b) Use of ¹⁹F NMR to probe protein structure and

conformational changes. *Annu. Rev. Biophys. Biomol. Struct.* **25**: 163-195.

Dantzig, A.H., Law, K.L., Cao, J. and Starling, J.J. (2001) Reversal of multidrug resistance by the P-glycoprotein modulator, LY3335979, from the bench to clinic. *Curr. Med. Chem.* **8**: 39-50.

Davis, J.H. (1983) The description of membrane lipid conformation, order and dynamics by ²H-NMR. *Biochim. Biophys. Acta.* **737**: 117-171.

de Lamotte, F., Boze, H., Blanchard, C., Klein, C., Moulin, G., Gautier, M.-F. and Delsuc, M.-A. (2001) NMR monitoring of accumulation and folding of ¹⁵N-labeled protein overexpressed in *Pichia pastoris*. *Protein Expression and Purification.* **22**: 318-324.

Del Grosso, M., Iannelli, F., Messina, C., Santagati, M., Petrosillo, N. and Stefani, S.e.a. (2002) Macrolide efflux genes *mef(A)* and *mef(E)* are carried by different genetic elements in *Streptococcus pneumoniae*. *J. Clin. Microbiol.* **40**: 774-778.

Dewolf, F.A., Demel, R.A., Bets, D., Vankats, C. and Dekruiff, B. (1991) Characterization of the Interaction of Doxorubicin with (Poly)Phosphoinositides in Model Systems - Evidence for Specific Interaction with Phosphatidylinositol-Monophosphate and Phosphatidylinositol-Diphosphate. *FEBS Lett.* **288**: 237-240.

Dey, S., Ramachandra, M., Pastan, I., Gottesman, M.M. and Ambudkar, S.V. (1997) Evidence for two nonidentical drug-interaction sites in the human P-glycoprotein. *Proc. Natl. Acad. Sci. U.S.A.* **94**: 10594-10599.

DiDiodato, G. and Sharom, F.J. (1997) Interaction of combinations of drugs, chemosensitisers, and peptides with the P-glycoprotein multidrug transporter. *Biochem. Pharmacol.* **53**: 1789-1797.

Diederichs, K., Diez, J., Greller, G., Müller, C., Breed, J., Schnell, C., *et al* (2000) Crystal structure of MalK, the ATPase subunit of the trehalose/maltose ABC transporter of the archaeon *Thermococcus litoralis*. *EMBO J.* **9**: 5951-5961.

Dong, J., Yang, G. and Mchaourab, H.S. (2005) Structural basis of energy transduction in the transport cycle of MsbA. *Science.* **308**: 1023-1028.

Dougherty, D.A. (1996) Cation- π interactions in chemistry and biology: A new view of benzene, Phe, Tyr, and Trp. *Science.* **271**: 163-168.

Drew, D., Fröderberg, L., Baars, L. and J.-W.L., d.G. (2003) Assembly and overexpression of membrane proteins in *Escherichia coli*. *Biochim. Biophys. Acta.* **1610**: 3-10.

- Duer, M.J. (2002) Solid-state NMR spectroscopy. *Blackwell science Press*.
- Ecker, G.F., Pleban, K., Kopp, S., Csaszar, E., Poelarends, G.J., Putman, M., *et al* (2004) A three-dimensional model for the substrate binding domain of the multidrug ATP binding cassette transporter LmrA. *Mol. Pharmacol.* **66**: 1169-1179.
- Eckford, P.D.W. and Sharom, F.J. (2005) The reconstituted P-glycoprotein multidrug transporter is a flippase for glucosylceramide and other simple glycosphingolipids. *Biochem. J.* **389**: 517-526.
- Eden, M. and Levitt, M. (1999) Pulse sequence symmetries in the nuclear magnetic resonance of spinning solids: application to heteronuclear decoupling. *J. Chem. Phys.* **111**: 1511.
- Edgar, R. and Bibi, E. (1999) A single membrane-embedded negative charge is critical for recognizing positively charged drugs by the Escherichia coli multidrug resistance protein MdfA. *EMBO J.* **18**: 822-832.
- Eilers, M., Reeves, P.J., Ying, W.W., Khorana, H.G. and Smith, S.O. (1999) Magic angle spinning NMR of the protonated retinylidene Schiff base nitrogen in rhodopsin: Expression of N-15-lysine- and C-13-glycine-labeled opsin in a stable cell line. *Proc. Natl. Acad. Sci. U.S.A.* **96**: 487-492.
- Elbaz, Y., Tayer, N., Steinfelds, E., Steiner-Mordoch, S. and Schuldiner, S. (2005) Substrate-induced tryptophan fluorescence changes in EmrE, the smallest ion-coupled multidrug transporter. *Biochemistry.* **44**: 7369-7377.
- Ellena, J.F., Dominey, R.N., Archer, S.J., Xu, Z.C. and Cafiso, D.S. (1987) Localization of Hydrophobic Ions in Phospholipid-Bilayers Using H-1 Nuclear Overhauser Effect Spectroscopy. *Biochemistry.* **26**: 4584-4592.
- Eytan, G.D. (2005) Mechanism of multidrug resistance in relation to passive membrane permeation. *Biomed. Pharmacother.* **59**: 90-97.
- Eytan, G.D., Regev, R., Oren, G. and Assaraf, Y.G. (1996) The role of passive transbilayer drug movement in multidrug resistance and its modulation. *J. Biol. Chem.* **271**: 12897-12902.
- Fang, G., Friesen, R., Lanfermeijer, F., Hagting, A., Poolman, B. and Konings, W.N. (1999) Manipulation of activity and orientation of membrane-reconstituted di-tripeptide transport protein DtpT of Lactococcus lactis. *Mol. Membr. Biol.* **16**: 297-304.
- Ferte, J. (2000) Analysis of tangled relationships between P-glycoprotein-mediated multidrug resistance and the lipid phase of the cell membrane. *Eur. J. Biochem.* **267**: 277-294.

- Fetsch, E.E. and Davidson, A.L. (2002) Vanadate-catalyzed photocleavage of the signature motif of an ATP-binding cassette (ABC) transporter. *Proc. Natl. Acad. Sci. U.S.A.* **99**: 9685-9690.
- Frezard, F. and Garniersuillerot, A. (1991) DNA-Containing Liposomes as a Model for the Study of Cell-Membrane Permeation by Anthracycline Derivatives. *Biochemistry*. **30**: 5038-5043.
- Frezard, F., Pereira-Maia, E., Quidu, P., Priebe, W. and Garnier-Suillerot, A. (2001) P-Glycoprotein preferentially effluxes anthracyclines containing free basic versus charged amine. *Eur. J. Biochem.* **268**: 1561-1567.
- Fukuda, H., Kishii, R. and Takei, M. (2001) Contributions of the 8-methoxy group of gatifloxacin to resistance selectivity, target preference and antibacterial activity against *Streptococcus pneumoniae*. *Antimicrob. Agents Chemother.* **45**: 1649-1653.
- Fung, B.M., Khitritin, A.K. and Ermolaev, K. (2000) An improved broadband decoupling sequence for liquid crystals and solids *J. Magn. Reson.* **142**: 97.
- Gaggelli, E., Valensin, G., Stolowich, N.J., Williams, H.J. and Scott, A.I. (1992) Conformation of Vinblastine in Aqueous-Solution Determined by 2D H-1-NMR and C-13-NMR Spectroscopy. *J. Nat. Prod.* **55**: 285-293.
- Gallois, L., Fiallo, M., Laigle, A., Priebe, W. and Garnier Suillerot, A. (1996) The overall partitioning of anthracyclines into phosphatidyl-containing model membranes depends neither on the drug charge nor the presence of anionic phospholipids. *Eur. J. Biochem.* **241**: 879-887.
- Gan, Z.H. and Ernst, R.R. (1997) Frequency- and phase-modulated heteronuclear decoupling in rotating solids. *Solid-State Nucl. Magn. Reson.* **8**: 153.
- Garipova, I.Y. and Silnikov, V.N. (2003) New synthetic approaches to multifunctional phenazinium salt derivatives. *Molecules*. **8**: 505-519.
- Gaudet, R. and Wiley, D.C. (2001) Structure of the ABC ATPase domain of human TAP1, the transporter associated with antigen processing. *EMBO J.* **20**: 4964-4972.
- Geourjon, C., Orelle, C., Steinfels, E., Blanchet, C., Deleage, G., Di Pietro, A. and Jault, J.M. (2001) A common mechanism for ATP hydrolysis in ABC transporter superfamilies. *Trends Biochem. Sci.* **26**: 539-544.
- Gerig, J.T. (2001) Fluorine NMR. Biophysics textbook on-line, NMR section, chapter 24. www.biosci.umn.edu/biophys

- Getmanova, E., Patel, A.B., Klein-Seetharaman, J., Loewen, M.C., Reeves, P.J., Friedman, N., *et al* (2004) NMR spectroscopy of phosphorylated wild-type rhodopsin: mobility of the phosphorylated C-terminus of rhodopsin in the dark and upon light activation. *Biochemistry*. **43**: 1126-1133.
- Glaubitz, C., Gröder, A., Gottschalk, K., Spooner, P., Watts, A., Schuldiner, A. and Kessler, H. (2000) ³¹P-CP-NMR studies on TPP⁺ bound to the ion-coupled multidrug transport protein EmrE. *FEBS Lett.* **480**: 127-131.
- Gorzelle, B.M., Nagy, J.K., Oxenoid, K., Lonzer, W., Cafiso, D.S. and Sanders, C.R. (1999) Reconstitutive refolding of diacylglycerol kinase, an integral membrane protein *Biochemistry*. **38**: 16373-16382.
- Goto, N.K. and Kay, L.E. (2000) New developments in isotope labelling strategies for protein solution NMR spectroscopy. *Curr. Opin. Struct. Biol.* **10**: 585-592.
- Grimard, V., Vigano, C., Margolles, A., Wattiez, R., van Veen, H.W., Konings, W.N., *et al* (2001) Structure and dynamics of the membrane-embedded domain of LmrA investigated by coupling polarized ATR-FTIR spectroscopy and H-1/H-2 exchange. *Biochemistry*. **40**: 11876-11886.
- Grobner, G., Taylor, A., Williamson, P.T., Choi, G., Glaubitz, C., Watts, J.A., *et al* (1997) Macroscopic orientation of natural and model membranes for structural studies. *Anal. Biochem.* **254**: 132-138.
- Gullion, T. and Schaefer, J. (1989) Rotational-Echo Double-Resonance. *NMR J. Magn. Reson.* **90**: 330.
- Haeberlen, U. and Waugh, J.S. (1968) Coherent Averaging Effects in Magnetic Resonance. *Phys. Rev.* **175**: 453.
- Hagmann, W., Schubert, J., König, J. and Keppler, D. (2002) Reconstitution of transport-active multidrug resistance protein 2 (MRP2; ABCC2) in proteoliposomes. *Biol. Chem.* **383**: 1001-1009.
- Hallock, K., Henzler Wildman, K., Lee, D. and A., R. (2002) An innovative procedure using a sublimable solid to align lipid bilayers for solid-state NMR studies. *Biophys. J.* **82**: 2499-2503.
- Hebert, M.F., Roberts, J.P., Prueksaritanont, T. and Benet, L.Z. (1992) Bioavailability of cyclosporine with concomitant rifampicin administration is markedly less than predicted by hepatic enzyme. *Clin. Pharmacol. Therapeutics*. **52**: 453-457.
- Hediger, S., Meier, B.H., Kurur, N.D., Bodenhausen, G. and Ernst, R.R. (1994) NMR Cross-Polarization by Adiabatic Passage through the Hartmann-Hahn Condition (Aphh). *Chem. Phys. Lett.*

223: 283.

Herzfeld, J., Mulliken, C.M., Siminovitch, D.J. and Griffin, R.G. (1987) Contrasting molecular dynamics in red and purple membrane fractions of the *Halobacterium halobium*. *Biophys. J.* **52**: 855-858.

Higgins, C.F. (1992) ABC transporters: from microorganism to man. *Ann. Rev. Cell Dev. Biol.* **8**: 67-113.

Higgins, C.F. and Gottesman, M.M. (1992) Is the Multidrug Transporter a Flippase. *Trends Biochem. Sci.* **17**: 18-21.

Higgins, C.F. and Linton, K.J. (2004) The ATP switch model for ABC transporters. *Nat. Struct. Mol. Biol.* **11**: 918-926.

Higgins, C.F. (1986a) A family of related ATP-binding subunits coupled to many distinct biological processes in bacteria. *Nature.* **323**: 448-450.

Hologne, M. and Hirschinger, J. (2004) Molecular dynamics as studied by static-powder and magic-angle spinning 2H NMR. *Solid-State Nucl. Magn. Reson.* **26**: 1-10.

Holte, L.L. and Gawrisch, K. (1997) Determining ethanol distribution in phospholipid multilayers with MAS-NOESY spectra. *Biochemistry.* **36**: 4669-4674.

Homolya, L., Hollo, Z., Germann, U.A., Pastan, I., Gottesman, M.M. and Sarkadi, B. (1993) Fluorescent cellular indicators are extruded by the multidrug resistance protein. *J. Biol. Chem.* **268**: 21493-21496.

Hong, M. and Jakes, K. (1999) Selective and extensive C-13 labelling of a membrane protein for solid-state NMR investigations. *J. Biomol. NMR.* **14**: 71-74.

Hopfner, K.P., Karcher, A., Shin, D.S., Craig, L., Arthur, L.M., Carney, J.P. and Tainer, J.A. (2000) Structural biology of Rad50 ATPase: ATP-driven conformational control in DNA double-strand break repair and the ABC-ATP-ase superfamily. *Cell.* **101**: 789-800.

Hore, P.J. (1995) Nuclear magnetic resonance. *Oxford university press.*

Huestis, W.H. and Raftery, M.A. (1978) Bromotrifluoroacetone alkylates hemoglobin at cysteine b83. *Biochem. Biophys. Res. Commun.* **81**: 892-899.

Hung, L.W., Wang, I.X.Y., Nikaido, K., Liu, P.Q., Ames, G.F.L. and Kim, S.H. (1998) Crystal structure of the ATP-binding subunit of an ABC transporter. *Nature.* **398**: 703-707.

Huster, D., Arnold, K. and Gawrisch, K. (1998) Influence of docosahexaenoic acid and cholesterol on lateral lipid organization in phospholipid mixtures. *Biochemistry*. **37**: 17299-17308.

Huster, D., Arnold, K. and Gawrisch, K. (1999) Investigation of lipid organization in biological membranes by two-dimensional nuclear overhauser enhancement spectroscopy. *J. Phys. Chem. B*. **103**: 243-251.

Huster, D., Muller, P., Arnold, K. and Herrmann, A. (2003a) Dynamics of lipid chain attached fluorophore 7-nitrobenz-2-oxa-1,3-diazol-4-yl (NBD) in negatively charged membranes determined by NMR spectroscopy. *Eur. Biophys. J.* **32**: 47-54.

Huster, D., Vogel, A., Katzka, C., Scheidt, H.A., Binder, H., Dante, S., *et al* (2003b) Membrane insertion of a lipidated Ras peptide studied by FTIR, solid-state NMR, and neutron diffraction spectroscopy. *J. Am. Chem. Soc.* **125**: 4070-4079.

Jelinski, L.W., Sullivan, C.E. and Torchia, D.A. (1980a) ²H NMR study of molecular motion in collagen fibrils. *Nature*. **284**: 531-534.

Jelinski, L.W., Sullivan, C.E., Batchelder, L.S. and Torchia, D.A. (1980b) Deuterium nuclear magnetic resonance of specifically labeled native collagen. *Biophys. J.* **10**: 515-529.

Jones, D.H., Rigby, A.C., Barber, K.R. and Grant, C.W.M. (1997) Oligomerization of the EGF receptor transmembrane domain: a ²H NMR study in lipid bilayers. *Biochemistry*. **36**: 12616-12624.

Kamihira, M., Vosegaard, T., Mason, A.J., Straus, S.K., Nielsen, N.C. and Watts, A. (2005) Structural and orientational constraints of bacteriorhodopsin in purple membranes determined by oriented-sample solid-state NMR spectroscopy. *J. Struct. Biol.* **149**: 7-16.

Karcher, A., Büttner, K., Märten, B., Jansen, R.-P. and Hopfner, K.P. (2005) X-ray structure of PLI, an essential twin cassette ABC ATPase involved in ribosome biogenesis and HIV capsid assembly. *Structure*. **13**: 649-659.

Karczmar, G.S. and Tritton, T.R. (1979) Interaction of adryamycin with small unilamellar vesicle liposomes - fluorescence study. *Biochim. Biophys. Acta*. **557**: 306-319.

Karpowich, N., Martisinkevich, O., Millen, L., Yuan, Y.R., Dai, P.L., MacVey, K., *et al* (2001) Crystal structure of the MJ1267 ATP binding cassette reveal an induced-fit effect at the TPase active site of an ABC transporter. *Structure*. **9**: 571-586.

Keniry, M.A., Gutowsky, H.S. and Oldfield, E. (1984a) Surface dynamics of the integral membrane protein bacteriorhodopsin. *Nature*. **307**: 383-386.

- Keniry, M.A., Rothgeb, T.M., Smith, R.L., Gutowsky, H.S. and Oldfield, E. (1983) Nuclear magnetic resonance studies of amino acids and proteins. Side-chain mobility of methionine in the crystalline amino acid and in crystalline sperm whale (Physeter catodon) myoglobin. *Biochemistry*. **22**: 1917-1926.
- Keniry, M.A., Kintanar, A., Smith, R.L., Gutowsky, H.S. and Oldfield, E. (1984b) Nuclear magnetic resonance studies of amino acids and proteins. Deuterium nuclear magnetic resonance relaxation of deuteriomethyl-labeled amino acids in crystals and in Halobacterium halobium and Escherichia coli cell membranes. *Biochemistry*. **23**: 288-298.
- Kihara, A., Akiyama, Y., Ito, K. (1995) FtsH is required for proteolytic elimination of uncomplexed forms of SecY, an essential protein translocase subunit. *Proc. Natl. Acad. Sci. U.S.A.* **92**: 4532-4536.
- Kikuchi, J., Williamson, M.P., Shimada, K. and Asakura, T. (2000) Structure and dynamics of photosynthetic membrane-bound proteins in Rhodospirillum rubrum, studied with solid-state NMR spectroscopy. *Photosynthesis Res.* **63**: 259-267.
- Kim, H.-W., Perez, J.A., Ferguson, S.J. and Campbell, I.D. (1990) The specific incorporation of labelled amino acids into proteins through growth of bacteria in the presence of glyphosate. *FEBS Lett.* **272**: 34-36.
- Kinsey, R.A., Kintanar, A. and Oldfield, E. (1981) Dynamics of amino acid side chains in membrane proteins by high field solid state deuterium nuclear magnetic resonance spectroscopy. *J. Biol. Chem.* **256**: 9028-9036.
- Klammt, C., Lohr, F., Schafer, B., Haase, W., Dotsch, V., Ruterjans, H., *et al* (2004) High level cell-free expression and specific labelling of integral membrane proteins. *Eur. J. Biochem.* **271**: 568-580.
- Klopman, G., Shi, L.M. and Ramu, A. (1997) Quantitative structure-activity relationship of multidrug resistance reversal agents. *Mol. Pharmacol.* **52**: 323-334.
- Knol, J., Veenhoff, L.M. and Poolman, B. (1997) Unidirectional reconstitution of a secondary transport protein. *FASEB J.* **11**: A1082-A1082.
- Knol, J., Sjollem, K. and Poolman, B. (1998) Detergent-mediated reconstitution of membrane proteins. *Biochemistry*. **37**: 16410-16415.
- Konings, W.N., Kok, J., Kuipers, O.P. and Poolman, B. (2000) Lactic acid bacteria: the bugs of the new millennium. *Curr. Opin. Microbiol.* **3**: 276-282.
- Kristensen, J.H., Bildsoe, H., Jakobsen, H.J. and Nielsen, N.C. (1999) Separation of ²H MAS NMR

spectra by two-dimensional spectroscopy. *J. Magn. Reson.* **139**: 314-333.

Krueger-Koplin, R.D., Sorgen, P.L., Krueger-Koplin, S.T., Rivera-Torres, I.O., Cahill, S.M., Hicks, D.B., *et al* (2004) An evaluation of detergents for NMR structural studies of membrane proteins. *J. Biomol. NMR.* **17**: 43-57.

Kumar, A. and Schweizer, H.R. (2005) Bacterial resistance to antibiotics: active efflux and reduced uptake. *Adv. Drug Delivery Rev.* **57**: 1486-1513.

Kunji, E.R.S., Slotboom, D.J. and Poolman, B. (2003) *Lactococcus lactis* as host for overproduction of functional membrane proteins. *Biochim. Biophys. Acta.* **1610**: 97-108.

Lam, F.C., Liu, R.H., Lu, P.H., Shapiro, A.B., Renoir, J.M., Sharom, F.J. and Reiner, P.B. (2001) beta-Amyloid efflux mediated by p-glycoprotein. *J. Neurochem.* **76**: 1121-1128.

Lau, F.W. and Bowie, J.U. (1997) A method for assessing the stability of a membrane protein. *Biochemistry.* **36**: 5884-5892.

Laws, D.D., Bitter, H.-M. and Jerschow, A. (2002) Solid-state NMR spectroscopic methods in chemistry. *Angew. Chem. Int.* **41**: 3096-3129.

Lee, J.-Y., Urbatsch, I.L., Senior, A.E. and Wilkens, S. (2002) Projection structure of P-glycoprotein by electron microscopy. *J. Biol. Chem.* **277**: 40125-40131.

LeMaster, D.M. (1994) Isotope labelling in solution protein assignment and structural analysis. *Proc. Natl. Acad. Sci. U.S.A.* **26**: 371-419.

Leo, G.C., Colnago, L.A., Valentine, K.G. and Opella, S.J. (1987) Dynamics of fd coat protein in lipid bilayers. *Biochemistry.* **26**: 854-862.

Levitt, M. (2001) Spin dynamics. *John Wiley Press.*

Lewis, H.A., Buchanan, S.G., Burley, S.K., Conners, K., Dickey, M. and Dorwart, M.E.A. (2004) Structure of nucleotide-binding domain 1 of the cystic fibrosis transmembrane conductance regulator. *EMBO J.* **23**: 282-293.

Li, X.Z., Barre, N. and Poole, K. (2000) Influence of the MexA-MexB-OprM multidrug efflux system on expression of the MexC-MexD-OprJ and MexE-MexF-OprN multidrug efflux systems in *Pseudomonas aeruginosa*. *J. Antimicrob. Chemother.* **46**: 885-893.

Lian, L.Y. and Middleton, D.A. (2001a) Labelling approaches for protein structural studies by solution-state and solid-state NMR. *Prog. Nucl. Magn. Res. Spectrosc.* **39**: 171-190.

- Lindholm, A., Mäki-Arvela, P., Toukoniitty, E., Pakkanen, T.Y., Hirvi, J.T., Salmi, T., *et al* (2002) Hydrosilylation of cinchonidine and 9-O-TMS-cinchonidine with triethoxysilane: application of 11-(triethoxysilyl)-10, 11-dihydrocinchonidine as a chiral modifier in the enantioselective hydrogenation of 1-phenylpropane-1, 2-dione. *J. Chem.Soc. Perk. T. 1*: 2605-2612.
- Liu, R., Siemiarczuk, A. and Sharom, F.J. (2000) Intrinsic fluorescence of the P-glycoprotein multidrug transporter: sensitivity of tryptophan residues to binding of drugs and nucleotides. *Biochemistry*. **39**: 14927-14938.
- Locher, K.P., Lee, A.T. and Rees, D.C. (2002) The E.coli BtuCD structure: A framework for ABC transporter architecture and mechanism. *Science*. **296**: 1091-1098.
- Loewen, M.C., Klein-Seetharaman, J., Getmanova, E., Reeves, P.J., Schwalbe, H. and Khorana, H.G. (2001) Solution 19F nuclear overhauser effects in structural studies of the cytoplasmic domain of mammalian rhodopsin. *Proc. Natl. Acad. Sci. U.S.A.* **98**: 4888-4892.
- Loo, T.W. and Clarke, D.M. (2001) Determining the dimensions of the drug-binding domain of human P-glycoprotein using thiol cross-linking compounds as molecular rulers. *J. Biol. Chem.* **276**: 36877-36880.
- Loo, T.W. and Clarke, D.M. (2002) Vanadate trapping of nucleotide at the ATP-binding sites of human multidrug resistance P-glycoprotein exposes different residues to the drug-binding site. *Proc. Natl. Acad. Sci. U.S.A.* **99**: 3511-3516.
- Loo, T.W. and Clarke, D.M. (2005) Do drug substrates enter the common drug-binding pocket of P-glycoprotein through "gates"? *Biochem. Biophys. Res. Commun.* **329**: 419-422.
- Loo, T.W., Bartlett, M.C. and Clarke, D.M. (2003) Substrate-induced conformational, changes in the transmembrane segments of human P-glycoprotein - Direct evidence for the substrate-induced fit mechanism for drug binding. *J. Biol. Chem.* **278**: 13603-13606.
- Loo, T.W., Bartlett, M.C. and Clarke, D.M. (2004a) Processing mutations located throughout the human multidrug resistance P-glycoprotein disrupt interactions between the nucleotide binding domains. *J. Biol. Chem.* **279**: 38395-38401.
- Loo, T.W., Bartlett, M.C. and Clarke, D.M. (2004b) The drug-binding pocket of the human multidrug resistance P-glycoprotein is accessible to the aqueous medium. *Biochemistry*. **43**: 12081-12089.
- Lowry, O.H., Rosebrough, N.J., Farr, A.L. and Randall, R.J. (1951) Protein Measurement with the Folin Phenol Reagent. *J. Biol. Chem.* **193**: 265-275.

- Lu, G., Westbrook, J.M., Davidson, A.L. and Chen, J. (2005) ATP hydrolysis is required to reset the ATP-binding cassette dimer into the resting-state conformation. *Proc. Natl. Acad. Sci. U.S.A.* **102**: 17969-17974.
- Lu, P.H., Liu, R.H. and Sharom, F.J. (2001) Drug transport by reconstituted P-glycoprotein in proteoliposomes - effect of substrates and modulators, and dependence on bilayer phase state. *Eur. J. Biochem.* **268**: 1687-1697.
- Lu, W.C., Wang, C.Z., Yu, E.W. and Ho, K.M. (2006) Dynamics of the trimeric AcrB transporter protein inferred from a B-Factor analysis of the crystal structure. *Proteins-Structure Function and Bioinformatics.* **62**: 152-158.
- Lubelski, J., van Merkerk, R., Konings, W. and Driessen, A.J.M. (2006) Nucleotide-binding sites of the heterodimeric LmrCD ABC-multidrug transporter of *Lactococcus lactis* are asymmetric. *Biochemistry.* **45**: 648-656.
- Lubelski, J., Mazurkiewicz, P., van Merkerk, R., Konings, W. and Driessen, A.J.M. (2004) ydaG and YbdA of *Lactococcus lactis* encode a heterodimeric ATP-binding cassette-type multidrug transporter. *J. Biol. Chem.* **279**: 34449-34455.
- Luca, S., Heise, H. and Baldus, M. (2005) Investigation of ligand-receptor systems by high-resolution solid-state NMR: recent progress and perspectives. *Arch. Pharm. Chem. Life Sci.* **338**: 217-228.
- Lugo, M.R. and Sharom, F.J. (2005a) Interaction of LDS-751 with P-glycoprotein and mapping of the location of the R drug binding site. *Biochemistry.* **44**: 643-655.
- Lugo, M.R. and Sharom, F.J. (2005b) Interaction of LDS-751 and rhodamine 123 with P-glycoprotein: Evidence for simultaneous binding of both drugs. *Biochemistry.* **44**: 14020-14029.
- Lynch, J.P. and Martinez, F.J. (2002) Clinical relevance of macrolide-resistant *Streptococcus pneumoniae* for community-acquired pneumonia. *Clin. Inf. Dis.* **34**: S27-46.
- Macdonald, P.M. and Seelig, A. (1988) Dynamic properties of gramicidin A in phospholipid membranes. *Biochemistry.* **27**: 2357-2364.
- Mack, J.W., Usha, M.G., Long, J., Griffin, R.G. and Witterbort, R.J. (2000) Backbone motions in a crystalline protein from field-dependent ²H-NMR relaxation and line-shape analysis. *Biopolymers.* **53**: 9-18.
- Mahmoud, M., Gentil, E. and Robins, R.J. (2004) Natural-abundance ratio mass spectrometry as a means of evaluating carbon redistribution during glucose-citrate cofermentation by *Lactococcus lactis*.

Eur. J. Biochem. **271**: 4392-4400.

Mao, Q.C., Deeley, R.G. and Cole, S.P.C. (2000) Functional reconstitution of substrate transport by purified multidrug resistance protein MRP1 (ABCC1) in phospholipid vesicles. *J. Biol. Chem.* **275**: 34166-34172.

Margolles, A., Putman, M., van Veen, H.W. and Konings, W.N. (1999) The purified and functionally reconstituted multidrug transporter LmrA of *Lactococcus lactis* mediates the transbilayer movement of specific fluorescent phospholipids. *Biochemistry.* **38**: 16298-16306.

Markham, P.N. and Neyfakh, A.A. (2001) Efflux-mediated drug resistance in Gram-positive bacteria. *Curr. Opin. Microbiol.* **4**: 509-514.

Marly, J., Lu, M. and C., B. (2001) A method for efficient isotopic labelling of recombinant proteins. *J. Biomol. NMR.* **20**: 71-75.

Martin, C., Higgins, C.F. and Callaghan, R. (2001) The vinblastine binding site adopts high- and low-affinity conformations during a transport cycle of P-glycoprotein. *Biochemistry.* **40**: 15733-15742.

Masuda, N., Sakagawa, E., Ohya, S., Gohot, N., Tsujimoto, H. and Nishino, T. (2000) Contribution of the MexX-MexY-OprM efflux system to intrinsic resistance in *Pseudomonas aeruginosa*. *Antimicrob. Agents Chemother.* **44**: 2242-2246.

Mazurkiewicz, P., Sakamoto, K., Poelarends, G.J. and Konings, W.N. (2005) Multidrug transporters in lactic acid bacteria. *Mini-Rev. Med. Chem.* **5**: 173-181.

Mazzariol, A., Cornaglia, G. and Nikaido, H. (2000) Contributions of the AmpC beta-lactamase and the AcrAB multidrug efflux system in intrinsic resistance of *Escherichia coli* K-12 to beta-lactams. *Antimicrob. Agents Chemother.* **44**: 1387-1390.

McDonnell, P.A., Shon, K., Kim, Y. and Opella, S.J. (1993) fd coat protein structure in membrane environments. *J. Mol. Biol.* **233**: 447-463.

Meadows, M.D. (1979) In Chemistry. *University of Illinois at Urbana-Champaign: Urbana, IL.*: 140.

Meng, Z., Simmons-Willis, T.A. and Limbach, P.A. (2004) The use of mass spectroscopy in genomics. *Biomol. Eng.* **21**: 1-13.

Metz, C., Wu, X. and Smith, S.O. (1994) Ramped-Amplitude Cross-Polarization in Magic-Angle-Spinning NMR. *J. Magn. Reson. Ser. A.* **110**: 219.

Middleton, D.A., Reid, D.G. and Watts, A. (2004) Combined quantitative and mechanistic study of

- drug-membrane interactions using a novel H-2 NMR approach. *J. Pharmaceutical Sci.* **93**: 507-514.
- Middleton, D.A., Rankin, S., Esmann, M. and Watts, A. (2000a) Structural insights into the binding of cardiac glycosides to the digitalis receptor revealed by solid-state NMR. *Proc. Natl. Acad. Sci. U.S.A.* **97**: 13602-13607.
- Middleton, D.A., Ahmed, Z., Glaubitz, C. and Watts, A. (2000b) REDOR NMR on a Hydrophobic Peptide in Oriented Membranes. *J. Magn. Reson.* **147**.
- Mierau, I. and Kleerebezem, M. (2005) 10 years of the nisin-controlled gene expression system (NICE) in *Lactococcus lactis*. *Appl. Microbiol. Biotechnol.* **68**: 705-717.
- Mierau, I., Olieman, K., Mond, J. and Smid, E.J. (2005) Optimization of the *Lactococcus lactis* nisin-controlled gene expression system NICE for industrial applications. *Microb. Cell Fact.* **4**: 16.
- Milett, F. and Raftery, M.A. (1972) A ¹⁹F nuclear magnetic resonance study of the binding of trifluoroacetylglucosamine oligomers to lysozyme. *Biochemistry.* **11**: 1639-1643.
- Millet, O., Muhandiram, D.R., Skrynnikov, N.R. and Kay, L.E. (2002) Deuterium spin probes of side-chain dynamics in proteins. 1. Measurement of five relaxation rates per deuteron in ¹³C-labeled and fractionally deuterated proteins in solution. *J. Am. Chem. Soc.* **124**: 6439-6448.
- Mitchell, B.A., Paulsen, I.T., Brown, M.H. and Skurray, R.A. (1999) Bioenergetics of the Staphylococcal multidrug export protein QacA. *J. Biol. Chem.* **274**: 3541-3548.
- Morgan, W.D., Kragt, A. and Feeney, J. (2000) Expression of deuterium-isotope labelled protein in the yeast *Pichia pastoris* for NMR studies. *J. Biomol. NMR.* **17**: 337-347.
- Muhandiram, D.R., Yamazaki, T., Sykes, B.D. and Kay, L.E. (1995) Measurements of ²H T₁ and T_{1ρ} relaxation times in uniformly ¹³C-labeled and fractionally ²H-labeled proteins in solution. *J. Am. Chem. Soc.* **117**: 11536-11544.
- Muhl, P., Likussar, W. and Schubert-Zsilavecz, M. (1996) Structure investigation and proton and carbon-13 assignments of digitonin and cholesterol using multidimensional NMR techniques. *Magn. Reson. Chem.* **34**: 137-142.
- Murakami, S., Nakasima, R., Yamashita, E. and Yamaguchi, A. (2002) Crystal structure of bacterial multidrug efflux transporter AcrB. *Nature.* **419**: 587-593.
- Muth, T.R. and Schuldiner, S. (2000) A membrane-embedded glutamate is required for ligand binding to the multidrug transporter EmrE. *EMBO J.* **19**: 234-240.

- Neyfakh, A.A. (2002) Mystery of multidrug transporters: the answer can be simple. *Mol. Microbiol.* **44**: 1123-1130.
- Nikaido, H. (1996) Multidrug efflux pumps of Gram-negative bacteria. *J. Bacteriol.* **178**: 5853-5859.
- Nikaido, H. (2001) Preventing drug access to targets: cell surface permeability barriers and active efflux in bacteria. *Sem. Cell Dev. Biol.* **12**: 215-223.
- Novak, L. and Loubiere, P. (2000) The metabolic network of *Lactococcus lactis*: Distribution of C-14-labeled substrates between catabolic and anabolic pathways. *J. Bacteriol.* **182**: 1136-1143.
- Novak, L., Cocaign-Bousquet, M., Lindley, N.D. and Loubiere, P. (1997) Metabolism and energetics of *Lactococcus lactis* during growth in complex or synthetic media. *Appl. Environ. Microbiol.* **63**: 2665-2670.
- Ojjima, I. (2005) Design, synthesis and structure-activity relationships of novel taxane-based multidrug resistance agents. *J. Med. Chem.* **48**: 2218-2228.
- Oloo, E.O. and Tieleman, D.P. (2004) Conformational transitions induced by the binding of MgATP to the vitamin B12 ABC-transporter BtuCD. *J. Biol. Chem.* **279** (43): 45013-9.
- Onishi Y., H.H., Nakata K., Oosumi K., Nagakura M., Tarui Sh., and Ishikawa T. (2003) High-speed screening and structure-activity relationship analysis for the substrate specificity of P-glycoprotein. *Chemi-Bio Informatics J.* **3**: 175-193.
- Opella, S.J. (1982) Solid-state NMR of biological systems. *Ann. Rev. Phys. Chem.* **33**: 53-562.
- Otten, D., Brown, M.F. and Beyer, K. (2000) Softening of membrane bilayers by detergents elucidated by Deuterium NMR spectroscopy. *J. Phys. Chem. B.* **104**: 12119-12129.
- Otto, R., ten Brink, B., Veldkamp, H. and Konings, W.N. (1983) The relation between growth rate and electrochemical proton gradient of *Streptococcus cremoris*. *FEMS Microbiol. Lett.* **16**: 69-74.
- Palmer, A.G. (1997) Probing molecular motion by NMR. *Curr. Opin. Struct. Biol.* **7**: 732-737.
- Palmer, A.G. (2004) NMR characterization of the dynamics of biomolecules. *Chem. Rev.* **104**: 3623-3640.
- Parker, M.A., King, V. and Howard, K.P. (2001) Nuclear magnetic resonance study of doxorubicin binding to cardiolipin containing magnetically oriented phospholipid bilayers. *Biochim. Biophys. Acta.* **1514**: 206-216.

Patching, S.G., Herbert, R.B., O'Reilly, J., Brough, A.R. and Henderson, P.J.F. (2004a) Low C-13-background for NMR-based studies of ligand binding using C-13-depleted glucose as carbon source for microbial growth: C-13-labeled glucose and C-13-forskolin binding to the galactose-H⁺ symport protein GalP in Escherichia coli. *J. Am. Chem. Soc.* **126**: 86-87.

Patching, S.G., Brough, A.R., Herbert, R.B., Rajakarier, J.A., Henderson, P.J.F. and Middleton, D.A. (2004b) Substrate affinities for membrane transport proteins determined by C-13 cross-polarization magic-angle spinning nuclear magnetic resonance spectroscopy. *J. Am. Chem. Soc.* **126**: 3072-3080.

Paternostre, M.T., Roux, M. and Rigaud, J.L. (1988) Mechanisms of Membrane-Protein Insertion into Liposomes During Reconstitution Procedures Involving the Use of Detergents .1. Solubilization of Large Unilamellar Liposomes (Prepared by Reverse-Phase Evaporation) by Triton X-100, Octyl Glucoside, and Sodium Cholate. *Biochemistry.* **27**: 2668-2677.

Paulsen, I.T. (2003) Multidrug efflux pumps and resistance: regulation and evolution. *Curr. Opin. Microbiol.* **6**: 446-451.

Paulsen, I.T., Sliwinski, M.K. and Saier, M.H. (1998) Microbial genome analyses: Global comparisons of transport capabilities based on phylogenies, bioenergetics and substrate specificities. *J. Mol. Biol.* **277**: 573-592.

Pawagi, A.B., Wang J., Silverman, M., Reithmeier, R.A. and Deber, C.M. (1994) Transmembrane aromatic amino acid distribution in P-glycoprotein. A functional role in broad substrate specificity. *J. Mol. Biol.* **235**: 554-564.

Peer, M., Csaszar, E., Vorlauffer, E., Kopp, S. and Chiba, P. (2005) Photoaffinity labelling of P-glycoprotein. *Mini-Rev. Med. Chem.* **5**: 165-172.

Peersen, O.B., Wu, X., Kustanovich, I. and Smith, S.O. (1993) Variable-amplitude cross-polarization MAS NMR. *J. Magn. Reson. A.* **104**: 334.

Peng, X.D., Jonas, A. and Jonas, J. (1995) One-Dimensional and 2-Dimensional H-1-Nmr Studies of Pressure and Tetracaine Effects on Sonicated Phospholipid-Vesicles. *Chem. Phys. Lipids.* **75**: 59-69.

Phan-Thanh, L. and Gormon, T. (1997) A chemilal defined medium for the optimal culture of Listeria. *J. Food Microbiol.* **35**: 91-95.

Pinciroli, V., Rizzo, V., Angelucci, F., Tato, M. and Vigevani, A. (1997) 1H NMR characterization of mrthacrylamide polymer comjugates with the anti-cancer derug doxorubicin. *Magn. Reson. Chem.* **35**: 2-8.

Pleban, K., Macchiarulo, A., Costantino, G., Pellicciari, R., Chiba, P. and Ecker, G.F. (2004) Homology model of the multidrug transporter LmrA from *Lactococcus lactis*. *Bioorg. Med. Chem. Lett.* **14**: 5823-5826.

Pleban, K., Kopp, S., Csaszar, E., Peer, M., Hrebicek, T., Rizzi, A., *et al* (2005b) P-glycoprotein substrate binding domains are located at the transmembrane domain/transmembrane domain interface: a combined photoaffinity labelling-protein homology modeling approach. *Mol. Pharmacol.* **67**: 365-374.

Poelarends, G.J. and Konings, W.N. (2002) The transmembrane domains of the ABC multidrug transporter LmrA form a cytoplasmic exposed, aqueous chamber within the membrane. *J. Biol. Chem.* **277**: 42891-42898.

Poelarends, G.J., Mazurkiewicz, P., Putman, M., Cool, R.H., van Veen, H.W. and Konings, W.N. (2000) An ABC-type multidrug transporter of *Lactococcus lactis* possesses an exceptionally broad substrate specificity. *Drug Res. Updates.* **3**: 330-334.

Poole, K. (2000) Efflux-mediated resistance to fluoroquinolones in Gram-positive bacteria and the Mycobacteria. *Antimicrob. Agents Chemother.* **44**: 2595-2599.

Poolman, B. and Konings, W.N. (1988) Relation of growth of *Streptococcus lactis* and *Streptococcus cremoris* to Amino acids transport. *J. Appl. Bacteriol.* **170**: 700-707.

Porcar, I., Codoner, A., Gomez, C.M., Abad, C. and Campos, A. (2003) Interaction of quinine with model lipid membranes of different compositions. *J. Pharm. Sci.* **92**: 45-57.

Prosser, R.S. and Davis, J.H. (1994b) Dynamics of an Integral Membrane Peptide - a Deuterium NMR Relaxation Study of Gramicidin. *Biophys. J.* **66**: 1429-1440.

Prosser, R.S., Davis, J.H., Mayer, C., Weisz, K. and Kothe, G. (1992) Deuterium NMR Relaxation Studies of Peptide-Lipid Interactions. *Biochemistry.* **31**: 9355-9363.

Putman, M., van Veen, H., Poolman, B. and Konings, W.N. (1999) Restrictive use of detergents in the functional reconstitution of the secondary multidrug transporter LmrP. *Biochemistry.* **38**: 1002-1008.

Putman, M., van Veen, H.W., Degener, J.E. and Konings, W.N. (2000) Antibiotic resistance: era of the multidrug pump. *Mol. Microbiol.* **36**: 772-773.

Qu, Q. and Sharom, F.J. (2002) Proximity of bound Hoechst 33342 to the ATPase catalytic sites places the drug binding site of P-glycoprotein within the cytoplasmic membrane leaflet. *Biochemistry.* **41**: 4744-4752.

- Qu, Q., Chu, J.W.K. and Sharom, F.J. (2003) Transition state P-glycoprotein binds drugs and modulators with unchanged affinity, suggesting a concerted transport mechanism. *Biochemistry*. **42**: 1345-1353.
- Raleigh, D.P., Levitt, M. and Griffin, R.G. (1988) Rotational Resonance in Solid-State NMR. *Chem. Phys. Letters*. **146**: 71.
- Ramachandra, M., Ambudkar, S.V., Chen, D., Hrycyna, C.A., Dey, S., Gottesman, M.M. and Pastan, I. (1998) Human P-glycoprotein exhibits reduced affinity for substrates during a catalytic transition state. *Biochemistry*. **37**: 5010-5019.
- Ravault, S., Soubias, O., Saurel, O., Thomas, A., Brasseur, R. and Milon, A. (2005) Fusogenic Alzheimer's fragment Ab (29-42) in interaction with lipid bilayers: secondary structure, dynamics, and specific interaction with phosphatidyl ethanolamine polar heads as revealed by solid-state NMR. *Protein Sci*. **14**: 1181-1189.
- Reyes, C.L. and Chang, G. (2005) Structure of the ABC transporter MsbA in complex with ADP-vanadate and lipopolysaccharide. *Science*. **308**: 1028-1031.
- Rhim, W.-K., Elleman, D.D. and Vaughan, R.W. (1973) Analysis of Multiple Pulse NMR in Solids. *J. Chem. Phys.* **59**: 3740.
- Rigaud, J.L. and Levy, D. (2003) Reconstitution of membrane proteins into liposomes. In *Liposomes, Pt B*, pp. 65-86.
- Roberts, M.C. (1996) Tetracycline resistance determinants: mechanisms of action, regulation of expression, genetic mobility, and distribution. *FEMS Microbiol. Rev.* **19**: 1-24.
- Rogl, H., Kosemund, K., Kulbrandt, W. and I, C. (1998) Refolding of Escherichia coli produced membrane protein inclusion bodies immobilised by nickel chelating chromatography. *FEBS Lett.* **432**: 21-26.
- Romsicki, Y. and Sharom, F.J. (1999) The membrane lipid environment modulates drug interactions with the P-glycoprotein multidrug transporter. *Biochemistry*. **38**: 6887-6896.
- Rosenberg, M.F., Callaghan, R., Ford, R.C. and Higgins, C.F. (1997) Structure of the multidrug resistance P-glycoprotein to 2.5 nm resolution determined by electron microscopy and image analysis. *J. Biol. Chem.* **272**: 10685-10694.
- Rosenberg, M.F., Kamis, A.B., Callaghan, R., Higgins, C.F. and Ford, R.C. (2003) Three-dimensional structures of the mammalian multidrug resistance P-glycoprotein demonstrate major conformational

- changes in the transmembrane domains upon nucleotide binding. *J. Biol. Chem.* **278**: 8294-8299.
- Rosenberg, M.F., Kamis, A.B., Aleksandrov, L.A., Ford, R.C. and Riordan, J.R. (2004) Purification and crystallization of the cystic fibrosis transmembrane conductance regulator (CFTR). *J. Biol. Chem.* **279**: 39051-39057.
- Rosenberg, M.F., Callaghan, R., Modok, S., Higgins, C.F. and Ford, R.C. (2005) Three-dimensional structure of P-glycoprotein. *J. Biol. Chem.* **280**: 2857-2862.
- Rosenberg, M.F., Mao, Q., Holzenburg, A., Ford, R.C., Deeley, R.G. and Cole, S.P. (2001a) The structure of the multidrug resistance protein 1 (MRP1/ABCC1). *J. Biol. Chem.* **276**: 16076-16082.
- Rosenberg, M.F., Velarde, G., Ford, R.C., Martin, C., Berridge, G., Kerr, I.D., *et al* (2001b) Repacking of the transmembrane domains of P-glycoprotein during the transport ATPase cycle. *EMBO J.* **20**: 5615-5625.
- Rotem, D. and Schuldiner, S. (2004) EmrE, a multidrug transporter from *Escherichia coli*, transports monovalent and divalent substrates with the same stoichiometry. *J. Biol. Chem.* **279**: 48787-48793.
- Rozovsky, S. and McDermott, A.E. (2001) The time scale of the catalytic loop motion in triosephosphate isomerase. *J. Mol. Biol.* **310**: 259-270.
- Sanders, C.R. and Oxenoid, K. (2000) Customizing model membranes and samples for NMR spectroscopic studies of complex membrane proteins. *Biochim. Biophys. Acta.* **1508**: 129-145.
- Santos, J.S., Lee, D.K. and Ramamoorthy, A. (2004) Effects of antidepressants on the conformation of phospholipid headgroups studied by solid-state NMR. *Magn. Reson. Chem.* **42**: 105-114.
- Scheidt, H.A., Pampel, A., Nissler, L., Gebhardt, R. and Huster, D. (2004) Investigation of the membrane localization and distribution of flavonoids by high-resolution magic angle spinning NMR spectroscopy. *Biochim. Biophys. Acta.* **1663**: 97-107.
- Schmitt, L. (2002) The first view of an ABC transporter: the x-ray crystal structure of MsbA from *E. coli*. *Chembiochem.* **3**: 61-165.
- Schmitt, L. and Tampe, R. (2002) Structure and mechanism of ABC transporters. *Curr. Opin. Struct. Biol.* **12**: 754-760.
- Schmitt, L., Benabdelhak, H., Blight, M.A., Holland, I.B. and Stubbs, M.T. (2003) Crystal structure of the nucleotide-binding domain of the ABC-transporter haemolysin B: identification of a variable region within ABC helical domain. *J. Mol. Biol.* **330**: 333-342.

- Scrutton, N.S. and Raine, A.R.C. (1996) Cation- π bonding and amino-aromatic interactions in the biomolecular recognition of substituted ammonium ligands. *Biochem. J.* **319**.
- Seelig, A. (1998) A general pattern for substrate recognition by P-glycoprotein. *Eur. J. Biochem.* **251**: 252-261.
- Seelig, A. and Landwojtowicz, E. (2000) Structure-activity relationship of P-glycoprotein substrates and modifiers. *Eur. J. Pharm. Sci.* **12**: 31-40.
- Shapiro, A.B. and Ling, V. (1995) Reconstitution of Drug Transport by Purified P-Glycoprotein. *J. Biol. Chem.* **270**: 16167-16175.
- Shapiro, A.B. and Ling, V. (1998) Transport of LDS-751 from the cytoplasmic leaflet of the plasma membrane by the rhodamine-123-selective site of P-glycoprotein. *Eur. J. Biochem.* **254**: 181-188.
- Sharom, F.J., Yu, X.H., Didiodato, G. and Chu, J.W.K. (1996) Synthetic hydrophobic peptides are substrates for P-glycoprotein and stimulate drug transport. *Biochem. J.* **320**: 421-428.
- Sharom, F.J., Lu, P., Liu, R. and Yu, X.H. (1998) Linear and cyclic peptides as substrates and modulators of P-glycoprotein: peptide binding and effects on drug transport and accumulation. *Biochem. J.* **333**: 621-630.
- Sharom, F.J., Liu, R.H., Romsicki, Y. and Lu, P.H. (1999a) Insights into the structure and substrate interactions of the P-glycoprotein multidrug transporter from spectroscopic studies. *Biochim. Biophys. Acta.* **1461**: 327-345.
- Sharom, F.J., Liu, R.H., Qu, Q. and Romsicki, Y. (2001) Exploring the structure and function of the P-glycoprotein multidrug transporter using fluorescence spectroscopic tools. *Sem. Cell Dev. Biol.* **12**: 257-265.
- Sharom, F.J., Yu, X.H., Lu, P.H., Liu, R.H., Chu, J.W.K., Szabo, K., *et al* (1999b) Interaction of the P-glycoprotein multidrug transporter (MDR1) with high affinity peptide chemosensitizers in isolated membranes, reconstituted systems, and intact cells. *Biochem. Pharmacol.* **58**: 571-586.
- Shilling, R., Federici, L., Walas, F., Venter, H., Velamakanni, S., Woebking, B., *et al* (2005) A critical role of a carboxylate in proton conduction by the ATP-binding cassette multidrug transporter LmrA. *FASEB J.* **19**.
- Shilling, R.A., Balakrishnan, L., Shahi, S., Venter, H. and van Veen, H.W. (2003) A new dimer interface for an ABC transporter. *Int. J. Antimicrobial Agents.* **22**: 200-204.

Siminovitch, D.J. (1998) Solid-state NMR studies of proteins: the view from static ^2H NMR experiments. *Biochem. Cell Biol.* **76**: 411-422.

Smith, P.C., Karpowich, N., Millen, L., Moody, J.E., Rosen, J., Thomas, P.J. and Hunt, J.F. (2002) ATP binding to the motor domain from an ABC transporter drives formation of a nucleotide sandwich dimer. *Mol Cell.* **10**: 139-149.

Smith, R.L. and Oldfield, E. (1984) Dynamic structure of membranes by deuterium NMR. *Science.* **225**: 280-288.

Sparman, T. and Westlund, P.-O. (2003) An NMR line shape and relaxation analysis of heavy water powder spectra of the La, Lb and Pb phases in the DPPC/water system. *Phys. Chem.* **5**: 2114-2121.

Speelmans, G., Staffhorst, R.W.H.M., Dekruiff, B. and Dewolf, F.A. (1994) Transport Studies of Doxorubicin in Model Membranes Indicate a Difference in Passive Diffusion across and Binding at the Outer and Inner Leaflets of the Plasma-Membrane. *Biochemistry.* **33**: 13761-13768.

Spooner, P., Rutherford, N., Watts, A. and Henderson, P.J.F. (1994) NMR observation of substrate in the binding site of an active sugar- H^+ symport protein in native membranes. *Proc. Natl. Acad. Sci. U.S.A.* **91**: 3877-3881.

Spooner, P., Veenhoff, L.M., Watts, A. and Poolman, B. (1999) Structural information on a membrane transport protein from nuclear magnetic resonance spectroscopy using sequence-selective nitroxide labelling. *Biochemistry.* **38**: 9634-9639.

Spooner, P., O'Reilly, J., Homans, S.W., Rutherford, N.G., Henderson, P.J.F. and Watts, A. (1998) Weak substrate binding to transport proteins studied by NMR. *Biophys. J.* **75**: 2794-2800.

Stejskal, E.O., Schaefer, J. and Waugh, J.S. (1977) Magic-Angle Spinning and Polarization Transfer in Proton-Enhanced Nmr. *J. Magn. Reson.* **28**: 105-112.

Stopar, D., Strancar, J., Spruijt, R.B. and Hemminga, M.A. (2005) Exploring the local conformational space of a membrane protein by site-directed spin labelling. *J. Chem. Inf. Model.* **45**: 1621-1627.

Straus, S.K. (2004) Recent developments in solid-state magic-angle spinning, nuclear magnetic resonance of fully and significantly isotopically labelled peptides and proteins. *Philos. Trans. R. Soc. London Ser. B.* **359**: 997-1008.

Stryer, L. (1988) *Biochemistry. 3rd edn. New York: W.H. Freeman and company.*

Subczynski, W.K., Wisniewska, A., Yin, J.-J., Hyde, J.S. and Kusumi, A. (1994) Hydrophobic

barriers of lipid bilayer membranes formed by reduction of water penetration by alkyl chain saturation and cholesterol. *Biochemistry*. **33**: 7670-7681.

Suwalsky, M., Villena, F., Aguilar, F. and Sotomayor, C.P. (1996) Interaction of penicillin G with the human erythrocyte membrane and models. *Z. Naturforsch.* 51c: 243-248.

Takegoshi, K., Mizokami, J. and Terao, T. (2001) ¹H decoupling with third averaging in solid NMR. *Chem. Phys. Lett.* 341: 540-544.

Tanizaki, S. and Feig, M. (2006) Molecular dynamics simulations of large integral membrane proteins with an implicit membrane model. *J. Phys. Chem. B*. **110**: 548-556.

Thomas, M.R. and Boxer, S.G. (2001) ¹⁹F NMR of trifluoroacetyl-labeled cysteine mutants of myoglobin: structural probes of nitric oxide bound to the H93G cavity mutant. *Biochemistry*. **40**: 8588-8596.

Tiburru, E.K., Karp, E.S., Dave, P.C., Damodaran, K. and Lorigan, G.A. (2004) Investigating the dynamic properties of the transmembrane segment of phospholamban incorporated into phospholipid bilayers utilizing ²H and ¹⁵N solid-state NMR spectroscopy. *Biochemistry*. **43**: 13899-13909.

Torchia, D.A. (1984) Solid-state NMR studies of protein internal dynamic. *Ann. Rev. Biophys. Bioeng.* **13**: 125-144.

Tung, J.C., Gonzales, A.J., Sadowsky, J.D. and O'Leary, D.J. (2000) On the ¹H NMR chemical shift assignments for ampicillin. *Magn. Reson. Chem.* **38**: 126-128.

Tycko, R. and Dabbagh, G. (1990) Measurement of Nuclear Magnetic Dipole-Dipole Couplings in Magic Angle Spinning NMR. *Chem. Phys. Lett.* **173**: 461-465.

Ueda, K., Taguchi, Y. and Morishima, M. (1997) How does P-glycoprotein recognize its substrates? *Cancer Biol.* **8**: 151-159.

Van Bambeke, F., Balzi, E. and Tulkens, P.M. (2000) Antibiotic efflux pumps - Commentary. *Biochem. Pharmacol.* **60**: 457-470.

Van Bambeke, F., Glupczynski, Y., Plesiat, P., Pechere, J.C. and Tulkens, P.M. (2003) Antibiotics efflux pumps in prokaryotic cells: occurrence, impact on resistance and strategies for the future of antimicrobial therapy. *J. Antimicrob. Chemother.* **51**: 1055-1065.

van Berg van Saparoeva, H.B., Lubelski, J., van Merkerk, R., Mazurkiewicz, P. and Driessen, A.J.M. (2005) Proton motive force-dependent Hoechst 33342 transport by the ABC transporter LmrA of

Lactococcus lactis. *Biochemistry*. **44**: 16931-16938.

van der Does, C. and Tampe, R. (2004) How do ABC transporter drive transport? *Biol. Chem.* **385**: 927-933.

van Niel, E.W.J. and Hahn-Hagerdal, B. (1999) Nutrient requirements of lactococci in defined growth media. *Appl. Microbiol Biotechnol.* **52**: 617-627.

van Niel, E.W.J., Hofvendahl, K. and Hahn-Hagerdal, B. (2002) Formation and conversion of oxygen metabolites by *Lactococcus lactis* subsp *lactis* ATCC 19435 under different growth conditions. *Appl. Environ. Microbiol.* **68**: 4350-4356.

van Veen, H.W. (2001) Towards the molecular mechanism of prokaryotic and eukaryotic multidrug transporters. *Sem. Cell Dev. Biol.* **12**: 239-245.

van Veen, H.W. and Konings, W.N. (1997) Multidrug transporters from bacteria to man: similarities in structure and function. *Sem. Cancer Biol.* **8**: 183-191.

van Veen, H.W., Higgins, C.F. and Konings, W.N. (2001) Multidrug transport by ATP binding cassette transporters: a proposed two-cylinder engine mechanism. *Res. Microbiol.* **152**: 365-374.

van Veen, H.W., Putman, M., Heijne, R., Margolles, A. and Konings, W. (1998a) Basic mechanisms of antibiotic resistance: molecular properties of multidrug transporters. *MJM Focus.* **4**: 56-66.

van Veen, H.W., Margolles, A., Muller, M., Higgins, C.F. and Konings, W.N. (2000a) The homodimeric ATP-binding cassette transporter LmrA mediates multidrug transport by an alternating two-site (two-cylinder engine) mechanism. *EMBO J.* **19**: 2503-2514.

van Veen, H.W., Putman, M., Margolles, A., Sakamoto, K. and Konings, W.N. (2000b) Molecular pharmacological characterization of two multidrug transporters in *Lactococcus lactis*. *Pharmacol. Therapeutics.* **85**: 245-249.

van Veen, H.W., Callaghan, R., Soceneantu, L., Sardini, A., Konings, W.N. and Higgins, C.F. (1998b) A bacterial antibiotic-resistance gene that complements the human multidrug-resistance P-glycoprotein gene. *Nature.* **391**: 291-295.

van Veen, H.W., Venema, K., Bolhuis, H., Oussenko, I., Kok, J., Poolman, B., *et al* (1996) Multidrug resistance mediated by a bacterial homolog of the human multidrug transporter MDR1. *Proc. Natl. Acad. Sci. U.S.A.* **93**: 10668-10672.

Van't Land, C.W., Mocek, U. and Floss, H.G. (1993) Biosynthesis of the phenazine antibiotics, the

- Saphenamycins and Esmeraldins, in *Streptomyces antibioticus*. *J. Org. Chem.* **58**: 6576-6582.
- Varma, M.V.S., Ashokraj, Y., Dey, C.S. and Panchagnula, R. (2003) P-glycoprotein inhibitors and their screening: a perspective from bioavailability enhancement. *Pharmacol. Res.* **48**: 347-359.
- Venter, H., Ashcrofr, A.E., Keen, J.N., Henderson, P.J.F. and Herbert, R.B. (2002) Molecular dissection of membrane-transport proteins: mass spectrometry and sequence determination of the galactose-H⁺ symport protein, GalP, of *Escheriachia coli* and quantitative assay of the incorporation of [ring-213C] histidine and 15NH₃. *Biochem. J.* **363**: 243-252.
- Venter, H., Shilling, R.A., Velamakanni, S., Balakrishnan, L. and van Veen, H.W. (2003) An ABC transporter with a secondary-active multidrug translocator domain. *Nature.* **426**: 866-870.
- Venter, H., Shahi, S., Balakrishnan, L., Velamakanni, S., Bapha, A., Woebking, B. and W., v.V.H. (2005) Similarities between ATP-dependent and ion-coupled multidrug transporters. *Biochem. Soc. Trans.* **33**: 1008-1011.
- Vergani, P., Lockless, S.W. and Gadsby, D.C. (2005) CFTR chanel opening by ATP-driven tight dimerization of its nucleotide-binding domains. *Nature.* **433**: 876-880.
- Vigano, C., Grimard, V., Margolles, A., Goormaghtigh, E., van Veen, H.W., Konings, W.N. and Ruyschaert, J.M. (2002) A new experimental approach to detect long-range conformational changes transmitted between the membrane and cytosolic domains of LmrA, a bacterial multidrug transporter. *FEBS Lett.* **530**: 197-203.
- Vinogradova, O., Sonnichsen, F.D. and Sanders, C.R. (1998) On choosing a detergent for solution NMR studies of membrane proteins. *J. Biomol. NMR.* **4**: 381-386.
- von Heijne, G. (1992) Membrane protein structure prediction. Hydrophobicity analysis and the positive-inside rule. *J. Mol. Biol.* **225**: 487-494.
- Walsh, C. (2003) Antibiotics: actions, origins, resistance. *ASM Press, Washington, D.C.*
- Wang, E.-J., Casciano, C.N., Clement, R.P. and Johnson, W.W. (2000) In Vitro Flow Cytometry Method to Quantitatively Assess Inhibitors of P-Glycoprotein. *Drug Matab. Dispos.* **28**: 522-528.
- Watts, A., Spooner, P., Middleton, D., Henderson, P.J.F., O'Reilly, W.J. and Rutherford, N. (1998) Probing the structure and mechanism of binding of an inhibitor to a P-type-ATPase and of sugars during translocation by expressed transporters, using solid state MAS NMR. *Biophys. J.* **74**: A130-A130.

- White, G.F., Racher, K.I., Lipski, A., Hallett, F.R. and Wood, J.M. (2000) Physical properties of liposomes and proteoliposomes prepared from *Escherichia coli* polar lipids. *Biochim. Biophys Acta*. **1468**: 175-186.
- Wiedmer, S.K., Hautala, J., Holopainen, J.M., Kinnunen, P.K.J. and Riekkola, M.L. (2001) Study on liposomes by capillary electrophoresis. *Electrophoresis*. **22**: 1305-1313.
- Wiese, M. and Pajeva, I.K. (2001) Structure-activity relationships of multidrug resistance reversers. *Curr. Med. Chem.* **8**: 685-713.
- Williamson, P.T.F., Watts, J.A., Addona, G.H., Miller, K.W. and Watts, A. (2001) Dynamics and orientation of N⁺(CD3)3-bromoacetylcholine bound to its binding site on the nicotinic acetylcholine receptor. *Proc. Natl. Acad. Sci. U.S.A.* **98**: 2346-2351.
- Wüthrich, K. (2002) NMR studies of structure and function of biological macromolecules. *Nobel Lecture*.
- Wyss, D.F., McCoy, M.A. and Senior, M.M. (2002) NMR-based approaches for lead discovery. *Curr. Opin. Drug Discov.* **5**: 630-647.
- Xu, Y., Seto, T., Tang, P. and Firestone, L. (2000) NMR study of volatile anesthetic binding to nicotinic acetylcholine receptors. *Biophys. J.* **78**: 746-751.
- Yau, W.M., Wimley, W.C., Gawrisch, K. and White, S.H. (1998) The preference of tryptophan for membrane interfaces. *Biochemistry*. **37**: 14713-14718.
- Yerushalmi, H. and Schuldiner, A. (2000) A model for coupling of H⁺ and substrate fluxes based on 'time-sharing' of a common binding site. *Biochemistry*. **39**: 14711-14719.
- Yokono, S., Ogi, K., Miura, S. and Ueda, I. (1989) 400 Mhz Two-Dimensional Nuclear Overhauser Spectroscopy on Anesthetic Interaction with Lipid Bilayer. *Biochim. Biophys. Acta*. **982**: 300-302.
- Yokota, A., Veenstra, M., Kurdi, P., van Veen, H.W. and Konings, W. (2000) Cholera resistance in *Lactococcus lactis* is mediated by an ATP-dependent multispecific organic anion transporter. *J. Bacteriol.* **182**: 5196-5201.
- Yu, Y. and Fung, B.M. (1998) An efficient broadband decoupling sequence for liquid crystals. *J. Magn. Reson.* **130**: 317.
- Yuan, Y.R., Blecker, S., Martsinkevich, O., Millen, L., Thomas, P.J. and Hunt, J.F. (2001) The crystal structure of the MJ0796 ATP-binding cassette. Implications for the structural consequences of ATP

hydrolysis in the active site of an ABC transporter. *J. Biol. Chem.* **276**: 32313-32321.

Zaitseva, J., Jenewein, S., Wiedenmann, A., Benabdelhak, H., Holland, I.B. and Schmitt, L. (2005) Functional characterization and ATP-induced dimerization of the isolated ABC-domain of the Haemolysin B transporter. *Biochemistry.* **44**: 9680-9690.

Zech, S.G., Olejniczak, E., Hajduk, P., Mack, J. and McDermott, A.E. (2004) Characterization of protein-ligand interactions by high-resolution solid-state NMR spectroscopy. *J. Am. Chem. Soc.* **126**: 13948-13953.

Zgurskaya, H.I. and Nikaido, H. (2000) Multidrug resistant mechanisms: drug efflux across two membranes. *Mol. Microbiol.* **37**: 219-225.

Zheleznova, E.E., Markham, P.N., Neyfakh, A.A. and Brennan, R.G. (1999) Structural basis of multidrug recognition by BmrR, a transcriptional activator of a multidrug transporter. *Cell.* **96**: 353-362.

Zheleznova, E.E., Markham, P., Edgar, R., Bibi, E., Neyfakh, A.A. and Brennan, R.G. (2000) A structure-based mechanism for drug binding by multidrug transporters. *Trends Bioch. Sci.* **25**: 39-43.

Zolek, T., Paradowska, K., Krajewska, D., Rozanski, A. and Wawer, I. (2003) H-1, C-13 MAS NMR and GIAO-CPHF calculations of chloramphenicol, thiamphenicol and their pyrrole analogues. *J. Mol. Struct.* **646**: 141-149.

Zusammenfassung

Festkörper NMR Experimente an dem ABC Transporter LmrA

Multidrug Resistenz ist ein wachsendes Problem bei einer Anzahl von infektiösen Erkrankungen und Krebs. Das Phänomen der Multidrug Resistenz (MDR) basiert auf dem synergetischen Zusammenspiel von verschiedenen Mechanismen; Proteindeaktivierung, Proteinveränderung, Prevention von Wirkstoffinflux sowie aktiver Ausstoss des Wirkstoffes aus der Zelle. Dieser zuletzt genannte Mechanismus wird durch die Überexpression von Multidrug Effluxpumpe bewirkt. Die zuerst entdeckte und bis heute am besten charakterisierte Multidrug Effluxpumpe ist der menschliche MDR Transporter P-glycoprotein (Ambudkar *et al.*, 2003). Es ist ein Mitglied der Familie der ATP Bindekassetten (ABC) Superfamilie und fungiert als aktiver Transporter für eine Reihe von Antitumor Wirkstoffen unter Verwendung der Energie der ATP Hydrolyse (Higgins, 1986b).

ABC Transporter haben vier Hauptdomänen. Zwei Transmembrandomänen (TMD) jede bestehend aus multiplen membranspannenden α -Helices die zusammen den Substratkanal durch die Membran formen. Zwei Nukleotidbindedomänen (NBD) formen die ATP Bindetasche und koppeln Konformationsänderungen, die von ATP-Bindung, -Hydrolyse und ADP-Abgabe hervorgerufen werden, an den Substrattransportprozess. Diese vier Domänen sind entweder als separate Polypeptide kodiert oder als Multidomänenprotein fusioniert (Higgins, 1986b).

Die ABC Transporterfamilie ist gross und vielseitig. Die Gemeinsamkeit der Familie beruht auf den streng konservierten Motive der ABC-Kassetten, die sowohl in der Bindung als auch in der Hydrolyse von ATP involviert sind (Geourjon *et al.*, 2001).

Die konservierten Motive sind P-Schleife oder Walker A Motiv, Walker B Motiv, ein Glutamat in der Q-Schleife sowie ein Histidine in der Schalterregion.

Zusätzlich besitzen ABC Kassetten grundsätzlich eine D-Schleife mit (..LSGG..), die auch als ABC – Signatursequenz bezeichnet wird (Ambudkar *et al.*, 1999).

Membranproteine sind äußerst schwierig aufzureinigen und zu kristallisieren. Trotzdem gab es erhebliche Fortschritte in der Strukturanalyse von ABC Transportern. In den letzten fünf Jahren

wurden mehrere ABC Transporter Strukturen von MsbA (Reyes and Chang, 2005; Chang, 2003a; Chang and Roth, 2001) und die Struktur von BtuCD aus *E. coli* (Locher et al., 2002) gelöst. Der Mechanismus von ABC Transportern ist trotz einer Vielzahl von ausführlichen Untersuchungen biochemischer und struktureller Natur immernoch ungeklärt. Aufgrund der Ähnlichkeiten zwischen den NBDs verschiedener Transporter wird allgemein angenommen, dass derselbe Mechanismus zum Substrattransport genutzt wird (van der Does and Tampe, 2004). Unser Verständnis des Mechanismus der ABC Transporter beruht auf PGP Strukturen mit geringer Auflösung in verschiedenen Konformationen, unterstützt von biochemischen Daten. Diese Daten zeigen, dass die Hauptkonformationsänderung der TMD bei der Bindung des ATP stattfindet, sich dabei die Affinität für Wirkstoffe reduziert und eine zentrale Pore geöffnet wird. Diese Konformationsänderungen können möglicherweise das Eintreten von Wirkstoffen von der Lipidmembran in die wassergefüllte Pore des Transporters erleichtern (Rosenberg *et al.*, 2003; Rosenberg *et al.*, 2001b).

Obwohl eine grosse Menge an strukturellen und funktionellen Daten in Bezug auf verschiedene Aspekte der ABC MDR Transporter im Allgemeinen und PGP im Besonderen existieren, gibt es noch viele offene Fragen.

Ein Teil dieser offenen Fragen sind 1) wie das Substrat an das Protein gebunden wird, 2) wieviele ATP Moleküle pro Substrattransport hydrolysiert werden, 3) wieviele Konformationsänderungen von NBD auf TMD übertragen und umgekehrt werden, 4) wie der Transportzyklus abläuft, 5) wie der Transportzyklus reguliert wird. Kristallstrukturen von ABC MDR Transportern in offener und geschlossener Konformation, sowie mit und ohne gebundenem Substrat müssen noch gelöst werden.

Wie schon erwähnt ist einer der am besten charakterisierten MDR ABC Transporter sicherlich P-glycoprotein und als solches wird es als Modellprotein für die ganze ABC MDR Familie angesehen. Das strukturell und funktional ähnlichste Protein in Bakterien ist LmrA aus *Lactococcus lactis*.

Motivation

Es ist oft schwierig mit Proteinen aus Säugetieren zu arbeiten und diese in ausreichender Menge nicht nur für Kristallisationsansätze sondern auch für biochemische Versuche zu produzieren. Daher ist LmrA ein praktisches Modellsystem für strukturelle und funktionale Analysen.

Die Hauptziele dieser Arbeit sind die Etablierung einer selektiven Isotopenmarkierungsmethode für

LmrA in *Lactococcus lactis*, Optimierung von LmrA für Festkörper NMR und erste Festkörper NMR Experimente, die die Substratbindung und den katalytischen Zyklus von LmrA untersuchen sollen.

Lange Zeit wurde Festkörper NMR in den Biowissenschaften fast ausschliesslich für die Untersuchung kleiner Moleküle genutzt. Nun konnte gezeigt werden, dass Festkörper NMR auch für Struktur- und Funktionsuntersuchungen grosser Membranproteine und deren Liganden geeignet ist. Jedoch wurde nach unserem Wissen bis jetzt weder ein ABC Transporter aminosäureselektiv mit Isotopen markiert noch ein kompletter ABC Transporter mit Hilfe von NMR untersucht. Für Festkörperexperimente an Membranproteinen müssen diese aufgereinigt werden und hochkonzentriert in Lipide rekonstituiert werden. Weiterhin müssen das Protein oder ein Ligand isotopenmarkiert werden. Daher wurden grosse Mengen an Protein hergestellt, in hoher Konzentration rekonstituiert und in dieser Form auch auf Funktionalität untersucht.

Kapitel 1: Einleitung

Kapitel 1 gibt einen Literaturüberblick. Es beginnt mit einer Erläuterung des Phänomens der Multiwirkstoff-Resistenz und Multidrug Transportern. Im zweiten Teil werden MDR ABC Transporter, insbesondere P-glycoprotein und LmrA sowie deren Funktionsweise besprochen. Der dritte Teil der Einleitung führt allgemein in die Festkörper NMR ein und zeigt Anwendungen für membranständige Transportproteine auf.

Kapitel 2: Entwicklung eines Definierten Mediums für Isotopenmarkierung von LmrA in *Lactococcus lactis*.

Kapitel 2 dieser Dissertation beschreibt die Etablierung einer kosteneffizienten aminosäureselektiven Methode der Isotopenmarkierung Methode für LmrA in *Lactococcus lactis*. Es wurde ein chemisch definiertes Medium zur selektiven Aminosäuremarkierung im ABC Transporter LmrA in *Lactococcus lactis* für NMR Anwendungen etabliert. Die ersten Spektren von inside-out Vesikeln mit circa 30% LmrA Überexpression und ^{13}C Glycin/Tyrosin Markierung bestätigen eine erfolgreiche Isotopenmarkierung. Die neue *Lactococcus lactis* Methode benötigt lediglich die Hälfte der ursprünglich benötigten Menge an isotopenmarkierten Aminosäuren. Die Funktionalität des, in diesem System überexprimierten LmrA wurde mit Hilfe von dem Hoechst-33342 Fluoreszenzassay bestätigt.

Kapitel 3: Herstellung von in verschiedenen Lipiden rekonstituierten LmrA für Festkörper NMR Versuche.

In Kapitel 3 dieser Dissertation wird gezeigt, dass LmrA in *E.coli* Lipiden und einer Reihe von künstlichen Lipiden (PE/PG, und PC/PG/cardiolipin) mit Hilfe der Detergenz basierten Liposomendestabilisationsmethode in einem hohen Protein:Lipid Verhältnis von 1:300 mol:mol rekonstituiert werden kann. Die Qualität der Rekonstitution und Proteinfunktionalität sind mit Hilfe von Gefrierbrüchelektronenmikroskopie, Sukrose Gradienten, Gel Filtration, ATPase Aktivitätsnachweis, und Hoechst 33342 Transport untersucht worden. Die ersten Spektren von ^{13}C und ^{15}N Tyrosin markiertem LmrA, welches in *E. coli* Liposomen rekonstituiert wurde, zeigte ein gutes Signal zu Rauschen Verhältnis und bestätigten, dass die Menge an selektiv isotopenmarkiertem LmrA ausreichend ist für Festkörper NMR Experimente. Zum ersten Mal sind jetzt ein 64kDa Membranprotein LmrA und damit die Klasse der ABC Transporter Superfamilie für NMR Analyse zugänglich gemacht worden. Nach Etablierung der Prozedur zur aminosäureselektiven Markierung von LmrA in *Lactococcus lactis* und Rekonstituierung in *E. coli* Lipiden in einem hohen Protein Lipid Verhältnis konnten wir nun Untersuchung zur Ligandenbindung und Dynamik des Proteins während der ATP Bindung und Hydrolyse durchführen.

Kapitel 4: Dynamik von LmrA untersucht mit Deuterium-Linienformanalyse und Relaxationsmessungen.

Unter Benutzung der in Kapitel 2 beschriebenen Methode für die selektive Aminosäurenmarkierung wurde LmrA mit deuteriertem Alanin hergestellt und in *E. coli* Liposomen rekonstituiert. Statische Deuterium NMR Experimente zeigen, dass die Dynamik von LmrA Domänen komplex ist. Während ein Teil der LmrA Domänen sehr immobil auf der NMR Zeitskala ist sind andere sehr dynamisch. Der Vergleich von Deuteriumlinienform in LmrA im Ruhezustand zu den AMP-PNP und ATP/ADP-Vanadate gebundenen Zuständen zeigt, dass das Protein in diesen Fällen unterschiedliche Bewegungsmodi besitzt. Im Zustand der ATP Bindung und Hydrolyse bleiben die TMD von LmrA während der NMR-Zeitskala relativ immobil. In der gleichen Zeit wird die Mobilität der NBDs durch ATP-Bindung und – Hydrolyse stark eingeschränkt.

Kapitel 5: Untersuchung der Ligandenbindung an LmrA durch Fluoreszenzspektroskopie und

Festkörper NMR

Experimente zum Quenching der intrinsischen Fluoreszenz von Tryptophan in LmrA wurden an in *E. coli* Lipiden rekonstituierten Proben vorgenommen. Zum ersten Mal konnte gezeigt werden, dass Norfloxacin ein antibakterieller Wirkstoff aus der Fluoroquinolon Familie ein Substrat von LmrA ist. Die Bindungskonstante von Norfloxacin, Vinblastine und TPP^+ wurden aus der konzentrationsabhängigen intrinsischen Tryptophan Fluoreszenz erhalten. Die Analyse der Fluoreszenz Emissionspektren von LmrA deutet auf eine relativ unpolare Umgebung für alle fünf LmrA Tryptophane hin. Zusätzlich wurde gezeigt, dass durch Substratbindung induzierte Konformationsänderungen von den Transmembran Helices zur zytosolischen Domäne übertragen werden. Jedoch erhöhen diese Konformationsänderungen der NBD nicht die Tryptophan Zugänglichkeit zur Lösung. Ausserdem kann das Quenching von der intrinsische Fluoreszenz von Tryptophan als Test für Substratbindung und Proteinaktivität benutzt werden.

Die Untersuchung von Ligand/Protein Wechselwirkungen an Protein rekonstituiert in Liposomen wird erschwert, da die Unterscheidung zwischen einer spezifischen Interaktion von Ligand/Protein, jedoch nicht einer spezifischen Interaktion von Ligand/Lipid erzielt werden muss. Am Beispiel von Norfloxacin und unter Nutzung der hohen ^{19}F Sensitivität und Dekonvolution konnte Ligandenbindung an LmrA beobachtet werden. Experimente, die die Bindung von TPP^+ an LmrA untersuchen sollten, erzielten zweideutige Ergebnisse. Jedoch konnte ein besseres Verständnis der Limitationen der Ligandenobservation mittels Festkörper NMR erreicht werden, und es zeigten sich Möglichkeiten diese zu überwinden. In der hier vorliegenden Studie wurde zum ersten Mal gezeigt, dass der Echtzeit Hoechst-33342 Transport von LmrA in inside-out Vesikeln mit Hilfe einer Leupeptin Zugabe unterbrochen werden kann. Ähnliche Experimente können für Hochdurchsatz Echtzeit Fluoreszenz Experimente zur Untersuchung einer Wirkstoffbibliothek nach potentiellen ABC Transporter Substraten und Modulatoren benutzt werden. Im Prinzip kann diese Echtzeit Methode auch mit anderen fluoreszierenden LmrA Substraten wie etwa Verapamil Derivaten benutzt werden. Die LmrA ATPase wurde bei verschiedenen Leupeptin Konzentrationen untersucht. Leupeptin erzeugt eine bimodale ATPase Modulation und suggeriert damit die Existenz von inhibierenden und stimulierenden Bindungstaschen in LmrA und Leupeptininteraktion mit beiden.

Kapitel 6: Die Lokalisierung von Multidrug Transporter Substraten in einer Modellmembran.

Die Lokalisierung von sieben P-glycoprotein und LmrA Substraten sowie zwei Modulatoren innerhalb einer neutral geladenen Phospholipidmembran wurde mit Hilfe von NOESY-MAS-NMR bestimmt. Obwohl strukturell divers zeigten alle Moleküle ein ähnliches Verhalten in der Membran. Die Moleküle sind überwiegend in der Membran/Lösungs Region zu finden und kaum im hydrophoben Kern der Membran. Zusätzlich zeigen sowohl Substrate als auch Modulatoren ein ähnliches Membranlokalisationsprofil. Es folgt, dass PGP Substrate und Modulatoren die Bindestellen von der Membran/Lösungsregion aus erreichen können. Dieses Ergebnis könnte relevant sein für das Verständnis von sekundären Multidrug Effluxpumpen. Diese zeigen eine partiell überlappende Substratspezifität und haben die Möglichkeit Substrate aus der Membran heraus zu binden, wie bereits für LmrP beschrieben (Bolhuis *et al.*, 1996a).

ERKLÄRUNG

Ich erkläre hiermit, dass ich mich bisher keiner Doktorprüfung unterzogen habe.

Frankfurt am Main, den.....

.....

(Unterschrift)

Eidesstattliche Versicherung

Ich erkläre hiermit an Eides Statt, dass ich die vorgelegte Dissertation über **``Solid-state NMR investigations of the ATP binding cassette multidrug transporter LmrA``** selbständig angefertigt und mich anderer Hilfsmittel als der in ihr angegebenen nicht bedient habe, insbesondere, dass aus Schriften Entlehnungen, soweit sie in der Dissertation nicht ausdrücklich als solche mit Angabe der betreffenden Schrift bezeichnet sind, nicht stattgefunden haben.

Frankfurt am Main, den.....

(Unterschrift)

Lebenslauf



Name Alena Siarheyeva
Geboren am 4 April 1979 in Minsk

Ausbildung

Schule 1986 -1996 Höhere Schule, Minsk,

Studium 1996 – 2001 Studium der Strahlenbiologie und Medicinische Ökologie
an der International Sakharov Ökologisch Universität, Minsk
Thema der Abschlussarbeit: “Investigation of pharmacokinetic and
pharmacodynamic properties of new bloodsubstitute solution Microdez”
Betreuer: Prof. V. N. Gapanovich

Promotion Februar 2003 – in der Abteilung von Prof. Dr. Glaubitz am der Institut
für Biophysikalische Chemie, Johann Wolfgang Goethe Universität in
Frankfurt am Main
Thema der Dissertation: “Solid-State NMR Investigations on the ATP
Binding Cassete Multidrug Transporter LmrA”
Betreuer: Prof. C. Glaubitz

Publications

Siarheyeva A., Lopez J., Glaubitz C.: The localization of P-glycoprotein substrates within model membranes, *Biochemistry*, in press 2006.

Siarheyeva A., Glaubitz C.: Deuterium solid-state NMR investigation of LmrA dynamic changes under ATP binding, in preparation.

Lorch M., Lehner I., Siarheyeva A., Basting D., Pflieger N., Manolikas T., Glaubitz C.: NMR and fluorescence spectroscopy approaches to secondary and primary active multidrug efflux pumps, *Biochem. Soc. Trans.*; 33 (Pt 4):873-7 August 2005.

Mason A.J., Siarheyeva A., Haase W., Lorch M., van Veen H., Glaubitz C.: Amino acid type selective isotope labelling of the multidrug ABC transporter LmrA for solid-state NMR studies, *FEBS Letters*, 568 (1-3): 117-121 June 18 2004.

List of Conferences Contributions and Talks

CONFERENCES

- March 2006 “A systematic approach to study the multidrug ABC transporter LmrA substrate binding by solid-state NMR” at FEBS special meeting: ATP-binding cassette (ABC) proteins: from multidrug resistance genetic diseases, Innsbruck, Austria
- March 2005 “First solid-state NMR Experiments on ABC multidrug transporter LmrA” at 1st Joint German/British bioenergetics meeting, Wilhelm-Kempf-Haus, Wiesbaden, Germany
- September 2004 “Solid-State NMR investigations on ABC-transporter LmrA” at Annual Meeting of the German Biophysical Society, Freiburg, Germany

TALKS

- October 2005 “Solid-State NMR investigations on ABC-transporter LmrA” at Forschungsinstitute für Molekulare Pharmakologie, Berlin, Germany
- June 2005 “Solid-State NMR investigations on ABC-transporter LmrA” at the International School of Structural Biology and Magnetic resonance, 7th Course Structure and Biophysics New Technologies for Current Challenges in Biology and beyond, Erice, Sicily
- May 2004 “Solid-State NMR investigations on ABC-transporter LmrA” at Summer school Membrane proteins, Bioinformatics and Proteomics, Spetses, Greece

WORKSHOPS

- March 2006 Workshop on Computational Biophysics ‘Hands-on’, giving by K. Schulten, MPI of Biophysics, Frankfurt (M), Germany
- June - July 2005 The International School of Structural Biology and Magnetic resonance, 7th Course Structure and Biophysics New Technologies for Current Challenges in Biology and beyond, Erice, Sicily

- November 2004 Workshop 'Scientific presentation skills', Saarbücken, Germany
- May 2004 Summer school 'Membrane proteins, Bioinformatics and Proteomics',
Spetses, Greece
- April 2004 Workshop 'Membrane protein biophysics', Aalborg, Denmark